



01 Feb 2011

Calibration of Load and Resistance Factors in LRFD Foundation Design Specifications

Zuocai Wang

Genda Chen

Missouri University of Science and Technology, gchen@mst.edu

Oh-Sung Kwon

Sarah Orton

Follow this and additional works at: https://scholarsmine.mst.edu/civarc_enveng_facwork



Part of the [Structural Engineering Commons](#)

Recommended Citation

Z. Wang et al., "Calibration of Load and Resistance Factors in LRFD Foundation Design Specifications," Center for Transportation Infrastructure and Safety/NUTC program, Missouri University of Science and Technology, Feb 2011.

This Technical Report is brought to you for free and open access by Scholars' Mine. It has been accepted for inclusion in Civil, Architectural and Environmental Engineering Faculty Research & Creative Works by an authorized administrator of Scholars' Mine. This work is protected by U. S. Copyright Law. Unauthorized use including reproduction for redistribution requires the permission of the copyright holder. For more information, please contact scholarsmine@mst.edu.



MISSOURI
S&T

CENTER FOR TRANSPORTATION INFRASTRUCTURE AND SAFETY

Calibration of Load and Resistance Factors in LRFD Foundation Design Specifications

by

Zuocai Wang
Genda Chen
Oh-Sung Kwon
Sarah Orton



**NUTC
R237**

**A National University Transportation Center
at Missouri University of Science and Technology**

Disclaimer

The contents of this report reflect the views of the author(s), who are responsible for the facts and the accuracy of information presented herein. This document is disseminated under the sponsorship of the Department of Transportation, University Transportation Centers Program and the Center for Transportation Infrastructure and Safety NUTC program at the Missouri University of Science and Technology, in the interest of information exchange. The U.S. Government and Center for Transportation Infrastructure and Safety assumes no liability for the contents or use thereof.

Technical Report Documentation Page

1. Report No. NUTC R237		2. Government Accession No.		3. Recipient's Catalog No.	
4. Title and Subtitle Calibration of Load and Resistance Factors in LRFD Foundation Design Specifications				5. Report Date February 2011	
				6. Performing Organization Code	
7. Author/s Zuocai Wang, Genda Chen, Oh-Sung Kwon, and Sarah Orton				8. Performing Organization Report No. 00022979	
9. Performing Organization Name and Address Center for Transportation Infrastructure and Safety/NUTC program Missouri University of Science and Technology 220 Engineering Research Lab Rolla, MO 65409				10. Work Unit No. (TRAIS)	
				11. Contract or Grant No. DTRT06-G-0014	
12. Sponsoring Organization Name and Address U.S. Department of Transportation Research and Innovative Technology Administration 1200 New Jersey Avenue, SE Washington, DC 20590				13. Type of Report and Period Covered Final	
				14. Sponsoring Agency Code	
15. Supplementary Notes					
16. Abstract This report summarizes the findings and recommendations on the impact of foundation settlements on the reliability of bridge superstructures. As a collaborative effort of an overall initiative for the development of LRFD foundation design specifications, this study is focused on the investigation of pros and cons for including foundation settlements in bridge designs under gravity loads. Settlement was modeled both probabilistically and deterministically. In the case of a random settlement variable, a lognormal distribution was used in reliability analysis with a fixed coefficient of variation of 0.25. Dead and live loads were modeled as random variables with normal and Gumbel Type I distributions, respectively. Considering the regional traffic condition on Missouri roadways, the effect of a live load reduction factor on bridge reliability was also investigated. Therefore, a total of eight cases were discussed with a complete combination of settlement modeling (mean and extreme values), design consideration (settlements included and excluded), and live load reduction (unreduced and reduced live loads). Based on extensive simulations on multi-span bridges, bridges designed without due consideration on settlements can tolerate an extreme settlement of $L/3500 - L/450$ under unreduced live loads and up to $L/3500$ under reduced live loads without resulting in a reliability index below 3.5 (L =span length). Depending upon span lengths and their ratio, the reliability of existing steel-girder bridges is consistently higher than prestressed concrete and solid slab bridges. The shorter and stiffer the spans, the more significant the settlement's effect on the reliability of bridge superstructures. As the span length ratio becomes less than 0.75, the girder and solid slab bridges' reliability drops significantly at small settlements. A concrete diaphragm is very susceptible to the differential settlement of bridges, particularly for moment effects. Two recommended were made to address settlement effects in bridge design: (1) settlement is considered in structural design and no special requirement is needed for foundation designs unless settlement exceeds the AASHTO recommended settlement limit of $L/250$, and (2) settlement is not considered in structural design as in the current MoDOT practice but ensured below the tolerable settlement (e.g. $L/450$ for steel girders, $L/2500$ for slabs, and $L/3500$ for prestressed concrete girders). The first method provides a direct approach to deal with settlements and has potential to reduce overall costs in bridge design. The second method may result in oversized foundations.					
17. Key Words Reliability index, random variable, probabilistic distribution, tolerable settlement, girder bridge, prestressed concrete bridge, solidslab bridge, concrete diaphragm			18. Distribution Statement No restrictions. This document is available to the public through the National Technical Information Service, Springfield, Virginia 22161.		
19. Security Classification (of this report) unclassified		20. Security Classification (of this page) unclassified		21. No. Of Pages 143	22. Price

EXECUTIVE SUMMARY

Since October 2007, all state departments of transportation in the U.S. have been mandated to use the AASHTO Load and Resistance Factored Design (LRFD) Bridge Design Specifications in their federally funded bridge projects. In Missouri, these specifications had not been calibrated with its regional truck load and site conditions. As a critical part of a bridge system, the foundation not only affects the safety and stability of the overall system, but also constitutes a significant portion of bridge construction costs. Therefore, better calibrations with field data are imperative.

To this end, MoDOT recently launched a geotechnical study initiative for the development and calibration of load and resistance factors in LRFD foundation design specifications. As a support effort to that overall initiative, this study is aimed to investigate pros and cons for including foundation settlements in bridge designs under gravity loads and the effect of reducing live loads on the reliability of bridges. Settlement was modeled both probabilistically and deterministically. In the case of a random settlement variable, a lognormal distribution was adopted in reliability analysis with a fixed coefficient of variation of 0.25 based on limited studies reported in the literature. Dead and live loads were modeled as random variables with normal and Gumbel Type I distributions, respectively. In this study, a total of eight cases were analyzed with a complete combination of settlement modeling (characterized by mean and extreme values), settlement design consideration (included and excluded), and live load reduction (unreduced and reduced).

This report summarizes the findings and recommendations on the impact of foundation settlements on the reliability of the superstructure of both new and existing bridges. Based on extensive simulations on multi-span, continuous bridges, bridges designed without settlement consideration can tolerate an extreme settlement of $L/3500$ - $L/450$ under unreduced live loads and up to $L/3500$ under reduced live loads without resulting in a reliability index below 3.5 (L = span length). Depending upon span lengths and their ratio, the reliability of existing steel-girder bridges is consistently higher than prestressed concrete and solid slab bridges. The shorter and stiffer the spans, the more significant the settlement's effect on the reliability of bridge superstructures. As the span length ratio becomes less than 0.75, the girder and solid slab bridges' reliability drops significantly at small settlements. A concrete diaphragm is very susceptible to the differential settlement of bridges, particularly for moment effects.

Two methods are recommended to address settlement effects: (1) settlement is considered in superstructure and substructure design and no special requirement is needed for foundation designs unless settlement exceeds the AASHTO recommended limit of $L/250$, and (2) settlement is not considered in superstructure and substructure design as in the current MoDOT practice but ensured below the tolerable settlement (e.g. $L/450$ for steel girders, $L/2500$ for slabs, and $L/3500$ for prestressed concrete girders). The first method provides a direct approach to deal with settlements and has potential to reduce overall costs in bridge design. The potential increase in material and labor costs associated with structural design and construction expects to be trivial. The second method is an indirect approach to deal with settlements and may require oversized foundations to restrain settlement to the level that can be tolerated by the superstructure and substructure of a bridge designed without due consideration of settlement.

ACKNOWLEDGEMENTS

Financial support to complete this study by Missouri Department of Transportation (MoDOT) and Missouri S&T Center for Transportation Infrastructure and Safety are greatly appreciated. The authors are grateful to Jennifer Harper for her continuing efforts to seek and provide input from MoDOT engineers and coordinate various project meetings over the duration of this project. Special thanks are due to Greg Sanders, Alan Miller, David Hagemeyer, and Aaron Kemna for their service as the Technical Advisory Panel (TAP) members of this project. Thanks are also due to Drs. Erik Loehr and Ronaldo Luna for their input from a geotechnical engineers' point of view as well as MoDOT and Federal Highway Administration (FHWA) Missouri Division engineers for their valuable comments during various project meetings and review of the final report.

TABLE OF CONTENTS

TABLE OF CONTENTS.....	v
LIST OF FIGURES	vii
LIST OF TABLES	x
1 INTRODUCTION	1
1.1 Background.....	1
1.2 Objective and Scope of Work.....	2
1.3 Organization of This Report	2
2 BRIDGE ANALYSIS UNDER SUPPORT SETTLEMENTS.....	4
2.1 Random Settlement and its Effect on Bridge Responses.....	4
2.2 Analysis Methods.....	5
2.3 Bridge Analysis with MATLAB Program.....	7
2.3.1 Example 1: 2-span continuous steel girder bridge.....	8
2.3.2 Example 2: 3-span continuous prestressed concrete girder bridge.....	8
2.4 Bridge Analysis with Analytical Solutions.....	13
2.4.1 Prismatic girder bridge with equal spans	13
2.4.2 Non-prismatic girder bridges with unequal spans	15
2.5 Bridge Analysis with ANSYS Probabilistic Design Software	20
2.6 Analysis with New Steel-Girder Bridges.....	21
2.7 Settlement Effect on Overall Design Loads.....	22
3 STATISTICAL PROPERTIES OF LOADS AND RESISTANCES	25
3.1 Statistical Parameters for Dead Load.....	25
3.2 Statistical Parameters for Live Load.....	25
3.3 Statistical Parameters of Resistance.....	27
3.4 Statistical Parameters of Settlement Effects	28
4 RELIABILITY ANALYSIS WITH SETTLEMENT EFFECTS	31
4.1 Reliability Theory	31
4.2 Reliability Index with Settlement Effect.....	33
5 SETTLEMENT EFFECT ON SUPERSTRUCTURE RELIABILITY	36
5.1 Load Analysis	36
5.1.1 Dead load effect	36
5.1.2 Live load effect	39
5.2 Strength Resistance of Selected Bridges.....	41
5.3 Reliability Indices of 31 Bridge Designs with Equal Spans	42
5.4 Reliability Indices of 14 Existing Bridges	69
5.4.1 Based on minimum resistances.....	69
5.4.2 Based on actual resistances.....	82
5.4.3 Baseline at zero support settlement.....	85
5.5 Uneven Settlement Effect on Diaphragm	86
6 CONCLUSIONS AND RECOMMENDATIONS	89
6.1 Conclusions.....	89
6.2 Recommendations.....	90
REFERENCES	92
APPENDIX A: SUPPORT MOMENTS DUE TO UNIT SETTLEMENTS AT VARIOUS SUPPORTS.....	94

APPENDIX B: SHEAR IN SPAN DUE TO UNIT SETTLEMENTS AT VARIOUS SUPPORTS	97
APPENDIX C: SUPPORT REACTIONS DUE TO UNIT SETTLEMENTS AT VARIOUS SUPPORTS	100
APPENDIX D: BRIDGE ANALYSIS REPORT FROM ANSYS SOFTWARE.....	103
APPENDIX E: FORCES AND MOMENTS OF 31 NEW BRIDGES DUE TO A UNIT SETTLEMENT AT SUPPORT 1	120
APPENDIX F: FORCES AND MOMENTS OF 31 NEW BRIDGES DUE TO DEAD AND LIVE LOADS	123

LIST OF FIGURES

Figure 1.1 Organization of this report	3
Figure 2.1 Support settlement sample data with COV = 25%.....	5
Figure 2.2 Support and span definitions of bridges with various spans	7
Figure 2.3 Bridge A3101 under a 1-inch center support settlement (Support 2).....	9
Figure 2.4 Bridge A3101 under a random center support settlement (Support 2): mean=1 in. and COV=0.25	9
Figure 2.5 Maximum positive moment distribution of Bridge A3101 under the center support settlement (Support 2): mean=1 in. and COV=0.25	10
Figure 2.6 Bridge A4058 under a 1-inch deterministic settlement.....	11
Figure 2.7 Bridge A4058 under a random support settlement: mean=1 in. and COV=0.25	12
Figure 2.8 Histograms of the maximum positive and negative moments of Bridge A4058 under random support settlements: mean=1 in. and COV=0.25.....	12
Figure 2.9 Special bridge cases.....	13
Figure 2.10 Moment distribution of a prismatic 2-span girder of equal spans	14
Figure 2.11 Maximum moments at Support 2 of the 2-span bridge	14
Figure 2.12 Moment diagrams of a 3-span girder.....	15
Figure 2.13 Maximum positive and negative moments of a 3-span bridge.....	16
Figure 2.14 $f(\alpha, \beta)$ for 2-span continuous girders	18
Figure 2.15 $f(\alpha, \beta)$ for 3-span continuous interior girders under settlement at Support 1 (left end support)	19
Figure 2.16 $f(\alpha, \beta)$ for 3-span continuous interior girders under settlement at Support 2 (left intermediate support)	19
Figure 2.17 Models of curved bridges with ANSYS.....	20
Figure 2.18 Cross section of new girder bridges	21
Figure 2.19 Minimum moments of inertia for new bridges.....	23
Figure 2.20 Moment and shear ratios between two cases: with and without settlement effects	24
Figure 3.1 Daily maximum moment fitted into Gumbel Type I distribution	26
Figure 3.2 Comparison between daily and 75-year maximum moment.....	26
Figure 3.3 Comparison of maximum positive and negative moment distributions of Bridge A3101: mean=1 in., COV=0.25.....	29
Figure 3.4 Comparison of maximum positive and negative moment distributions of Bridge A4058 due to settlements: mean=1 in., COV=0.25	30
Figure 5.1 Multiple-lane load	39
Figure 5.2 The ratio of the real resistance to the minimum resistance	42
Figure 5.3 Reliability indices of 2-span bridges (No.1 to No.11 in Table 2.3): Case 1	43
Figure 5.4 Reliability indices of 3-span bridges (No.12 to No.22 in Table 2.3): Case 1	44
Figure 5.5 Reliability indices of 4-span bridges (No.23 to No.31 in Table 2.3): Case 1	45
Figure 5.6 Reliability indices of 2-span bridges (No.1 to No.11 in Table 2.3): Case 2	46
Figure 5.7 Reliability indices of 3-span bridges (No.12 to No.22 in Table 2.3): Case 2	47
Figure 5.8 Reliability indices of 4-span bridges (No.23 to No.31 in Table 2.3): Case 2	48
Figure 5.9 Reliability indices of 2-span bridges (No.1 to No.11 in Table 2.3): Case 3	49
Figure 5.10 Reliability indices of 3-span bridges (No.12 to No.22 in Table 2.3): Case 3	50
Figure 5.11 Reliability indices of 4-span bridges (No.23 to No.31 in Table 2.3): Case 3	51
Figure 5.12 Reliability indices of 2-span bridges (No.1 to No.11 in Table 2.3): Case 4	52

Figure 5.13 Reliability indices of 3-span bridges (No.12 to No.22 in Table 2.3): Case 4	53
Figure 5.14 Reliability indices of 4-span bridges (No.23 to No.31 in Table 2.3): Case 4	54
Figure 5.15 Reliability indices of 2-span bridges (No.1 to No.11 in Table 2.3): Case 5	55
Figure 5.16 Reliability indices of 3-span bridges (No.12 to No.22 in Table 2.3): Case 5	56
Figure 5.17 Reliability indices of 4-span bridges (No.23 to No.31 in Table 2.3): Case 5	57
Figure 5.18 Reliability indices of 2-span bridges (No.1 to No.11 in Table 2.3): Case 6	58
Figure 5.19 Reliability indices of 3-span bridges (No.12 to No.22 in Table 2.3): Case 6	59
Figure 5.20 Reliability indices of 4-span bridges (No.23 to No.31 in Table 2.3): Case 6	60
Figure 5.21 Reliability indices of 2-span bridges (No.1 to No.11 in Table 2.3): Case 7	61
Figure 5.22 Reliability indices of 3-span bridges (No.12 to No.22 in Table 2.3): Case 7	62
Figure 5.23 Reliability indices of 4-span bridges (No.23 to No.31 in Table 2.3): Case 7	63
Figure 5.24 Reliability indices of 2-span bridges (No.1 to No.11 in Table 2.3): Case 8	64
Figure 5.25 Reliability indices of 3-span bridges (No.12 to No.22 in Table 2.3): Case 8	65
Figure 5.26 Reliability indices of 4-span bridges (No.23 to No.31 in Table 2.3): Case 8	66
Figure 5.27 Reliability indices of 14 existing bridges: Case 1	70
Figure 5.28 Reliability indices of 14 existing bridges: Case 2	72
Figure 5.29 Reliability indices of 14 existing bridges: Case 3	73
Figure 5.30 Reliability indices of 14 existing bridges: Case 4	75
Figure 5.31 Reliability indices of 14 existing bridges: Case 5	76
Figure 5.32 Reliability indices of 14 existing bridges: Case 6	78
Figure 5.33 Reliability indices of 14 existing bridges: Case 7	79
Figure 5.34 Reliability indices of 14 existing bridges: Case 8	81
Figure 5.35 Reliability indices of 14 existing bridges: Case 1	83
Figure 5.36 Reliability indices of 14 existing bridges: Case 2	84
Figure 5.37 Reliability indices of 14 existing bridges without settlement effects.....	86
Figure 5.38 Typical concrete bent diaphragm	87
Figure 5.39 Typical steel bent diaphragm.....	87
Figure 5.40 Bent diaphragm of Bridge A6569	87
Figure 5.41 Bent rotation due to the uneven settlement of bridge foundations.....	88
Figure 6.1 Design flow chart with two recommendations.....	91
Figure D.1 Finite element model of each bridge	103
Figure D.2 Probability density function and probability distribution function of input random variable A defined in Table D.3.....	104
Figure D.3 Histograms of maximum moment	106
Figure D.4 Histograms of minimum moment.....	107
Figure D.5 Histograms of maximum absolute shear force	108
Figure D.6 Histograms of minimum absolute shear force.....	109
Figure D.7 Sample histories of maximum moment.....	110
Figure D.8 Sample histories of minimum moment.....	111
Figure D.9 Sample histories of maximum shear force	112
Figure D.10 Sample histories of minimum shear force	113
Figure D.11 Probability distribution functions of maximum moment	114
Figure D.12 Probability distribution function of minimum moment.....	115
Figure D.13 Probability distribution function of maximum shear force	116
Figure D.14 Probability distribution function of minimum shear force	117
Figure D.15 Settlement versus maximum moment.....	118

Figure D.16 Settlement versus minimum moment	119
--	-----

LIST OF TABLES

Table 2.1 Select bridges for analysis	6
Table 2.2 Means of maximum positive and negative moments in interior girders.....	21
Table 2.3 Summary of new designs of girder bridges with equal spans.....	22
Table 2.4 Bridges analyzed under gravity loads.....	23
Table 3.1 Statistical values of dead load (Nowak, 1999)	25
Table 3.2 Statistical parameters of resistance	27
Table 4.1 Eight design cases investigated.....	33
Table 4.2 Strength resistance factors in AASHTO LRFD specifications (2007)	34
Table 5.1 Maximum positive moments of each interior girder due to dead loads excluding wearing surface	36
Table 5.2 Maximum negative moments of each interior girder due to dead loads excluding wearing surface	37
Table 5.3 Maximum shear forces of each interior girder due to dead loads excluding wearing surface	37
Table 5.4 Maximum positive moments of each interior girder due to weight of wearing surface only	38
Table 5.5 Maximum negative moments of each interior girder due to weight of wearing surface only	38
Table 5.6 Maximum shears of each interior girder due to weight of wearing surface only	39
Table 5.7 Maximum positive moments of each interior girder due to live load.....	40
Table 5.8 Maximum negative moments of each interior girder due to live load.....	40
Table 5.9 Maximum shear forces of each interior girder due to live load.....	41
Table 5.10 Minimum resistances of negative and positive moments and shear	41
Table 5.11 Actual resistances of negative and positive moments	42
Table 5.12 Average tolerable settlements of new bridges in terms of loading effects	67
Table 5.13 Average tolerable settlements of new bridges in terms of bridge span numbers	67
Table 5.14 Average tolerable settlements of existing bridges (% of span length) using the minimum resistances.....	81
Table 5.15 Average tolerable settlements of existing bridges (% of span length) using the actual moment strength.....	85
Table 5.16 Nominal resistance and maximum moment and shear due to uneven settlement	88
Table A.1 Support moments due to unit settlements for 2-span continuous bridges	94
Table A.2 Support moments due to unit settlements for 3-span continuous bridges	94
Table A.3 Support moments due to unit settlements for 4- and 5-span continuous bridges	95
Table B.1 Shear in spans due to unit settlements for 2-span continuous bridges.....	97
Table B.2 Shear in spans due to unit settlements for 3-span continuous bridges.....	97
Table B.3 Shear in spans due to unit settlements for 4- and 5-span continuous bridges.....	98
Table C.1 Support reactions due to unit settlements for 2-span continuous bridges.....	100
Table C.2 Support reactions due to unit settlements for 3-span continuous bridges.....	100
Table C.3 Support reactions due to unit settlements for 4- and 5-span continuous bridges.....	101
Table D.1 Details of the finite element model.....	104
Table D.2 Material properties	104
Table D.3 Random input variable specifications.....	104
Table D.4 Statistics of the random output parameters.....	105
Table E.1 Moments at various supports.....	120

Table E.2 Shear forces at various supports	121
Table E.3 Reactions at various supports	122
Table F.1 Maximum negative moments due to dead load excluding wearing surface	123
Table F.2 Maximum positive moments due to dead load excluding wearing surface	124
Table F.3 Maximum shear forces due to dead load excluding wearing surface	125
Table F.4 Maximum negative moments due to weight of wearing surface	126
Table F.5 Maximum positive moments due to weight of wearing surface	127
Table F.6 Maximum shear forces due to weight of wearing surface	128
Table F.7 Maximum negative moments due to 75-year live load including dynamic effect	129
Table F.8 Maximum positive moments due to 75-year live load including dynamic effect	130
Table F.9 Maximum shear forces due to 75-year live load including dynamic effect	131
Table F.10 Maximum negative moments due to HL-93 load including dynamic effect	132
Table F.11 Maximum positive moments due to HL-93 load including dynamic effect	133
Table F.12 Maximum shear forces due to HL-93 load including dynamic effect	134

1 INTRODUCTION

1.1 Background

Since October 2007, all state departments of transportation in the U.S. have been mandated to use the AASHTO load and resistance factored design (LRFD) specifications (2007) in their federally funded bridge projects. In Missouri, these specifications, including the effects of foundation settlement in bridge designs, had not been calibrated with its load conditions and environmental factors. As a critical part of a bridge system, the foundation not only affects the safety and stability of the overall system, but also constitutes a significant portion of bridge construction costs. Therefore, better calibrations with field data are imperative.

In the current design practice of bridges in Missouri, support settlement is not considered mainly because of the lack of well-founded criteria for the tolerable support settlement of bridges and due to shallow conditions at most bridge sites. This design practice implies that all continuous bridges be supported on rock directly or on deep piles/shafts that are socketed into rock. In the latter case, deep foundations may be unnecessarily long and costly. One alternative to the above practice is to reduce foundation length, allow for foundation settlement, and design for settlement-induced stress in the superstructure and substructure. In this case, the foundation costs less while the superstructure and substructure costs the same or more. Such an alternative that may result in satisfactory bridge performance at a lower overall cost has never been investigated before.

A bridge foundation settles nonlinearly as the vertical load applied on it increases. Under a given design load, the more settlement is allowed, the smaller the foundation. However, differential foundation settlement as an external load as specified in the AASHTO design specifications may induce additional responses in both the superstructure and substructure, such as deflection, moment, shear, and support reaction. How these responses affect the design of the superstructure and substructure is a critical issue to investigate in this study. If this effect is insignificant and does not govern the design of superstructures and substructures, the net gain of foundation cost reductions can be achieved. Otherwise, several design options can be exercised, including the use of larger and longer piles/shafts for reduced foundation settlements and the use of larger structural members to accommodate the increased demands. In this case, collaboration between structural and geotechnical engineers is a key to realizing a cost-effective design of the overall bridge system, offering the best long-term performance and economy.

The current AASHTO Bridge Design Specifications (2007) recommend that an angular distortion greater than 0.008 rad in simple spans and 0.004 rad in continuous spans should not be permitted in settlement criteria (Moulton et al. 1985; DiMillio, 1982; Barker et al. 1991). These criteria correspond to the differential settlements of $L/125$ and $L/250$ for simple and continuous spans, respectively, where L denotes the span length. The differential settlement on a continuous span can cause additional moment, shear and support reaction on the superstructure even when it is less than the AASHTO recommended settlement limit ($L/250$). In the AASHTO specifications, the extreme differential settlement is considered as an external load with a load factor $\gamma_{SE} = 1.0$ when combined with other loads in strength limit states (I, II, III, and V) and service limit states (I, III and IV).

The AASHTO recommended settlement limit was determined mainly based on the serviceability requirements in the development of allowable stress design specifications (AASHTO, 2007). Previous studies by Moulton et al. (1985, 1986) concluded that a 1-inch differential settlement can considerably stress a bridge girder or solid slab, depending upon its span length and flexural rigidity (EI). This effect is particularly significant for short spans up to 60 ft. To date, little has been investigated on how much settlement highway bridges can tolerate based on reliability theory in LRFD bridge design practices. This study intends to fill the gap between the past research and the current LRFD design practice.

1.2 Objective and Scope of Work

This study is a collaborative effort of the development of LRFD foundation design specifications initiated by the Missouri Department of Transportation (MoDOT). The overall goal of the initiative is to develop and calibrate the load and resistance factors considering the distribution of foundation settlements at various bridge sites in Missouri. The objective of this study is to evaluate the impact of foundation settlements on the design of superstructures and substructures in the context of LRFD design of bridges, particularly if MoDOT implements a new live load reduction factor based on the recent live load calibration study by Kwon et al. (2010). The reduced live load may lead to lower resistance requirements for the design of superstructures and substructures. As such, the ability of bridge structures to withstand differential support settlements is reduced and the effect of settlements on the reliability of the bridges could become critical in design.

Due to uncertainty in long-term settlement estimates, support settlement is considered as a deterministic extreme value or a random variable with a lognormal distribution. To achieve the objective, the scope of work of this study includes: (1) to analyze with three methodologies the force effect of the differential support settlement of bridges in various types, (2) to evaluate the reliability index of bridges taking into account the support settlement and the new live load factors for different design criteria, and (3) to recommend two strategies considering differential support settlements in bridge design to achieve a target reliability index.

1.3 Organization of This Report

This report is organized in six sections, including introduction, bridge analysis, statistical property, reliability analysis, settlement effect, and conclusions and recommendations. Section 1 provides the background information about this study and defines the objective and scope of work in this study. Section 2 develops and describes three bridge analysis methodologies due to deterministic and random settlements. Section 3 discusses the statistical properties of loads, settlements, and resistances. Section 4 summarizes the reliability analysis procedure for potential design criteria using the first order reliability method (FORM). Section 5 evaluates the effect of differential settlements on the reliability of superstructure design. Section 6 summarizes the findings from this study and recommends a simplified design procedure to take into account the force effects of differential support settlements.

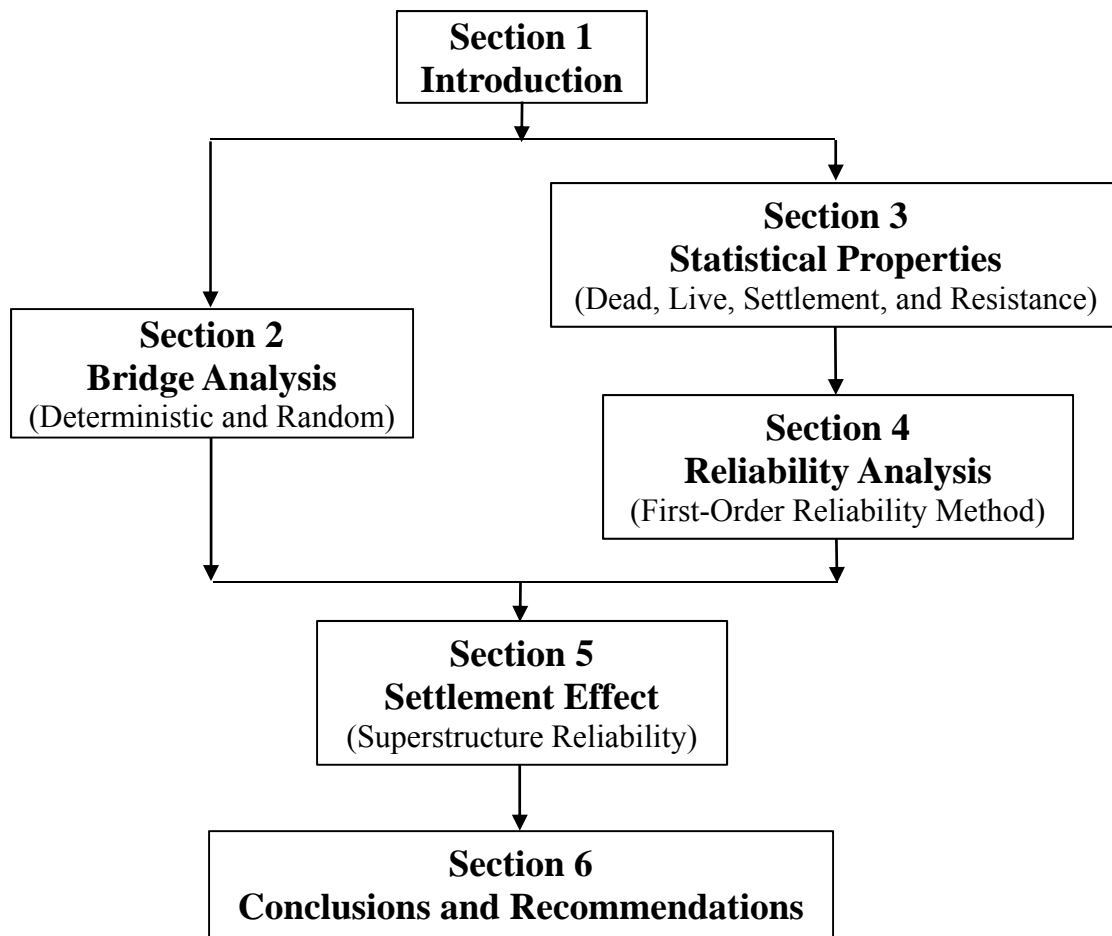


Figure 1.1 Organization of this report

2 BRIDGE ANALYSIS UNDER SUPPORT SETTLEMENTS

The section introduces three methods to analyze girder or solid slab bridges of various types under support settlements. In this study, the support settlements are assumed to be either deterministic with extreme values or random with a lognormal distribution.

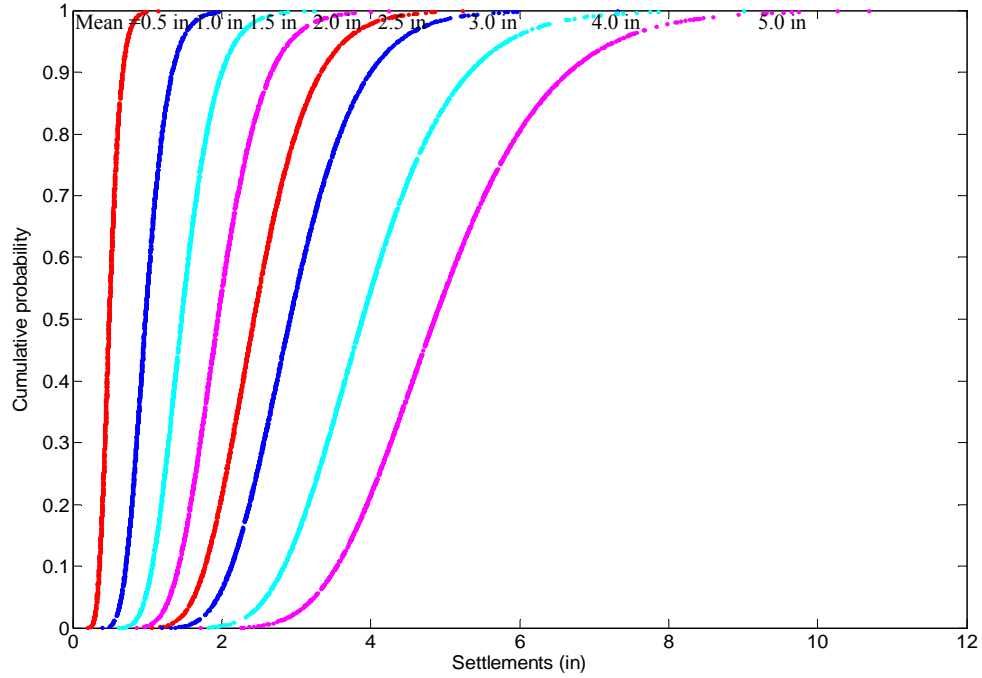
2.1 Random Settlement and its Effect on Bridge Responses

The current AASHTO LRFD Bridge Design Specifications (2007) require that the angular distortion between adjacent foundations be less than 0.008 rad for simple spans and 0.004 rad for continuous spans (Moulton et al. 1985; DiMillio, 1982; Barker et al., 1991). They correspond to the differential support settlements of $L/125$ and $L/250$ for simple and continuous spans, respectively. Therefore, the mean values of support settlement selected in this study do not exceed the AASHTO recommended limits.

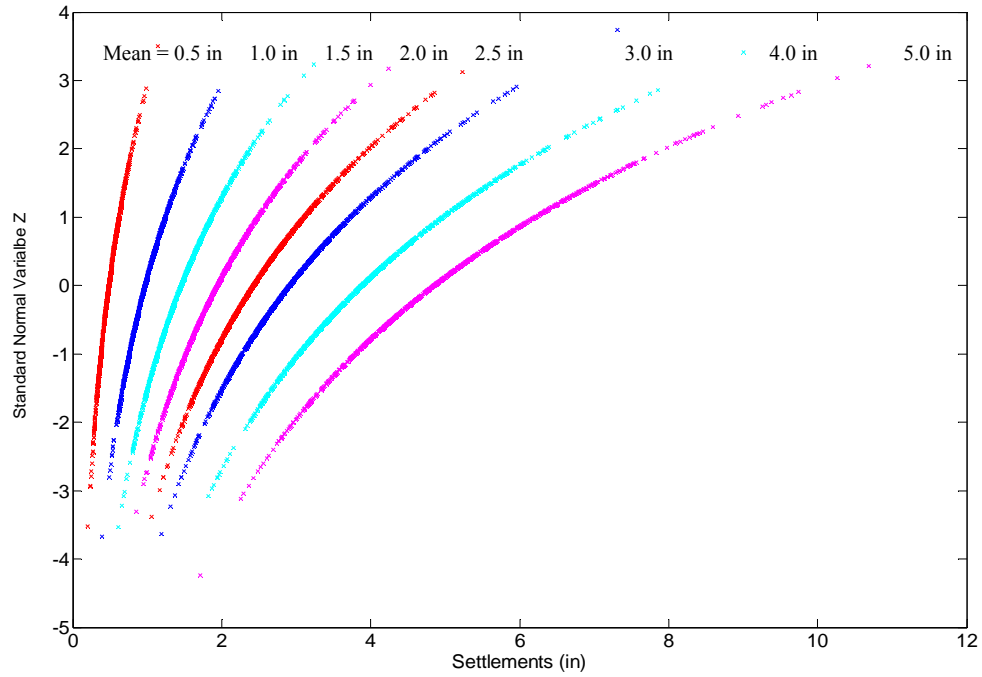
Another important parameter for the random variable of differential settlement is the coefficient of variation (COV). For granular soils, there are a wide variety of methods currently in use for settlement prediction. However, the settlement of granular soils occurs so rapidly that at each stage of loading during the construction process, the settlement is essentially completed before the next stage of loading is applied. Most part of the settlement occurs after the bridge deck is in place. If deemed necessary, adjustments can be made during construction to minimize the post-construction differential settlement imposed on the bridge superstructure. For cohesive soils, a few sophisticated methods are available for settlement prediction. Based on a comparative study by Moulton et al. (1986), the ultimate foundation settlement can be numerically estimated to within 25% of its measured value so long as reliable subsurface exploration and consolidation test data are available. In this study, the 25% relative difference is considered as the coefficient of variation for the support settlement.

To fully describe the random variable, differential settlement is considered to follow a lognormal distribution. Lognormal distribution has been widely used in various engineering applications based on observed histogram shapes (Ang and Tang, 1975; Abramowitz and Stegan, 1972; Nour et al., 2002). For a COV value of 0.25, the probability distribution function of a settlement variable with various mean values generated by Monte Carlo simulations is presented in Figure 2.1(a). The corresponding standard normal variable Z , a normalized settlement by mean and standard deviation, is shown in Figure 2.1(b).

The effect of support settlements on the shear and moment of girder or solid slab bridges was investigated as a function of span length, number of spans, stiffness and other parameters such as the ratio of end span length to center span length. The settlement-induced force and moment can be significant in design (Hearn and Nordheim, 1998). For example, the settlement-induced moment can not only affect the moment magnitude under gravity loads, but also change the distribution of the overall moment. The negative moment at intermediate supports under gravity loads alone could be changed to positive moment due to support settlements. Moulton et al. (1986) concluded that, for two and four span steel-girder bridges, a differential settlement of 1.0 in. for spans up to 50 ft or 3.0 in. for 100-foot spans would produce unacceptable stresses. The effect of a 3-inch support settlement was small for spans of above 200 ft.



(a) Probability distribution function with various mean values



(b) Standard normal variable with various mean values

Figure 2.1 Support settlement sample data with COV = 25%

2.2 Analysis Methods

The moment, shear, and support reaction due to support settlements depend on bridge properties, such as the moment of inertia, number of spans, and span length. In this study, three methods were adopted for various bridge analyses under different conditions:

1. A MATLAB program was developed for the maximum automation of numerical analyses for the straight girder bridges,
2. Analytical solutions were derived for special cases of straight girders to facilitate the development of design equations, and
3. An ANSYS probabilistic design software package was used to analyze both the superstructure and substructure of curved girder bridges under random support settlements.

A total of 20 highway bridges were analyzed using the above three methods as summarized in Table 2.1. They include multi-span continuous bridges with straight and curved, steel and concrete, non-prestressed and prestressed, girders and solid slabs. The span lengths and the AASHTO recommended settlement limits are given. As indicated in Table 2.1, Bridges 1-17 were analyzed using the MATLAB program and the analytical derivations. Bridges 18-20 are curved structures; they were analyzed using the ANSYS probabilistic design package.

Table 2.1 Select bridges for analysis

Bridge Index	Bridge No.		Bridge Description	Analysis Method	Minimum Span (ft)	Settlement Limit 0.004L (in)
	NBI	MoDOT				
1	2664	A3101	120'+120' steel girder	1 and 2	120	5.76
2	-	A6754	142'+110' steel girder	1 and 2	110	5.28
3	3945	A4840	138'+141' steel girder	1 and 2	138	6.62
4	31500	A7300	64.75'+64.75' steel girder	1 and 2	64.75	3.11
5	2852	A3386	75'+97'+75' steel girder	1 and 2	75	3.60
6	3332	A4058	37'+65'+42' prestressed concrete girder	1 and 2	37	1.78
7	3475	A4256	19.5'+26'+23.5' steel girder	1 and 2	19.5	0.94
8	4043	A4999	58'+119'+54' steel girder	1 and 2	54	2.59
9	11893	A5161	38'+65'+40' prestressed concrete girder	1 and 2	38	1.82
10	29023	A6569	65'+100'+74' prestressed concrete girder	1 and 2	65	3.12
11	3276	A3973	59'+59'+43'+43' prestressed concrete girder	1 and 2	43	2.06
12	3753	A4582	38'+38'+65'+38' prestressed concrete girder	1 and 2	38	1.82
13	new design	A7086	120'+125'+125'+120' prestressed concrete girder	1 and 2	120	5.76
14	2856	A3390	48'+60'+48'+55' slab bridge	1 and 2	48	2.30
15	2983	A3562	34'+46'+34' slab bridge	1 and 2	34	1.63
16	28993	A6450	18'+23'+18' slab bridge	1 and 2	18	0.86
17	3706	A4528	48'+48'+65'+48'+48' slab bridge	1 and 2	48	2.30
18	3190	A3848	68'+70'+68' curved steel girder	3	68	3.26
19	31528	A6723	90'+200'+90' curved steel girder	3	90	4.32
20	29559	A6477	110'+190'+110' curved steel girder	3	110	5.28

Table 2.1 includes continuous steel-girder, prestressed concrete-girder, and concrete slab bridges of two to five spans. To facilitate the following discussions, the support and span locations of 2-span, 3-span, 4-span, and 5-span bridges are defined below.

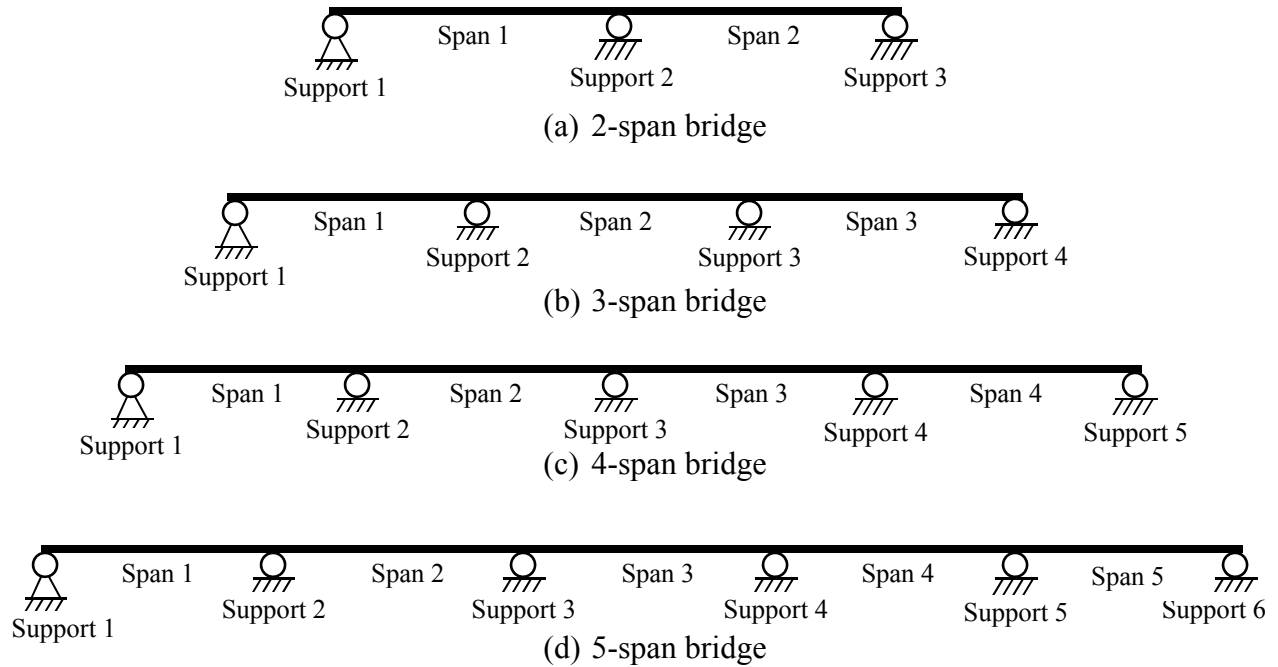


Figure 2.2 Support and span definitions of bridges with various spans

2.3 Bridge Analysis with MATLAB Program

The MATLAB program developed for this study can determine the moment, shear, and support reaction of straight continuous girder bridges of varying stiffness due to a deterministic or random support settlement. This program uses the finite element method to compute the girder responses to the support settlement. After the number of span and span length of a girder bridge are given, the program discretizes the girder into beam elements. Once the stiffness EI is defined for each beam element, the program formulates the global stiffness matrix and introduces the boundary conditions to solve for nodal displacements, shear forces, and moments under a deterministic or random support settlement. Note that for concrete bridges, EI changes with the moment in the bridge due to potential cracking. As the settlement increases, the cracking could reduce the stiffness and associated moment. The cracks and reduced moments are not included in this study in order to allow the application of the superposed effects of settlements at multiple supports in bridge analysis.

Based on the analyses of 17 bridges as indicated in Table 2.1 under both deterministic and random settlements, the following observations can be made:

- (1) Moment due to a support settlement is linearly distributed over the span length. Shear force is constant in each span.
- (2) The random distribution of moment and shear due to a settlement follow the same distribution of the settlement - lognormal.
- (3) The coefficient of variation of a moment and shear force due to settlement is the same as that of the settlement, which is 0.25.
- (4) The maximum moment due to a settlement always occurs at support locations, proportional to the settlement value.

The above observations indicate that, given the moment and shear diagrams due to a 1-inch settlement at each support individually, the moment and shear of a girder bridge due to combined support actions can be obtained by superimposing the solutions due to each support settlement. For example, the moment and shear of elastic bridges from any settlement at one support can be scaled up and down from those due to a 1-inch settlement at that support. For random settlements, the random properties of the moment and shear forces are the same as those of the random settlement, such as the lognormal distribution and equal coefficient of variation. For complete descriptions, the moment, shear, and reaction due to a 1-inch settlement at each support are included in Appendices A - C. According to the 2007 AASHTO Specification C3.12.6, for load combinations including support settlement, analysis should be repeated for the settlements that occur at individual substructure units or their combinations, creating the most critical force effects in the bridge structure. Therefore the critical force effects due to a combination of simultaneous support settlements are also calculated and shown in Appendices A - C.

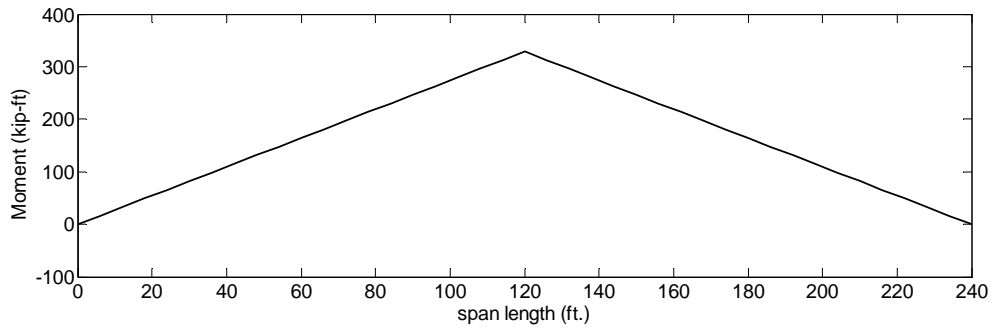
To illustrate the detailed information that the MATLAB program can provide for bridge analysis, following is a presentation of two example bridges. Both 2-span steel-girder and 3-span prestressed concrete-girder bridges are considered. The steel-girder bridges are continuous for both dead and live load effects. The prestressed concrete-girder bridges are simply supported for dead load effects and continuous for live load effects. Both examples are considered to be continuous structures as far as support settlement effects are concerned.

2.3.1 Example 1: 2-span continuous steel girder bridge

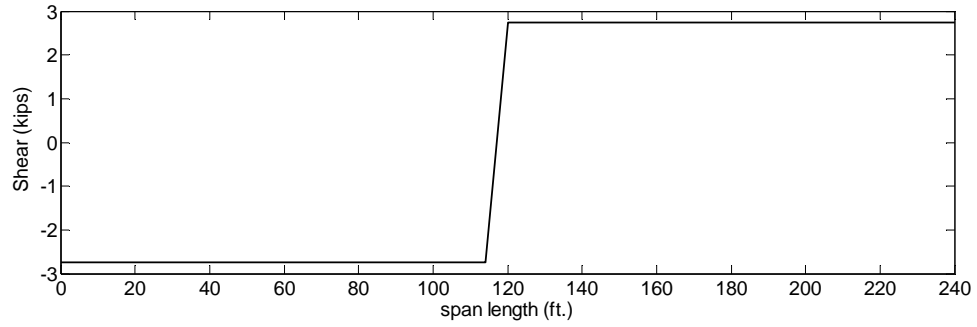
Bridge A3101 was analyzed as a two-span continuous steel bridge example. It has two equal spans of 120 ft each. For each interior steel girder, the moment of inertia was taken to be $I=68,532 \text{ in}^4$ from 0 to 82 ft and from 158 ft to 240 ft, and $I=116,536 \text{ in}^4$ from 82 ft to 158 ft. Their modulus of elasticity is $E=29,000 \text{ ksi}$. The moment and shear diagrams due to a deterministic settlement of 1.0 in. at the center support (Support 2 in Figure 2.2) are presented in Figures 2.3(a) and 2.3(b). The moment and shear diagrams due to random settlements with a mean of 1.0 in. and a COV of 25% at the center support are shown in Figures 2.4(a) and 2.4(b). The random distribution of the maximum moment is presented in Figure 2.5.

2.3.2 Example 2: 3-span continuous prestressed concrete girder bridge

Bridge A4058 was analyzed as a 3-span example bridge with prestressed concrete girders. The lengths of the three spans are 37 ft, 65 ft, and 42 ft, respectively. For each interior concrete girder, the moment of inertia and the modulus of elasticity were taken to be $I=319,300 \text{ in}^4$ and $E=3,600 \text{ ksi}$. The moment and shear diagrams due to a 1-inch settlement at the first (left end) and second supports (Supports 1 and 2 in Figure 2.2) are shown in Figures 2.6(a) and 2.6(b). The moment and shear diagrams under a random settlement of mean = 1.0 in. and COV = 25% at the first (left end) and second supports are presented in Figures 2.7(a) and 2.7(b). Each line in the moment and shear diagrams represents one sample of the random settlement variable. The random distributions of the maximum positive moment and maximum negative moment are shown in Figures 2.8(a) and 2.8(b).

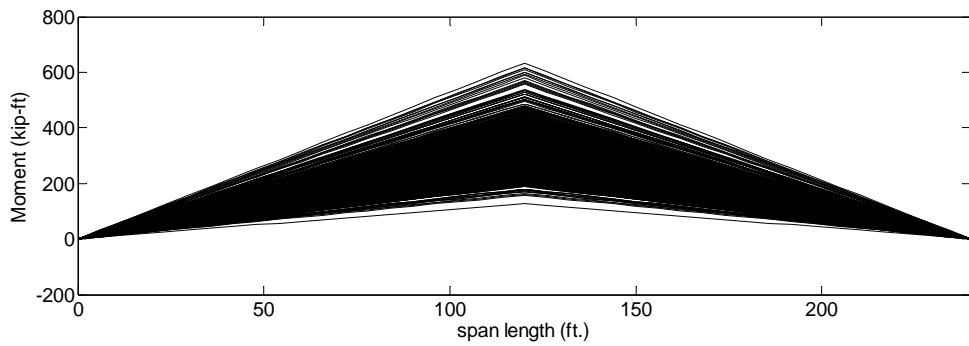


(a) Moment diagram

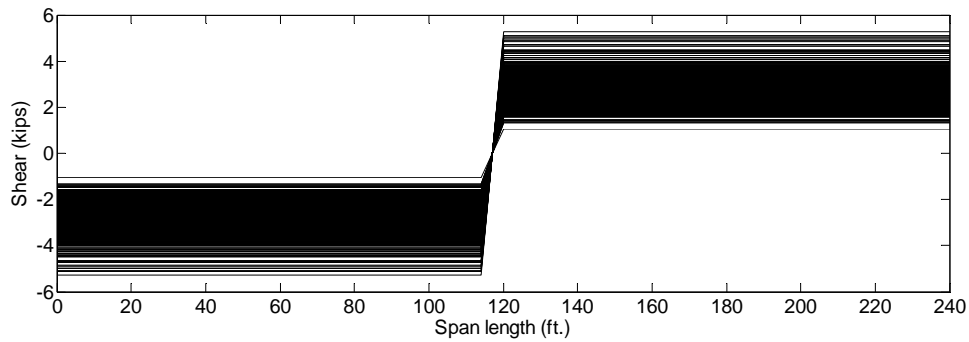


(b) Shear diagram

Figure 2.3 Bridge A3101 under a 1-inch center support settlement (Support 2)



(a) Moment diagram



(b) Shear diagram

Figure 2.4 Bridge A3101 under a random center support settlement (Support 2): mean=1 in. and COV=0.25

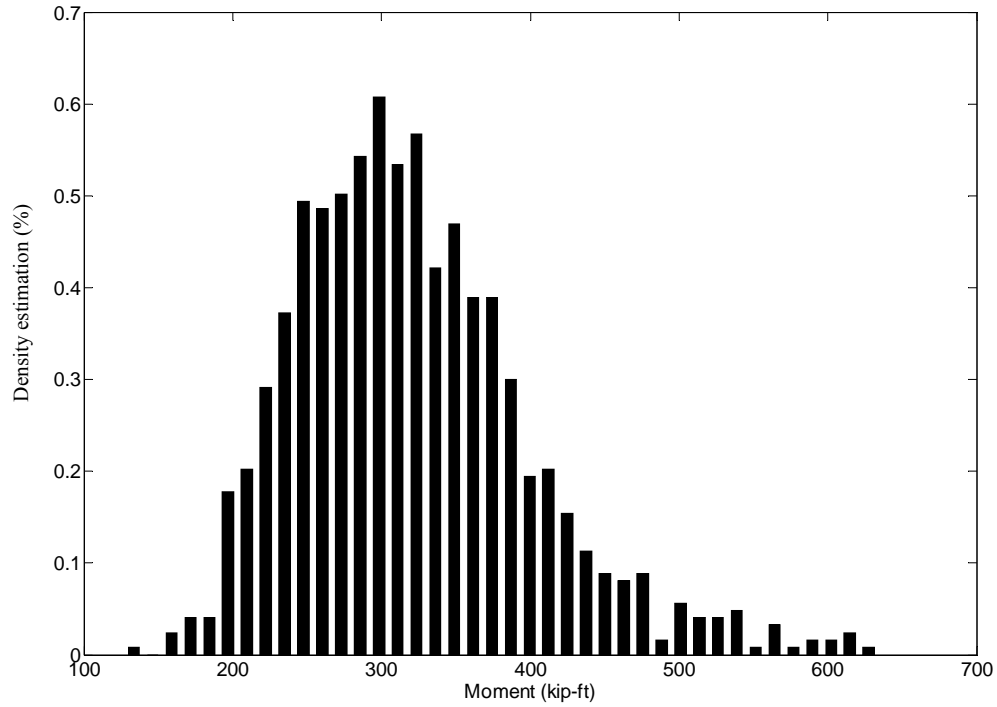
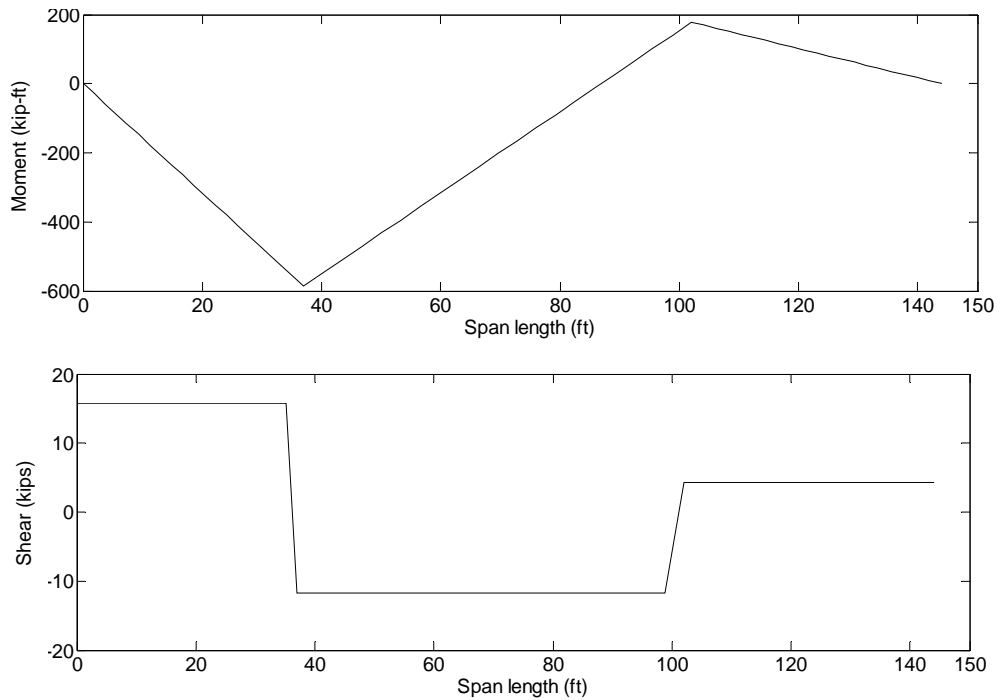
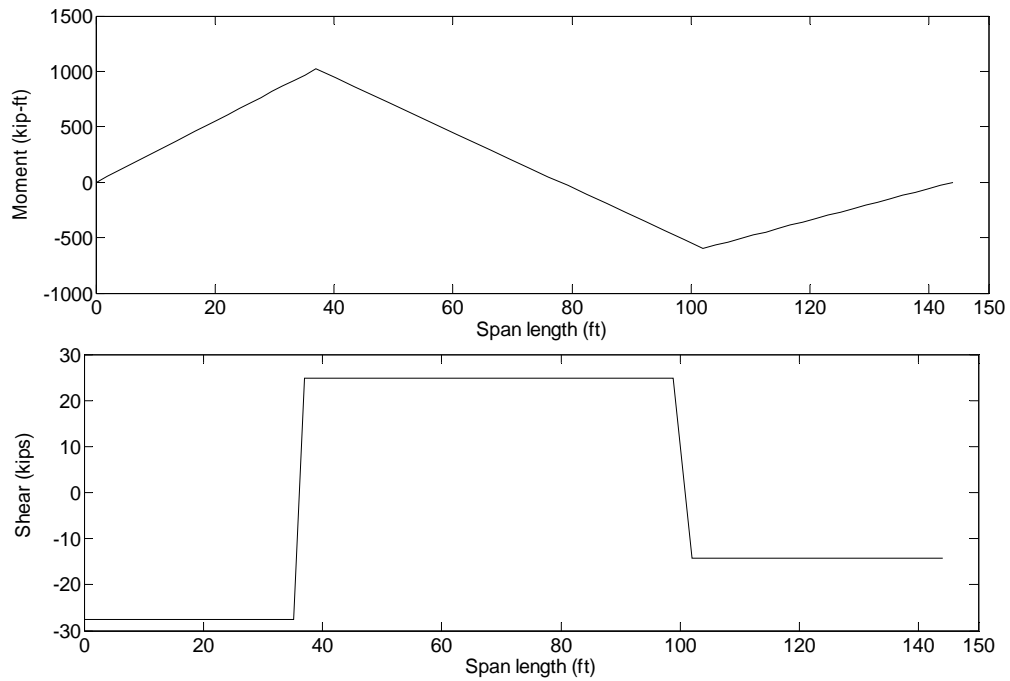


Figure 2.5 Maximum positive moment distribution of Bridge A3101 under the center support settlement (Support 2): mean=1 in. and COV=0.25

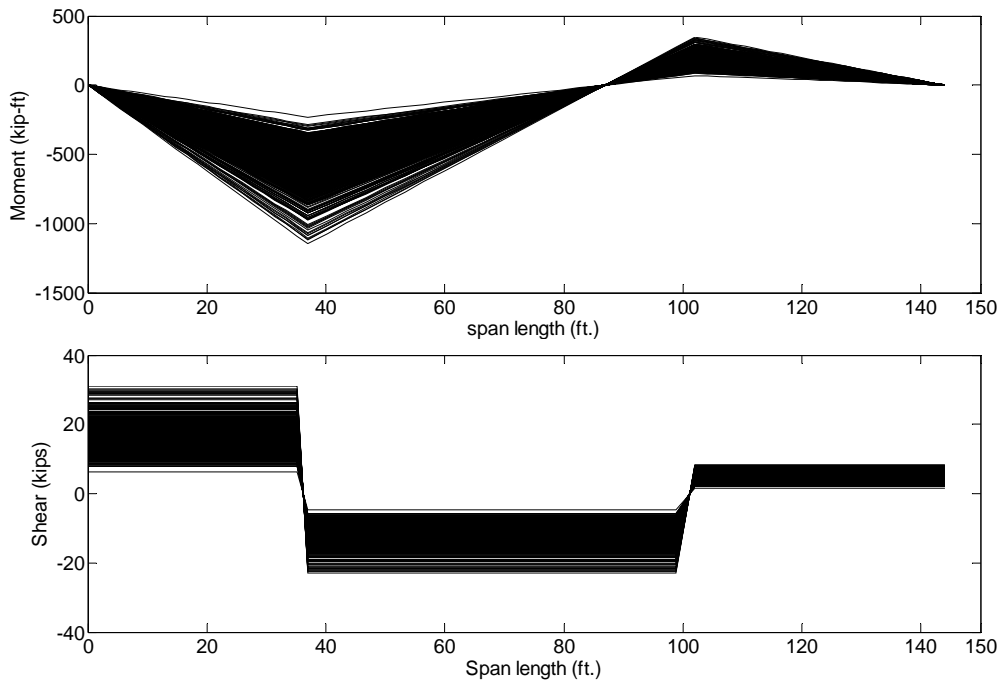


(a) Moment and shear diagrams due to settlement at Support 1 (left end support)

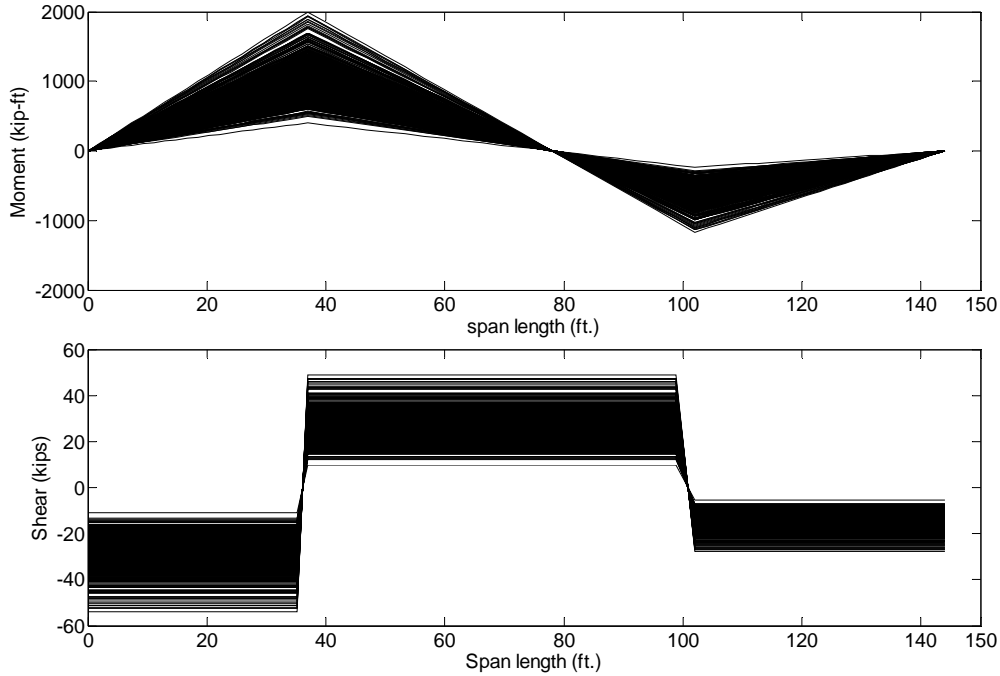


(b) Moment and shear diagrams due to settlement at Support 2 (left intermediate support)

Figure 2.6 Bridge A4058 under a 1-inch deterministic settlement



(a) Moment and shear diagrams due to settlement at Support 1 (left end support)



(b) Moment and shear diagrams due to settlement at Support 2 (left intermediate support)

Figure 2.7 Bridge A4058 under a random support settlement: mean=1 in. and COV=0.25

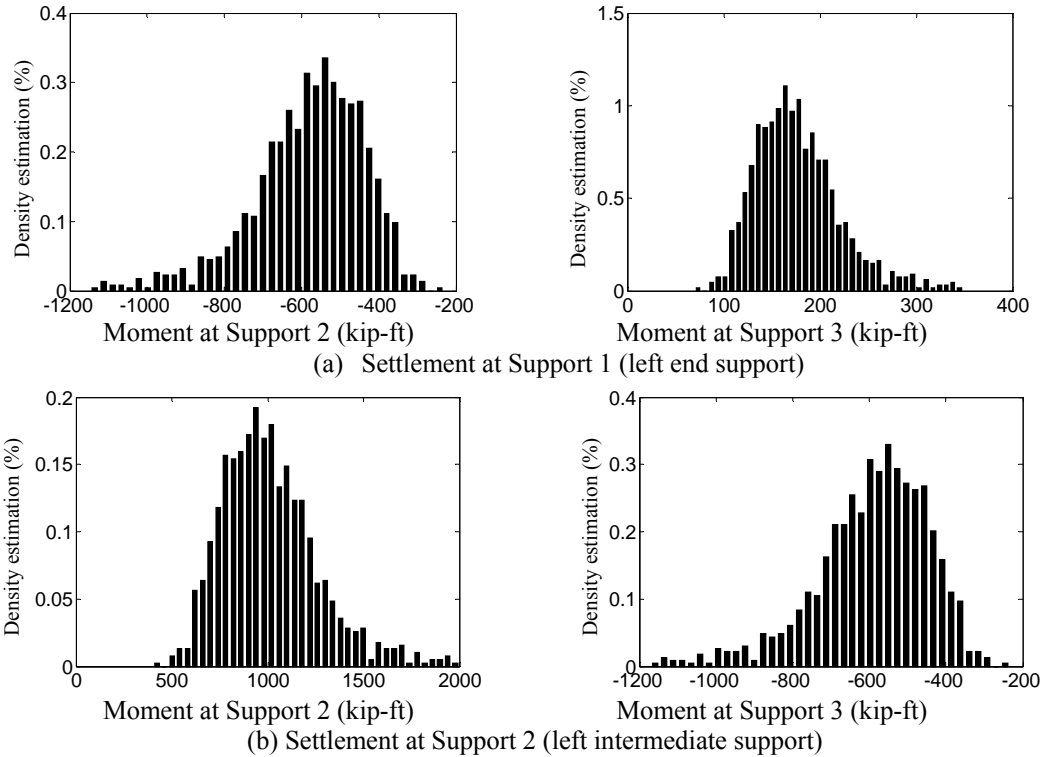


Figure 2.8 Histograms of the maximum positive and negative moments of Bridge A4058 under random support settlements: mean=1 in. and COV=0.25

2.4 Bridge Analysis with Analytical Solutions

For straight girder bridges with prismatic and nonprismatic girders, analytical solutions were derived to facilitate the determination of moment and shear forces using simple equations. Specifically, two cases were considered in this study as illustrated in Figure 2.9. In both cases, the flexural rigidity ratio and span ratio are defined by coefficients α and β , respectively.

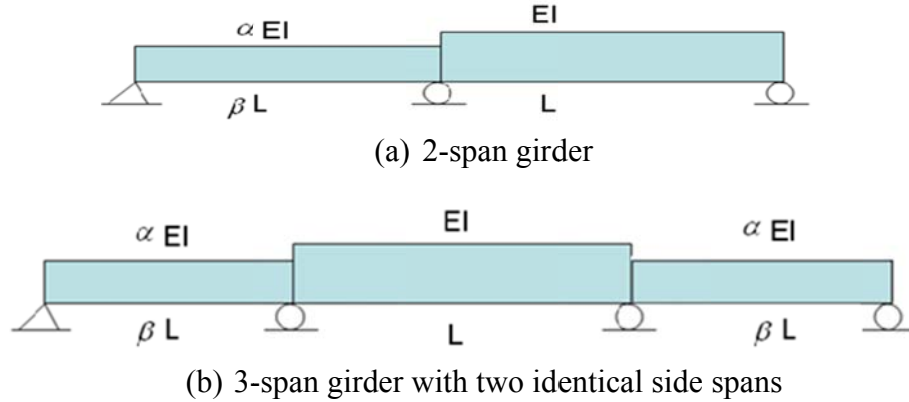


Figure 2.9 Special bridge cases

The settlement-induced moment diagram is composed of linear lines. The maximum moment, positive and negative, occurs at supports. Given the moment at all supports of a girder bridge, the moment diagram can be constructed by a linear interpolation between any two supports. The moment at each of the bridge supports as shown in Figure 2.9 can be expressed into:

$$M = C \frac{EI}{L^2} u f(\alpha, \beta) \quad (2.1)$$

in which EI is the flexural rigidity and L is the span length of the corresponding prismatic bridge girder with equal spans (equal to the longer span in 2-span and 3-span bridges as illustrated in Figure 2.9), and C represents the moment factor at different supports of the prismatic bridge girder with equal spans. In addition, u in Eq. (2.1) denotes the settlement at a support and $f(\alpha, \beta)$ is a moment modification coefficient for the girder with unequal spans as shown in Figure 2.9.

2.4.1 Prismatic girder bridge with equal spans

For a 2-span continuous girder with constant rigidity EI and equal span length L , the moments due to settlement at Supports 1 and 2 are distributed as shown in Figures 2.10(a) and 2.10(b). In this case, $f(\alpha, \beta) = 1.0$. The maximum moment (negative or positive) at the center support (Support 2 in Figure 2.2) must be determined as shown in Figure 2.11(a) and 2.11(b) for various settlements. The shear force can be derived from the moment diagram.

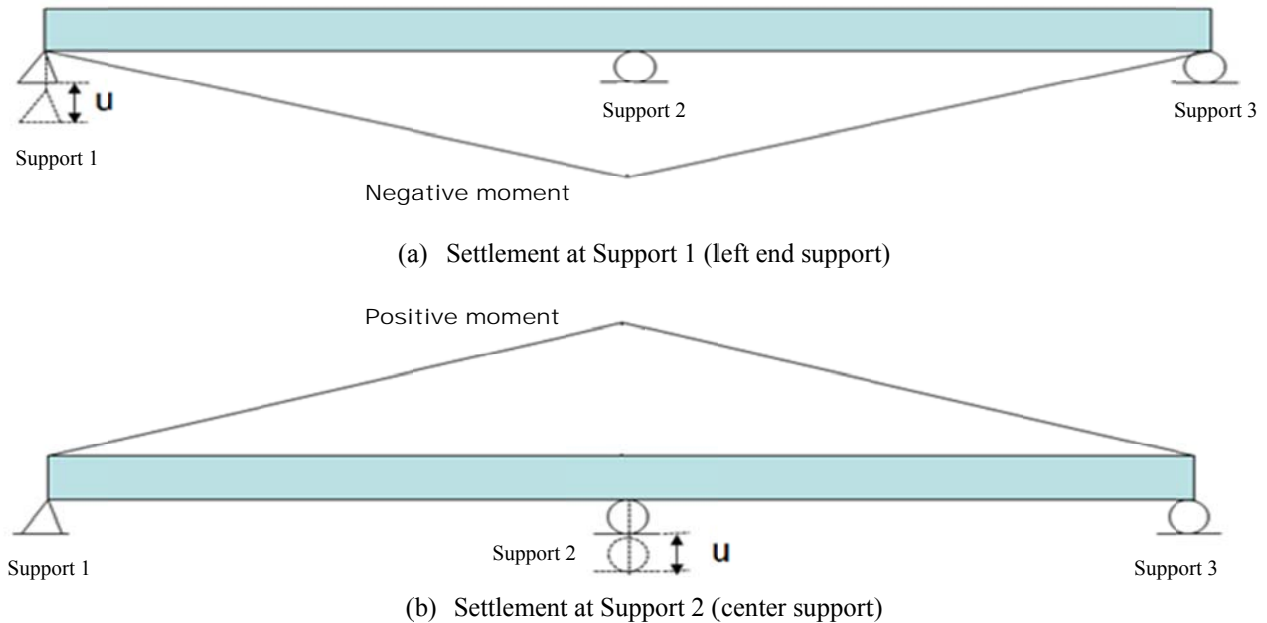


Figure 2.10 Moment distribution of a prismatic 2-span girder of equal spans

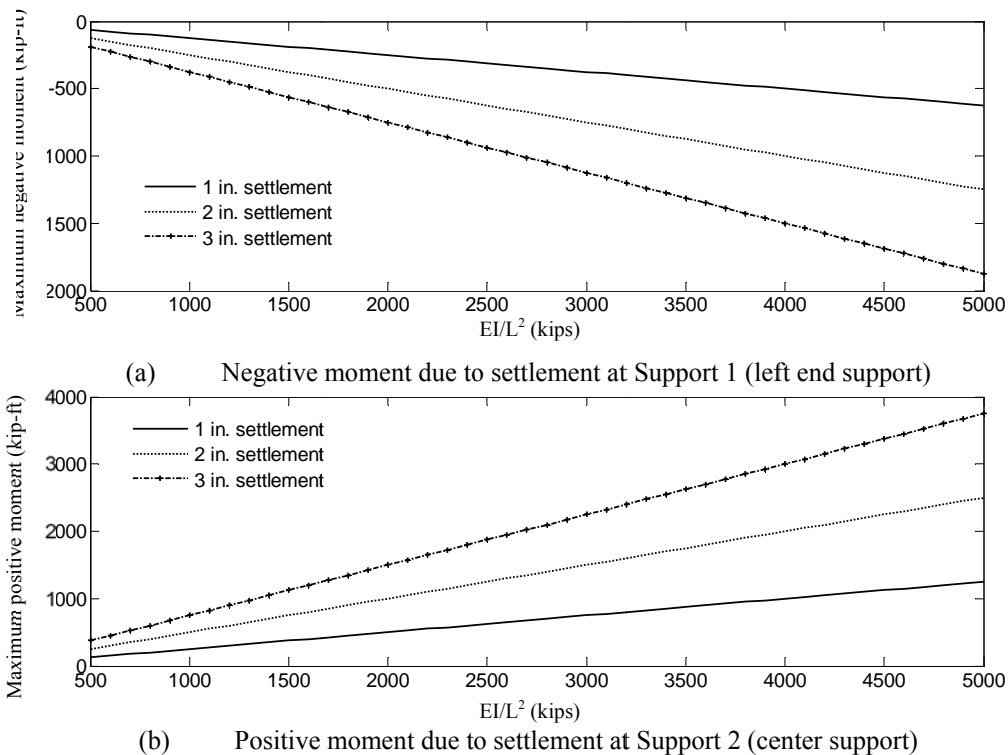


Figure 2.11 Maximum moments at Support 2 of the 2-span bridge

For verification purposes, Bridge A3101 was considered as an example. In this case, the average value of $EI/L^2 = 1,290$ kips. From Figure 2.11, the maximum positive moment is 320 kip-ft due to a 1-inch settlement at the center support, and the maximum negative moment is -160 kip-ft

due to a 1-inch settlement at the left end support, which is equal to their respective results from Method 1 using the MATLAB program.

For a 3-span continuous girder with constant rigidity EI and span length L , the moment distribution due to settlement at various supports is presented in Figures 2.12(a) and 2.12(b). In this case, both the negative and positive moments at the two intermediate supports must be determined to completely define a moment diagram. The shear force can thus be derived from the moment diagram. The moments at Supports 2 and 3 due to settlements at different supports are presented in Figures 2.13(a) and 2.13(b).

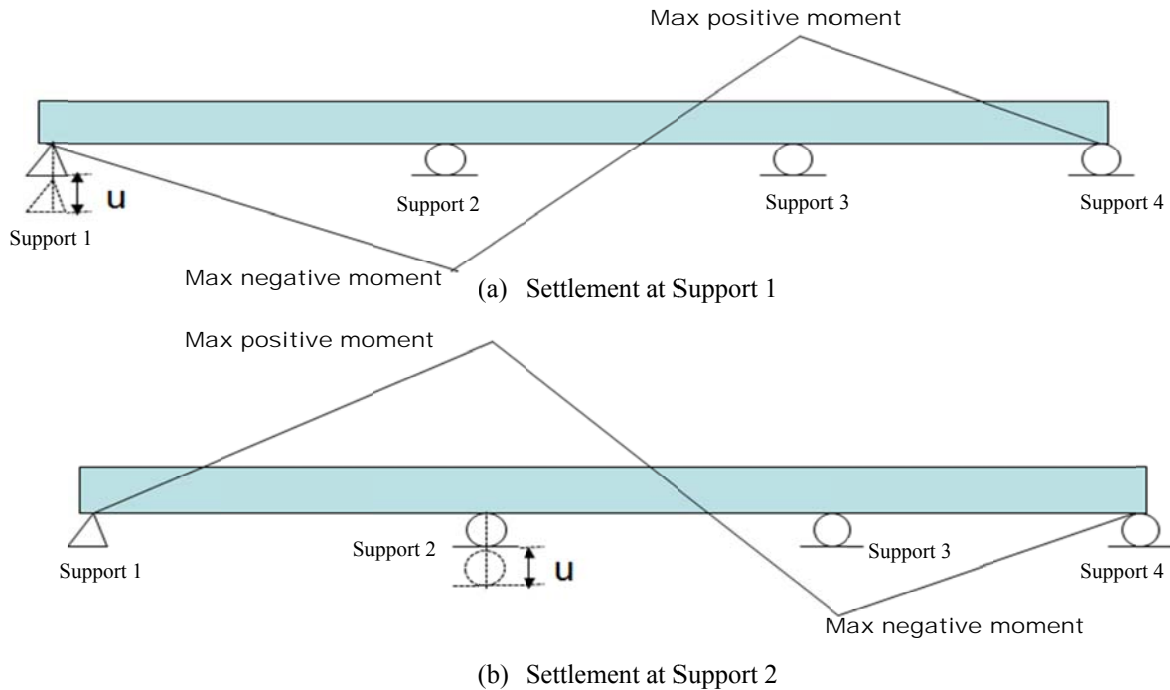


Figure 2.12 Moment diagrams of a 3-span girder

2.4.2 Non-prismatic girder bridges with unequal spans

As shown in Figure 2.9, the 2-span continuous girder bridge may have different cross sections and span lengths. These differences are represented by a moment modification coefficient $f(\alpha, \beta)$ as shown in Eq. (2.1). The modification coefficient for the 2-span continuous girder is presented in Figure 2.14(a) under an end support settlement and Figure 2.14(b) under the center support settlement. As the left span becomes stiffer by increasing its flexural rigidity and/or decreasing the span length, the moment at the intermediate support due to the left support settlement increases, corresponding to the increased reaction attracted at the left support.

To verify the analytical results, Bridge A6754 is analyzed as an example under a 1.0-inch settlement at the center support. In this case,

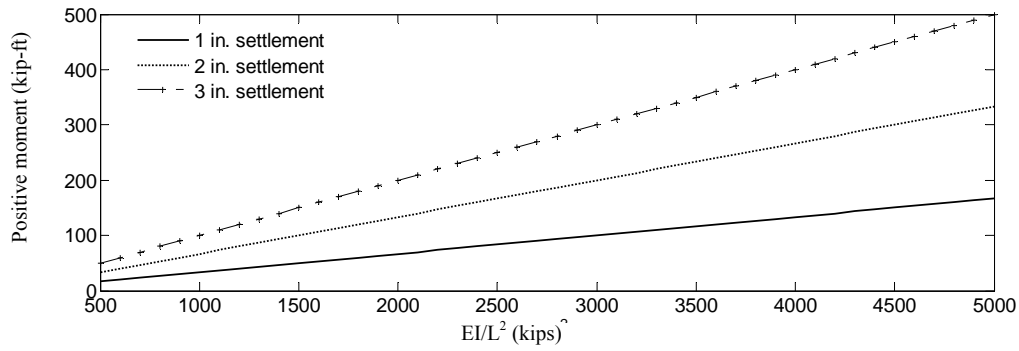
$$\alpha = 126015/132947 = 0.948$$

$$\beta = 110/142 = 0.774$$

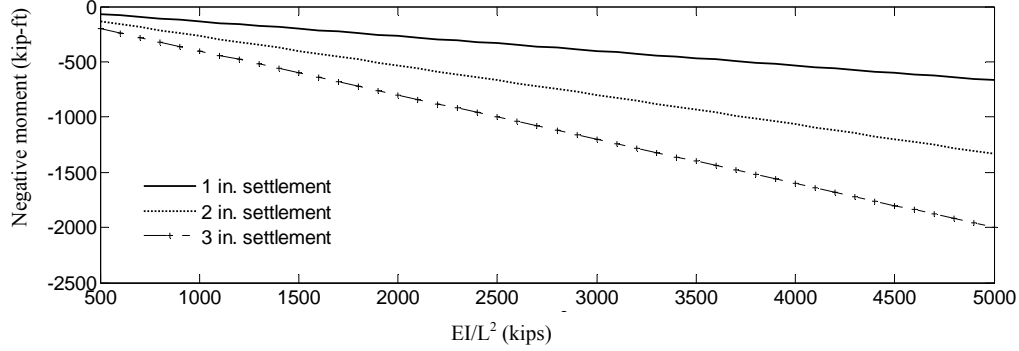
$$f(\alpha, \beta) = 1.26 \text{ from Figure 2.14(b)}$$

$$EI/L^2 = 29000 \times 132947/142^2 \times 144 = 1328 \text{ kips}$$

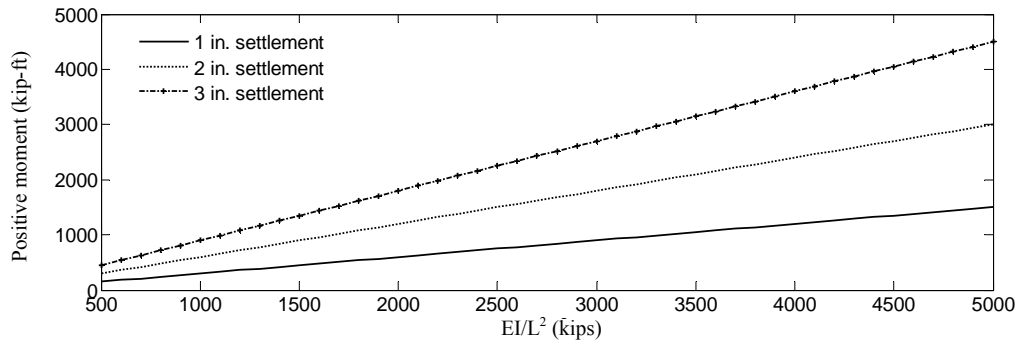
$$CEI/L^2 u = 330 \text{ kip-ft from Figure 2/11(b) for } EI/L^2 = 1328 \text{ kips.}$$



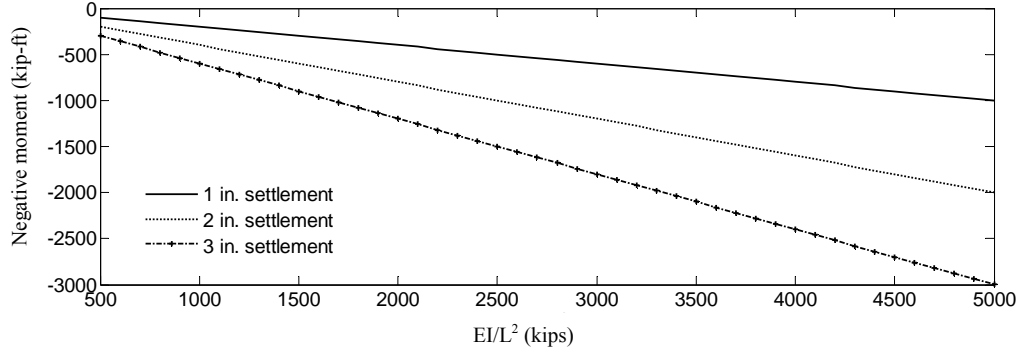
(a) Moment at Support 3 due to settlement at Support 1



(b) Moment at Support 2 due to settlement at Support 1



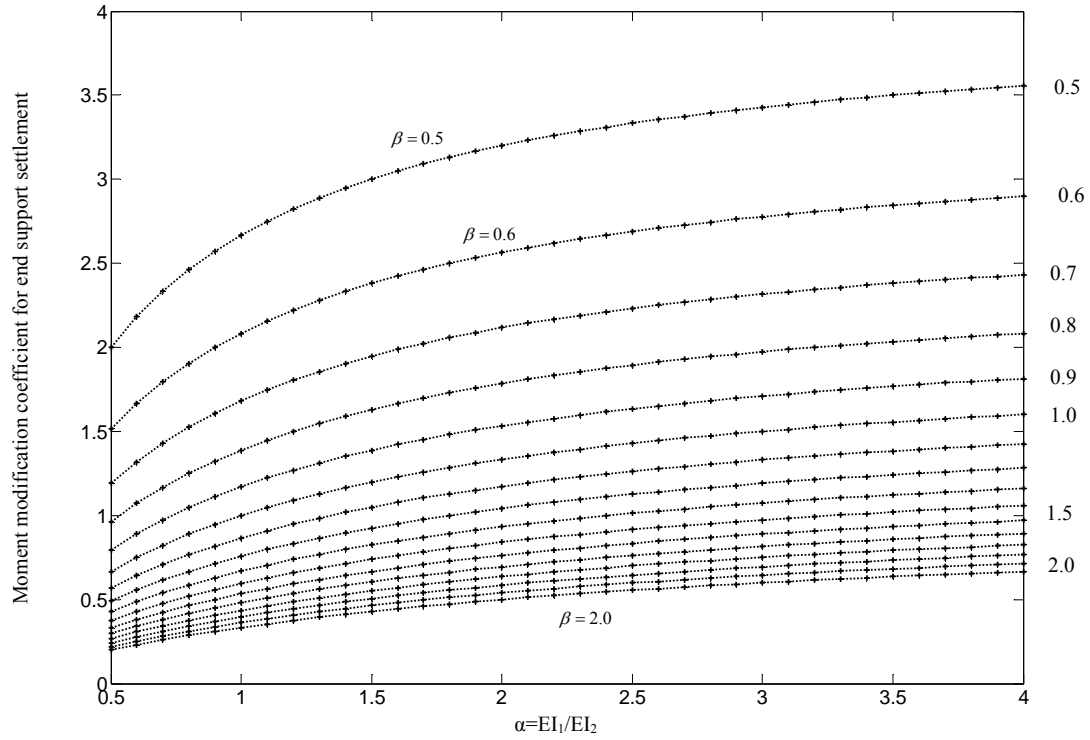
(c) Moment at Support 2 due to settlement at Support 2



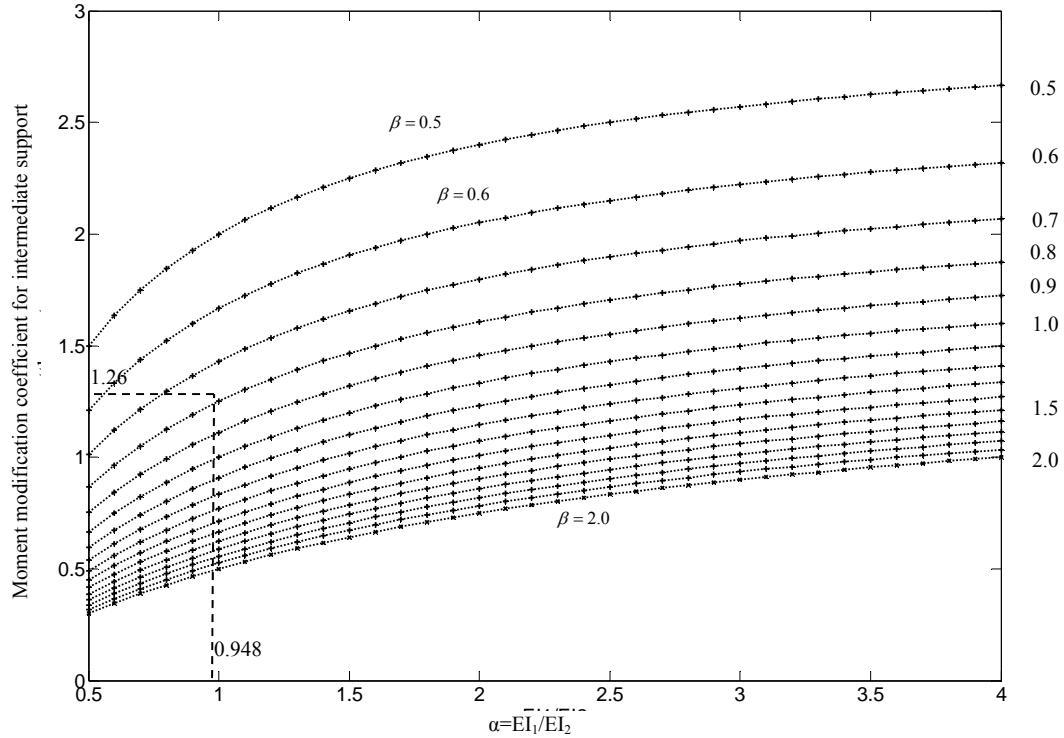
(d) Moment at Support 3 due to settlement at Support 2

Figure 2.13 Maximum positive and negative moments of a 3-span bridge

Therefore, the maximum moment of the interior girder of Bridge A6754 is $f(\alpha, \beta) \times 330 = 1.26 \times 330 = 415.8$ k-ft. This result is the same as that from the MATLAB program due to a 1-inch settlement at the center support.



(a) Due to a unit settlement at the left end support



(b) Due to a unit settlement at the intermediate support

Figure 2.14 $f(\alpha, \beta)$ for 2-span continuous girders

For the symmetric 3-span continuous girder as illustrated in Figure 2.9(b), the moment modification coefficient $f(\alpha, \beta)$ is shown in Figure 2.15 for settlement at the end support and Figure 2.16 for settlement at the intermediate support. To illustrate how to use the figures and verify the analytical results, Bridge A3386 under a 1-inch settlement at an intermediate support, Support 2, in Figure 2.11(b) is analyzed as an example. This continuous structure has three spans of 75 ft, 97 ft, and 75 ft. The moment of inertia of each interior girder is $I_1=I_3=93,366 \text{ in}^4$ and $I_2=151,300 \text{ in}^4$. For Bridge A3386,

$$\alpha = 93366/151300 = 0.617$$

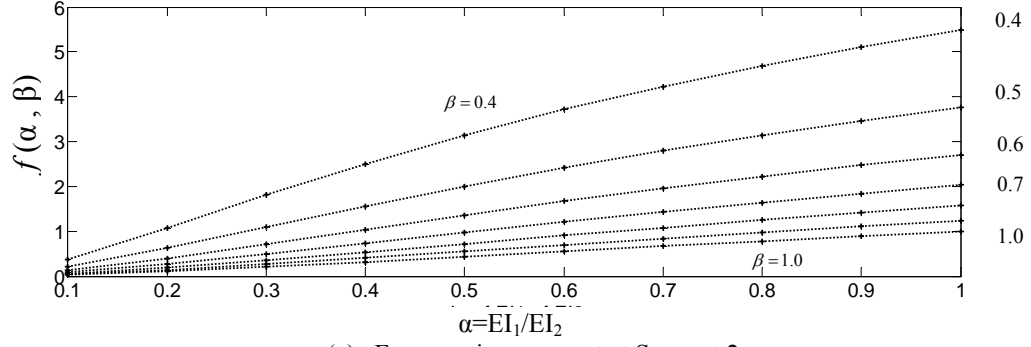
$$\beta = 75/97 = 0.773$$

$$f(\alpha, \beta) = 0.97 \text{ from Figure 2.16(a) and } 0.92 \text{ from Figure 2.16(b)}$$

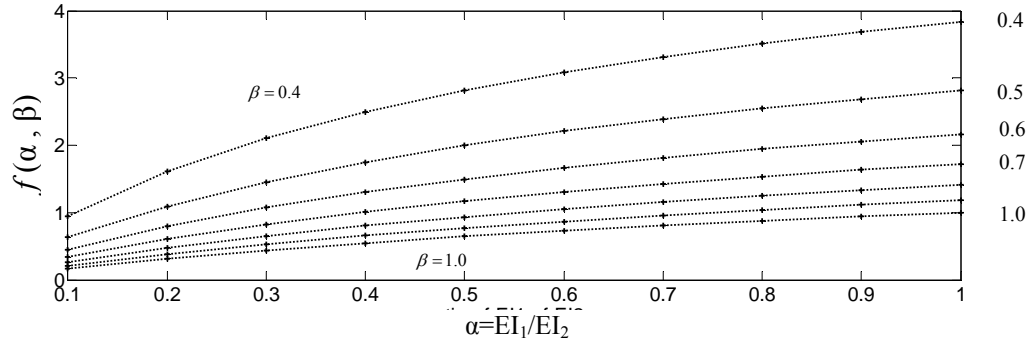
$$EI/L^2 = 29000 \times 151300 / (97^2 \times 144) = 3238 \text{ kips}$$

$$CEI/L^2 u = 972 \text{ kip-ft from Figure 2.13(c) and } -648 \text{ kip-ft from Figure 2.13(d).}$$

Therefore, the maximum positive moment and the maximum negative moment for a Bridge A3386 interior girder are $0.97 \times 972 = 943 \text{ kip-ft}$ and $0.92 \times (-648) = -596 \text{ kip-ft}$. Both agree well with the numerical results from the MATLAB program, which are 953 kip-ft and -609 kip-ft, respectively, as given in Table A.2 from Appendix A.

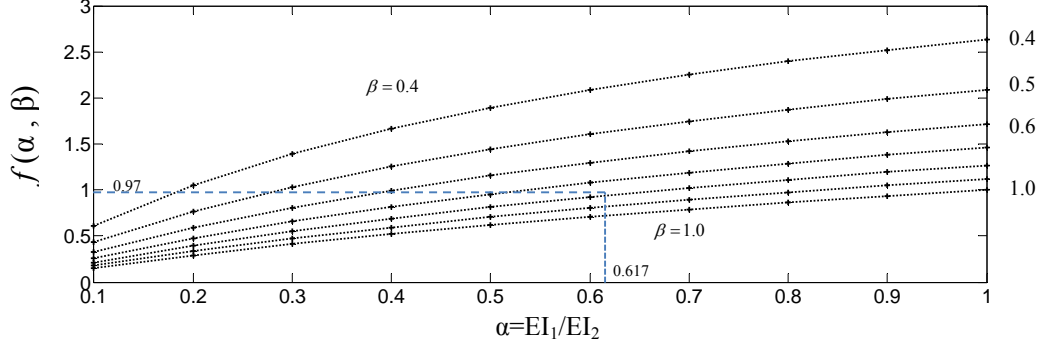


(a) For negative moment at Support 2

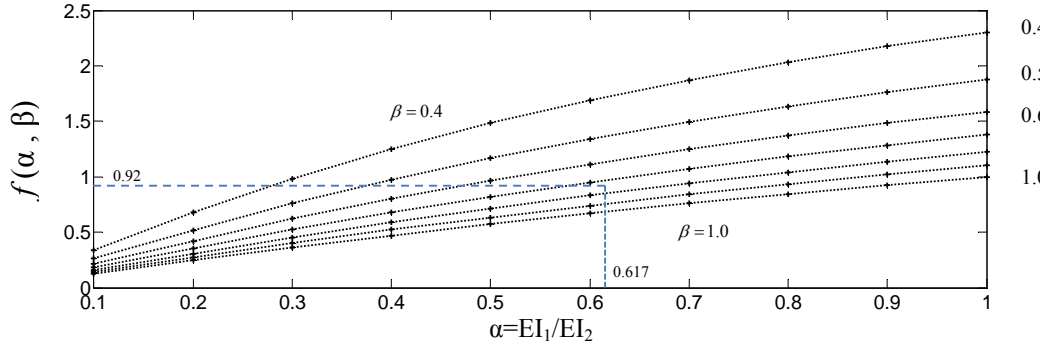


(b) For positive moment at Support 3

Figure 2.15 $f(\alpha, \beta)$ for 3-span continuous interior girders under settlement at Support 1 (left end support)



(a) For positive moment at support 2



(b) For negative moment at support 3

Figure 2.16 $f(\alpha, \beta)$ for 3-span continuous interior girders under settlement at Support 2 (left intermediate support)

2.5 Bridge Analysis with ANSYS Probabilistic Design Software

ANSYS has implemented a probabilistic design procedure for component or system analyses involving uncertain structural properties and/or external loads. The input parameters such as geometry, material property, and boundary condition are defined in the ANSYS computer model. The variations of these input parameters are defined as random input variables and are characterized by their distribution type with given mean and standard deviation, such as Gaussian and lognormal. Any interdependencies between random input variables can also be defined in the software by their correlation coefficients. The results are defined as random output parameters. During a probabilistic analysis, ANSYS computes the random output parameters as a function of the set of random input variables. The values for the input variables can be generated either randomly by Monte Carlo simulations or as prescribed samples by Response Surface methods.

In this study, only the support settlement as part of the external loads was treated as a random variable and all structural properties were considered in a deterministic fashion. Three curved bridges (A3848, A6477, and A6723) were analyzed with the ANSYS probabilistic design software. The models of these bridges are shown in Figure 2.17. The mean values of the maximum positive and negative moments of interior girders are summarized in Table 2.2 for three bridges under a random settlement of 1.0-inch mean and a COV of 0.25 at the left intermediate (second) support. The detailed probabilistic results of these bridges are reported in Appendix D.

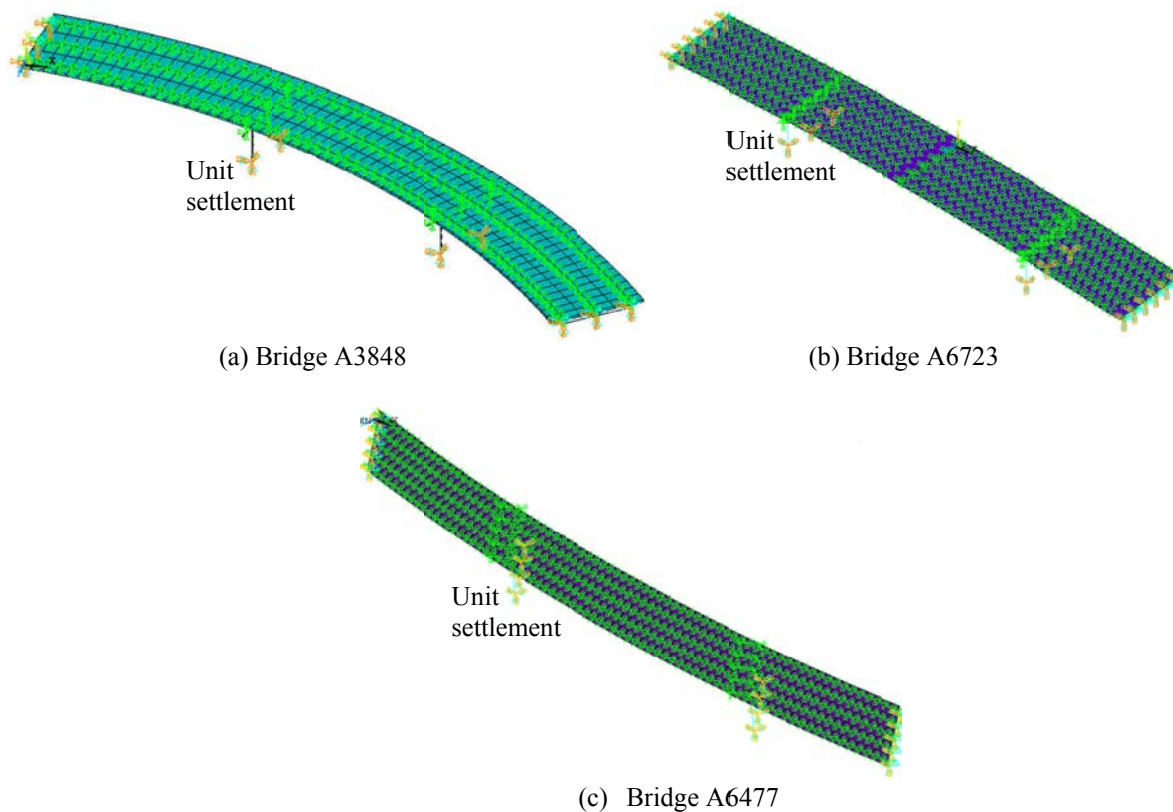


Figure 2.17 Models of curved bridges with ANSYS

Table 2.2 Means of maximum positive and negative moments in interior girders

Bridge No.	Girder No.	Maximum Positive Moment (kip-ft)	Maximum Negative Moment (kip-ft)
A3848	Interior girder	44.6	-30.6
A6723	Interior girder No.3	6.8	-4.9
A6477	Interior girder No.3	41.6	-16.6

2.6 Analysis with New Steel-Girder Bridges

As the public demands on roadways and structures, design specifications, and construction material availabilities change, the selection of the type of bridges and the use of construction materials may change significantly over time. In addition to existing bridges, the potential impacts of support settlement on superstructure and substructure are also evaluated on new bridges in this study. For this purpose, 31 steel girder bridges were designed based on the minimum strength and serviceability requirements. All of them have the same cross section configuration as illustrated in Figure 2.18. Although the exterior girder of an existing girder bridge is in general slightly smaller than the interior girder, all girders in the new bridges are considered to be identical. The number of spans and the span length of each bridge are detailed in Table 2.3. As presented in Figure 2.19, the minimum moment of inertia for each bridge was selected mainly based on the minimum plastic moment and deflection requirements ($L/800$). Note that the strength-required moment of inertia is governed by the larger effect of the positive and negative moments. The locally irregular changes of the strength-required moment curves in Figure 2.19 are due to switch of the magnitudes of the positive and negative moment effects. For all new bridges, the maximum moment, shear force and support reaction due to a unit settlement were analyzed using the MATLAB program. The critical forces and moments of the 31 bridges are reported in Appendix E.

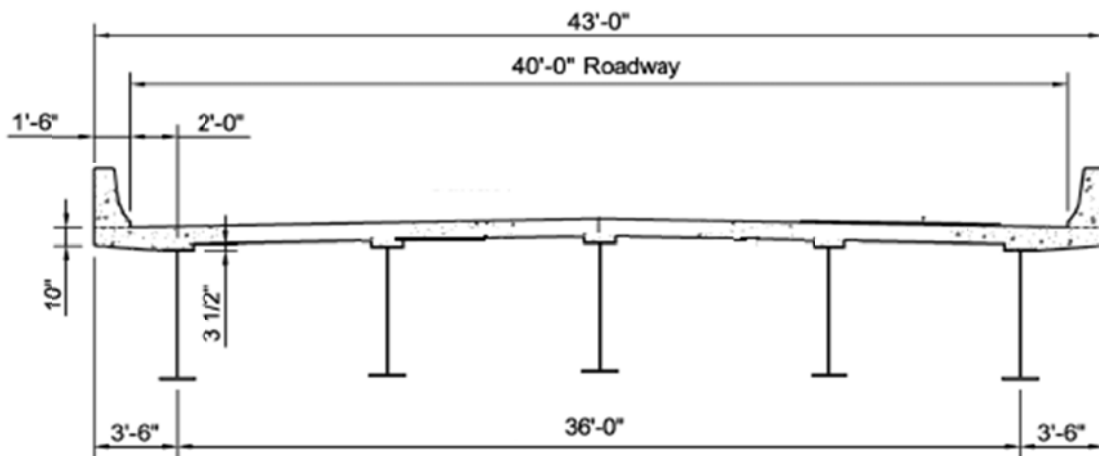
**Figure 2.18 Cross section of new girder bridges**

Table 2.3 Summary of new designs of girder bridges with equal spans

Bridge Index	Span Length (ft)			
	Span 1	Span 2	Span 3	Span 4
1	20	20		
2	30	30		
3	40	40		
4	50	50		
5	60	60		
6	70	70		
7	80	80		
8	90	90		
9	100	100		
10	110	110		
11	120	120		
12	20	20	20	
13	30	30	30	
14	40	40	40	
15	50	50	50	
16	60	60	60	
17	70	70	70	
18	80	80	80	
19	90	90	90	
20	100	100	100	
21	110	110	110	
22	120	120	120	
23	20	20	20	20
24	30	30	30	30
25	40	40	40	40
26	50	50	50	50
27	60	60	60	60
28	70	70	70	70
29	80	80	80	80
30	90	90	90	90
31	100	100	100	100

2.7 Settlement Effect on Overall Design Loads

To put settlement effects in the perspective of overall design loads, except for the missing NBI number, new design, 5-span, and curved bridges, 14 out of 20 bridges in Table 2.1 were analyzed under dead plus live loads. For clarity, these continuous structures are also reproduced in Table 2.4, including 6 steel-girder bridges, 5 prestressed concrete-girder bridges, and 3 slab concrete bridges. The moment and shear ratios between two cases, with and without settlement effects, are presented in Figures 2.20(a) and 2.20(b), respectively. It can be observed from Table 2.4 and Figure 2.20 that the settlement effect changes significantly, depending on the minimum span length and the span ratio of the bridges. For bridges of a minimum span length less than 40 ft, such as Bridge Nos. 5, 7, 8, 11, 12, and 13, the settlement effect is in general dominant, particularly in combination with a span ratio of less than 0.6, such as Bridge Nos. 7, 8, and 11.

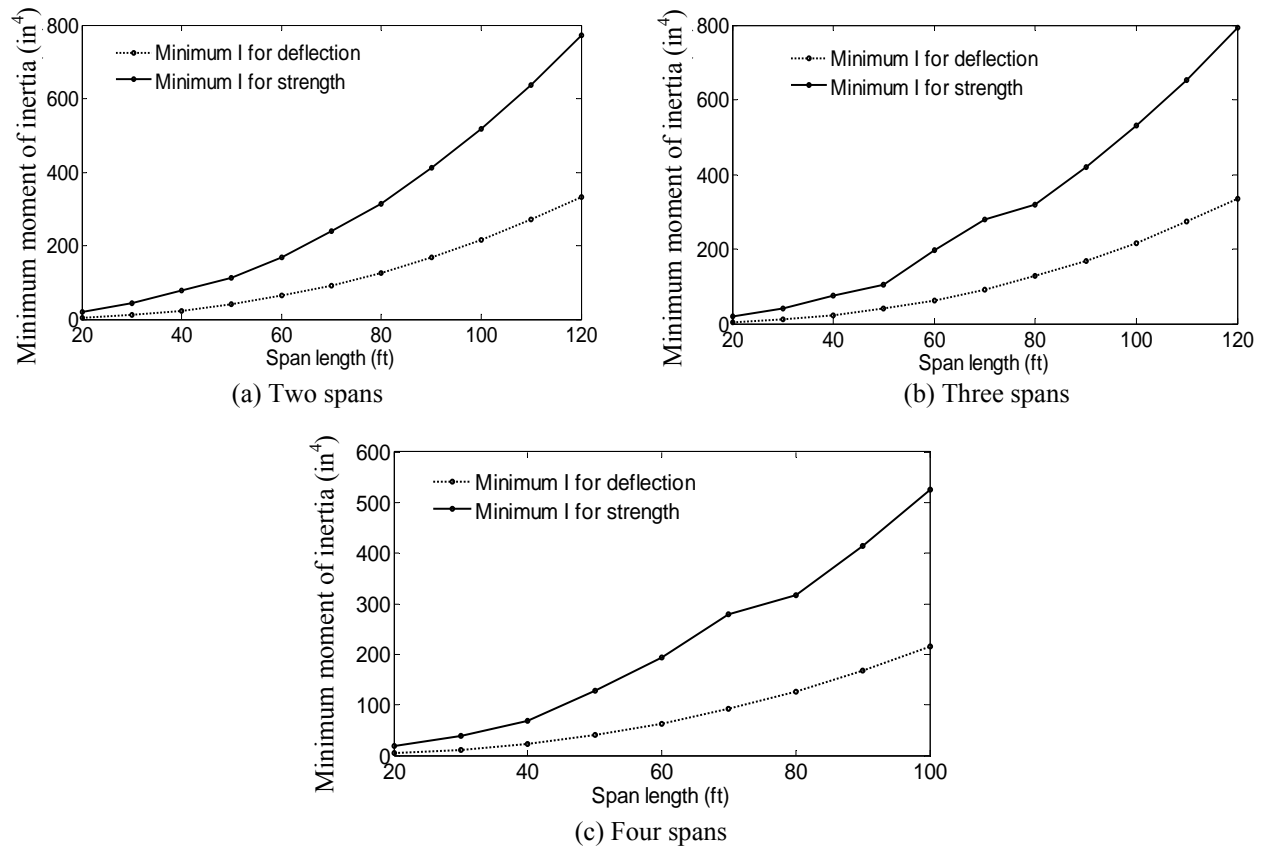
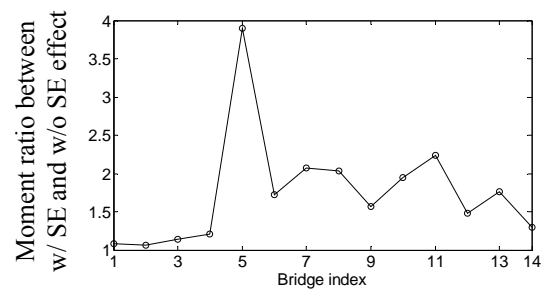


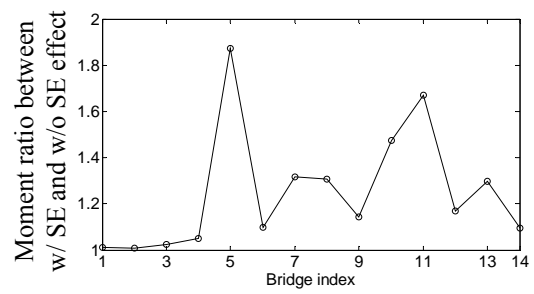
Figure 2.19 Minimum moments of inertia for new bridges

Table 2.4 Bridges analyzed under gravity loads

Bridge Index	Bridge No.		Description	Min Span Length (ft)	Max Span Length (ft)	Allowable Settlement 0.004L (in)
	NBI	MoDOT				
1	2664	A3101	Steel	120	120	5.76
2	3945	A4840	Steel	138	141	6.62
3	31500	A7300	Steel	64.8	64.8	3.11
4	2852	A3386	Steel	75	97	3.60
5	3475	A4256	Steel	19.5	26	0.94
6	4043	A4999	Steel	54	119	2.60
7	3332	A4058	Prestressed	37	65	1.78
8	11893	A5161	Prestressed	38	65	1.82
9	29023	A6569	Prestressed	65	100	3.12
10	3276	A3973	Prestressed	43	59	2.06
11	3753	A4582	Prestressed	38	65	1.82
12	2983	A3562	Slab	34	46	1.63
13	28993	A6450	Slab	18	23	0.86
14	2856	A3390	Slab	48	60	2.30



(a) Moment ratio



(b) Shear ratio

Figure 2.20 Moment and shear ratios between two cases: with and without settlement effects

3 STATISTICAL PROPERTIES OF LOADS AND RESISTANCES

3.1 Statistical Parameters for Dead Load

Dead load mainly represents the weights of structural and nonstructural elements that are permanently attached to bridges. It is often considered to be uniformly distributed along the length of each member. In this study, three components of bridge dead loads are considered: prefabricated members (steel and precast concrete), cast-in-place concrete members, and wearing surfaces (Nowak, 1999).

The mean and standard deviation of a dead load variable were estimated from the bias factor and the coefficient of variation (COV) listed in Table 3.1. The mean of the dead load is defined as the product of its nominal value and the bias factor. The standard deviation is defined as the product of the mean and COV values. They can be expressed into:

$$\mu_D = D_n \times \lambda_D \quad (3.1)$$

$$\sigma_D = \mu_D \times COV_D \quad (3.2)$$

in which μ_D and D_n represent the mean and nominal values, λ_D is the bias factor, σ_D is the standard deviation, and COV_D is the coefficient of variation of the dead load.

Table 3.1 Statistical values of dead load (Nowak, 1999)

Component	Bias Factor	COV	Distribution
Prefabricated members	1.03	0.08	Normal distribution
Cast-in-place members	1.05	0.10	
Wearing surfaces	1.00	0.25	

3.2 Statistical Parameters for Live Load

In bridge designs, live load basically means the weight of vehicles plus their impact effect. Vehicles move and provide temporary loads on bridges. The daily maximum value of a live load can be assumed to follow the extreme value distribution. In the recent study by Kwon et al. (2010), the Gumbel Type I distribution was adopted to represent the maximum daily load effect (Gumbel, 1958). Due to limited weigh-in-motion data over a short period of time in comparison with a bridge design life of 75 years, it is necessary to project the short-term field observations for a long-term prediction of the 75-year maximum load effect using the extreme value theory. The Gumbel Type I probability distribution function, $F_{X-1day}(x)$, and the probability density function, $f_{X-1day}(x)$, of the daily maximum load effect can be expressed into (Ang and Tang, 1975; 1984):

$$F_{X-1day}(x) = \exp(-\exp(-\frac{x-u}{\alpha})) \quad (3.3)$$

$$f_{X-1day}(x) = \frac{1}{\alpha} \exp(-\frac{x-u}{\alpha}) F_{X-1day}(x) \quad (3.4)$$

in which the scale parameter (α) and the location parameter (u) can be determined by the maximum likelihood estimation to fit the distribution model into the available observed data.

Note that α used here is different from that used in the moment modification coefficient $f(\alpha, \beta)$. Assuming that the maximum daily load effects are independent over 75 years, the probability distribution function of the 75-year maximum load effect can be projected by

$$F_{X-75years}(x) = \left[\exp\left(-\exp\left(-\frac{x-u}{\alpha}\right)\right) \right]^N = \exp\left\{-\exp\left(-\frac{x-u_n}{\alpha_n}\right)\right\} \quad (3.5)$$

where N is the number of days during 75 years. The scale parameter of $F_{X-75years}(x)$, α_n is the same as that of $F_{X-1day}(x)$, and the location parameter of $F_{X-75years}(x)$, u_n is equal to $u + \alpha \ln(N)$ (Ang and Tang, 1984). The daily and 75-year maximum moment for the interior girder of NBI Bridge No.11877 are illustrated in Figure 3.1 and Figure 3.2 (Kwon et al., 2010).

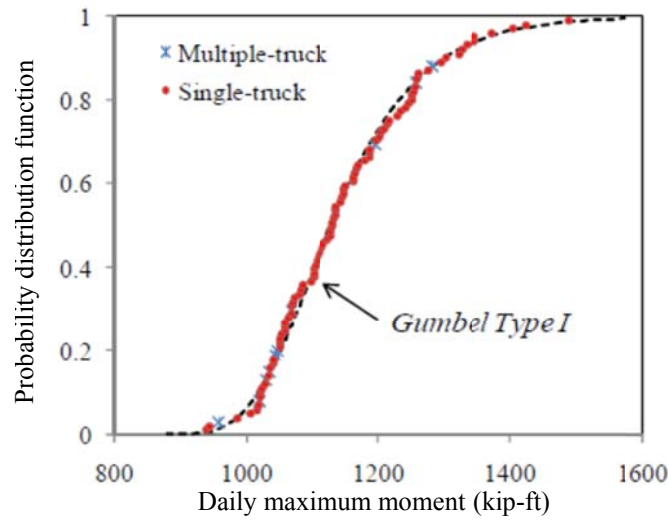


Figure 3.1 Daily maximum moment fitted into Gumbel Type I distribution

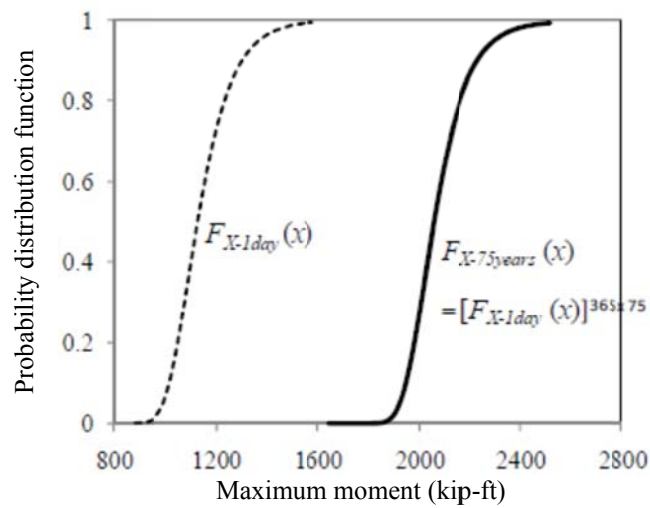


Figure 3.2 Comparison between daily and 75-year maximum moment

The mean value and standard deviation of the maximum live load effect in 75 years can be estimated by

$$\mu_L = u_n + \gamma \times \alpha_n \quad (3.6)$$

$$\sigma_L = \sqrt{\frac{\pi^2 \alpha_n^2}{6}} \quad (3.7)$$

in which μ_L and σ_L represent the mean value and standard deviation of the live load, α_n and u_n are the scale and location parameters of Gumbel Type I distribution for the 75-year maximum live load, and $\gamma=0.577216$ is the Euler number.

3.3 Statistical Parameters of Resistance

The statistical distribution of resistance is based on the uncertainties in material (strength, modulus of elasticity, etc), fabrication (geometry), and analysis (accuracy of analysis equations). The resistance R can thus be expressed into its nominal value R_n multiplied by three random factors: M for material properties, F for fabrication outcomes, and P for professional analyses (Nowak et al., 1994). That is,

$$R = R_n MFP \quad (3.8)$$

Since the three factors are associated with three independent processes in the creation of a bridge structure, they can be assumed to be statistically independent. In this case, the COV of the overall resistance can be determined by the square root of the sum of the squared COV values of individual factors provided they are small. That is,

$$COV_R = \left(COV_M^2 + COV_F^2 + COV_P^2 \right)^{1/2} \quad (3.9)$$

The statistical distribution of the resistance R can be characterized by a bias factor λ_R and the COV_R . The bias factor is the ratio of the mean to the nominal design value. The COV_R is the ratio of the standard deviation to the mean of resistance, giving an indication of uncertainty.

In order to determine the statistical distribution of resistance, Kwon et al. (2010) recently analyzed 100 sample bridges (14 reinforced concrete girder and slab, 58 prestressed girder, and 28 steel girder) from MoDOT's bridge inventory to determine the strength of representative bridges according to the 2007 AASHTO LRFD bridge design specifications. For each type of bridge, both material and geometry variations of structural members were taken into account in the determination of resistance distribution by Monte Carlo simulations. The effect of the professional analyses uncertainty is included in Eq. (3.8) and Eq. (3.9) after the Monte Carlo analysis. Based on Kwon et al. (2010), the moment statistical parameters were updated to reflect the bridge samples in MoDOT's inventory. They are presented in Table 3.2.

Table 3.2 Statistical parameters of resistance

Type of Structure	Moment (Nowak, 1999)		Shear Force (Nowak, 1999)		Moment (Kwon et al., 2010)		Distribution
	Bias	COV	Bias	COV	Bias	COV	
Steel girder	1.12	0.100	1.14	0.105	1.23	0.081	Lognormal
Concrete slab	1.14	0.130	1.20	0.156	1.17	0.090	
Prestressed concrete girder	1.05	0.075	1.15	0.140	1.055	0.069	

The mean value and standard deviation of resistance can then be determined using the bias factor and COV value like Eqs. (3.1) and (3.2):

$$\mu_R = R_n \times \lambda_R \quad (3.10)$$

$$\sigma_R = \mu_R \times COV_R \quad (3.11)$$

in which μ_R and σ_R are the mean value and standard deviation of resistance, R_n and λ_R are the nominal value and bias factor of resistance, and COV_R is the coefficient of variation of resistance.

3.4 Statistical Parameters of Settlement Effects

In Section 2, the mean and COV values of a differential settlement are assumed not to exceed $L/250$ for continuous girder bridges and to be 0.25, respectively. The mean value of settlement effects such as moment, shear, and support reaction is proportional to the mean value of the differential settlement. Therefore, the mean values of the settlement effects due to any differential settlement are equal to their mean values due to a 1-inch differential settlement, as given in Appendices A-C and E, multiplied by the differential settlement. In addition, the mean values of the effects of any differential settlements can be calculated with the MATLAB program or the Analytical Method developed in Section 2, using the Monte Carlo method.

Section 2 indicates that the settlement-induced moment, shear, and support reaction of girder bridges statistically follow the lognormal distribution. The mean value and standard deviation of settlement effects can be expressed into:

$$\mu_{SE} = u \times \mu_{SE=1"} \quad (3.12)$$

$$\sigma_{SE} = \mu_{SE} \times COV_{SE} \quad (3.13)$$

in which μ_{SE} and σ_{SE} are the mean value and standard deviation of the effect of a differential settlement, u represents the mean of the differential settlement, $\mu_{SE=1"}$ denotes the mean value of the effect due to a 1-inch differential settlement, and COV_{SE} ($= 0.25$ from Section 2) represents the coefficient of variation of the settlement effect.

To verify the distribution and COV value of the settlement effects, Bridges A3101 and A4058 were analyzed with the MATLAB program. For Bridge A3101, the moment distribution numerically calculated and the exact lognormal distribution with a COV of 0.25 are compared in Figure 3.3(a) and Figure 3.3(b) for a unit settlement at Supports 1 and 2 (left end and center supports), respectively. Similarly, they are compared in Figure 3.4(a) and Figure 3.4(b) for Bridge A4058 when Supports 1 and 2 experience a unit settlement. Figures 3.3 and 3.4 indicate that the moment distribution follows the lognormal distribution with a COV of 0.25 for two-span and three-span continuous girder bridges. Note that the notions of support designations are referred to Figures 2.2.

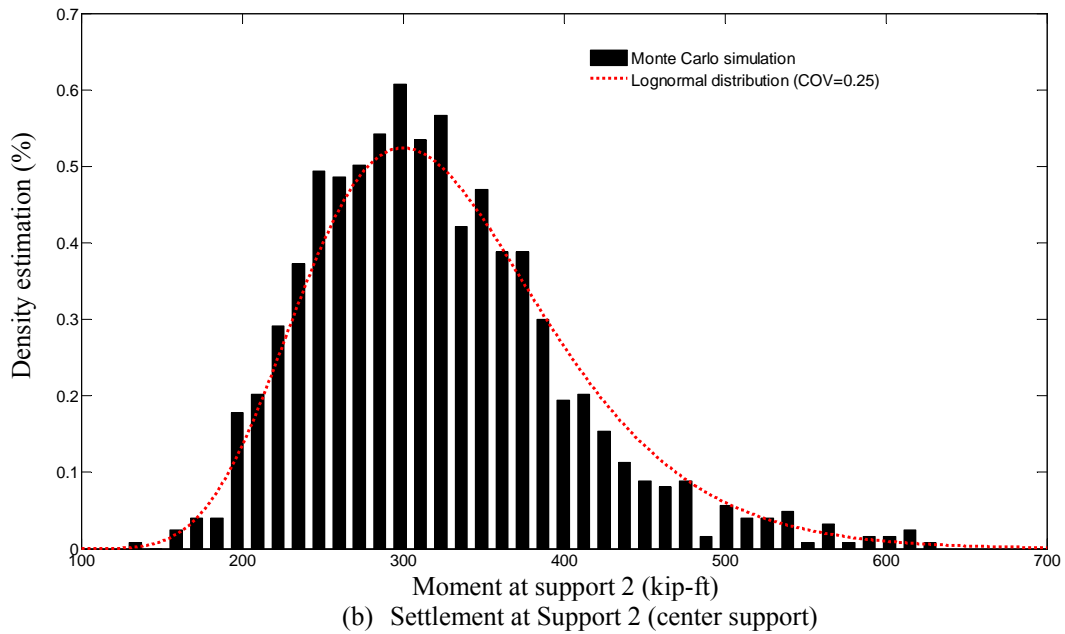
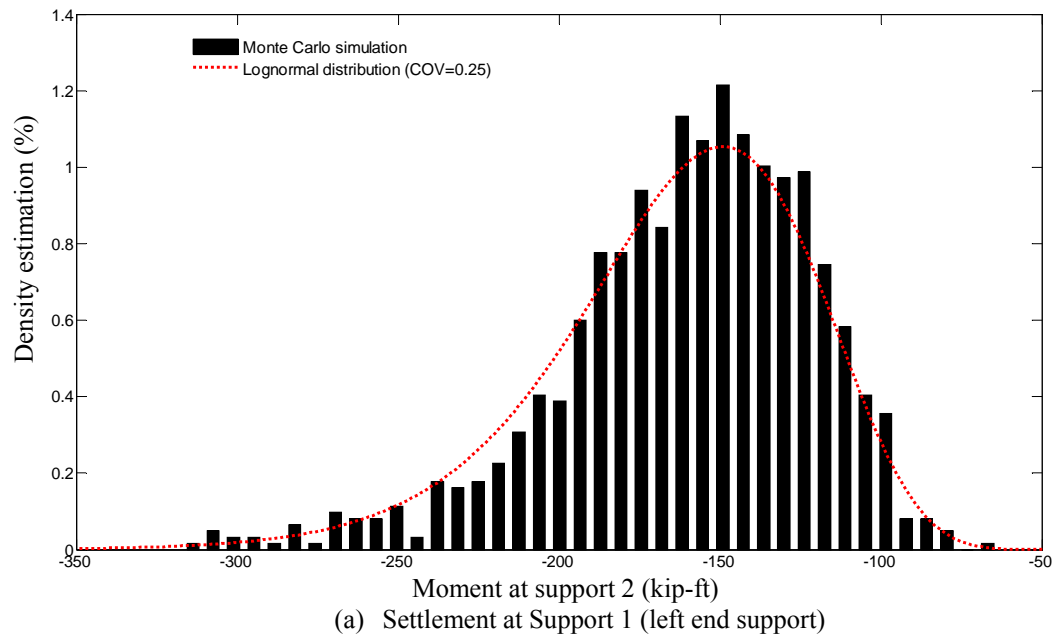


Figure 3.3 Comparison of maximum positive and negative moment distributions of Bridge A3101: mean=1 in., COV=0.25

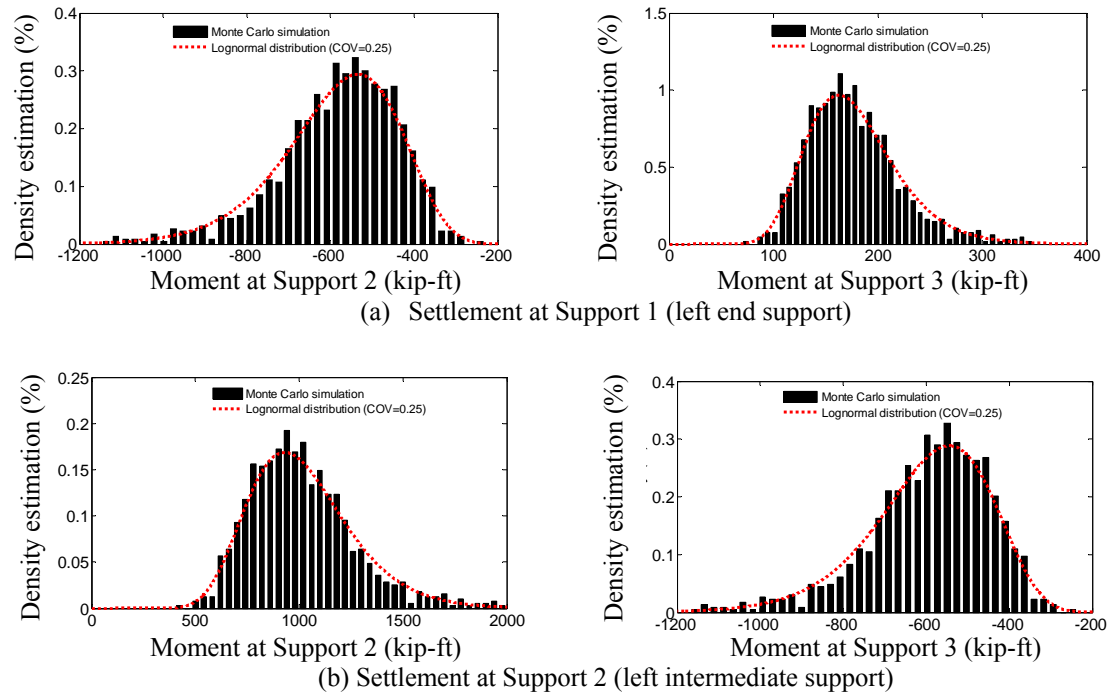


Figure 3.4 Comparison of maximum positive and negative moment distributions of Bridge A4058 due to settlements: mean=1 in., COV=0.25

4 RELIABILITY ANALYSIS WITH SETTLEMENT EFFECTS

4.1 Reliability Theory

The reliability indices of bridges will be evaluated based on the uncertainties in live load, dead load, settlement effect, and resistance. Minimum resistance is considered for new bridges; it represents the minimum design strength required to meet design specifications. The use of the minimum resistance is to avoid any unintended contribution from overdesign. For existing bridges, the actual resistance based on as-built drawings is considered to the extent practical.

In this study, the reliability indices are calculated using the First Order Reliability Method (FORM) (Der Kiureghian, 2005; Choi et al., 2006). To this end, a safety margin function g is defined as the difference of the resistance and the total load effect, which can be expressed into:

$$g = R - (DL + LL + SE) \quad (4.1)$$

where R , DL , LL , and SE are resistance, dead load effect, live load effect, and settlement effect, respectively. In the FORM, the safety margin function is represented by the first-order Taylor series expansion at the mean value point. For simplicity, let $\mathbf{X} = \{X_1, X_2, X_3, X_4\}^T$ in which $X_1=R$, $X_2=DL$, $X_3=LL$, and $X_4=SE$. Assume that the four variables are statistically independent. In general, n random variables are considered ($n=4$ in this study). The approximate safety margin function around the mean value is then written into:

$$\tilde{g}(\mathbf{X}) \approx g(\mu_X) + \nabla g(\mu_X)^T (X_i - \mu_{X_i}) \quad (4.2)$$

where $\mu_X = \{\mu_{X_1} \ \mu_{X_2} \ \dots \ \mu_{X_n}\}^T$ and $\nabla g(\mu_X)$ is the gradient of g evaluated at μ_X or

$$\nabla g(\mu_X) = \left\{ \frac{\partial g(\mu_X)}{\partial x_1} \ \frac{\partial g(\mu_X)}{\partial x_2} \ \dots \ \frac{\partial g(\mu_X)}{\partial x_n} \right\}^T.$$

The mean value and standard deviation of the approximate safety margin function $\tilde{g}(\mathbf{X})$ are:

$$\mu_{\tilde{g}} = E[g(\mathbf{X})] = g(\mu_X) \quad (4.3)$$

$$\sigma_{\tilde{g}} = \left[\sum_{i=1}^n \left(\frac{\partial g(\mu_X)}{\partial x_i} \right)^2 \sigma_{x_i}^2 \right]^{\frac{1}{2}} \quad (4.4)$$

The reliability index β is computed as:

$$\beta = \frac{\mu_{\tilde{g}}}{\sigma_{\tilde{g}}} \quad (4.5)$$

which in general is related to the inverse of the coefficient of variation of the safety margin function. However, the random variables in the safety margin function follow different probability distributions. In the case of a non-Gaussian distribution, the reliability index is iteratively estimated using the following FORM procedure:

- (1) Define the safety margin function with n number of random variables.

$$g(\mathbf{X}) = g(\{x_1 \ x_2 \ \dots \ x_n\}^T) \quad (4.6)$$

- (2) Assume a design point, starting with the mean value of \mathbf{X} .

$$\mathbf{X}^* = \{x_1^* \ x_2^* \ \dots \ x_n^*\}^T \quad (4.7)$$

(3) Transform the probability distribution function of each random variable into the normalized, standard variables corresponding to the design point.

$$u_i^* = \Phi^{-1}[F_{x_i}(x_i^*)] \quad (4.8)$$

in which $F_{x_i}(x_i)$ is the marginal probability distribution function of a random variable x_i , $\Phi^{-1}[\cdot]$ represents the inverse of the standard normal distribution function of the variable in the square bracket. The vector of the transformed random variables can be expressed into:

$$\mathbf{U}^* = \{u_1^* \ u_2^* \dots \ u_n^*\}^T \quad (4.9)$$

(4) Compute the equivalent means and standard deviations of the approximate normal distributions. Since the transformation is given by:

$$u_i = \Phi^{-1}[F_{x_i}(x_i)] \quad (4.10)$$

one way to get the equivalent normal distribution is to use the Taylor series expansion of the transformation at the design point \mathbf{X}^* . That is,

$$u_i = \Phi^{-1}[F_{x_i}(x_i^*)] + \frac{\partial}{\partial x_i}(\Phi^{-1}[F_{x_i}(x_i)]) \Big|_{x_i^*} (x_i - x_i^*) \quad (4.11)$$

$$\frac{\partial}{\partial x_i} \Phi^{-1}[F_{x_i}(x_i)] = \frac{f_{x_i}(x_i)}{\phi(\Phi^{-1}[F_{x_i}(x_i)])} \quad (4.12)$$

Therefore,

$$u_i = \frac{x_i - [x_i^* - \Phi^{-1}[F_{x_i}(x_i^*)]]\phi(\Phi^{-1}[F_{x_i}(x_i^*)])/f_{x_i}(x_i^*)}{\phi(\Phi^{-1}[F_{x_i}(x_i^*)])/f_{x_i}(x_i^*)} \quad (4.13)$$

which can be written as:

$$u_i = \frac{x_i - \mu_{x_i'}}{\sigma_{x_i'}} \quad (4.14)$$

in which $\sigma_{x_i'} = \frac{\phi(\Phi^{-1}[F_{x_i}(x_i^*)])}{f_{x_i}(x_i^*)}$ and $\mu_{x_i'} = x_i^* - \Phi^{-1}[F_{x_i}(x_i^*)]\sigma_{x_i'}$ are the equivalent mean and

standard deviation of the random variable x_i , $\phi(\cdot)$ is the probability density function of a standard normal variable u_i , and $f_{x_i}(x_i)$ is the probability density function of a random variable x_i . In Step (4), the non-Gaussian distribution of the random variable is transformed into a standard Gaussian distribution space.

(5) Compute the reliability index β at the design point. In the standard Gaussian distribution space, the reliability index is also defined as the shortest distance from the original to the new failure surface: $g(\mathbf{U}) = 0$.

$$\beta = \frac{g(\mathbf{U}^*) - \sum_{i=1}^n \frac{\partial g(\mathbf{U}^*)}{\partial x_i} \sigma_{x_i'} u_i^*}{\sqrt{\sum_{i=1}^n \left(\frac{\partial g(\mathbf{U}^*)}{\partial x_i} \sigma_{x_i'} \right)^2}} \quad (4.15)$$

Note that the reliability index β is significantly influenced by the standard deviations of various random variables.

(6) Calculate the direction cosine of the unit outward normal vector at the design point.

$$\cos \theta = \alpha_i = - \frac{\frac{\partial g(X^*)}{\partial x_i} \sigma_{x_i}}{\sqrt{\sum_{i=1}^n \left(\frac{\partial g(X^*)}{\partial x_i} \sigma_{x_i} \right)^2}} \quad (4.16)$$

where α_i defines the relative effect of the corresponding random variable on the total variation, which is called the sensitivity factor.

(7) Calculate the new design point.

$$x_i^* = \mu_{x_i} + \beta \sigma_{x_i} \alpha_i \quad (i = 1, 2, \dots, n) \quad (4.17)$$

(8) Repeat Steps (3) through (7) until the estimation of reliability index β converges.

4.2 Reliability Index with Settlement Effect

Nowak (1999) calibrated the load and resistance factor for the AASHTO LRFD Bridge Design Specifications (2007). Allen et al. (2005) calibrated the load and resistance factors for geotechnical and structural design. Neither considered the effect of differential settlements in their calibration.

In this study, only Strength I Load Combination Limit State was investigated for settlement effect, representing the basic load combination related to the nominal vehicular use of bridges without wind (AASHTO, 2007). As listed in Table 4.1, eight cases were considered to investigate the effect of support settlements on the reliability of superstructures and substructures. The settlement effect on the substructure is relatively small in comparison with the dead and live load effects. For each case, the evaluation of the reliability index is thus focused on superstructures only. The particular settlement corresponding to a reliability index of 3.5 is determined, which is the maximum settlement that could be neglected in bridge designs and is referred to as the tolerable settlement to the Strength I Limit State. The eight cases are described in detail as follows.

Table 4.1 Eight design cases investigated

Case	Brief Description	Represented Practice
1	Random settlement is not considered in design with unreduced live load	N/A
2	Deterministic settlement is not considered in design with unreduced live load	Current MoDOT
3	Random settlement is considered in design with unreduced live load	N/A
4	Deterministic settlement is considered in design with unreduced live load	Current AASHTO
5	Random settlement is not considered in design with reduced live load	N/A
6	Deterministic settlement is not considered in design with reduced live load	Potential MoDOT
7	Random settlement is considered in design with reduced live load	N/A
8	Deterministic settlement is considered in design with reduced live load	Potential AASHTO

Case 1: Random Settlement Not Considered in Design and Unreduced Live Load

This case represents the current MoDOT practice if settlement is considered and defined as a random variable with a mean of nominal value and a COV of 0.25. This practice recognizes that

most of the continuous bridges in Missouri are founded on rock or piles/shafts that are socketed into rock and settlement is negligible. However, a foundation actually settles. This case can shed light on how much settlement (mean value) a bridge that is not designed for settlement can tolerate to achieve a target reliability index of 3.5 under a combined dead, live, and settlement effect.

In this case, the minimum resistance R of a bridge and the safety margin function g are given by:

$$R = (1.25DC + 1.5DW + 1.75LL_{HL-93}) / \phi \quad (4.18)$$

$$g = R - (DC + DW + LL_{75-year} + SE) \quad (4.19)$$

in which R , DC , DW , LL_{HL-93} , $LL_{75-year}$, and SE are random variables, DW is the weight of the wearing surface, DC is the dead load excluding the wearing surface (DW), LL_{HL-93} is the HL-93 design load composed of an HS-20 design truck or a design tandem, and a uniformly distributed load, $LL_{75-year}$ is the 75-year live load based on the weight-in-motion data, and ϕ is the strength resistance factor as given in Table 4.2.

Table 4.2 Strength resistance factors in AASHTO LRFD specifications (2007)

Design Load	Resistance Factor		
	Concrete Slab	Steel Girder	Prestressed Girder
Moment	0.9	1.0	1.0
Shear	0.9	1.0	0.9

Case 2: Deterministic Settlement Not Considered in Design and Unreduced Live Load

This case also represents the current MoDOT practice when settlement is defined as an extreme value that can be considered as allowable settlement in bridge designs. In this case, settlement is not treated as a random variable or its COV is equal to zero. The minimum resistance is the same as Eq. (4-18). The safety margin function is also the same as Eq. (4.19) except that SE is now an extreme value. This case can shed light on how much settlement (extreme value) a bridge that is not designed for settlement can tolerate to achieve a target reliability index of 3.5 under a combined dead, live, and settlement effect.

Case 3: Random Settlement Considered in Design and Unreduced Live Load

In this case, settlement is represented by a random variable with a mean of nominal value and a COV of 0.25. Settlement is considered as part of the external load in design. The minimum resistance R and the safety margin function g of a bridge is given by:

$$R = (1.25DC + 1.5DW + 1.75LL_{HL-93} + 1.0SE) / \phi \quad (4.20)$$

$$g = R - (DC + DW + LL_{75-year} + SE) \quad (4.21)$$

Case 4: Deterministic Settlement Considered in Design and Unreduced Live Load

This case represents the current AASHTO LRFD requirement with COV=0 for an extreme settlement. The minimum resistance and the safety margin function are the same as Eq. (4-20) and Eq. (4-21) except that SE is a deterministic extreme value.

Case 5: Random Settlement Not Considered in Design and Reduced Live Load

This case represents a potential MoDOT future practice with reduced live loads when settlement is defined as a random variable. Based on the recent study by Kwon et al. (2010), a live load reduction factor (RF) of 0.7 for moment and 0.85 for shear force was recommended for MoDOT's adoption in the future. In this case, settlement is defined as a random variable with a mean of nominal value and a COV of 0.25. The minimum resistance R and the safety margin function g are given by:

$$R = (1.25DC + 1.5DW + RF \times 1.75LL_{HL-93}) / \phi \quad (4.22)$$

$$g = R - (DC + DW + LL_{75-year} + SE) \quad (4.23)$$

This case can shed light on how much settlement (mean value) a bridge that is not designed for settlement can tolerate to achieve a target reliability index of 3.5 under a combined dead, live, and settlement effect.

Case 6: Deterministic Settlement Not Considered in Design and Reduced Live Load

This case also represents a potential MoDOT future practice with reduced live loads when settlement is defined by its extreme value. In this case, SE is a deterministic extreme value. The minimum resistance is the same as Eq. (4.22) and the safety margin function is the same as Eq.(4.23) except that SE is a deterministic extreme value. This case can shed light on how much settlement (extreme value) a bridge that is not designed for settlement can tolerate to achieve a target reliability index of 3.5 under a combined dead, live, and settlement effect.

Case 7: Random Settlement Considered in Design and Reduced Live Load

In this case, settlement is defined as a random variable with a mean nominal value and a COV of 0.25. Live load is reduced by a live load reduction factor. The minimum resistance and the safety margin limit state function are given by:

$$R = (1.25DC + 1.5DW + RF \times 1.75LL_{HL-93} + 1.0SE) / \phi \quad (4.24)$$

$$g = R - (DC + DW + LL_{75-year} + SE) \quad (4.25)$$

Case 8: Deterministic Settlement Considered in Design and Reduced Live Load

For this case, the minimum resistance of a bridge and the safety margin function are the same as Eq.(4.24) and Eq. (4.25), except that settlement is a deterministic extreme value.

5 SETTLEMENT EFFECT ON SUPERSTRUCTURE RELIABILITY

To quantify the settlement effect on the reliability index of the superstructure, 31 new bridges and 14 existing bridges as described in Tables 2.3 and 2.4, respectively, were analyzed for the 8 cases presented in Section 4. Both load and resistance analyses are discussed before the reliability indices are presented for the new and existing bridges.

5.1 Load Analysis

5.1.1 Dead load effect

The nominal dead load of a bridge superstructure includes the weights of bridge girders, deck, barrier, and wearing surface that are permanently attached to the bridge as stipulated in as-built bridge drawings. In this study, a 3-inch (35 psf) future wearing surface was considered to calculate the dead load effect by wearing surface according to Engineering Policy Guide Article 751.10.1 in the MoDOT LRFD Bridge Design Guidelines.

In the case of steel girder bridges and slab bridges, the effects of all structural and nonstructural elements were evaluated with continuous spans. For prestressed concrete girder bridges, except for barriers and future wearing surfaces, the load effects of other components were calculated with simply supported spans; barriers and future wearing surfaces were constructed after installation of the girders and deck and thus computed with continuous spans.

The effects of the unfactored dead loads of 31 new designs on each girder (interior or exterior) are enclosed in Appendix F. For the 14 existing bridges, the unfactored dead load effects on each interior girder are presented in Table 5.1 to Table 5.6. Composite deck and girder action was taken into account. The load effect on the exterior girder is in general slightly smaller.

Table 5.1 Maximum positive moments of each interior girder due to dead loads excluding wearing surface

Bridge Index	Bridge No.		Positive Moment (kip-ft)			
	NBI	MoDOT	Span 1	Span 2	Span 3	Span 4
1	2664	A3101	912	912		
2	3945	A4840	1341	1443		
3	31500	A7300	375	375		
4	2852	A3386	1385	1560	1385	
5	3475	A4256	22	23	35	
6	4043	A4999	72	803	37	
7	3332	A4058	195	601	251	
8	11893	A5161	263	769	291	
9	29023	A6569	697	2224	1218	
10	3276	A3973	532	532	282	282
11	3753	A4582	242	242	708	242
12	2983	A3562	15	21	15	
13	28993	A6450	4	4	4	
14	2856	A3390	33	36	17	18

Table 5.2 Maximum negative moments of each interior girder due to dead loads excluding wearing surface

Bridge Index	Bridge No.		Negative moment (kip-ft)				
	NBI	MoDOT	Support 1	Support 2	Support 3	Support 4	Support 5
1	2664	A3101	0	1629	0		
2	3945	A4840	0	2486	0		
3	31500	A7300	0	669	0		
4	2852	A3386	0	2813	2813	0	
5	3475	A4256	0	54	54	0	
6	4043	A4999	0	1028	1021	0	
7	3332	A4058	0	0	0	0	
8	11893	A5161	0	0	0	0	
9	29023	A6569	0	0	0	0	
10	3276	A3973	0	0	0	0	
11	3753	A4582	0	0	0	0	
12	2983	A3562	0	35	35	0	
13	28993	A6450	0	7	7	0	
14	2856	A3390	0	65	55	33	0

Table 5.3 Maximum shear forces of each interior girder due to dead loads excluding wearing surface

Bridge Index	Bridge No.		Shear Force (kip)			
	NBI	MoDOT	Span 1	Span 2	Span 3	Span 4
1	2664	A3101	68	68		
2	3945	A4840	89	90		
3	31500	A7300	52	52		
4	2852	A3386	177	180	177	
5	3475	A4256	11	12	12	
6	4043	A4999	48	61	47	
7	3332	A4058	21	37	24	
8	11893	A5161	28	47	29	
9	29023	A6569	50	89	66	
10	3276	A3973	36	36	26	26
11	3753	A4582	25	25	44	25
12	2983	A3562	5	5	5	
13	28993	A6450	2	2	2	
14	2856	A3390	6	7	6	5

Table 5.4 Maximum positive moments of each interior girder due to weight of wearing surface only

Bridge Index	Bridge No.		Positive Moment (kip-ft)			
	NBI	MoDOT	Span 1	Span 2	Span 3	Span 4
1	2664	A3101	270	270		
2	3945	A4840	372	400		
3	31500	A7300	83	83		
4	2852	A3386	313	352	313	
5	3475	A4256	6	7	10	
6	4043	A4999	21	231	11	
7	3332	A4058	12	50	21	
8	11893	A5161	20	74	25	
9	29023	A6569	40	162	107	
10	3276	A3973	72	39	11	41
11	3753	A4582	38	38	68	17
12	2983	A3562	3	3	3	
13	28993	A6450	1	1	1	
14	2856	A3390	5	6	3	3

Table 5.5 Maximum negative moments of each interior girder due to weight of wearing surface only

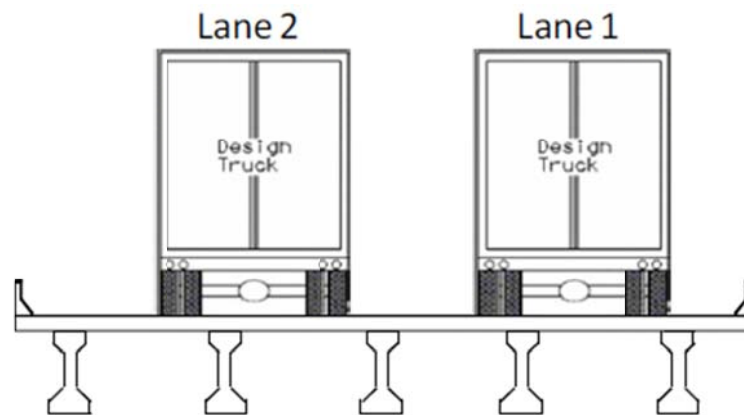
Bridge Index	Bridge No.		Negative Moment (kip-ft)				
	NBI	MoDOT	Support 1	Support 2	Support 3	Support 4	Support 5
1	2664	A3101	0	483	0		
2	3945	A4840	0	690	0		
3	31500	A7300	0	148	0		
4	2852	A3386	0	635	635	0	
5	3475	A4256	0	16	16	0	
6	4043	A4999	0	296	294	0	
7	3332	A4058	0	72	72	0	
8	11893	A5161	0	103	103	0	
9	29023	A6569	0	262	262	0	
10	3276	A3973	0	104	54	49	0
11	3753	A4582	0	83	91	91	0
12	2983	A3562	0	6	6	0	
13	28993	A6450	0	1	1	0	
14	2856	A3390	0	11	9	5	0

Table 5.6 Maximum shears of each interior girder due to weight of wearing surface only

Bridge Index	Bridge No.		Shear Force (kip)			
	NBI	MoDOT	Span 1	Span 2	Span 3	Span 4
1	2664	A3101	20	20		
2	3945	A4840	25	25		
3	31500	A7300	11	11		
4	2852	A3386	40	41	40	
5	3475	A4256	3	3	4	
6	4043	A4999	14	18	13	
7	3332	A4058	6	7	6	
8	11893	A5161	9	11	9	
9	29023	A6569	13	17	15	
10	3276	A3973	10	9	6	7
11	3753	A4582	6	7	10	8
12	2983	A3562	0.8	0.8	0.8	
13	28993	A6450	0.4	0.4	0.4	
14	2856	A3390	1.1	1.1	0.9	0.8

5.1.2 Live load effect

The daily maximum live load effect on bridge girders was selected among those due to single-truck and multiple-truck events each day. The live load effect is amplified due to vehicle-bridge dynamic interaction as a result of rough roadway surfaces. The additional live load effect due to the dynamic amplification is defined in the AASHTO LRFD Specifications (2007) as a percentage, referred to as dynamic impact factor (IM), of the live load effect of vehicles. The total live load effect is then distributed into bridge girders through a girder distribution factor (AASHTO, 2007). The girder distribution factor depends upon the cross section of a bridge and the number of vehicular lanes in the roadway, as illustrated in Figure 5.1.

**Figure 5.1 Multiple-lane load**

In this study, both the dynamic impact factor and girder distribution factors are considered as random variables. The dynamic impact factor has a mean of 0.1 and 0.15 for two parallel trucks and a single truck, respectively, with a COV of 0.8 (Hwang and Nowak, 1991). The girder

distribution factors have their bias factor and COV of 1.0 and 0.2, respectively (Nowak, 1999). Samples for the dynamic impact factor and girder distribution factors in single-lane and multiple-lane roads were randomly generated with the Monte Carlo Simulations using their statistical properties.

The unfactored live load induced moment and shear for the interior girders of bridges were calculated following the procedure by Kwon et al. (2010). The maximum live load effects for 14 existing bridges are presented in Tables 5.7 to 5.9. The maximum live load effects for 31 new designs of girder bridges are presented in Appendix F. Both include the dynamic impact effects.

Table 5.7 Maximum positive moments of each interior girder due to live load

Bridge Index	Bridge No.		Positive Moment (kip-ft)			
	NBI	MoDOT	Span 1	Span 2	Span 3	Span 4
1	2664	A3101	1383	1443		
2	3945	A4840	1707	1761		
3	31500	A7300	731	708		
4	2852	A3386	1774	1693	1775	
5	3475	A4256	193	184	212	
6	4043	A4999	748	992	707	
7	3332	A4058	505	624	555	
8	11893	A5161	623	736	619	
9	29023	A6569	985	1227	1244	
10	3276	A3973	774	639	541	564
11	3753	A4582	532	512	635	547
12	2983	A3562	59	61	59	
13	28993	A6450	38	34	37	
14	2856	A3390	77	71	63	57

Table 5.8 Maximum negative moments of each interior girder due to live load

Bridge Index	Bridge No.		Negative Moment (kip-ft)				
	NBI	MoDOT	Support 1	Support 2	Support 3	Support 4	Support 5
1	2664	A3101	0	990	0		
2	3945	A4840	0	1259	0		
3	31500	A7300	0	736	0		
4	2852	A3386	0	1474	1482	0	
5	3475	A4256	0	196	203	0	
6	4043	A4999	0	1317	1405	0	
7	3332	A4058	0	753	673	0	
8	11893	A5161	0	910	820	0	
9	29023	A6569	0	1424	1225	0	
10	3276	A3973	0	756	692	601	0
11	3753	A4582	0	821	668	765	0
12	2983	A3562	0	73	69	0	
13	28993	A6450	0	33	37	0	
14	2856	A3390	0	78	72	64	0

Table 5.9 Maximum shear forces of each interior girder due to live load

Bridge Index	Bridge No.		Shear Force (kip)			
	NBI	MoDOT	Span 1	Span 2	Span 3	Span 4
1	2664	A3101	122	134		
2	3945	A4840	128	135		
3	31500	A7300	100	98		
4	2852	A3386	212	220	205	
5	3475	A4256	58	64	64	
6	4043	A4999	98	132	101	
7	3332	A4058	73	94	83	
8	11893	A5161	86	105	92	
9	29023	A6569	99	132	119	
10	3276	A3973	101	97	84	87
11	3753	A4582	71	79	97	84
12	2983	A3562	9	9	11	
13	28993	A6450	12	11	12	
14	2856	A3390	9	9	9	10

5.2 Strength Resistance of Selected Bridges

As discussed in Section 4, the minimum resistances of 31 new bridges were calculated using their minimum required design strength without and with the effect of support settlements as defined in Eq. (4.18) and Eq. (4.20). As listed in Table 5.10, the minimum shear and moment resistances of the 14 existing bridges were also determined without considering the effect of differential settlements. For comparison, the actual resistances to negative and positive moments of the 14 existing bridges were calculated and included in Table 5.11 (Kwon et al., 2010).

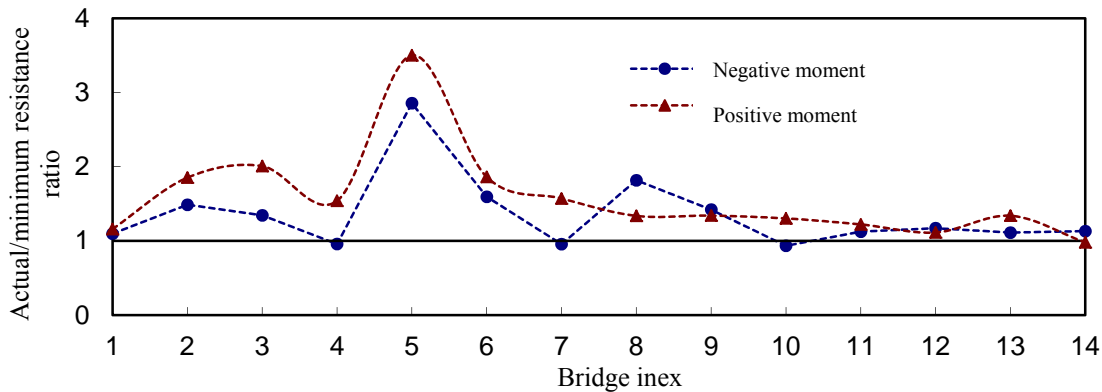
Table 5.10 Minimum resistances of negative and positive moments and shear

Bridge Index	Bridge No.		Negative Moment (kip-ft)				Positive Moment (kip-ft)				Shear Force (kip)			
	NBI	MoDOT	Span1	Span2	Span3	Span4	Span1	Span2	Span3	Span4	Span1	Span2	Span3	Span4
1	2664	A3101	5573	5573	0	0	4385	4385	0	0	307	307	0	0
2	3945	A4840	7727	7707	0	0	5711	5951	0	0	359	362	0	0
3	31500	A7300	2422	2422	0	0	1997	1995	0	0	242	242	0	0
4	2852	A3386	8798	8493	8798	0	6029	6278	6029	0	638	654	638	0
5	3475	A4256	343	360	367	0	335	345	414	0	108	112	116	0
6	4043	A4999	4119	3704	4141	0	1485	3389	1320	0	247	296	243	0
7	3332	A4058	1186	1040	1116	0	1051	1869	1222	0	148	187	158	0
8	11893	A5161	1558	1367	1519	0	1429	2441	1520	0	195	244	201	0
9	29023	A6569	3183	3092	3325	0	2829	5582	4193	0	253	328	290	0
10	3276	A3973	1329	1329	1103	841	2176	1811	1192	1380	210	201	170	177
11	3753	A4582	741	1374	1216	1332	1254	1055	2149	1244	167	163	215	172
12	2983	A3562	128	125	128	0	105	117	105	0	21	22	21	0
13	28993	A6450	51	47	51	0	51	48	51	0	17	16	17	0
14	2856	A3390	206	204	193	136	176	180	124	117	26	26	24	22

Table 5.11 Actual resistances of negative and positive moments

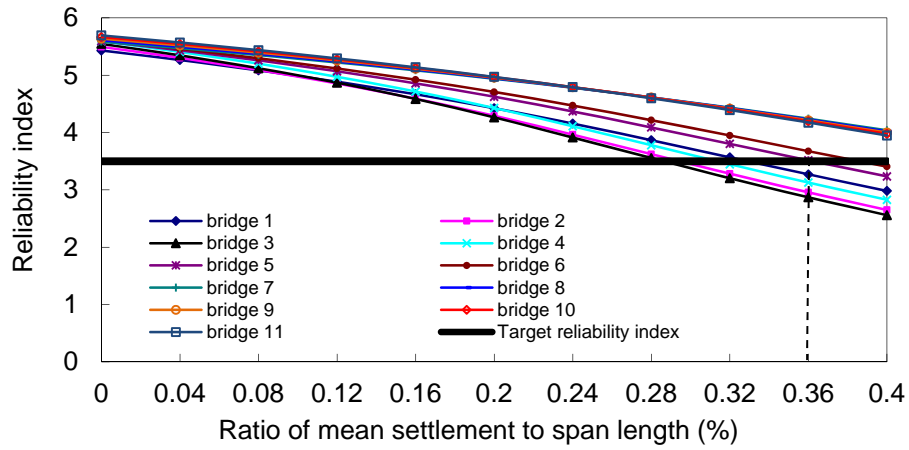
Bridge Index	Bridge No.		Negative Moment (kip-ft)				Positive Moment (kip-ft)			
	NBI	MoDOT	Span1	Span2	Span3	Span4	Span1	Span2	Span3	Span4
1	2664	A3101	6113	6113	0	0	5086	5086	0	0
2	3945	A4840	11461	11461	0	0	11025	11025	0	0
3	31500	A7300	3258	3258	0	0	4005	4005	0	0
4	2852	A3386	8139	8139	8139	0	9284	9666	9284	0
5	3475	A4256	1034	1027	1027	0	1219	1209	1248	0
6	4043	A4999	5907	5910	5910	0	8495	6312	8477	0
7	3332	A4058	994	994	994	0	1361	2938	1361	0
8	11893	A5161	2484	2484	2484	0	1862	3265	1862	0
9	29023	A6569	4395	4395	4395	0	3260	7487	4572	0
10	3276	A3973	1241	1241	1241	1241	2360	2360	1517	1517
11	3753	A4582	1546	1546	1546	1546	1289	1289	2641	1289
12	2983	A3562	146	146	146	0	130	130	130	0
13	28993	A6450	52	52	52	0	64	64	64	0
14	2856	A3390	231	231	158	158	205	176	135	148

The actual/minimum resistance ratio is presented in Figure 5.2. It is clearly seen that the actual moment resistances generally exceed their minimum required strengths stipulated by the current AASHTO LRFD Bridge Design Specifications (2007). The significantly overdesigned bridge, No. 5 in Figure 5.2, corresponds to the shortest spans of all steel girder bridges.

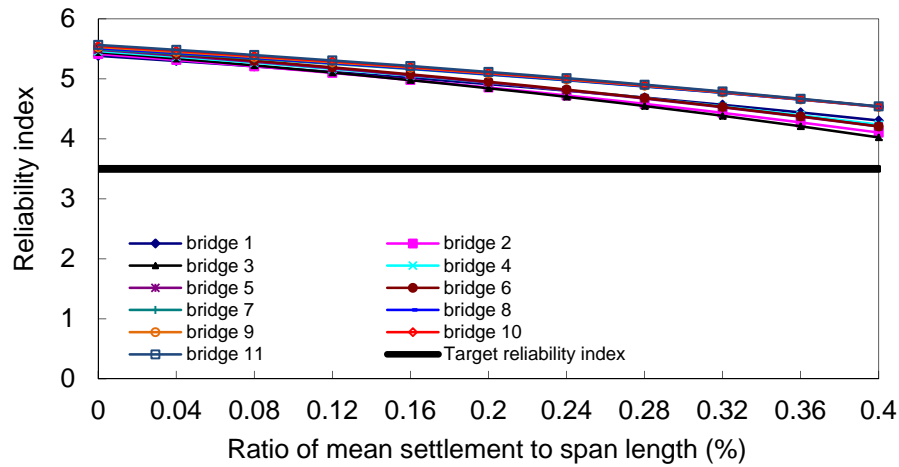
**Figure 5.2 The ratio of the real resistance to the minimum resistance**

5.3 Reliability Indices of 31 Bridge Designs with Equal Spans

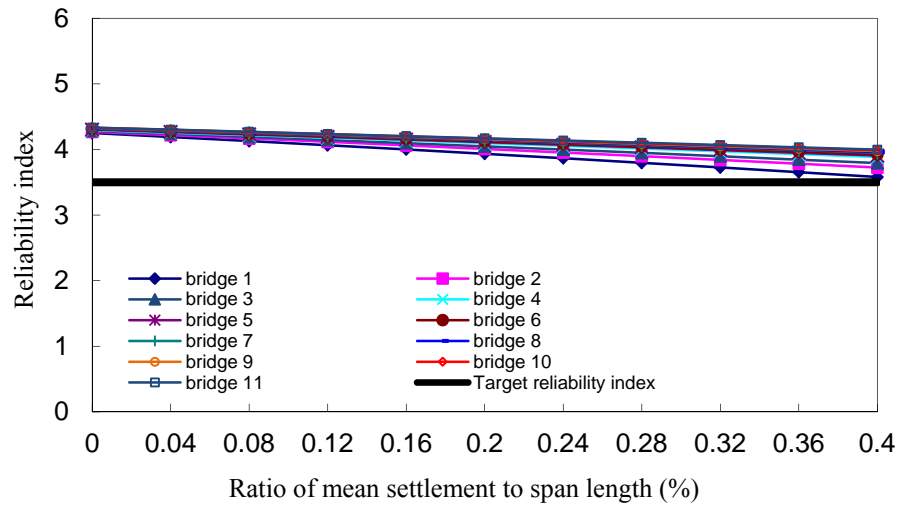
The 8 cases described in Section 4 were considered to understand the effect of differential settlements on the bridge safety margin under various design conditions. The reliability indices for the maximum negative moment, maximum positive moment, and shear of two-span, three-span, and four-span bridges are presented as a function of mean settlement up to the AASHTO recommended limit of $0.004L$ (L = span length, $COV = 0.25$) in Figures 5.3-5.5, 5.9-5.11, 5.15-5.17, and 5.21-5.23 for Cases 1, 3, 5, and 7, respectively. Similarly, the reliability indices are presented as a function of extreme settlement up to the AASHTO recommended limit of $0.004L$ in Figures 5.6-5.8, 5.12-5.14, 5.18-5.20, and 5.24-5.26 for Cases 2, 4, 6, and 8, respectively.



(a) Reliability indices for negative moment

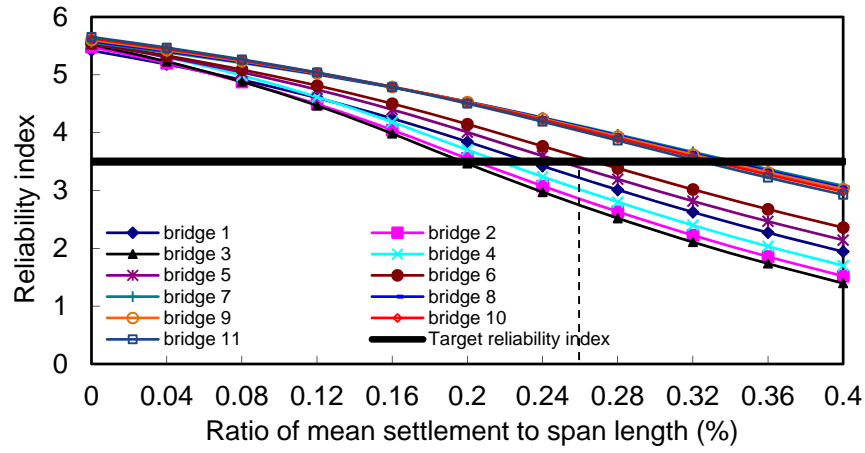


(b) Reliability indices for positive moment

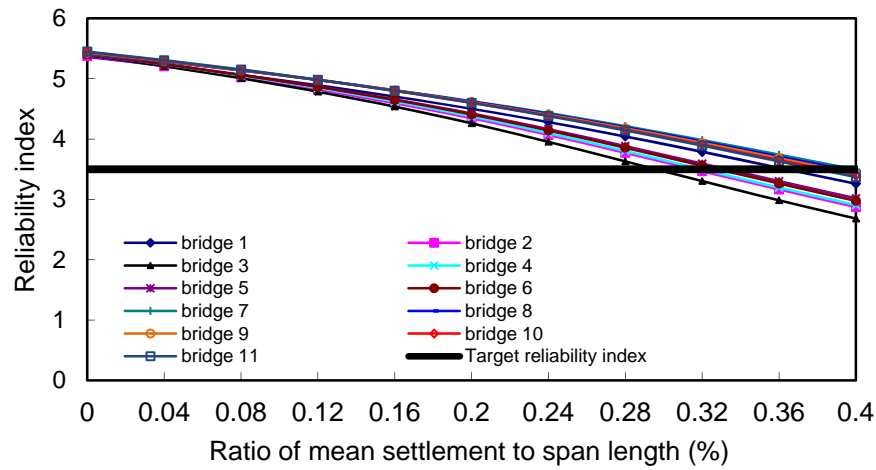


(c) Reliability indices for shear

Figure 5.3 Reliability indices of 2-span bridges (No.1 to No.11 in Table 2.3): Case 1



(a) Reliability indices for negative moment



(b) Reliability indices for positive moment

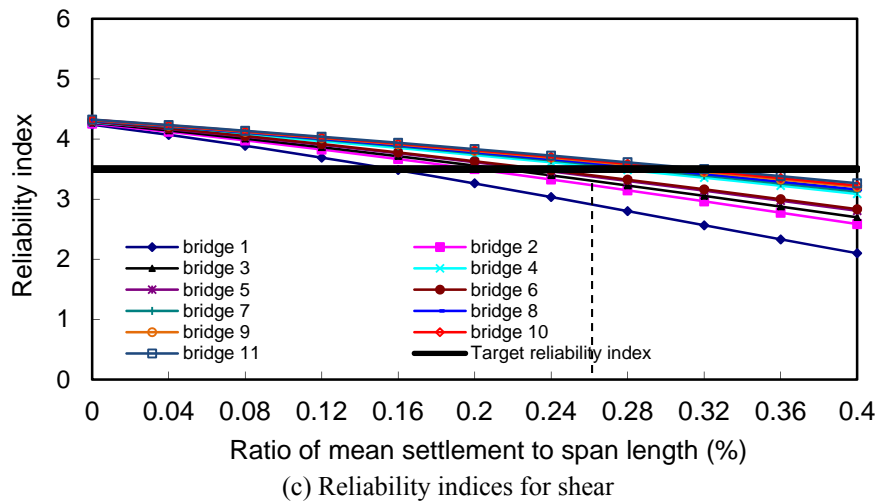
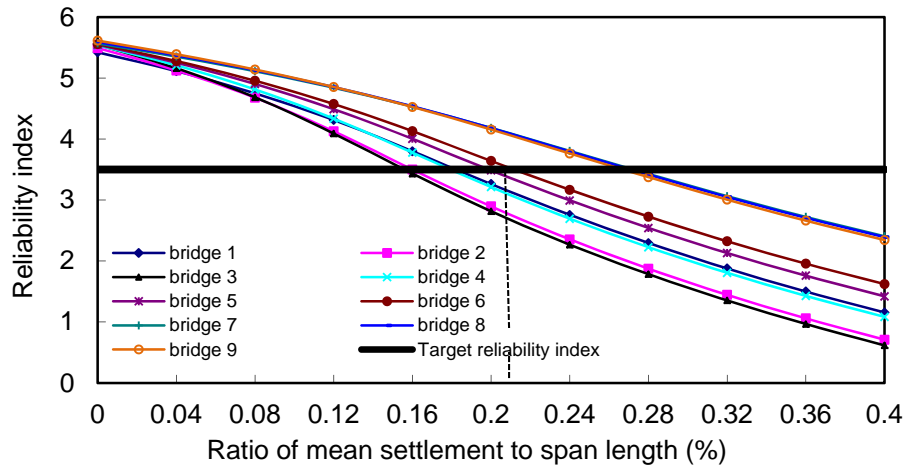
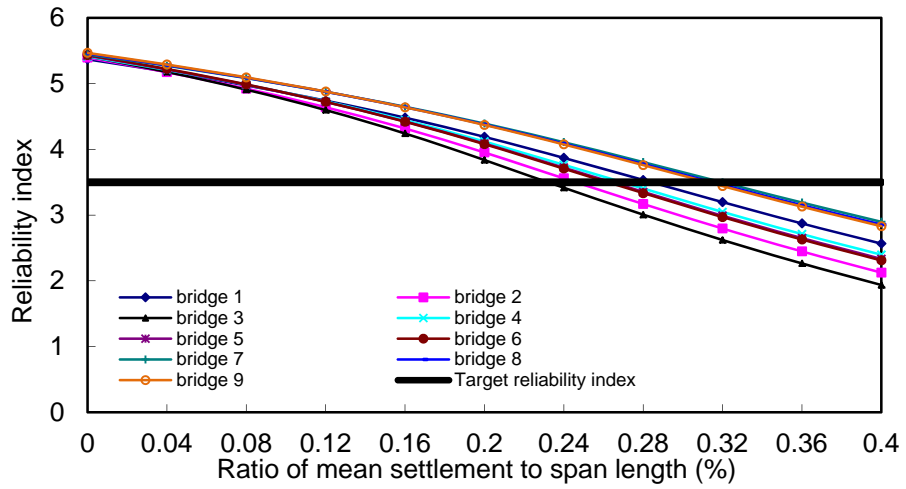


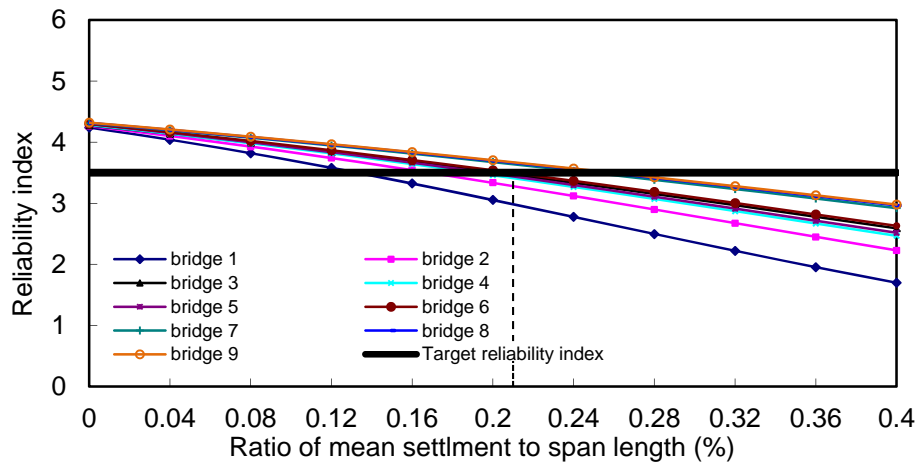
Figure 5.4 Reliability indices of 3-span bridges (No.12 to No.22 in Table 2.3): Case 1



(a) Reliability indices for negative moment

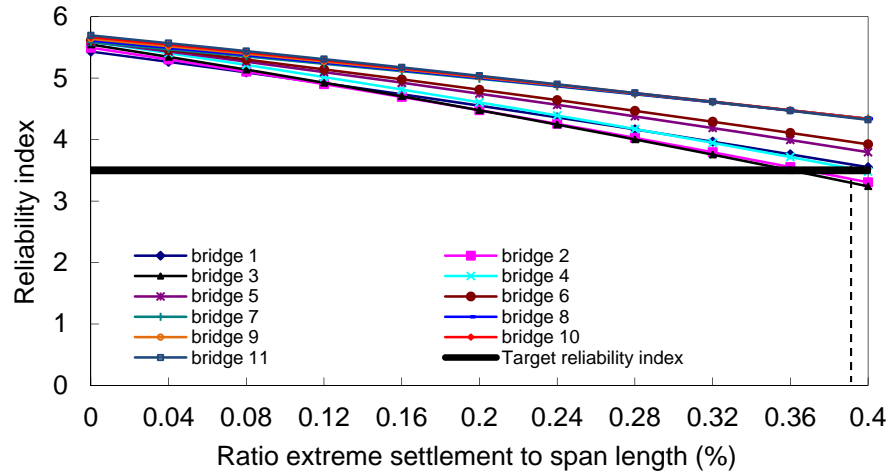


(b) Reliability indices for positive moment

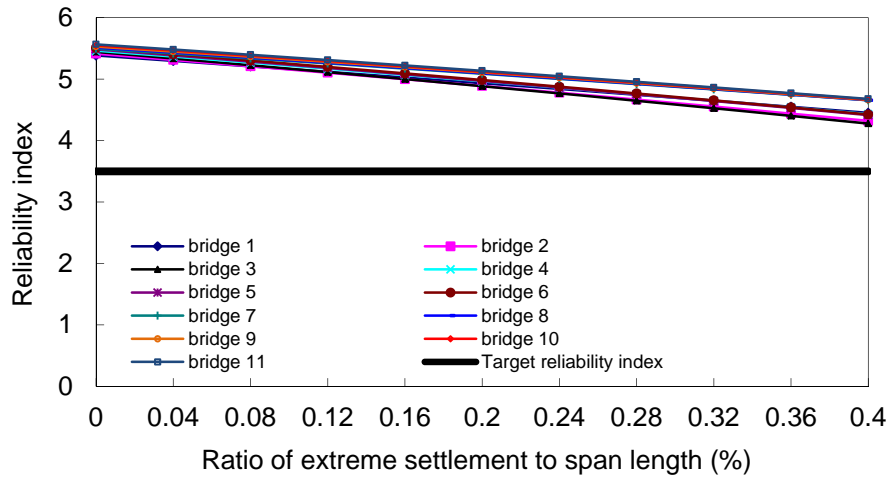


(c) Reliability indices for shear

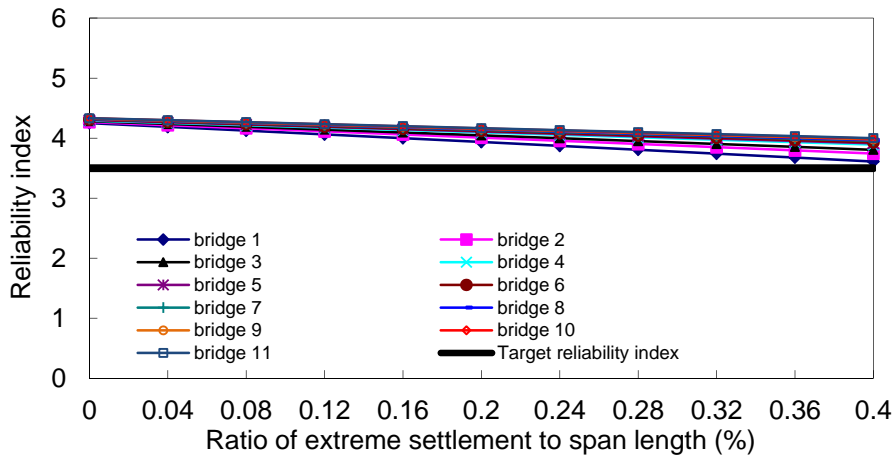
Figure 5.5 Reliability indices of 4-span bridges (No.23 to No.31 in Table 2.3): Case 1



(a) Reliability indices for negative moment

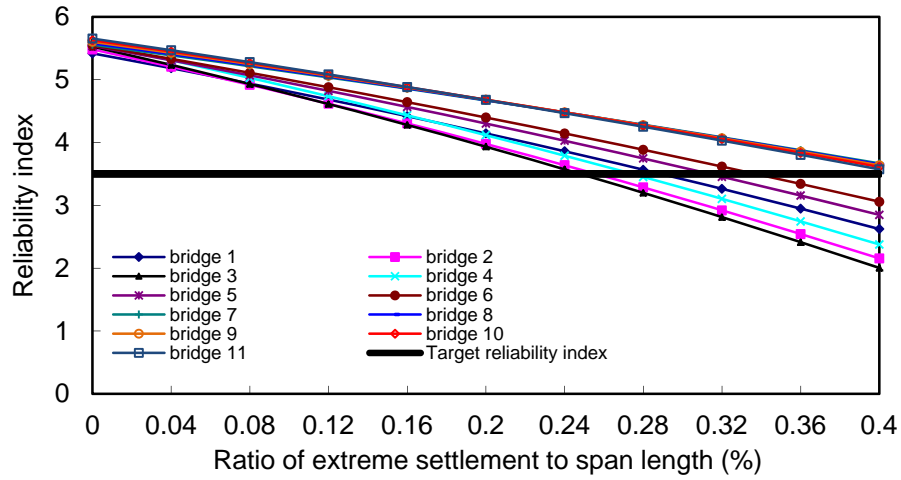


(b) Reliability indices for positive moment

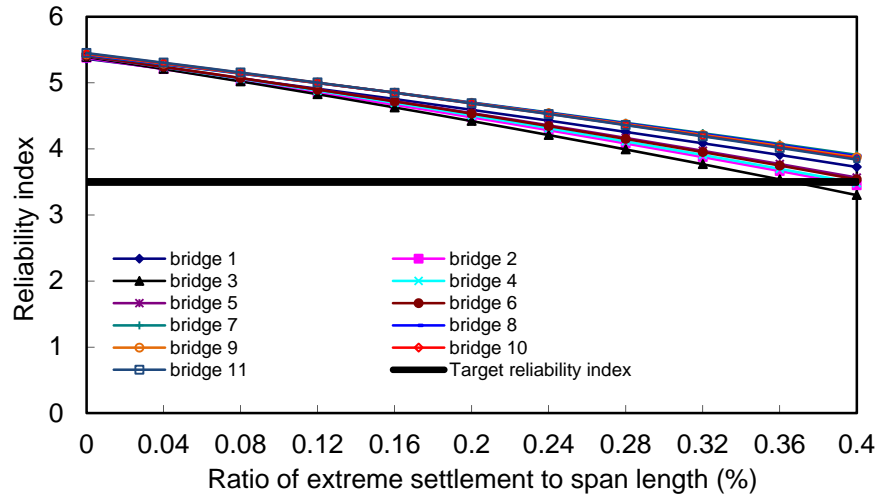


(c) Reliability indices for shear

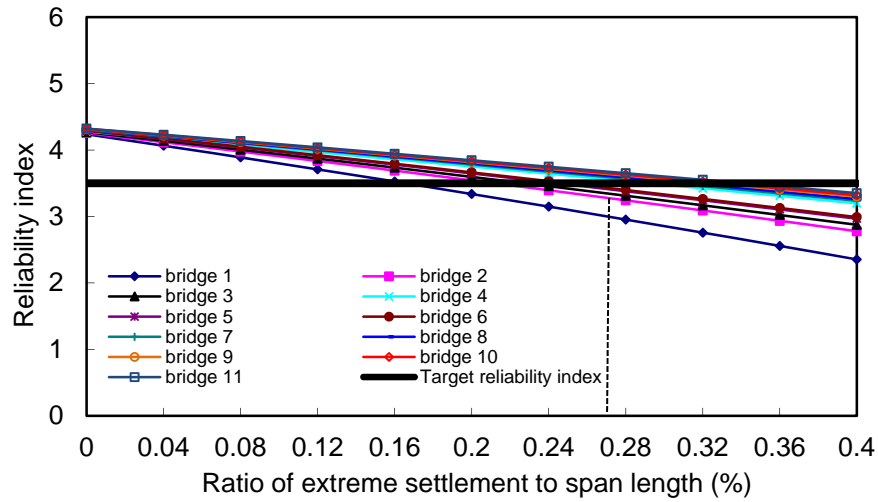
Figure 5.6 Reliability indices of 2-span bridges (No.1 to No.11 in Table 2.3): Case 2



(a) Reliability indices for negative moment

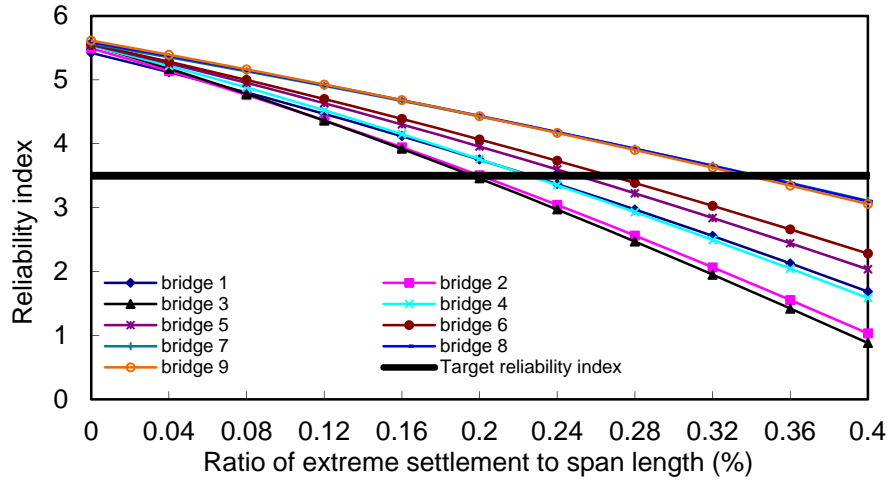


(b) Reliability indices for positive moment

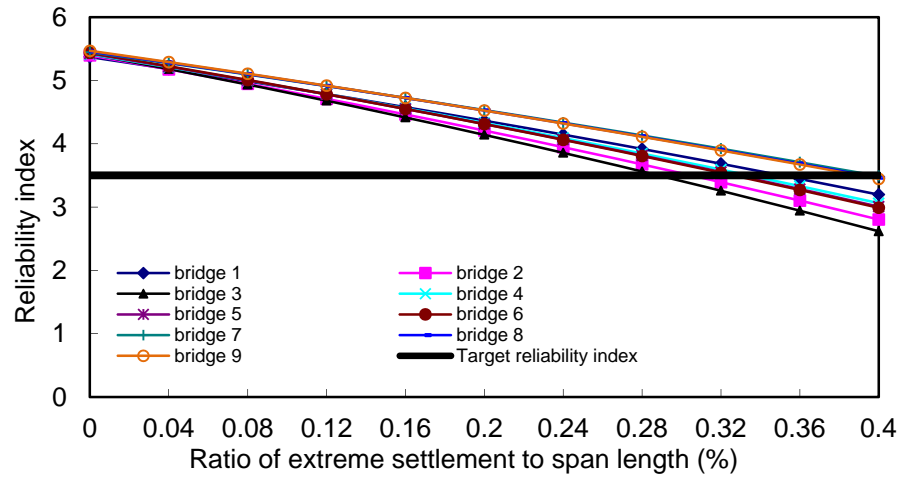


(c) Reliability indices for shear

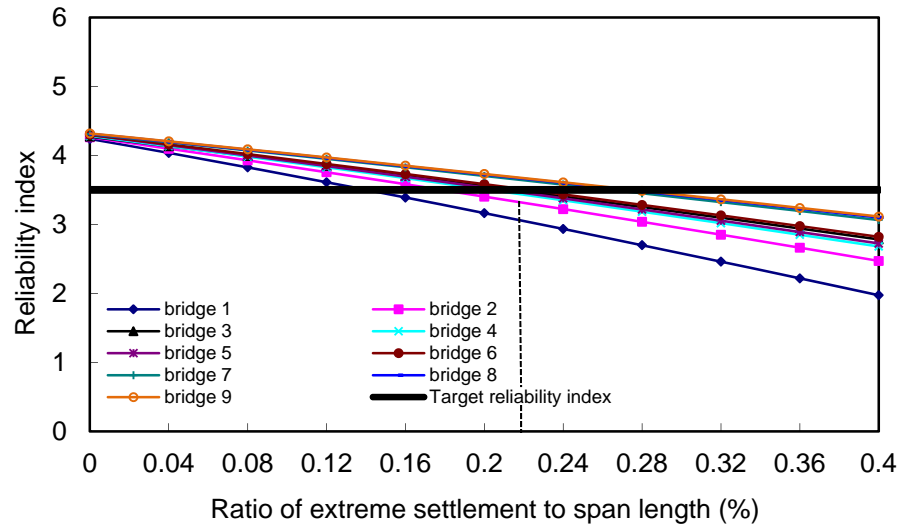
Figure 5.7 Reliability indices of 3-span bridges (No.12 to No.22 in Table 2.3): Case 2



(a) Reliability indices for negative moment

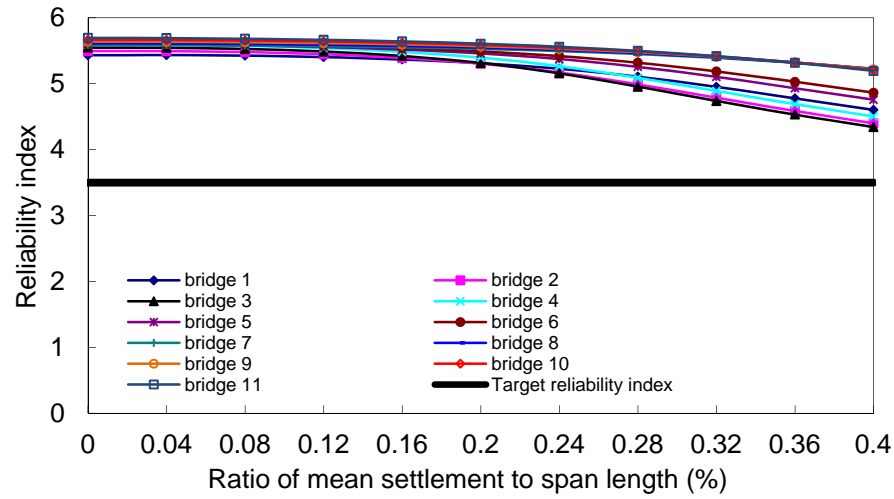


(b) Reliability indices for positive moment

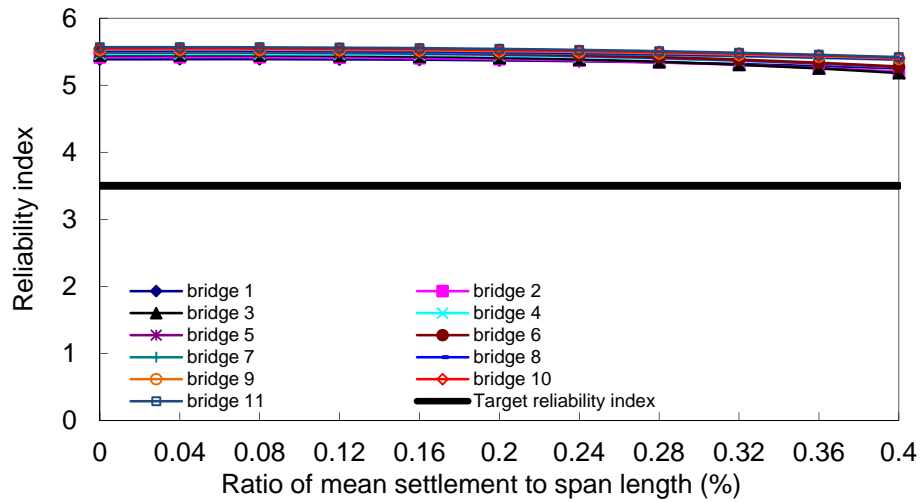


(c) Reliability indices for shear

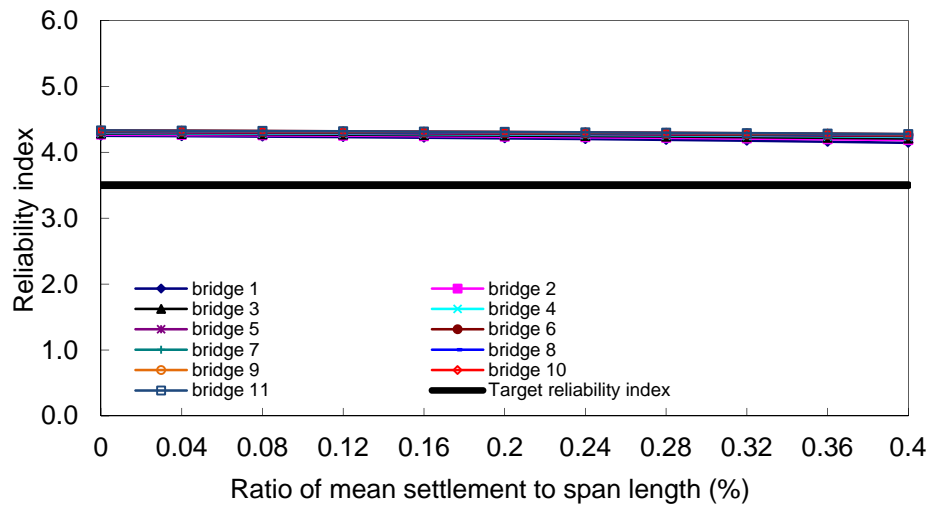
Figure 5.8 Reliability indices of 4-span bridges (No.23 to No.31 in Table 2.3): Case 2



(a) Reliability indices for negative moment



(b) Reliability indices for positive moment



(c) Reliability indices for shear

Figure 5.9 Reliability indices of 2-span bridges (No.1 to No.11 in Table 2.3): Case 3

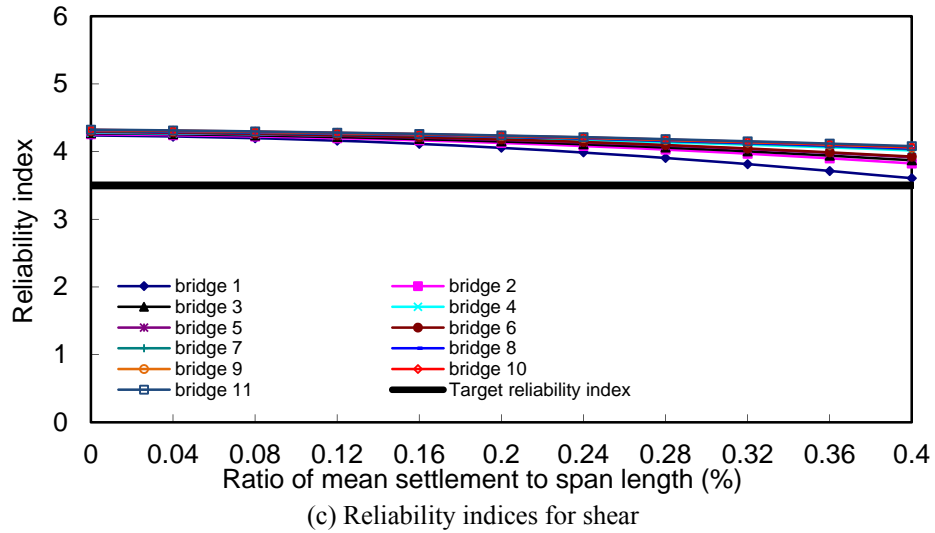
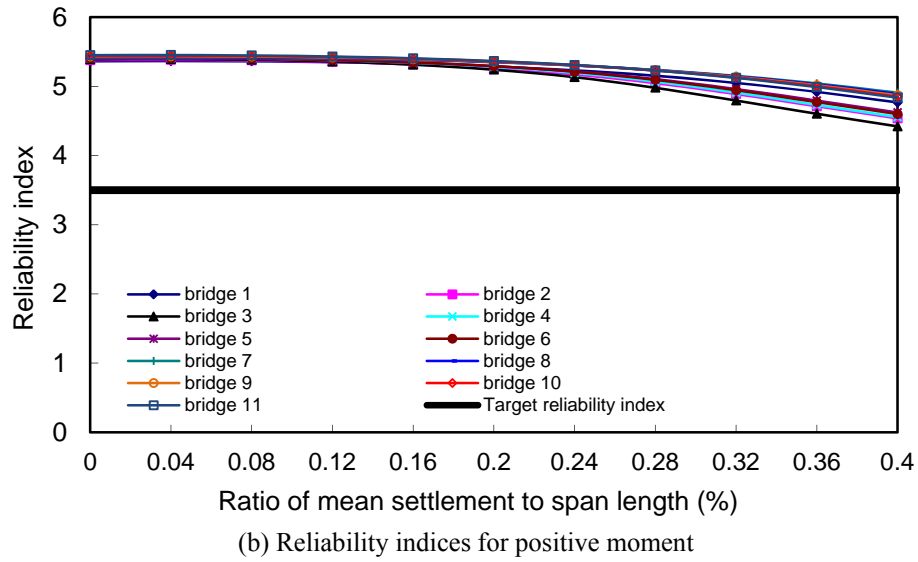
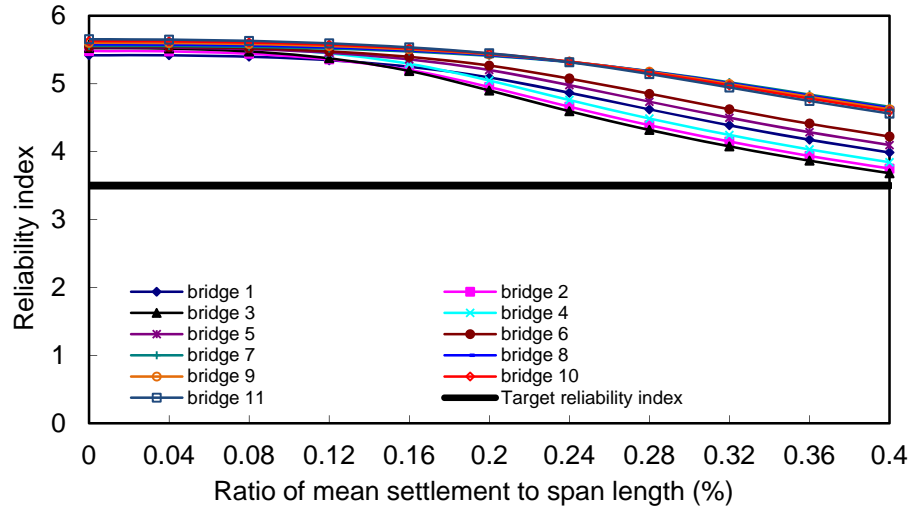
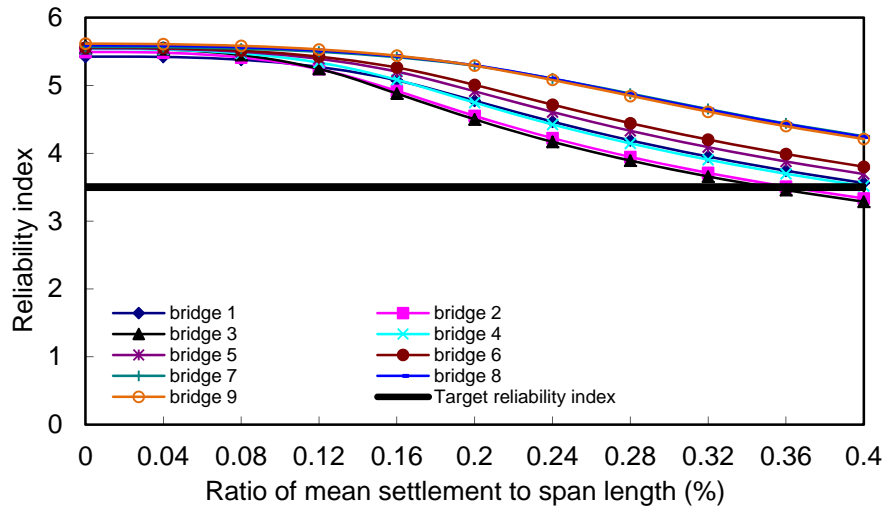
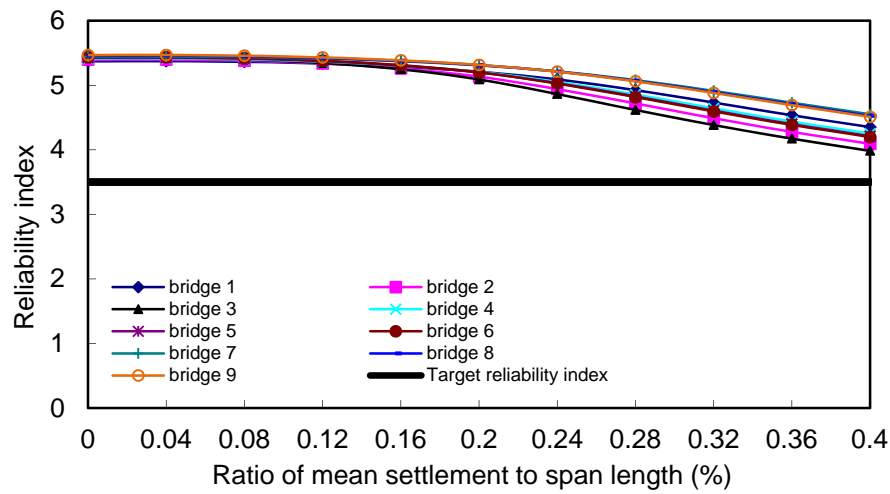


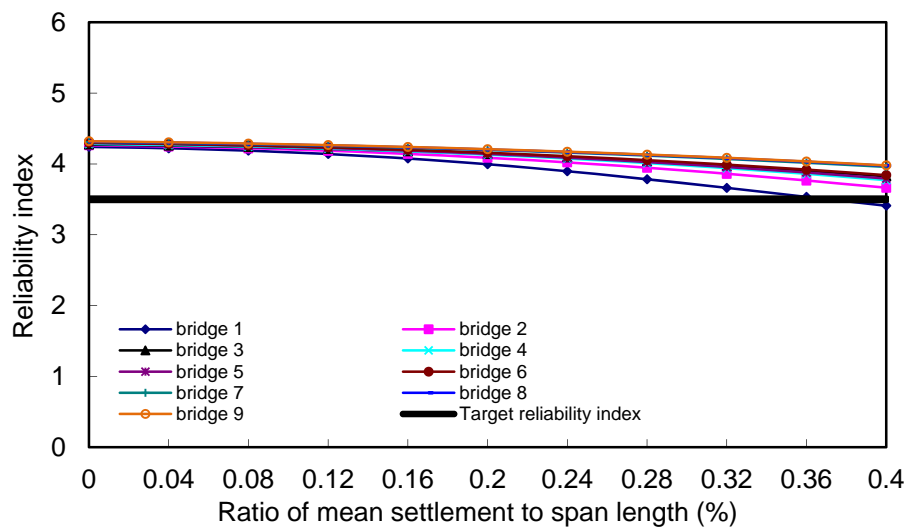
Figure 5.10 Reliability indices of 3-span bridges (No.12 to No.22 in Table 2.3): Case 3



(a) Reliability indices for negative moment



(b) Reliability indices for positive moment



(c) Reliability indices for shear

Figure 5.11 Reliability indices of 4-span bridges (No.23 to No.31 in Table 2.3): Case 3

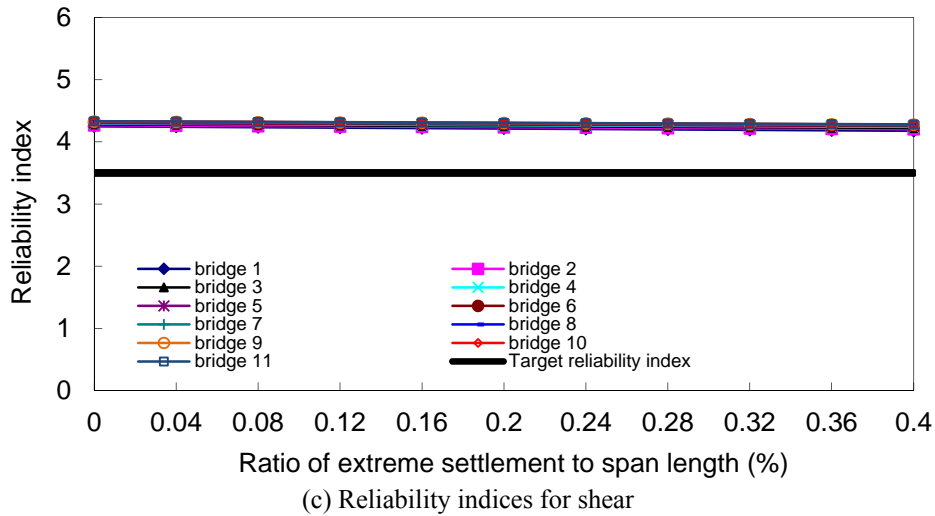
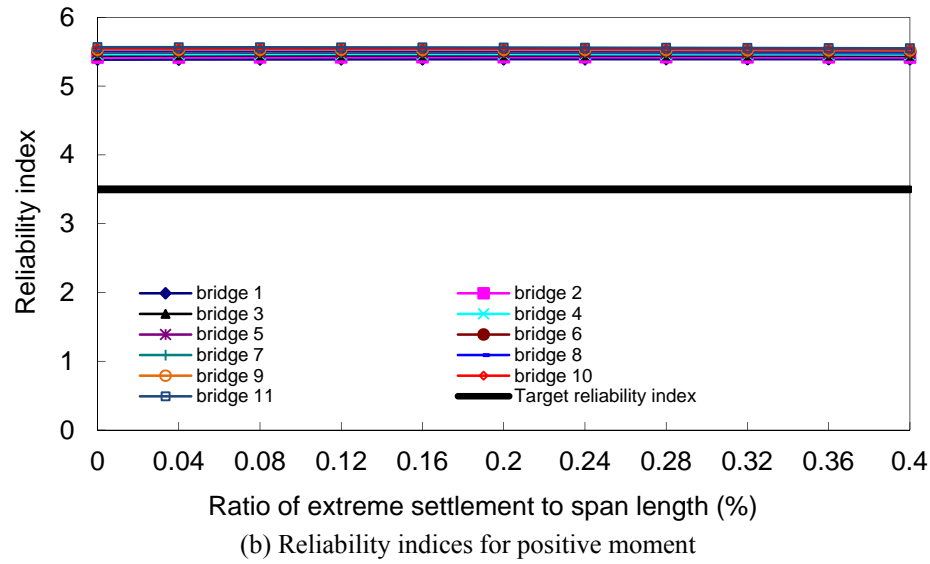
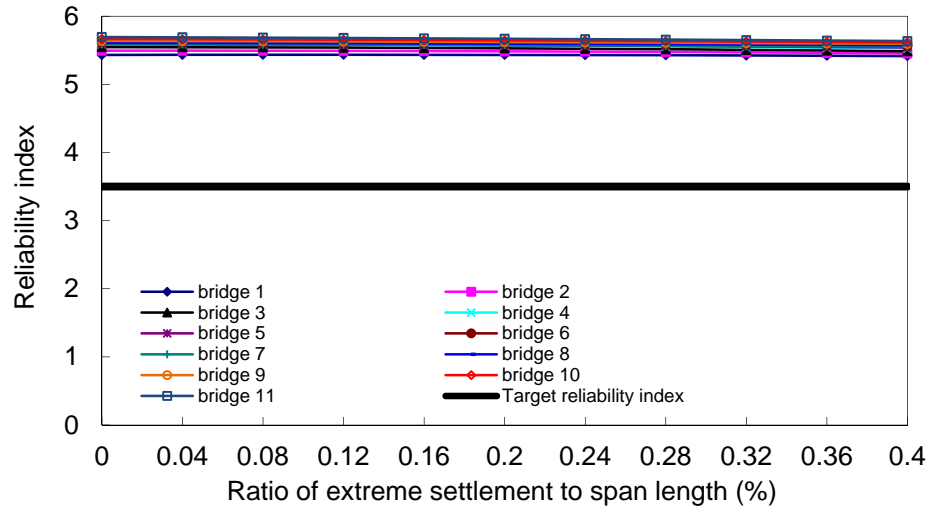
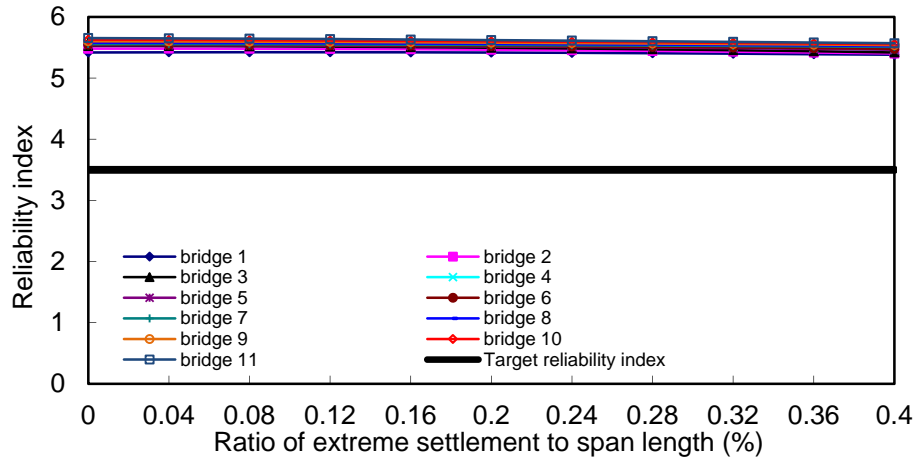
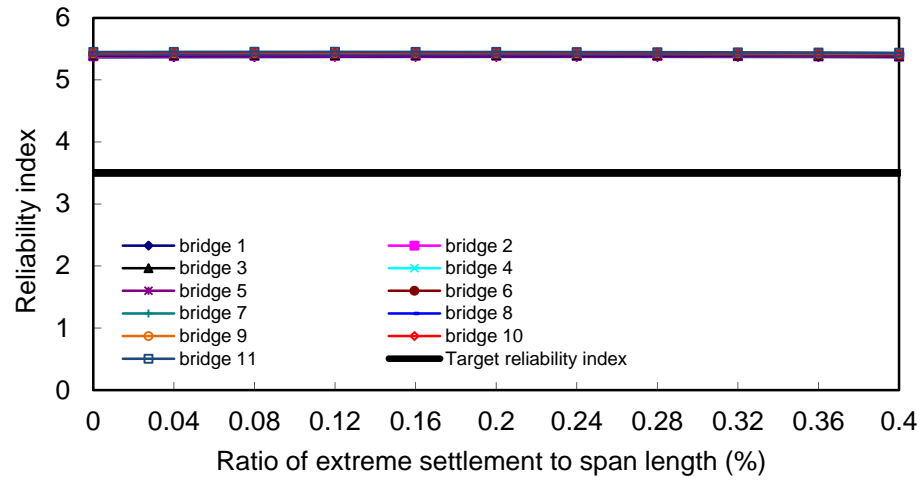


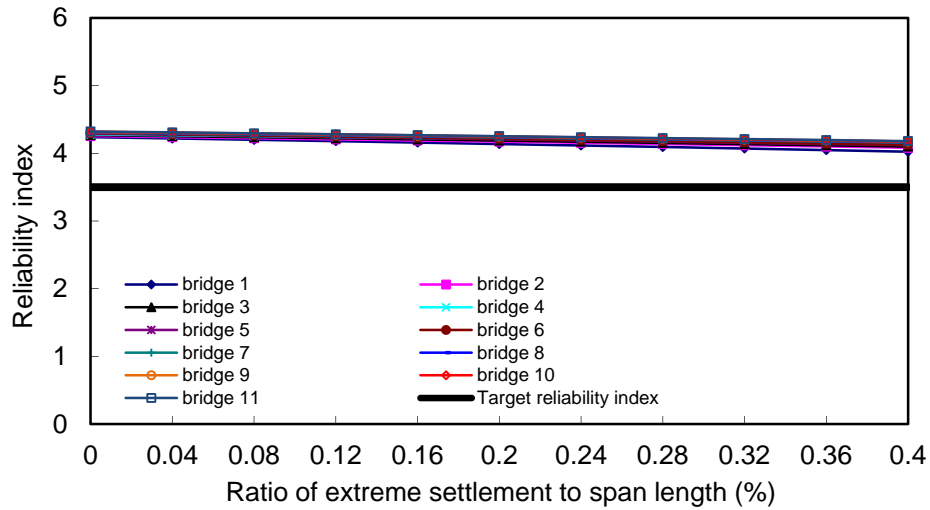
Figure 5.12 Reliability indices of 2-span bridges (No.1 to No.11 in Table 2.3): Case 4



(a) Reliability indices for negative moment

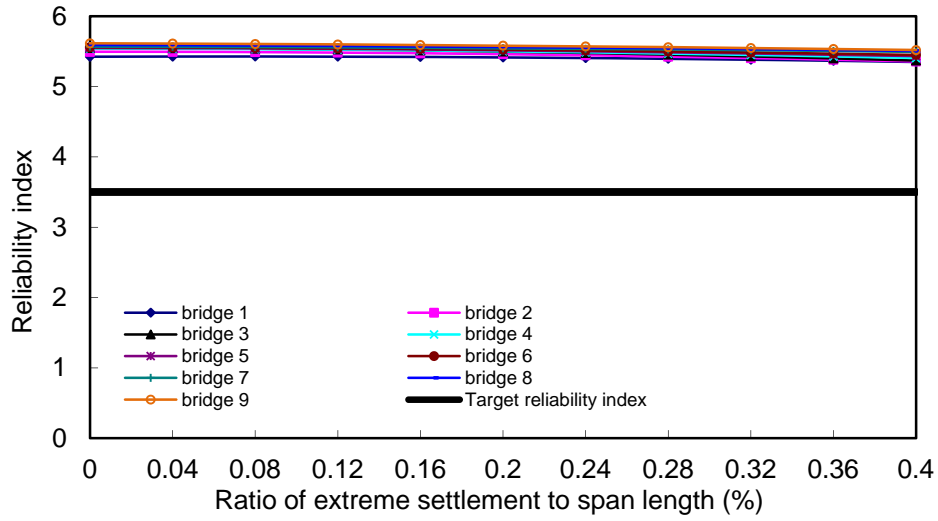


(b) Reliability indices for positive moment

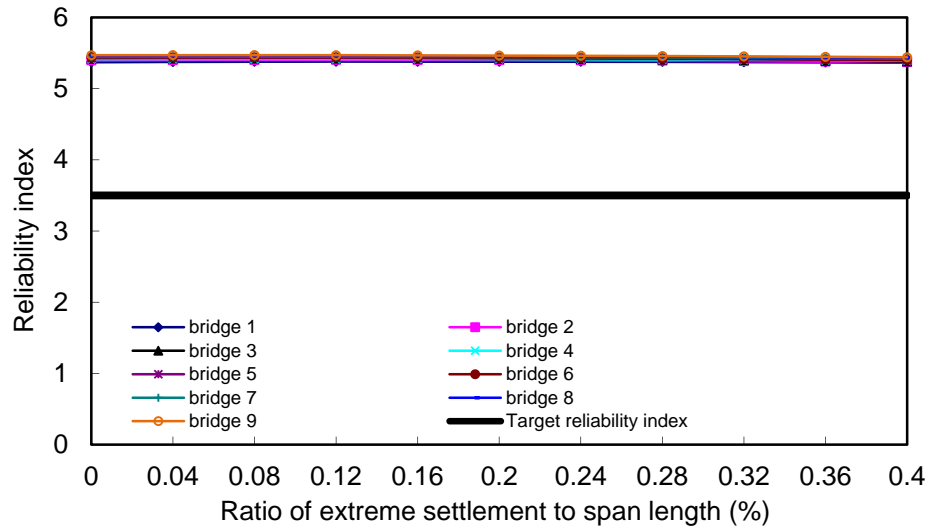


(c) Reliability indices for shear

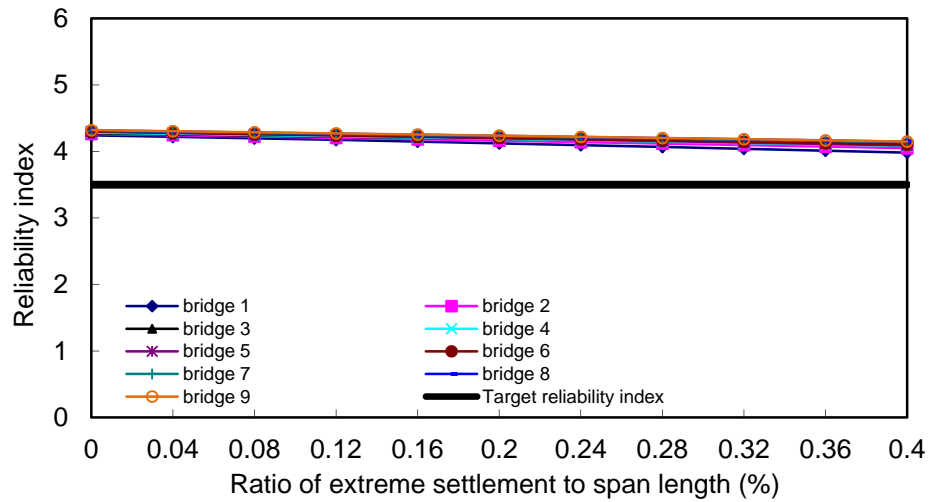
Figure 5.13 Reliability indices of 3-span bridges (No.12 to No.22 in Table 2.3): Case 4



(a) Reliability indices for negative moment



(b) Reliability indices for positive moment



(c) Reliability indices for shear

Figure 5.14 Reliability indices of 4-span bridges (No.23 to No.31 in Table 2.3): Case 4

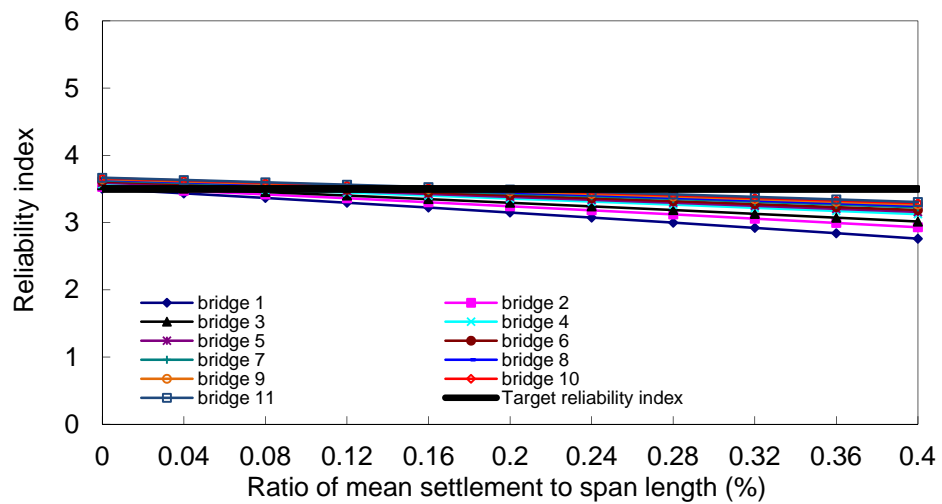
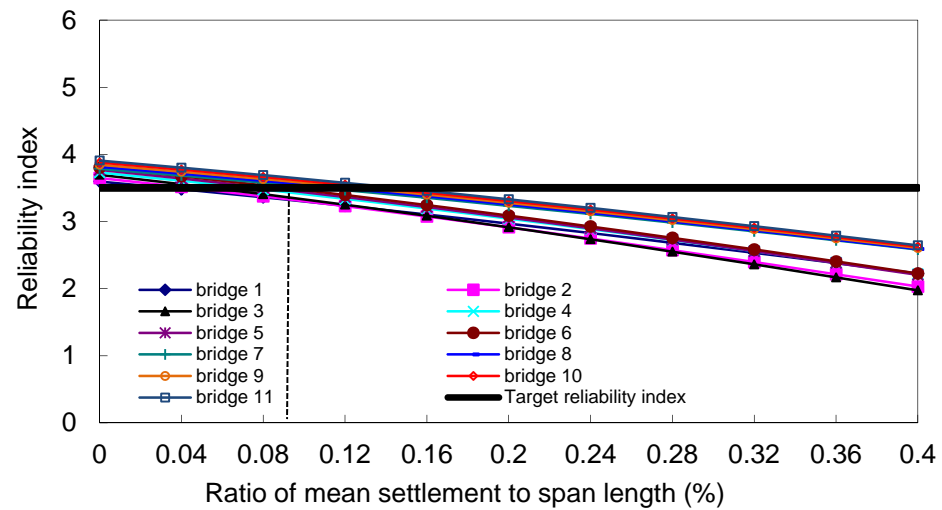
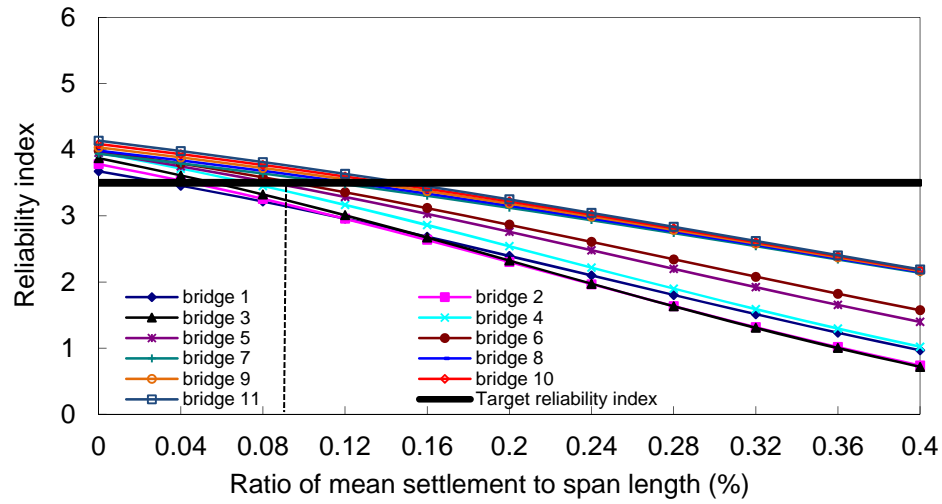
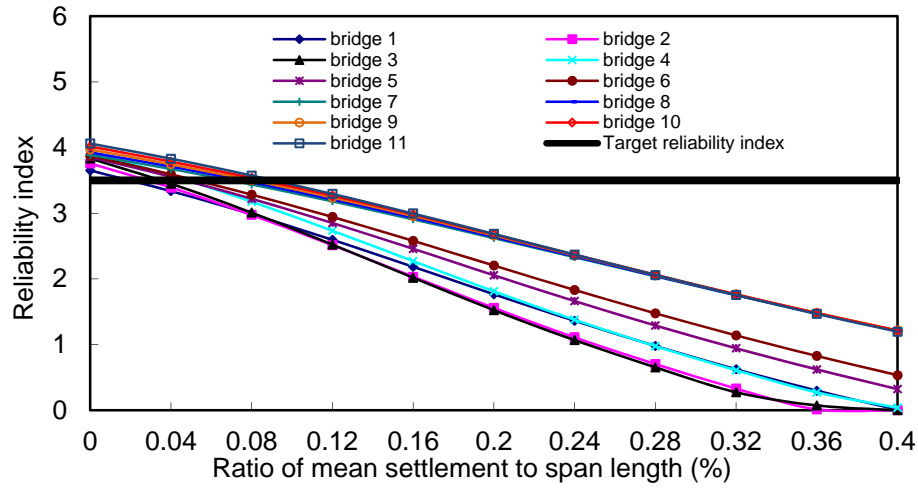
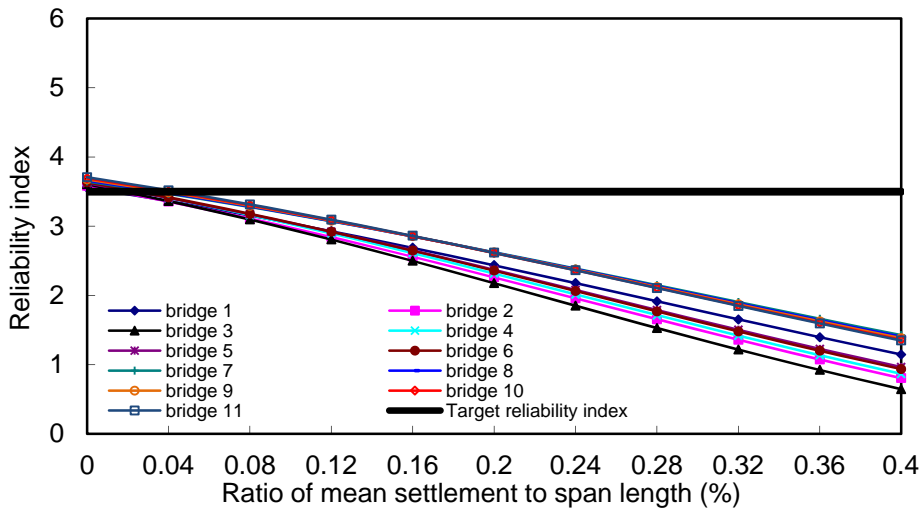


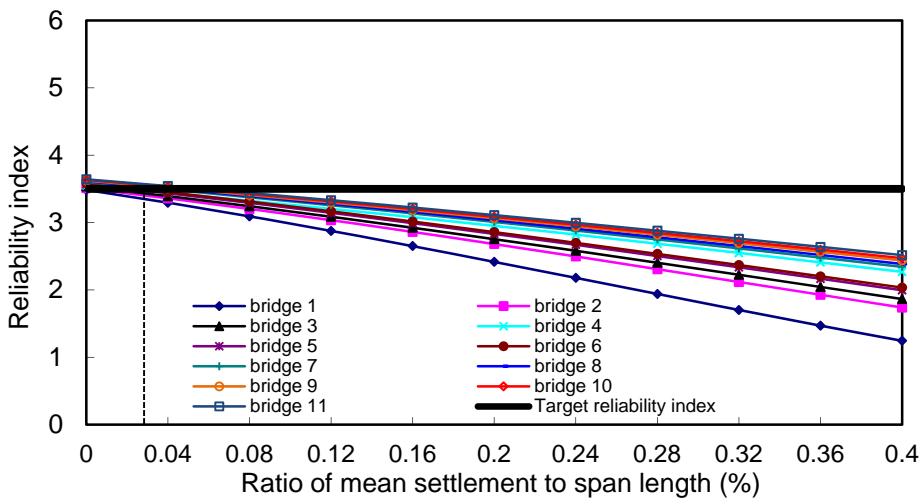
Figure 5.15 Reliability indices of 2-span bridges (No.1 to No.11 in Table 2.3): Case 5



(a) Reliability indices for negative moment

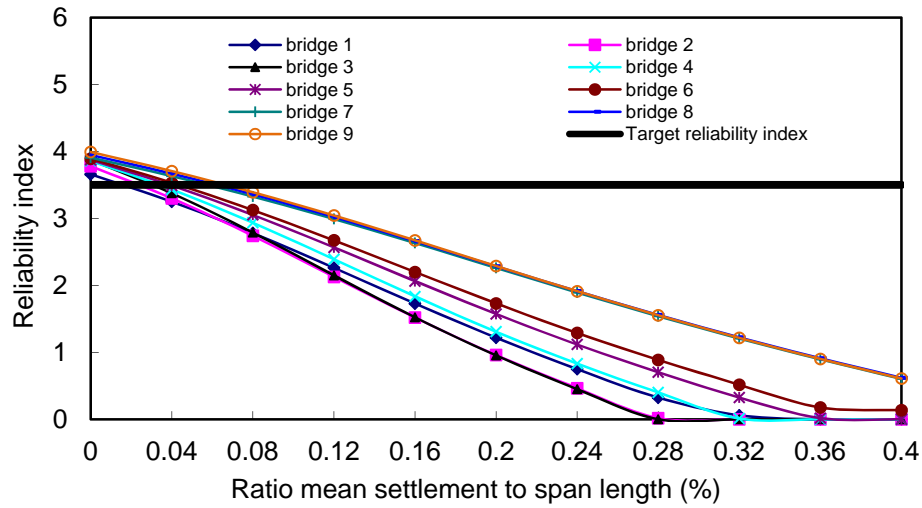


(b) Reliability indices for positive moment

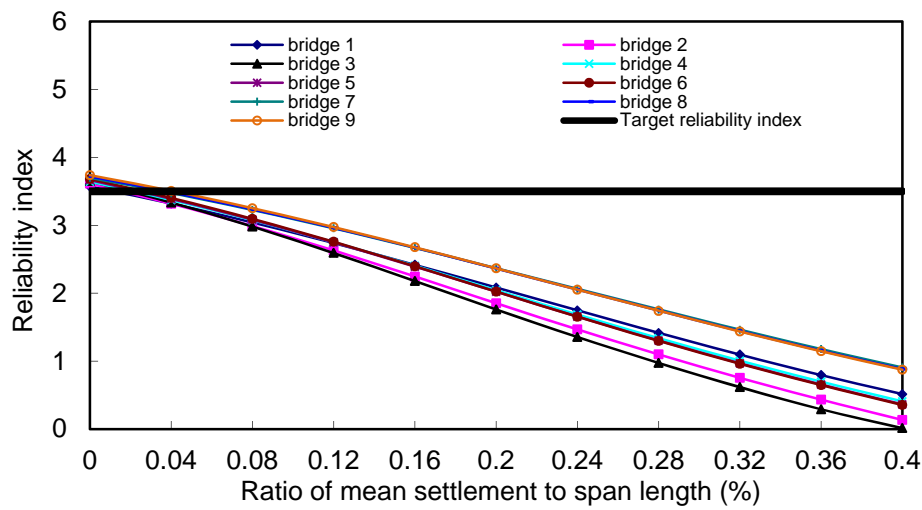


(c) Reliability indices for shear

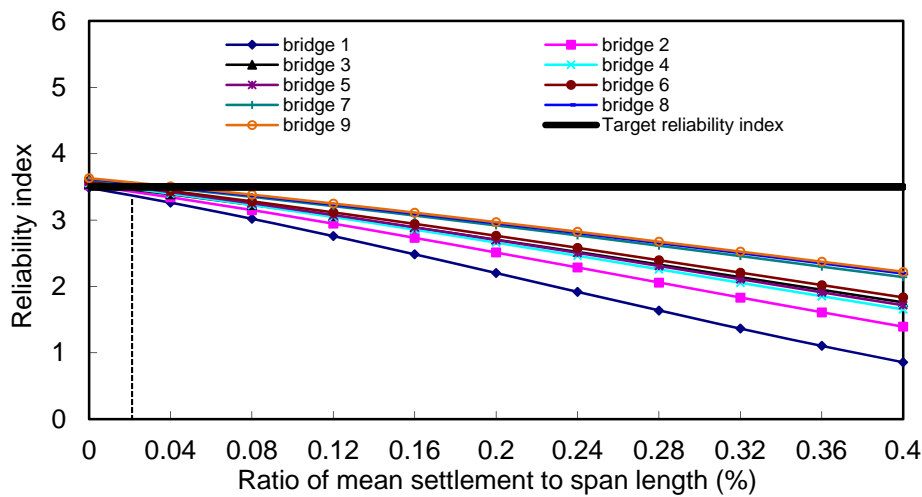
Figure 5.16 Reliability indices of 3-span bridges (No.12 to No.22 in Table 2.3): Case 5



(a) Reliability indices for negative moment

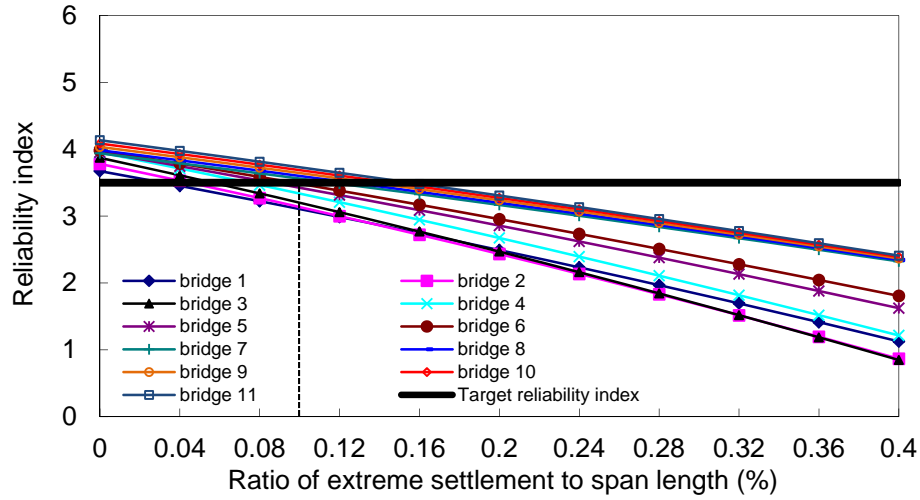


(b) Reliability indices for positive moment

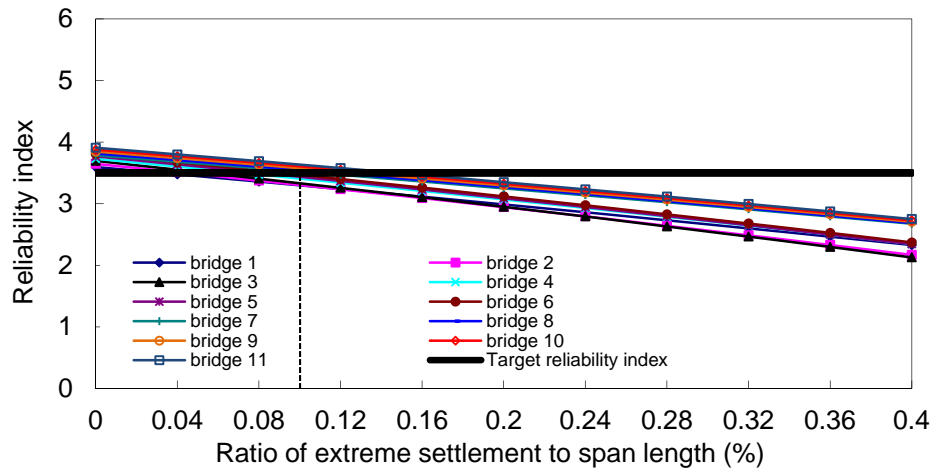


(c) Reliability indices for shear

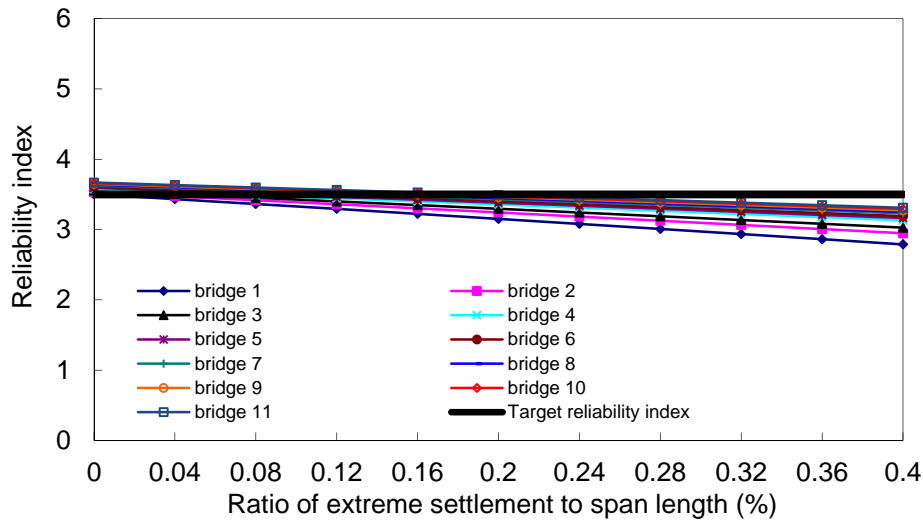
Figure 5.17 Reliability indices of 4-span bridges (No.23 to No.31 in Table 2.3): Case 5



(a) Reliability indices for negative moment

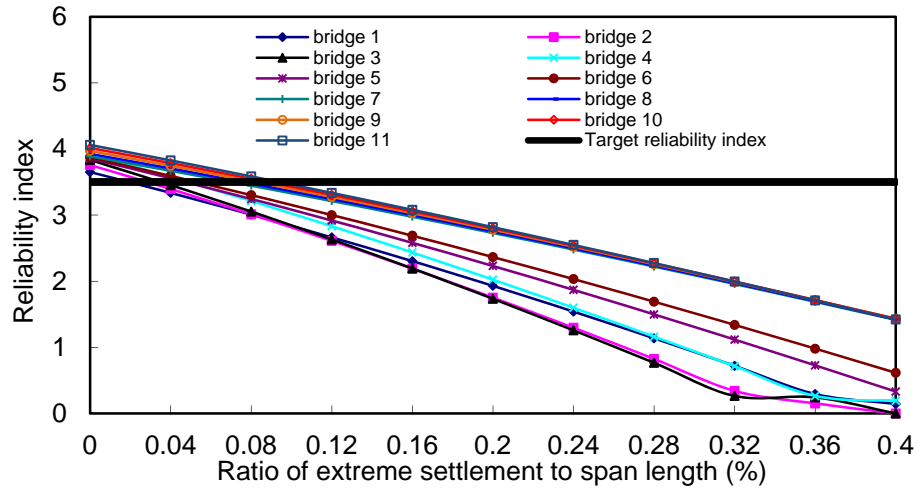


(b) Reliability indices for positive moment

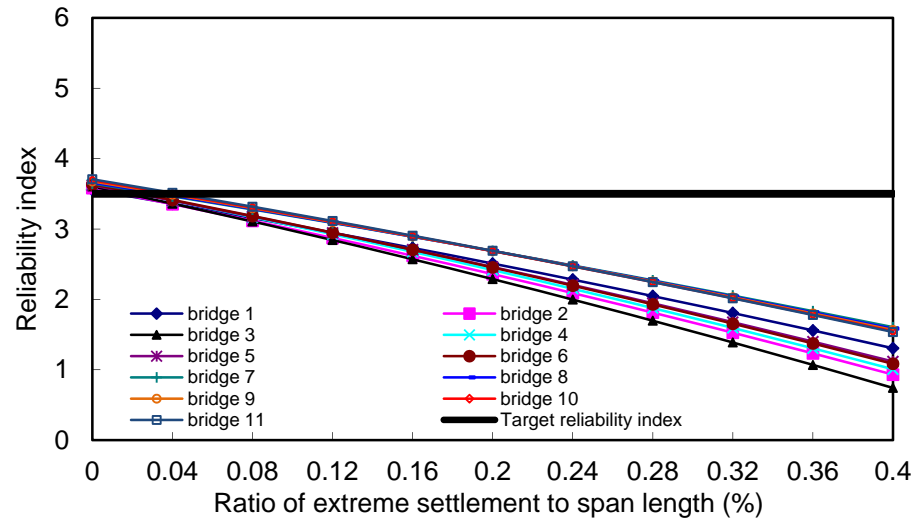


(c) Reliability indices for shear

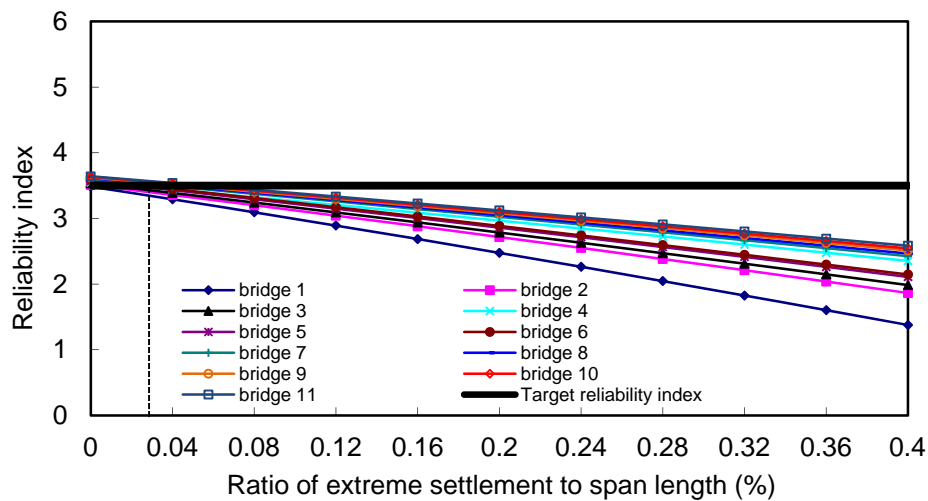
Figure 5.18 Reliability indices of 2-span bridges (No.1 to No.11 in Table 2.3): Case 6



(a) Reliability indices for negative moment

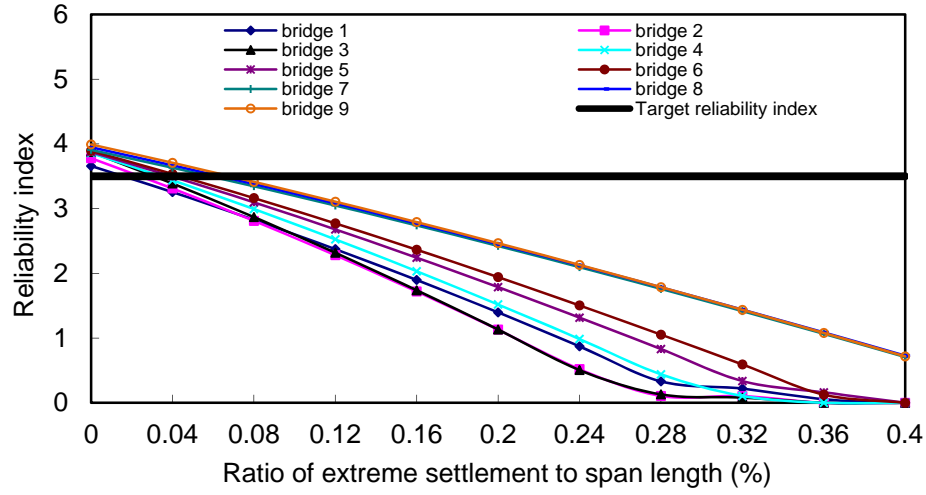


(b) Reliability indices for positive moment

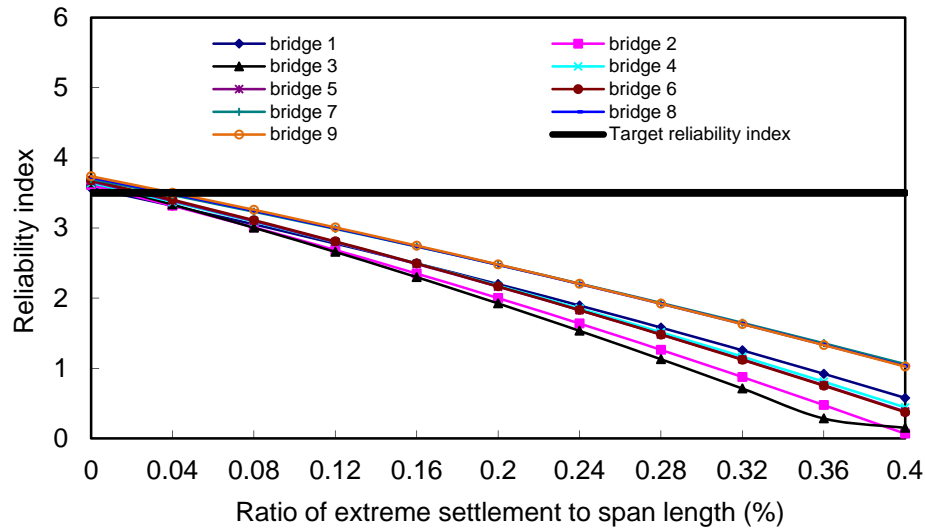


(c) Reliability indices for shear

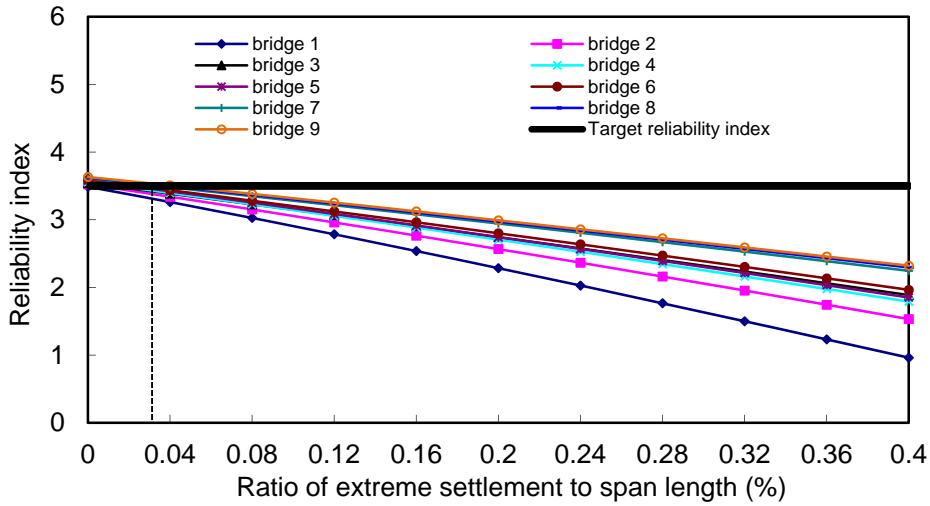
Figure 5.19 Reliability indices of 3-span bridges (No.12 to No.22 in Table 2.3): Case 6



(a) Reliability indices for negative moment



(b) Reliability indices for positive moment



(c) Reliability indices for shear

Figure 5.20 Reliability indices of 4-span bridges (No.23 to No.31 in Table 2.3): Case 6

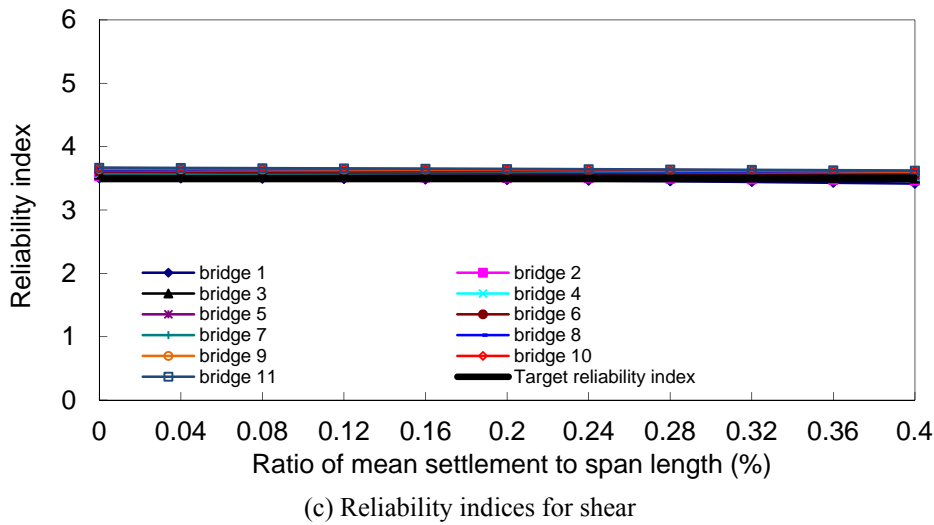
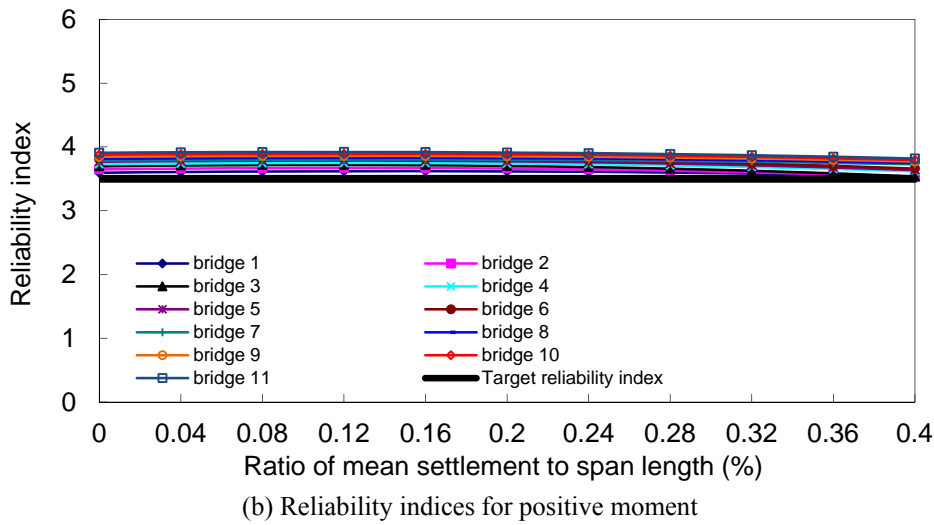
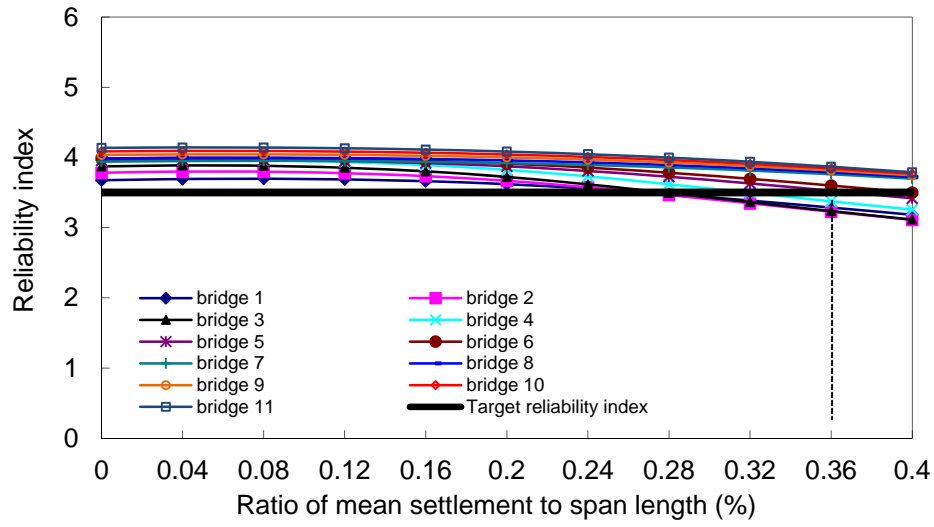
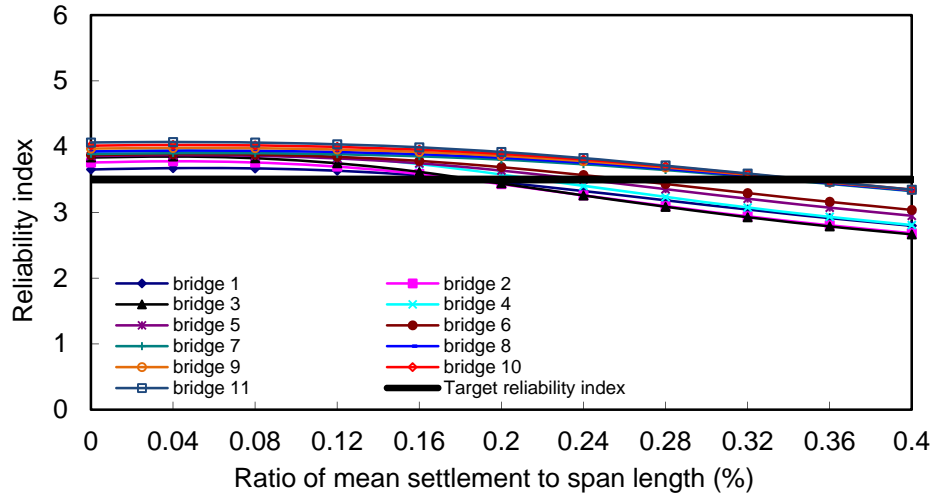
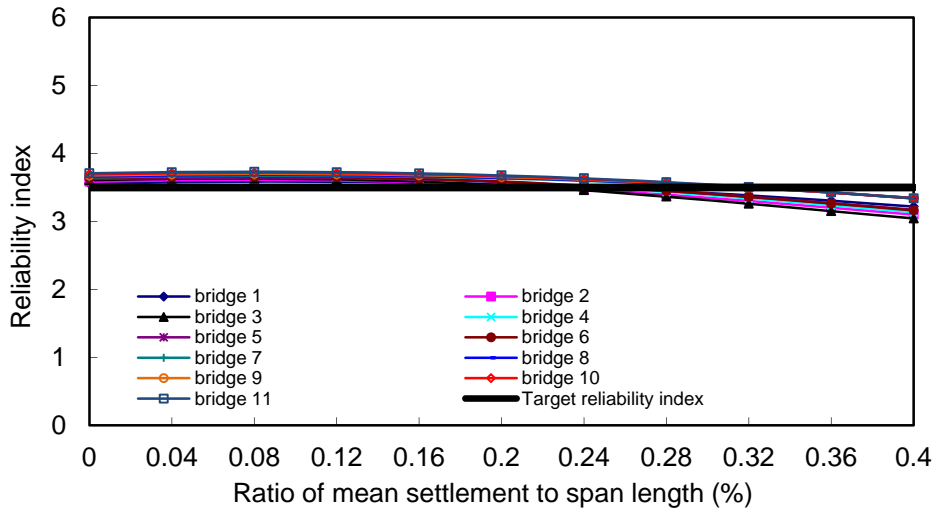


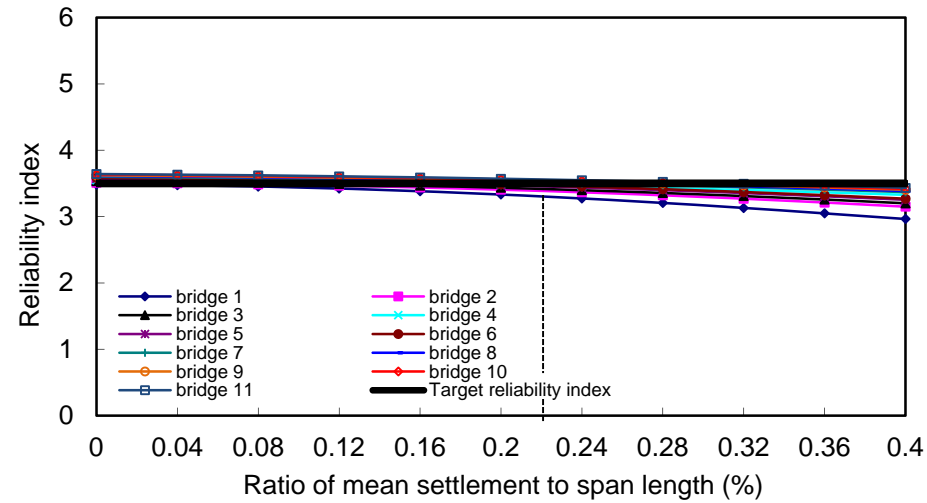
Figure 5.21 Reliability indices of 2-span bridges (No.1 to No.11 in Table 2.3): Case 7



(a) Reliability indices for negative moment

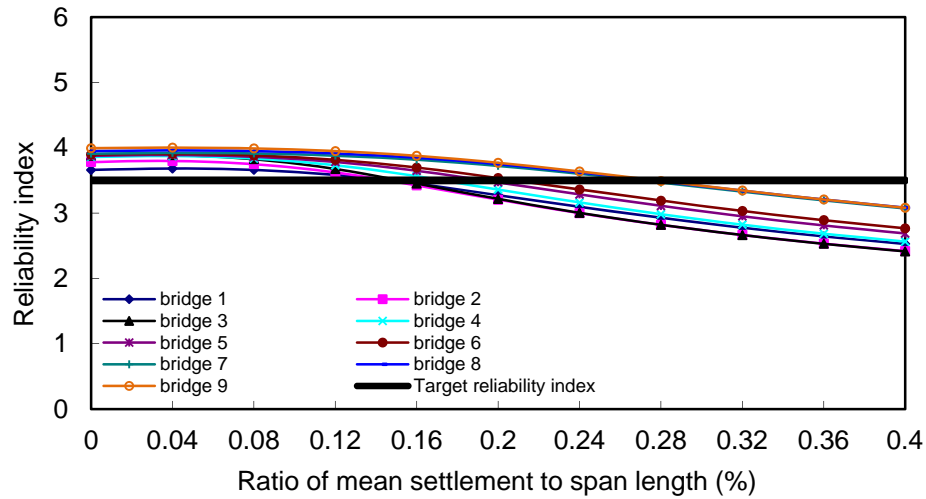


(b) Reliability indices for positive moment

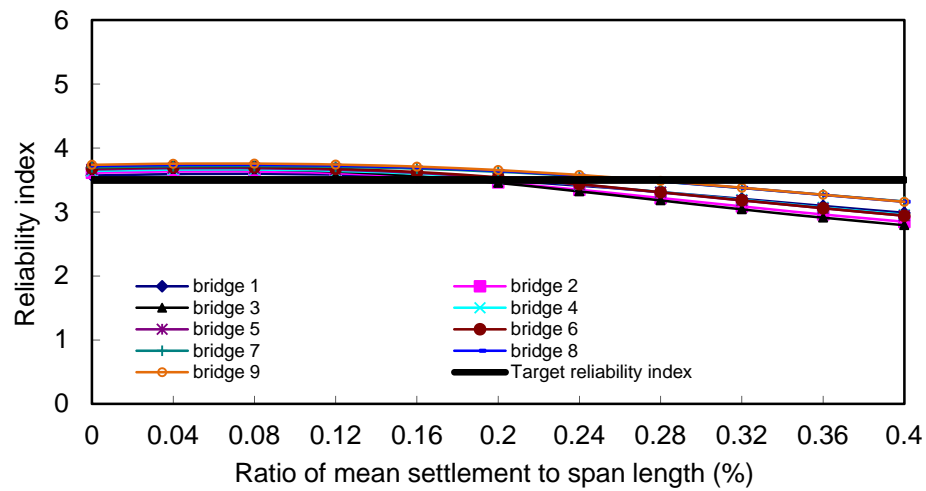


(c) Reliability indices for shear

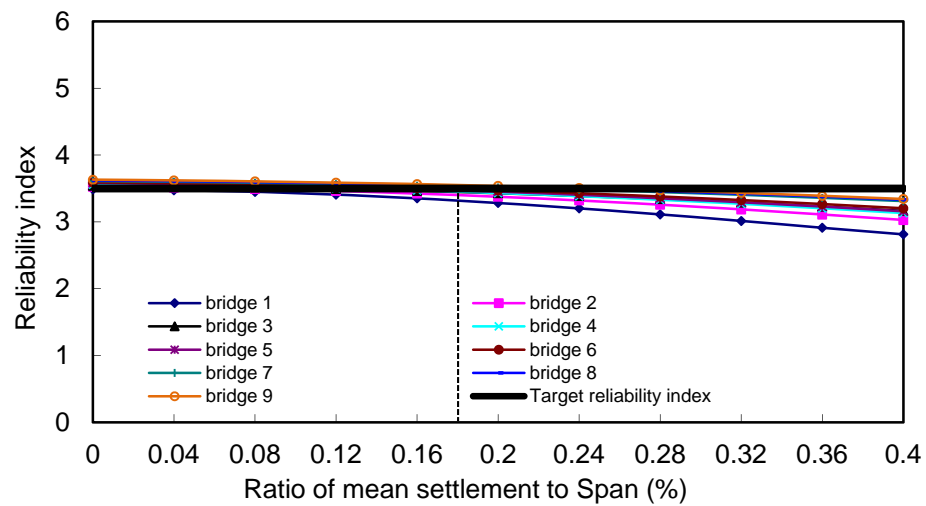
Figure 5.22 Reliability indices of 3-span bridges (No.12 to No.22 in Table 2.3): Case 7



(a) Reliability indices for negative moment

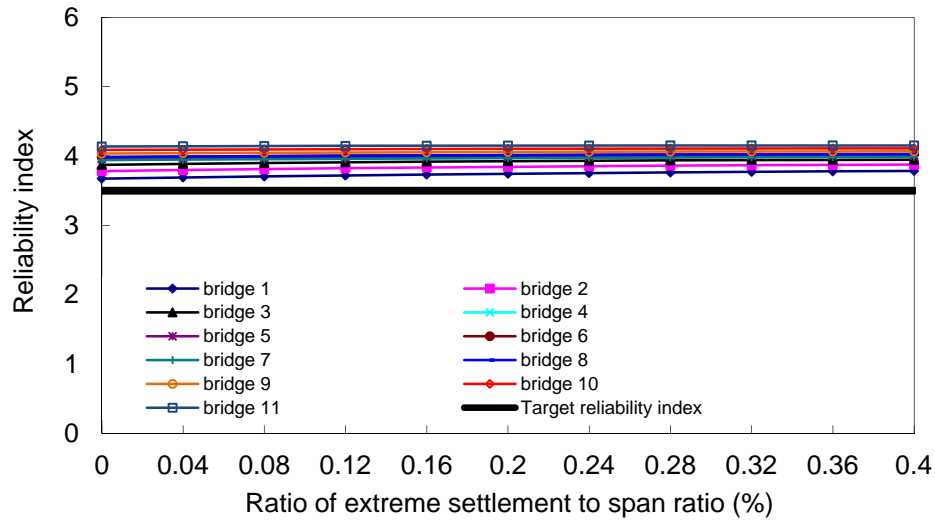


(b) Reliability indices for positive moment

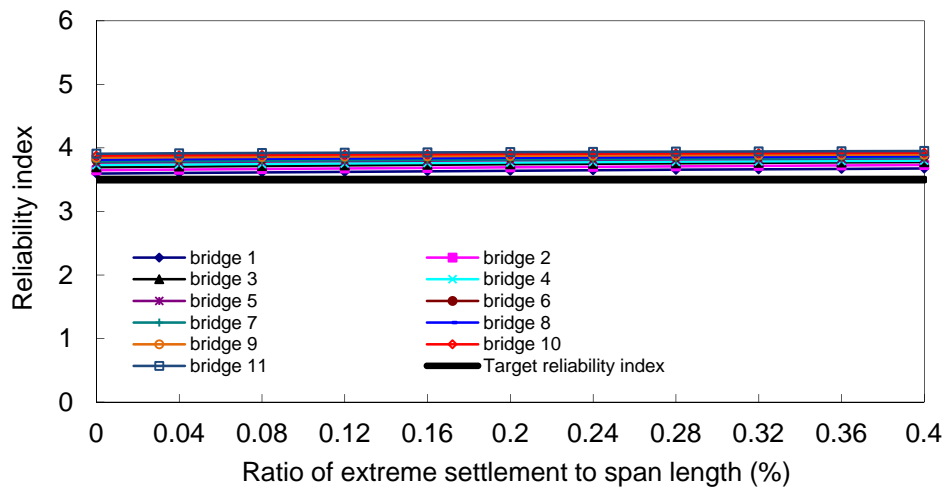


(c) Reliability indices for shear

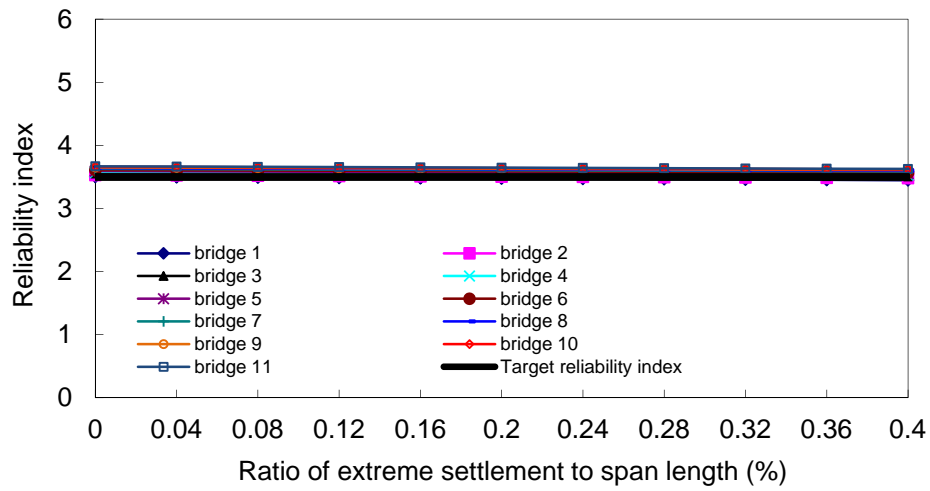
Figure 5.23 Reliability indices of 4-span bridges (No.23 to No.31 in Table 2.3): Case 7



(a) Reliability indices for negative moment

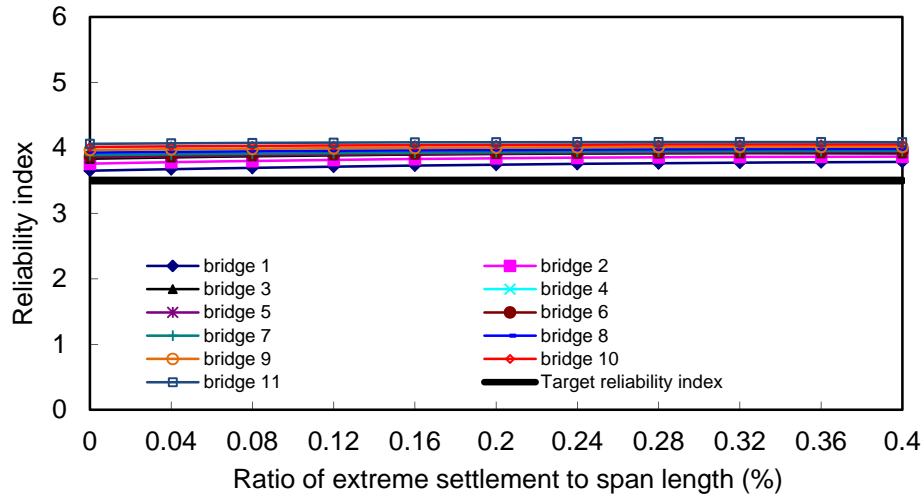


(b) Reliability indices for positive moment

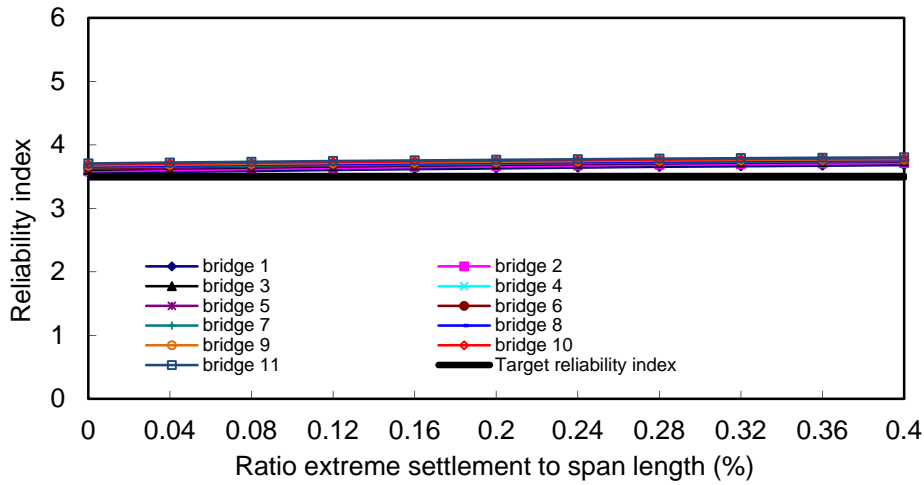


(c) Reliability indices for shear

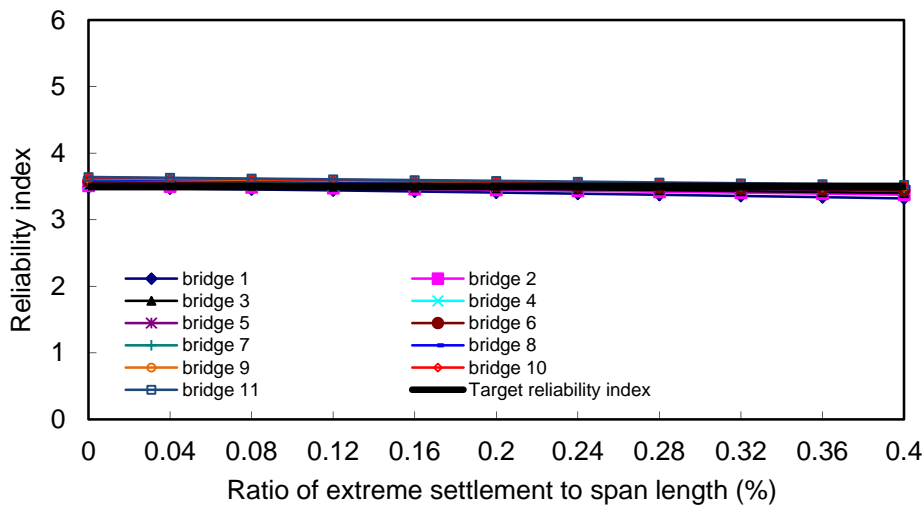
Figure 5.24 Reliability indices of 2-span bridges (No.1 to No.11 in Table 2.3): Case 8



(a) Reliability indices for negative moment

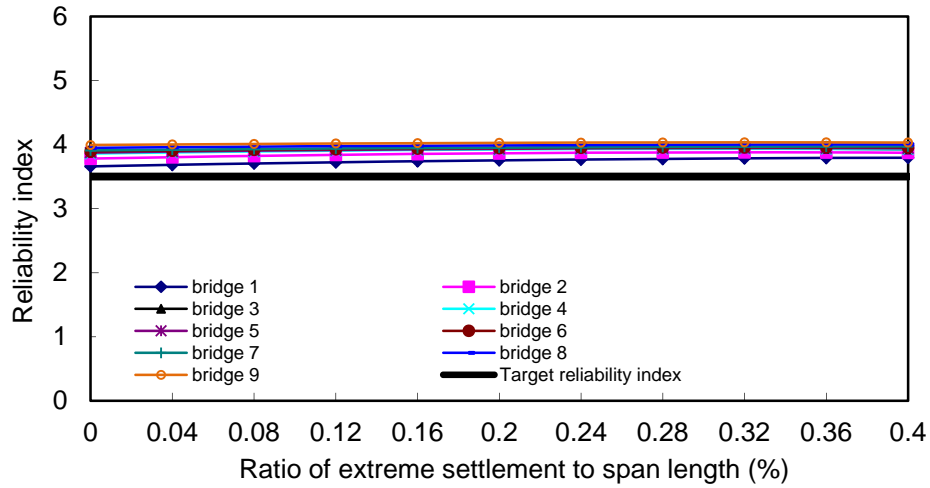


(b) Reliability indices for positive moment

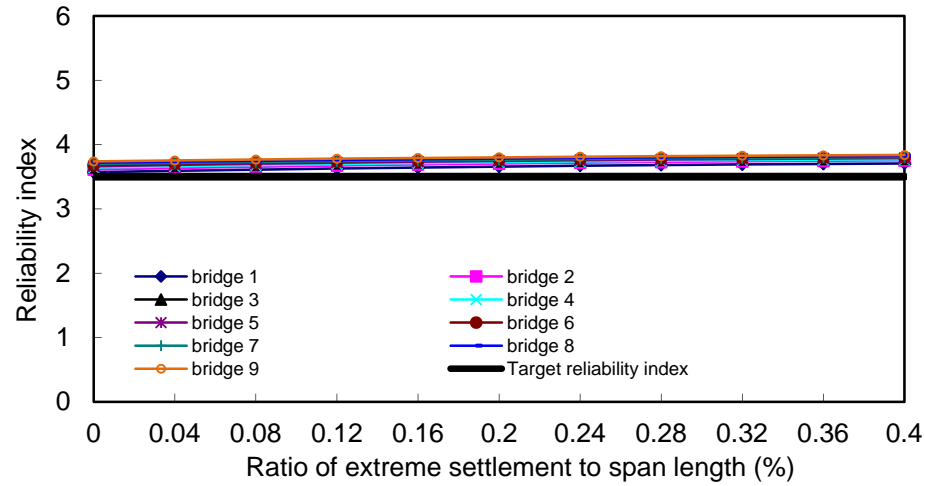


(c) Reliability indices for shear

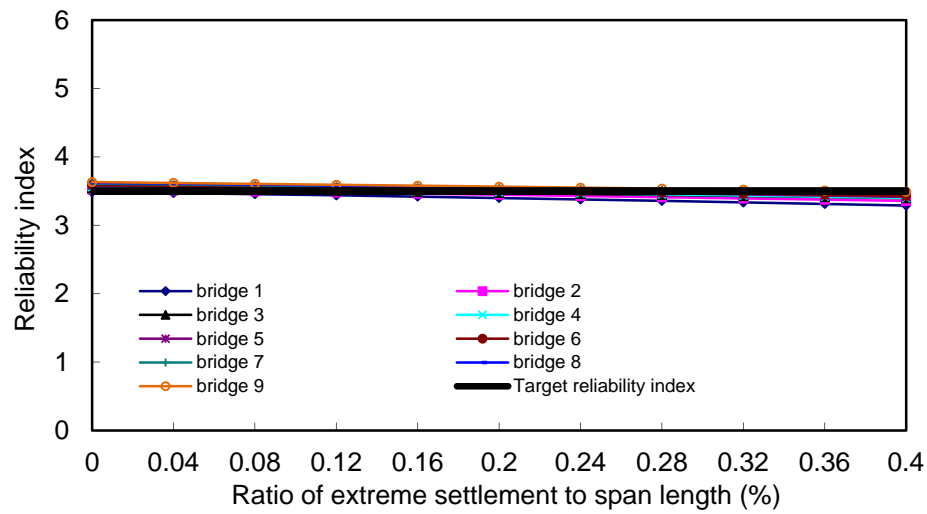
Figure 5.25 Reliability indices of 3-span bridges (No.12 to No.22 in Table 2.3): Case 8



(a) Reliability indices for negative moment



(b) Reliability indices for positive moment



(c) Reliability indices for shear

Figure 5.26 Reliability indices of 4-span bridges (No.23 to No.31 in Table 2.3): Case 8

The particular settlement of a bridge corresponding to a target reliability index of 3.5 is herein referred to as the tolerable settlement of the bridge under a certain design condition without requiring any settlement mitigation. For each case, type (2-span, 3-span, and 4-span), and parameter (positive moment, negative moment, and shear), the average value of the tolerable settlements less than $0.004L$ is presented in Table 5.12 in terms of span length and the overall control settlement for each case. Table 5.12 is represented in Table 5.13 to understand the average tolerable settlements in terms of span numbers, which corresponds to the vertical lines marked in Figures 5.3-5.26 if the average tolerable settlement is less than $0.004L$. By comparing with Table 5.12, Table 5.13 indicates that the tolerable settlement for 2-span bridges is slightly larger.

Table 5.12 Average tolerable settlements of new bridges in terms of loading effects

Tolerable Settlement (% of Span Length)		Without Live Load Reduction Factor				With Live Load Reduction Factor			
		Case 1	Case 2	Case 3	Case 4	Case 5	Case 6	Case 7	Case 8
Settlement effect on negative moment	2-span	0.36	0.39	0.4	0.4	0.09	0.1	0.36	0.4
	3-span	0.26	0.34	0.4	0.4	0.06	0.06	0.27	0.4
	4-span	0.21	0.28	0.4	0.4	0.04	0.04	0.22	0.4
	Minimum	0.21	0.28	0.4	0.4	0.04	0.04	0.22	0.4
Settlement effect on positive moment	2-span	0.4	0.4	0.4	0.4	0.09	0.1	0.4	0.4
	3-span	0.35	0.4	0.4	0.4	0.04	0.04	0.28	0.4
	4-span	0.28	0.34	0.4	0.4	0.04	0.04	0.24	0.4
	Minimum	0.28	0.34	0.4	0.4	0.04	0.04	0.24	0.4
Settlement effect on shear	2-span	0.4	0.4	0.4	0.4	0.11	0.11	0.4	0.4
	3-span	0.26	0.27	0.4	0.4	0.03	0.03	0.22	0.4
	4-span	0.21	0.22	0.4	0.4	0.02	0.03	0.18	0.4
	Minimum	0.21	0.22	0.4	0.4	0.02	0.03	0.18	0.4
Control tolerable settlement		0.21	0.22	0.4	0.4	0.02	0.03	0.18	0.4

Table 5.13 Average tolerable settlements of new bridges in terms of bridge span numbers

Tolerable Settlement (% of Span Length)		Without Live Load Reduction Factor				With Live Load Reduction Factor			
		Case 1	Case 2	Case 3	Case 4	Case 5	Case 6	Case 7	Case 8
2-span	Negative moment	0.36	0.39	0.4	0.4	0.09	0.1	0.36	0.4
	Positive moment	0.4	0.4	0.4	0.4	0.09	0.1	0.4	0.4
	Shear	0.4	0.4	0.4	0.4	0.11	0.11	0.4	0.4
	Minimum	0.36	0.39	0.4	0.4	0.09	0.1	0.36	0.4
3-span	Negative moment	0.26	0.34	0.4	0.4	0.06	0.06	0.27	0.4
	Positive moment	0.35	0.4	0.4	0.4	0.04	0.04	0.28	0.4
	Shear	0.26	0.27	0.4	0.4	0.03	0.03	0.22	0.4
	Minimum	0.26	0.27	0.4	0.4	0.03	0.03	0.22	0.4
4-span	Negative moment	0.21	0.28	0.4	0.4	0.04	0.04	0.22	0.4
	Positive moment	0.28	0.34	0.4	0.4	0.04	0.04	0.24	0.4
	Shear	0.21	0.22	0.4	0.4	0.02	0.03	0.18	0.4
	Minimum	0.21	0.22	0.4	0.4	0.02	0.03	0.18	0.4

The results presented in Figures 5.3 – 5.26 and summarized in Tables 5.12 and 5.13 leads to the following observations:

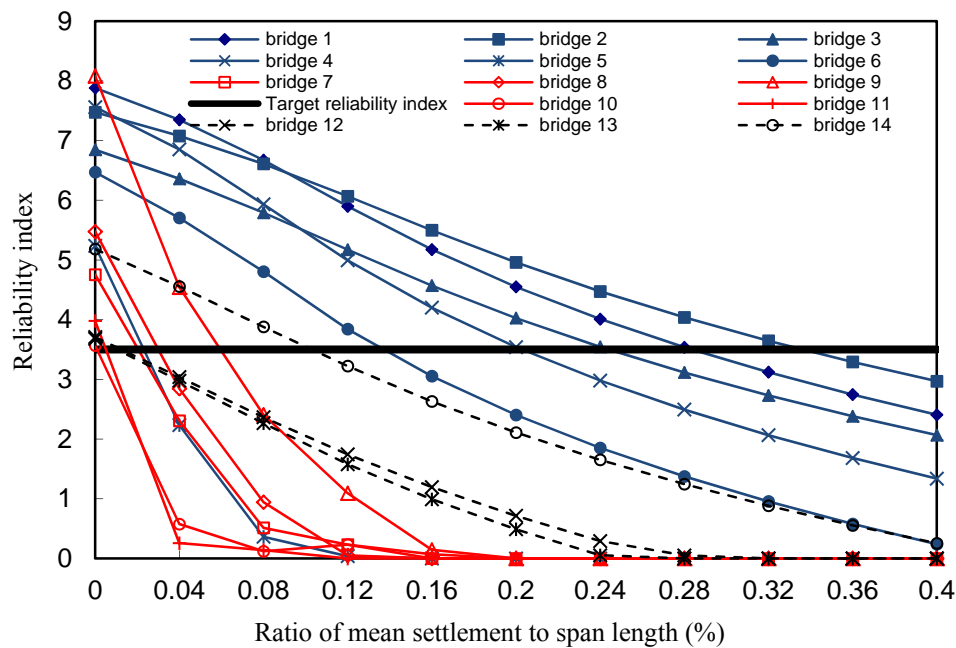
- (1) For bridges with the same number of spans, the minimum moment of inertia (I) to meet serviceability and strength requirements increases with span length, as shown in Figure 2.18. However, the settlement-induced moment is inversely proportional to L^2 as indicated by Eq. (2.1). The end effect of settlement on positive and negative moments depends upon I/L^2 . For shear, the settlement effect is a function of I/L^3 . Therefore, while the reliability indices for positive and negative moments increase with the increasing of span length, the reliability indices for shear are sometimes high for very short spans such as 20 ft.
- (2) As the number of spans increases, the moment and shear distributions under dead and live loads change and, more importantly, they become more sensitive to support settlement. Therefore, the average tolerable settlement is controlled by 4-span bridges.
- (3) When settlement is defined as a random variable with a mean value and a given COV = 0.25, the average tolerable settlements (represented by the mean of the random variable) in all cases are between 50% and 100% of their corresponding values when settlement is defined as an extreme value, as mostly demonstrated by comparing Cases 1 with 2, and by comparing Cases 7 with 8. This is because sample settlements can be larger than the mean settlement.
- (4) The maximum settlement-induced moment always occurs at supports, which coincides with the location of the maximum negative moment. Therefore, the reliability index for negative moment is more sensitive to differential settlement effects than positive moment, which is slightly smaller in all cases.
- (5) The reliability index for shear controls the average tolerable settlement of short span bridges because shear is more sensitive to support settlement than positive and negative moments for very short spans.
- (6) Cases 2 and 6 represent the current and potentially future MoDOT design practices using extreme settlement when settlement is not considered in design. Their tolerable settlements are $L/450$ and $L/3500$, respectively. When a bridge settles more than the tolerable settlement, the actual settlement is either taken into account in design phase to further check its impact on the reliability of bridge superstructures or mitigated by proper measures in foundation designs such as the use of oversized foundations.
- (7) Cases 4 and 8 represent the current AASHTO design practice and potentially future MoDOT design practices using extreme settlement when settlement is considered in design. The average tolerable settlements in both cases reach the AASHTO recommended limit of $L/250$.
- (8) Cases 3 and 4 include the unreduced live load and settlement in design. Their tolerable settlement is always equal to the AASHTO recommended settlement limit. Therefore, bridge designs using the current AASHTO design practice is adequate without special foundation requirements. On the other hand, Cases 5 and 6 include no settlement but the reduced live load in design. These cases substantially reduce the resistance of girders, resulting in a very small tolerable settlement ($L/3500$) for all bridges.
- (9) The tolerable settlements in this section are applicable to steel-girder bridges with equal spans. Those for bridges with unequal spans are discussed from the reliability evaluation of 14 existing bridges in Section 5.4.

5.4 Reliability Indices of 14 Existing Bridges

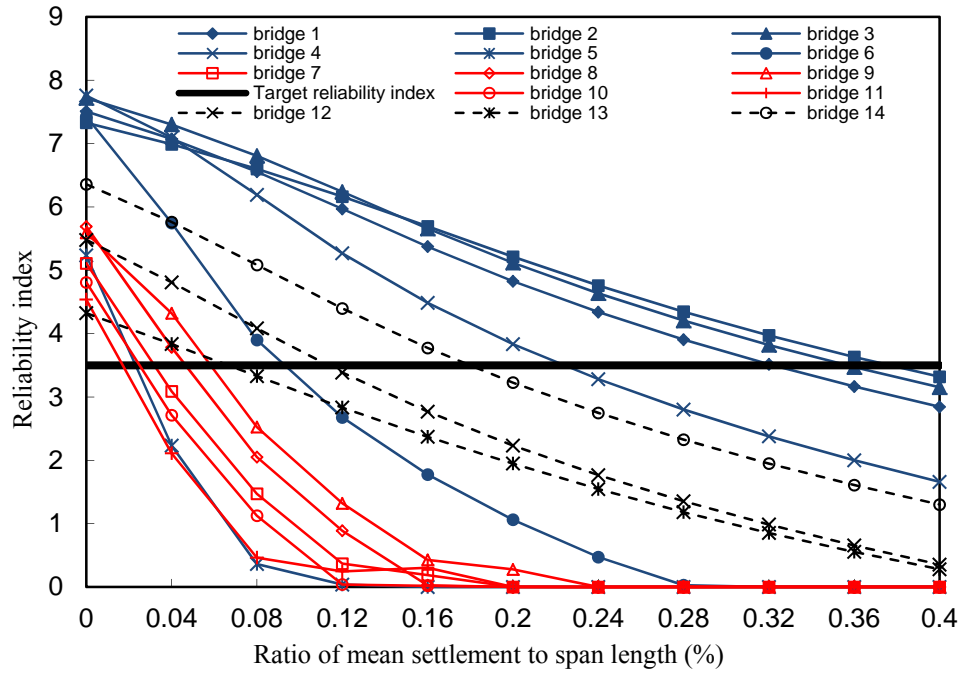
Section 5.3 only investigates the reliability of new steel-girder bridges that are designed based on the minimum moment of inertia requirements by the moment strength and girder deflection as stipulated in the AASHTO Specifications (2007). To compare the levels of tolerable settlement for various types of bridges, the 14 existing bridges (6 steel-girder, 5 prestressed concrete girder, and 3 slab bridges) are evaluated in Section 5.4.1 with the use of minimum required factored shear and moment resistances as did in Section 5.3 and in Section 5.4.2 with the use of actual positive and negative moment strengths. For steel-girder bridges, the results in Section 5.4.1 can also shed light on the tolerable settlement for continuous structures with unequal spans. The difference between Section 5.4.1 and Section 5.3 is the use of actual moments of inertia in the existing bridges.

5.4.1 Based on minimum resistances

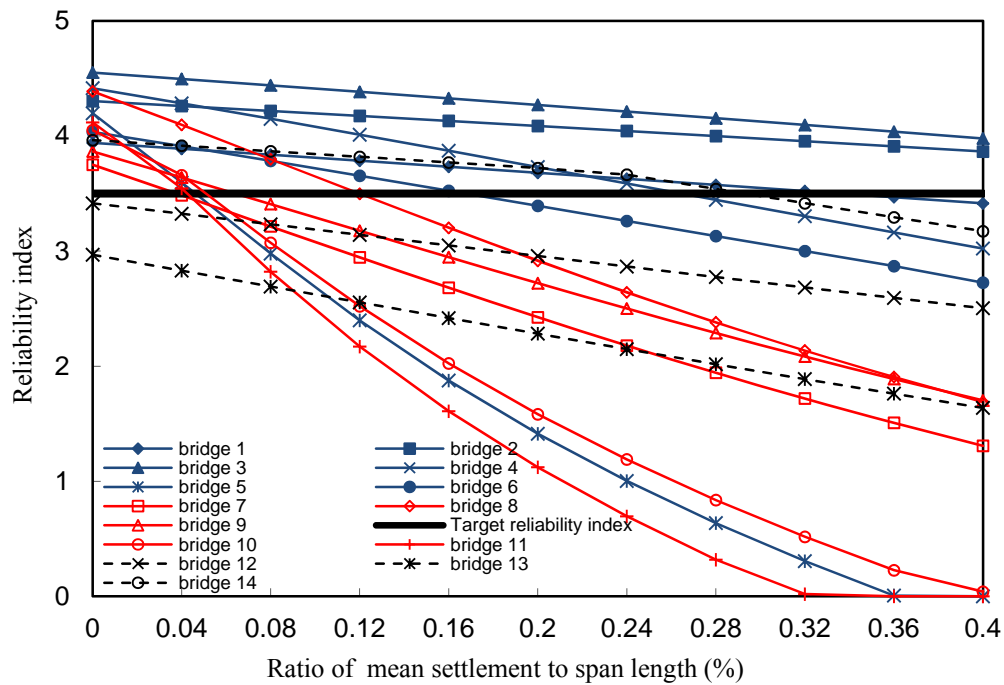
Like Section 5.3, the reliability indices of each of the 8 cases were analyzed for negative moment, positive moment, and shear force. They are presented in Figures 5.27 – 5.34. In each figure, the solid lines with unfilled and plus symbols and the remaining solid lines represent prestressed concrete-girder and steel-girder bridges, respectively. The dotted lines are for slab bridges. The target reliability index is represented by a heavy solid line. The average tolerable settlement for each type of the 14 existed bridges was determined and summarized in Table 5.14 for 8 cases.



(a) Reliability indices for negative moment

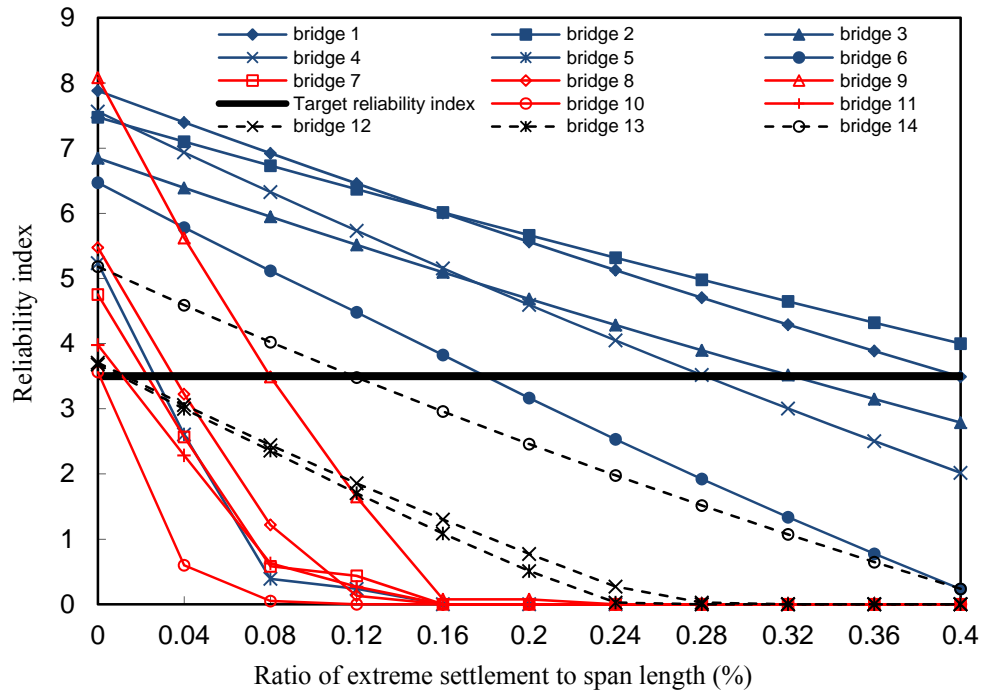


(b) Reliability indices for positive moment

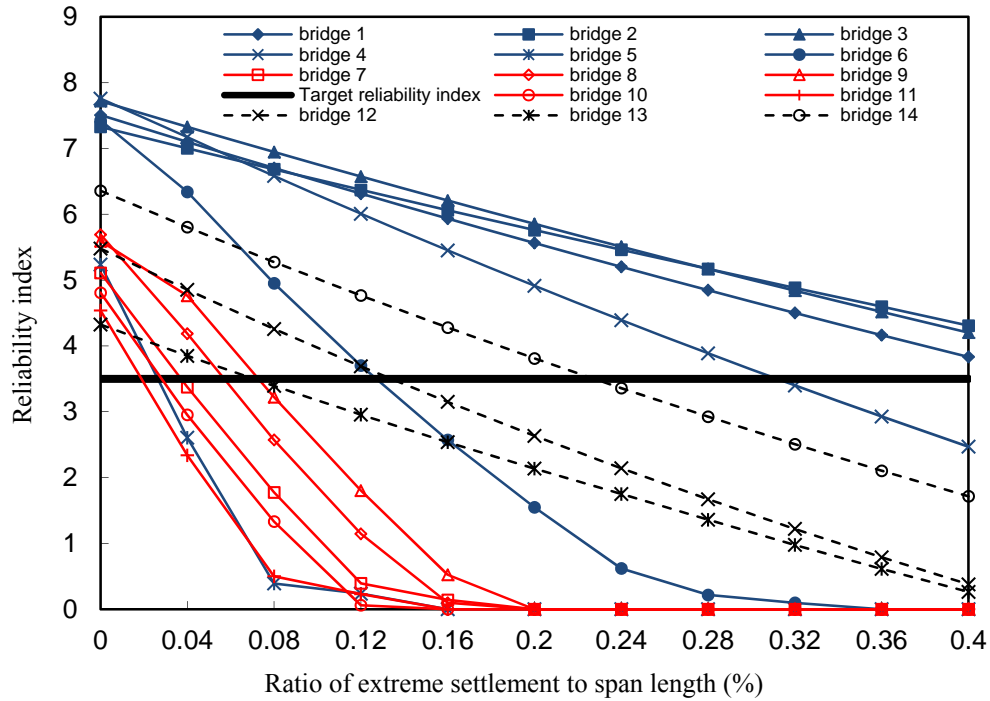


(c) Reliability indices for shear

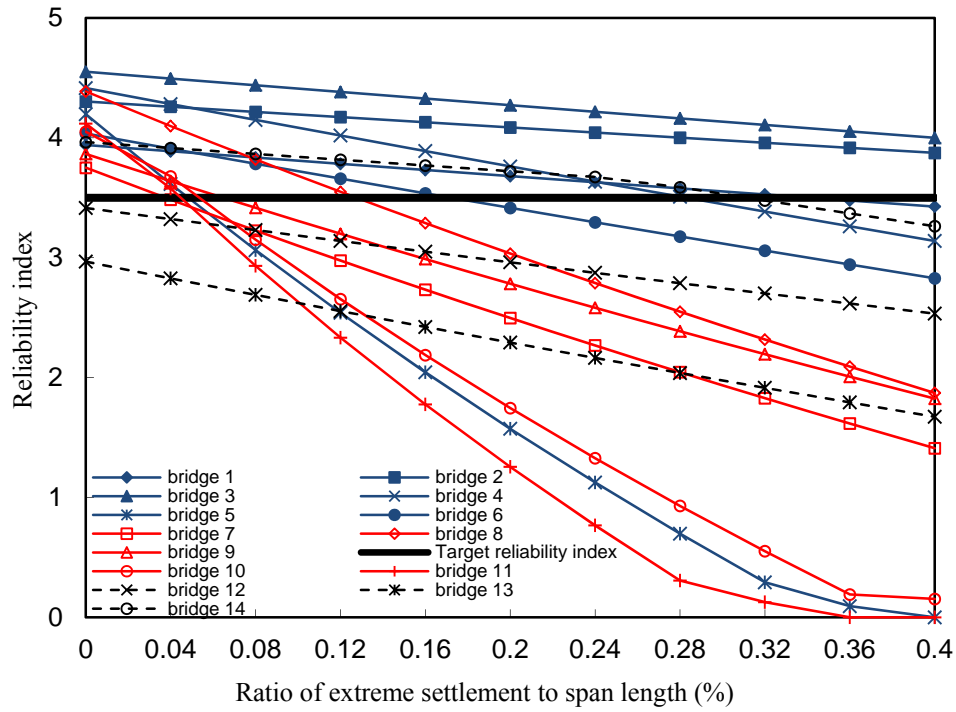
Figure 5.27 Reliability indices of 14 existing bridges: Case 1



(a) Reliability indices for negative moment

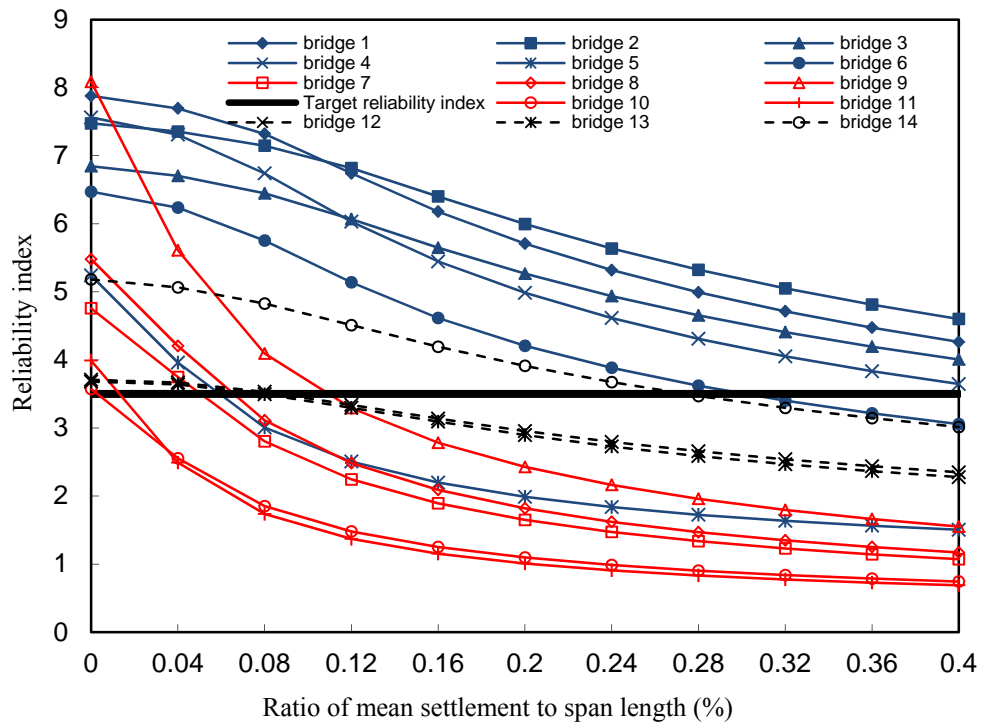


(b) Reliability indices for positive moment

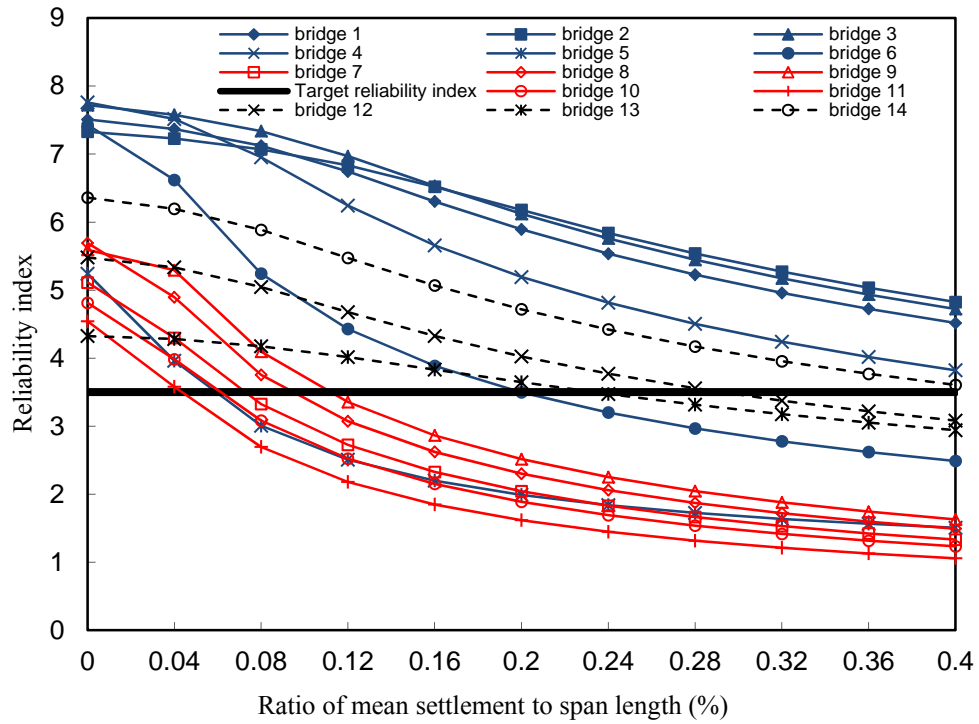


(c) Reliability indices for shear

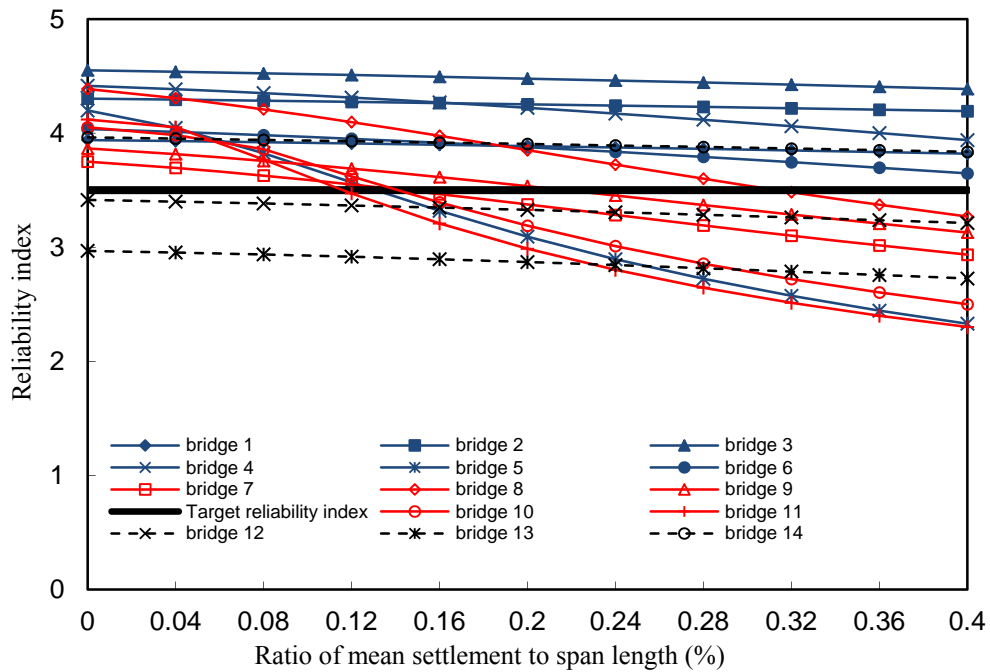
Figure 5.28 Reliability indices of 14 existing bridges: Case 2



(a) Reliability indices for negative moment

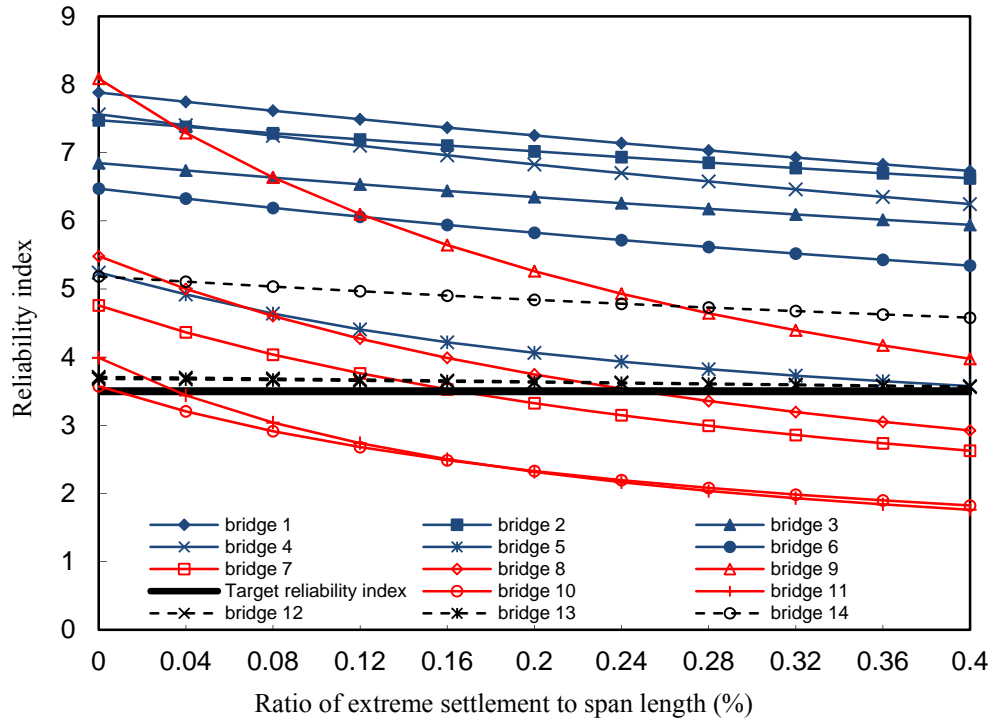


(b) Reliability indices for positive moment

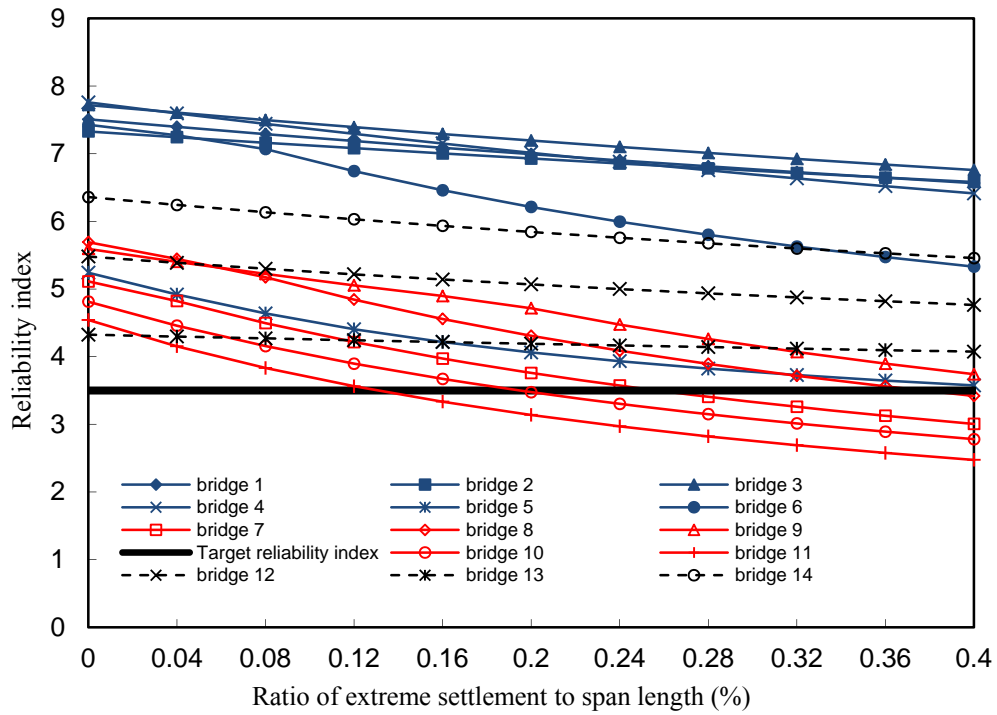


(c) Reliability indices for shear

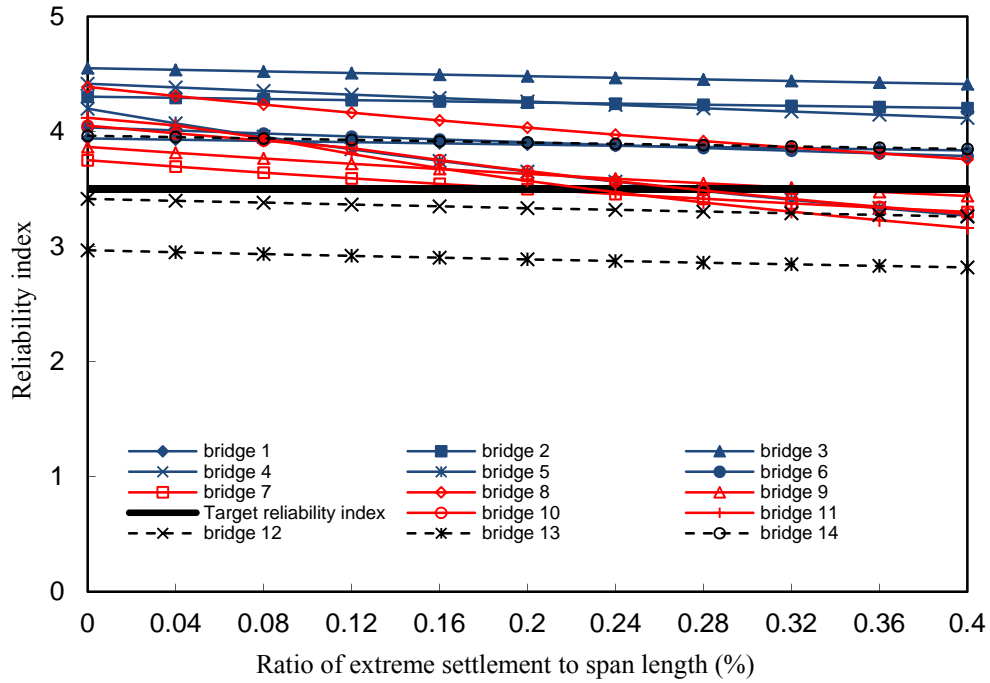
Figure 5.29 Reliability indices of 14 existing bridges: Case 3



(a) Reliability indices for negative moment

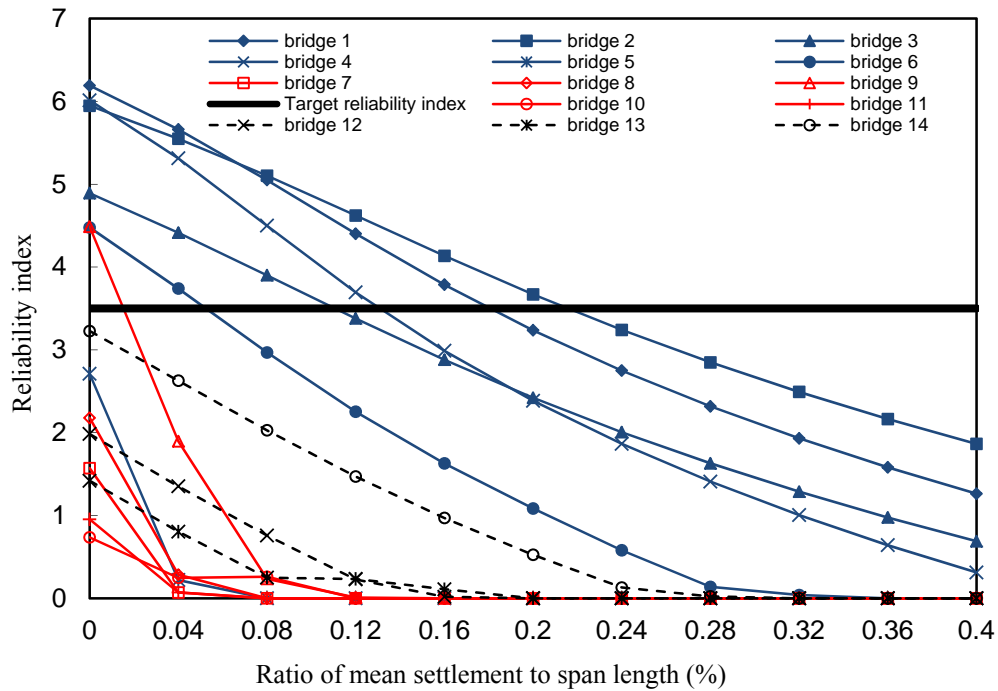


(b) Reliability indices for positive moment

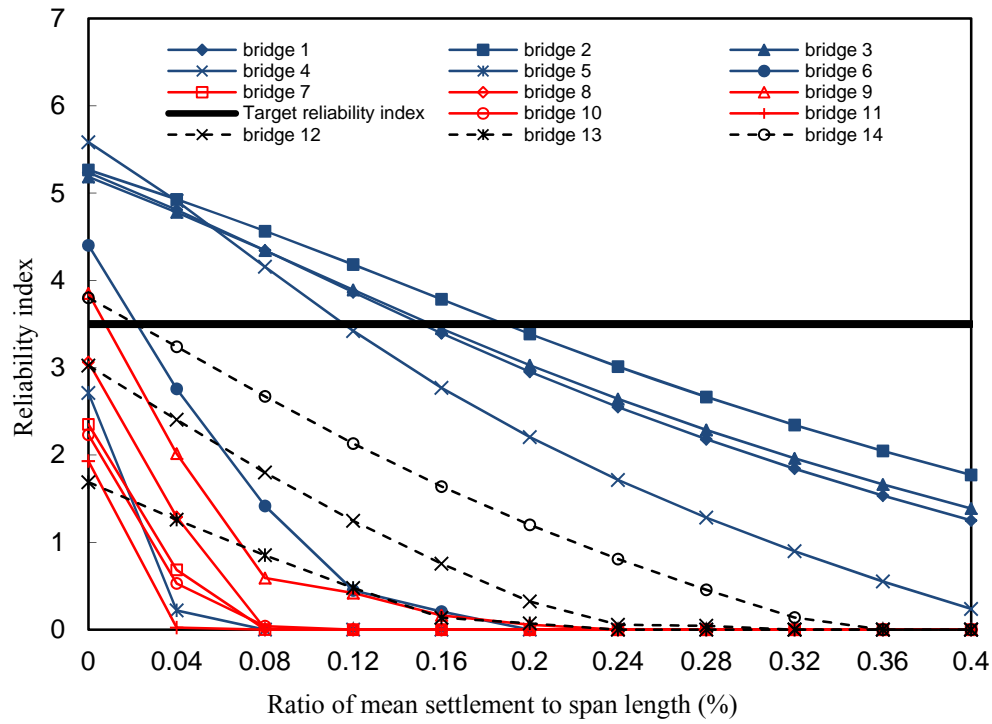


(c) Reliability indices for shear

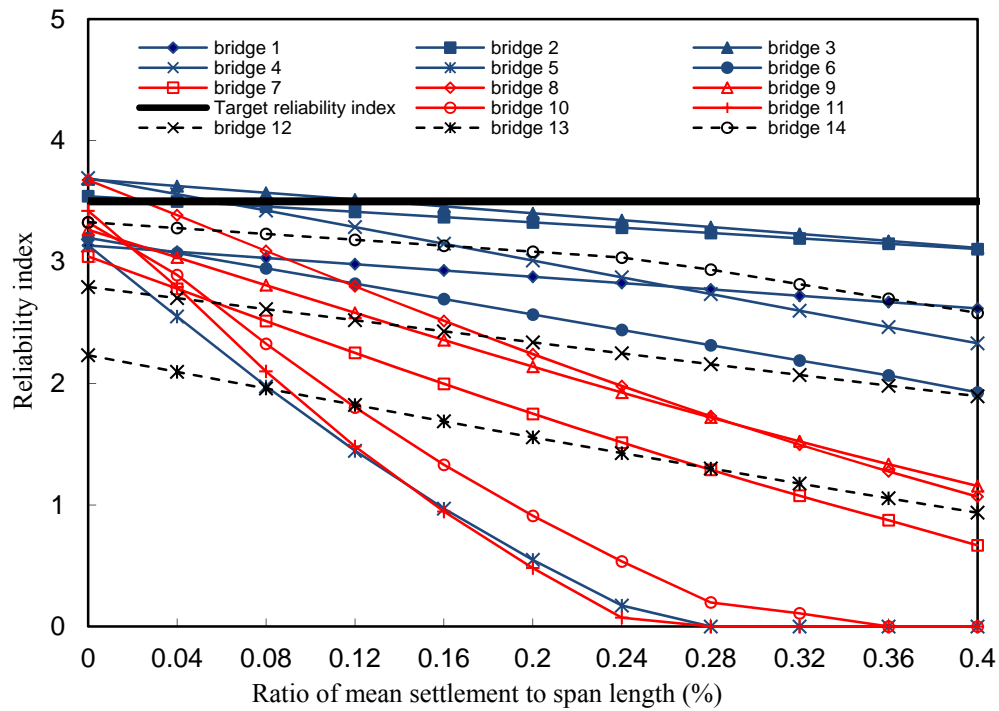
Figure 5.30 Reliability indices of 14 existing bridges: Case 4



(a) Reliability indices for negative moment

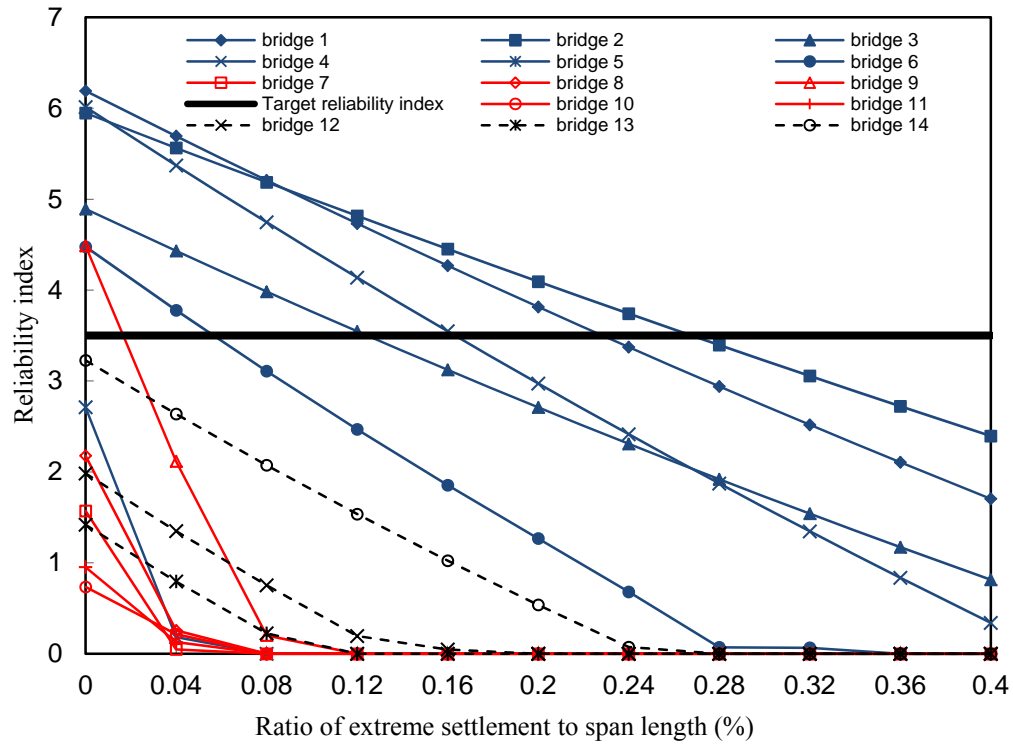


(b) Reliability indices for positive moment

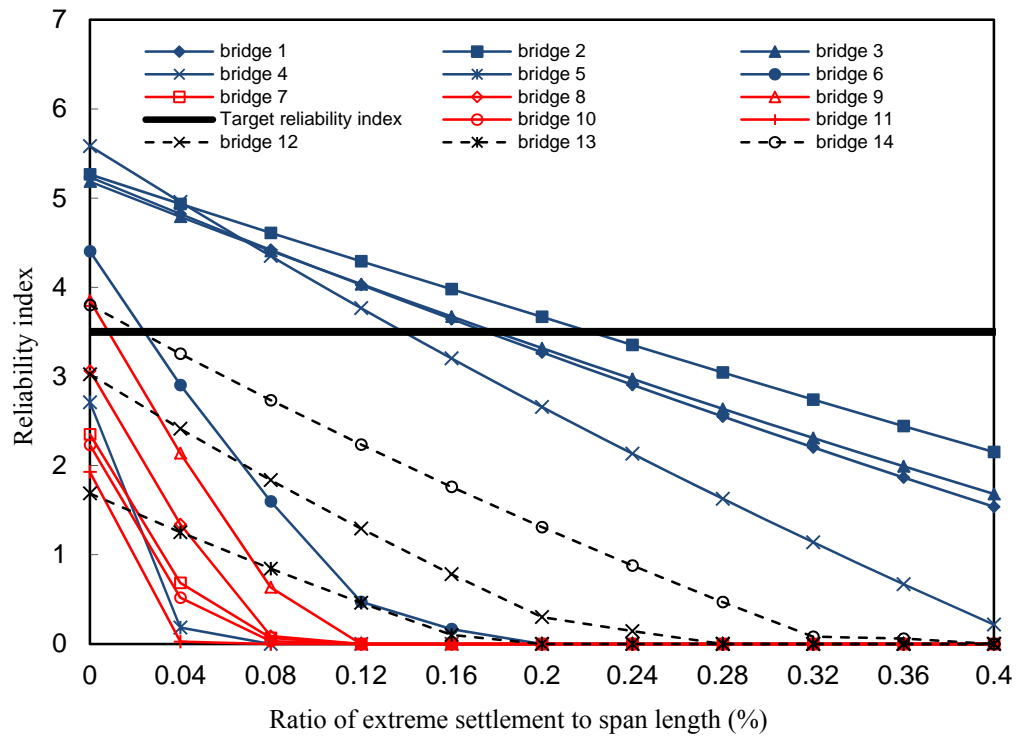


(c) Reliability indices for shear

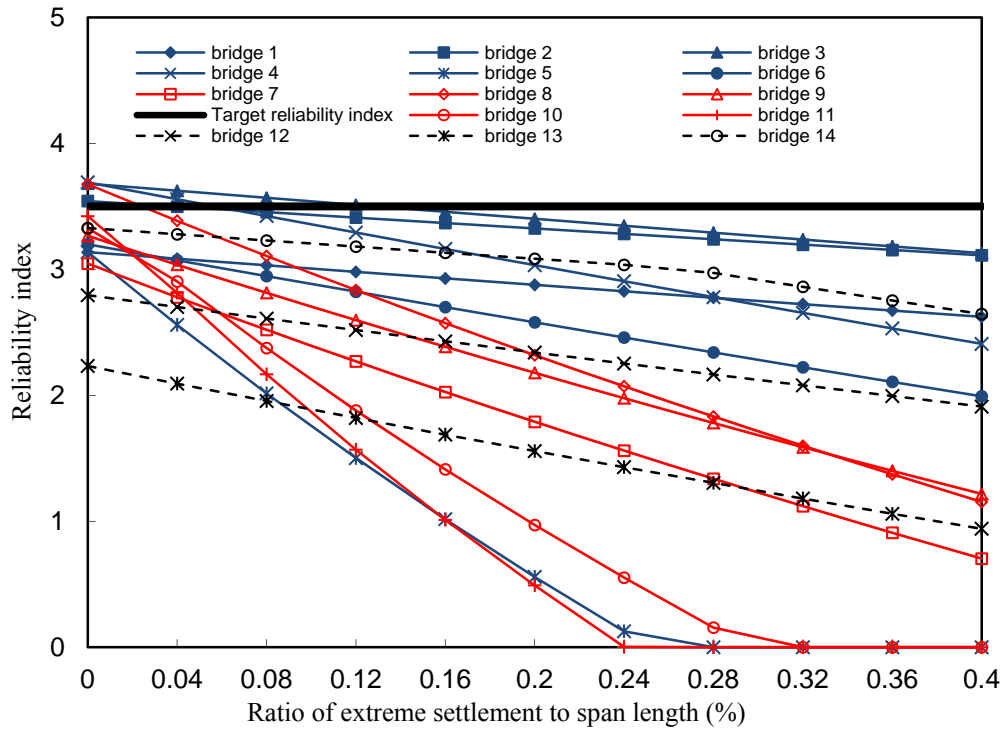
Figure 5.31 Reliability indices of 14 existing bridges: Case 5



(a) Reliability indices for negative moment

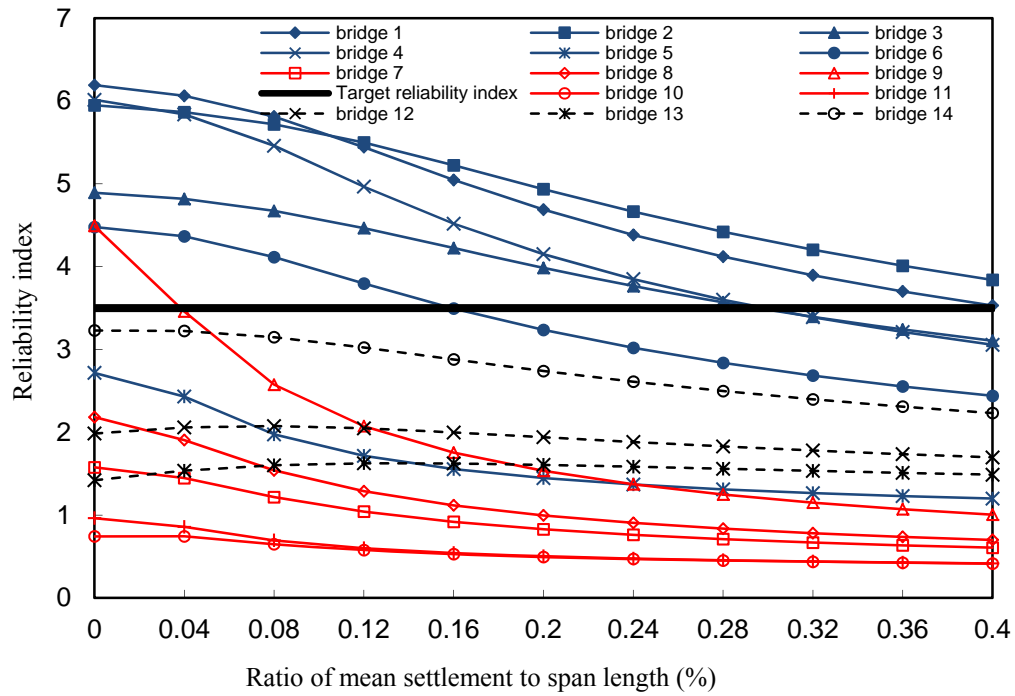


(b) Reliability indices for positive moment

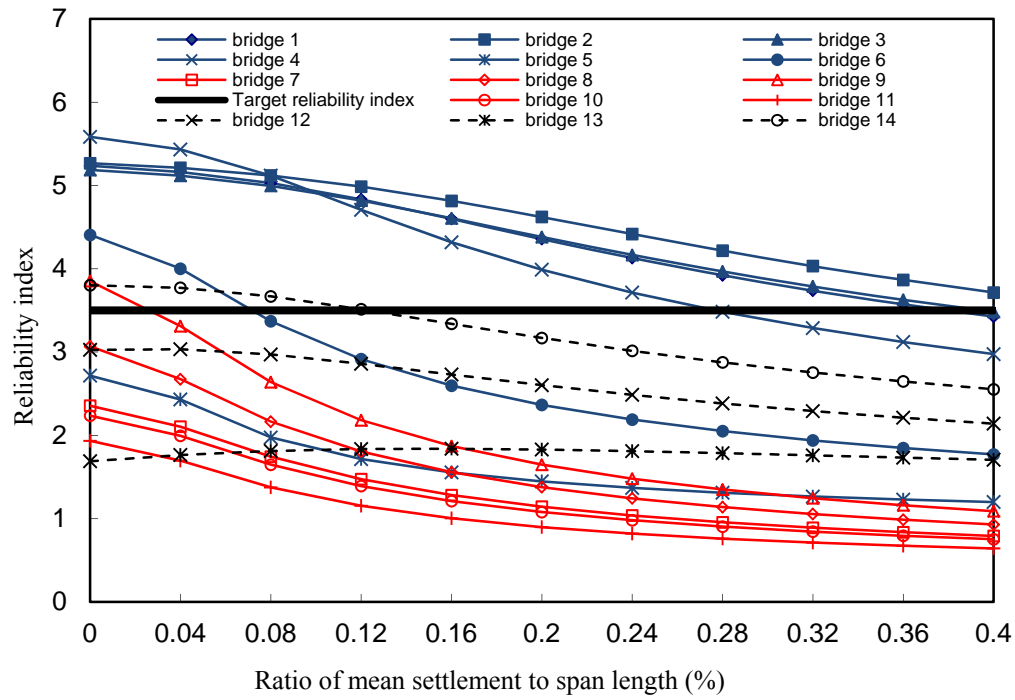


(c) Reliability indices for shear

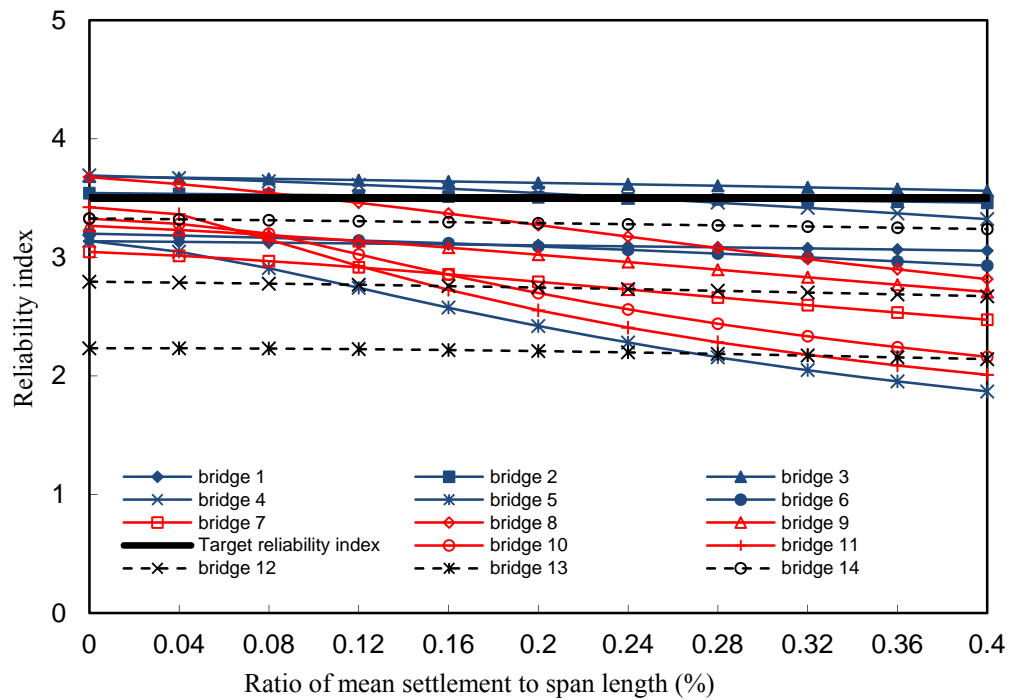
Figure 5.32 Reliability indices of 14 existing bridges: Case 6



(a) Reliability indices for negative moment

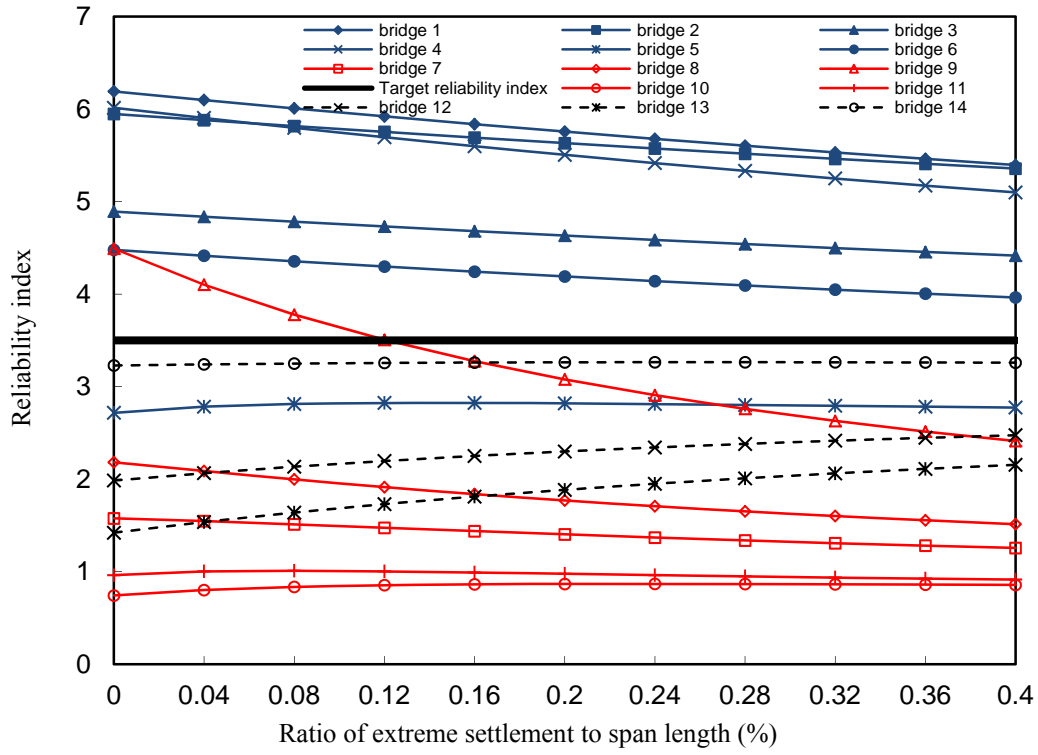


(b) Reliability indices for positive moment

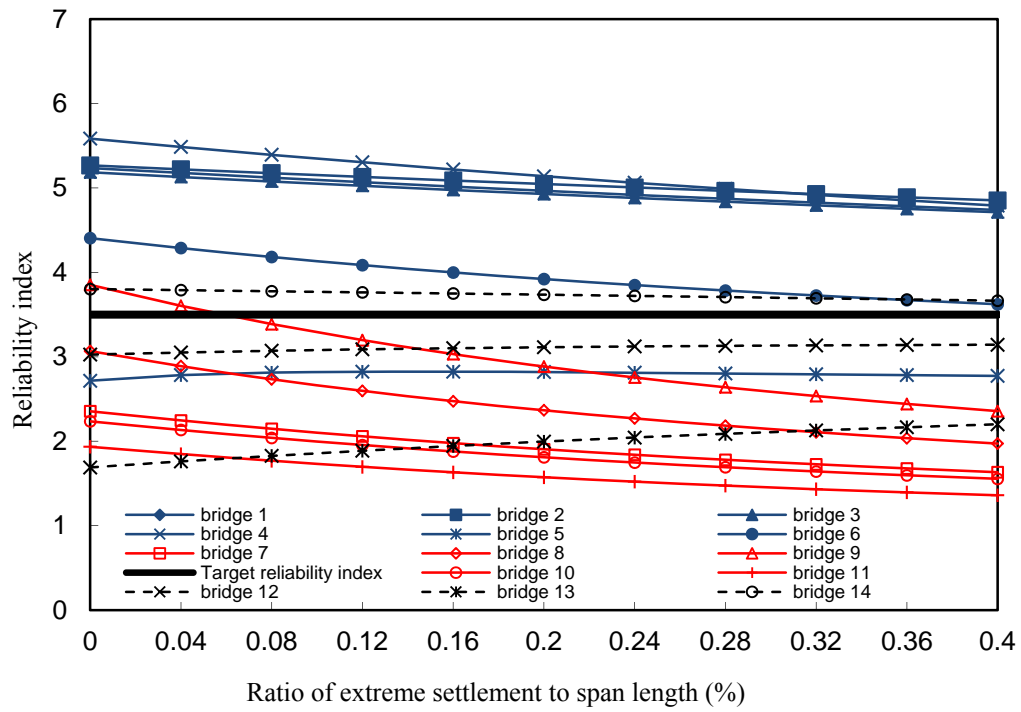


(c) Reliability indices for shear

Figure 5.33 Reliability indices of 14 existing bridges: Case 7



(a) Reliability indices for negative moment



(b) Reliability indices for positive moment

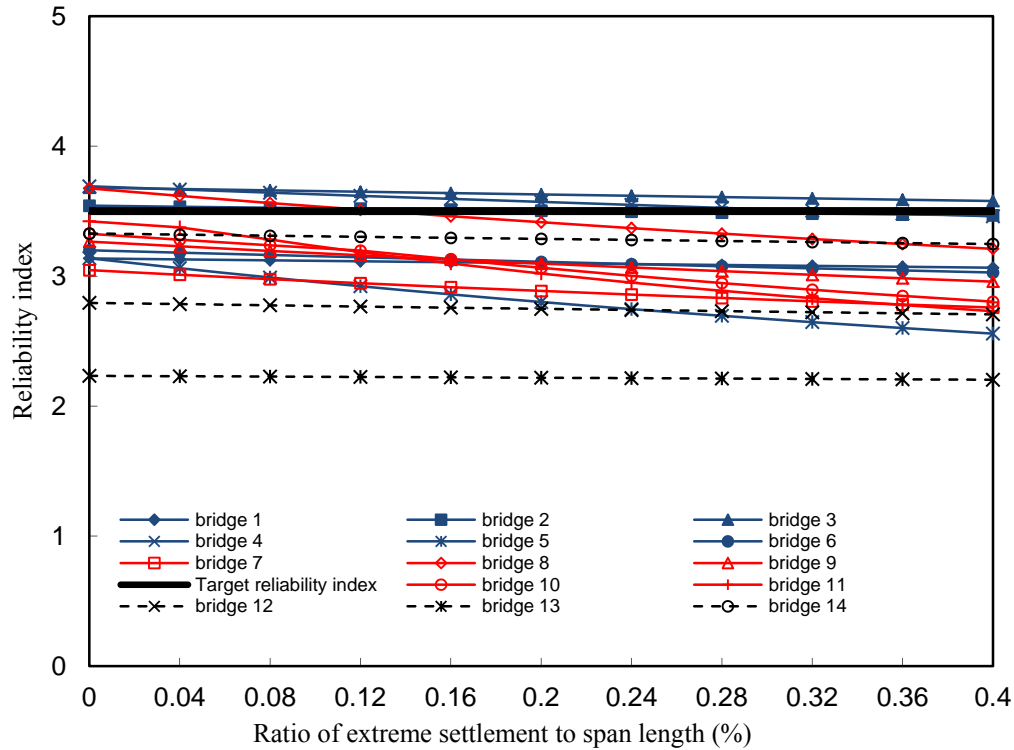


Figure 5.34 Reliability indices of 14 existing bridges: Case 8

Table 5.14 Average tolerable settlements of existing bridges (% of span length) using the minimum resistances

Average Tolerable Settlement (% of Span Length)		Without Live Load Reduction Factor				With Live Load Reduction Factor			
		Case 1	Case 2	Case 3	Case 4	Case 5	Case 6	Case 7	Case 8
Steel-girder bridges	Negative moment	0.20	0.27	0.33	0.4	0.11	0.14	0.26	0.33
	Positive moment	0.23	0.28	0.31	0.4	0.10	0.13	0.25	0.33
	Shear	0.27	0.28	0.35	0.4	0.05	0.05	0.18	0.19
	Minimum	0.20	0.27	0.31	0.4	0.05	0.05	0.18	0.19
Prestressed concrete- girder bridges	Negative moment	0.02	0.03	0.05	0.17	0	0	0.08	0.02
	Positive moment	0.04	0.04	0.08	0.28	0	0	0.01	0.01
	Shear	0.06	0.06	0.19	0.31	0	0	0.02	0.02
	Minimum	0.02	0.03	0.05	0.17	0	0	0.01	0.01
Slab bridges	Negative moment	0.04	0.04	0.15	0.40	0	0	0	0
	Positive moment	0.12	0.15	0.31	0.40	0	0	0.04	0.13
	Shear	0.10	0.11	0.13	0.13	0	0	0.13	0.13
	Minimum	0.04	0.04	0.13	0.13	0	0	0	0

The results presented in Figures 5.27 – 5.34 and summarized in Table 5.14 leads to the following observations:

- (1) For the 14 existing bridges, the reliability index based on the bending moment is more sensitive to support settlement than that on the shear force, regardless of steel-girder, prestressed concrete girder, and slab bridges. They are likely attributed to the fact that

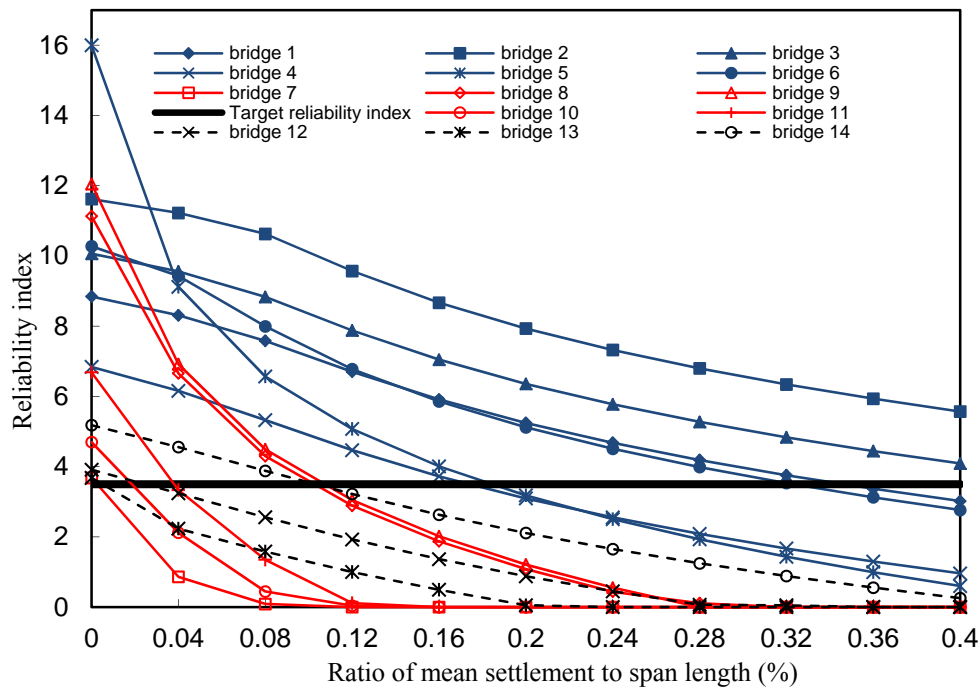
shear is proportional to I/L^3 instead of I/L^2 for bending moments and the fact that, except for Bridges #5 and #13, the minimum span length exceeds 34 ft, which is significantly longer than the shortest span (20 ft) of the 31 new bridge designs.

- (2) For steel-girder bridges, the reliability index of the 6 existing bridges is slightly more sensitive to support settlement than that of the 31 new bridge designs in most cases. This is due to the use of slightly higher moments of inertia for actual bridges. In addition, the variability of reliability indices for the existing bridges is significantly higher due to the use of unequal spans. In particular, the three-span continuous bridge (#5) has the shortest spans (19.5 ft to 26 ft), giving a significantly lower reliability index than other existing bridges due to its sensitivity to support settlement.
- (3) For Cases 5 – 8 when reduced live loads were used, the average tolerable settlements are substantially smaller than those for Cases 1 – 4.
- (4) For steel-girder bridges, the tolerable settlements of the 6 existing bridges are overall comparable to those from the 31 new bridge designs. While the use of unequal spans of the existing bridges generally increases the maximum moments at various supports as indicated in Figures 2.14 – 2.16, the maximum number of spans among the existing bridges is 3, which is less sensitive to the controlling 4-span bridges in the 31 new bridge designs. The net effect of the two competing factors gives the comparable reliability indices for the existing bridges and new designs, particularly evident for Cases 1 – 4 in Tables 5.13 and 5.14. For Case 2, a tolerable settlement of $L/450$ from the 31 new bridge designs can still be used for the existing steel-girder bridges. To ensure its applicability to bridges with unequal spans as more spans are used, the tolerable settlement should be determined by the minimum span length of multi-span bridges.
- (5) The reliability indices for prestressed concrete-girder and slab bridges are significantly lower than those of steel-girder bridges due partially to the fact that concrete-girder and slab bridges may be stiffer and the reliability indices of steel-girder bridges without settlement are significantly higher ($\beta = 3.8\sim 4.5$ for shear and $\beta = 5.1\sim 7.9$ for negative moment as will be discussed in Figure 5.37). Their corresponding tolerable settlements are much smaller, particularly for prestressed concrete-girder bridges. For Case 2, a tolerable settlement of $L/2500$ governed by negative moments can be used in design of slab bridges. Since prestressed concrete-girder bridges are simply supported for dead loads and continuous for live loads, the settlement-induced negative moments at various supports have a higher percentage of the negative moments induced by dead plus live loads, making concrete-girder bridges particularly sensitive to support settlement. Therefore, for Case 2, a tolerable settlement of $L/3500$ can be used in design of prestressed concrete-girder bridges.
- (6) For prestressed concrete-girder bridges under reduced live loads, the tolerable settlement does not reach the AASHTO recommended settlement limit of $L/250$ in all cases.

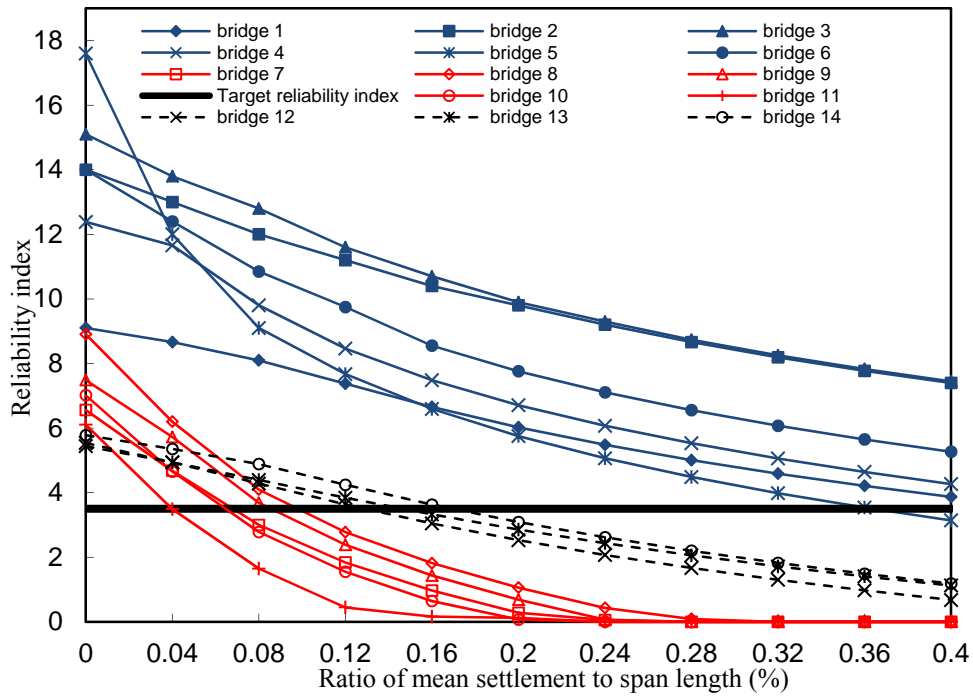
5.4.2 Based on actual resistances

The reliability indices of the 14 existing bridges described in Table 2.4 were calculated based on the uncertainties in the settlement-induced moment in Section 2, live and dead loads in Section 3, and the actual resistances for moment in Section 5.2. Since the existing bridges were designed with unreduced live loads and no settlement, only Cases 1 and 2 were considered in reliability analysis. Figures 5.35 and 5.36 present the reliability indices of the 14 existing bridges for the

two cases. The tolerable settlements for various types of bridges are summarized in Table 5.15. There is no appreciable difference in tolerable settlement when the actual moment strength or the minimum resistance is used.

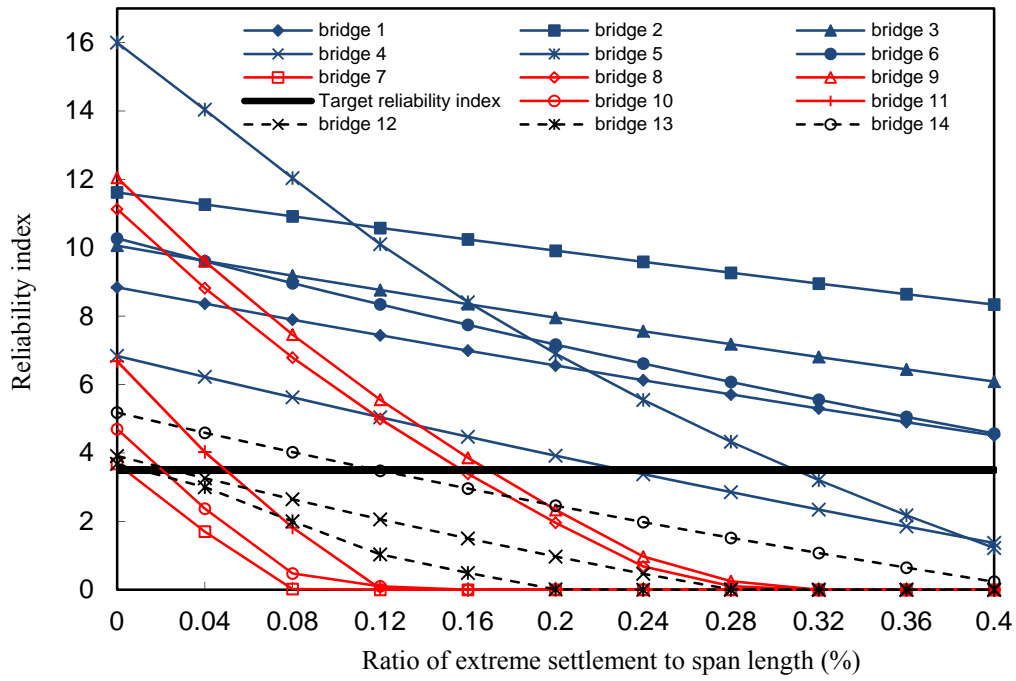


(a) Reliability indices for negative moment

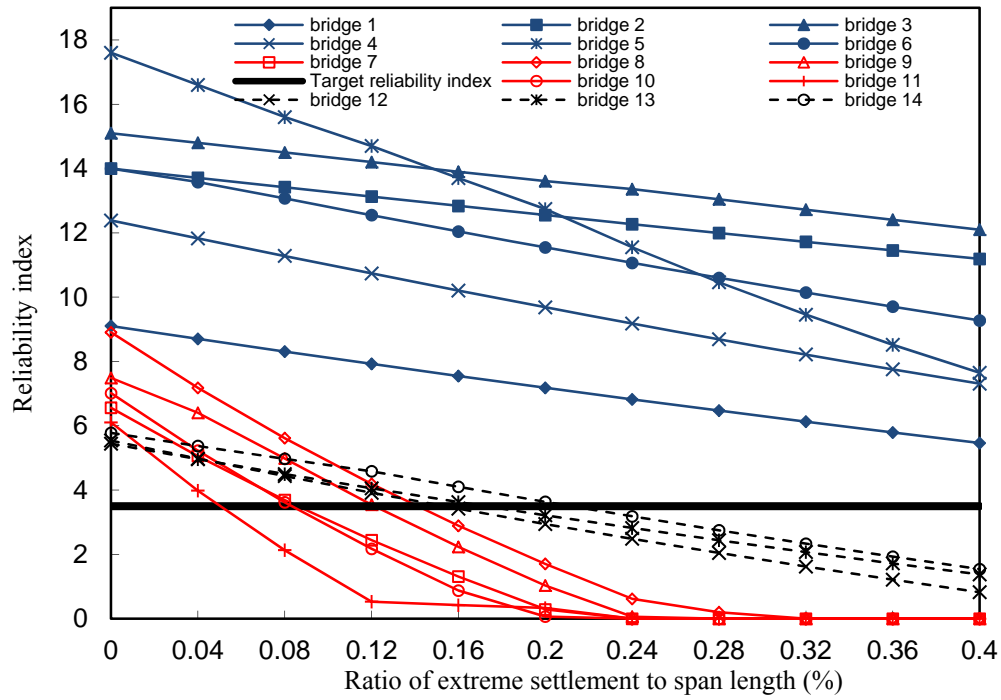


(b) Reliability indices for positive moment

Figure 5.35 Reliability indices of 14 existing bridges: Case 1



(a) Reliability indices for negative moment



(b) Reliability indices for positive moment

Figure 5.36 Reliability indices of 14 existing bridges: Case 2

Table 5.15 Average tolerable settlements of existing bridges (% of span length) using the actual moment strength

Average Tolerable Settlement (% of Span length)		Case 1	Case 2
Steel-girder bridges	Negative moment	0.31	0.36
	Positive moment	0.39	0.40
	Minimum	0.31	0.36
Prestressed concrete-girder bridges	Negative moment	0.05	0.08
	Positive moment	0.08	0.10
	Minimum	0.05	0.08
Slab bridges	Negative moment	0.05	0.06
	Positive moment	0.16	0.18
	Minimum	0.05	0.06

In comparison with Figures 5.27 – 5.34 and Table 5.14, Figures 5.35 and 5.36 as well as Table 5.15 indicate that the use of the actual moment resistances significantly increases the tolerable settlements for various types of bridges. This is because the actual resistance is higher than the minimum resistance based on the moments of inertia for strength and serviceability requirements as indicated by Figure 5.2. Reliability index is sensitive to the ratio of span lengths. As the span length ratio becomes less than 0.75, the reliability index drops significantly at small settlements.

5.4.3 Baseline at zero support settlement

To evaluate the reliability of the 14 existing bridges against the current AASHTO Specifications (2007), the design condition of the bridges without settlement effects was considered. Under this condition, the reliability indices for negative moment, positive moment, and shear of the 14 existing bridges using the unreduced and reduced live loads are presented in Figure 5.37. It can be clearly seen from Figure 5.37 that the overall reliability of the bridges meets the 2007 AASHTO requirements except for one solid slab bridge (No. 13) for shear reliability. The reliability of the steel-girder bridges for moment is higher than that of prestressed and solid slab bridges. Locally inconsistent changes in reliability occur for Bridge Nos. 5, 9, and 13 due to their irregular span length in each type of bridges. The lower reliability (No. 5 and 13) results from shorter span lengths and the higher reliability (No. 9) from longer span lengths. For shear, the reliability of the 14 bridges is basically independent of the type of bridges. Note that this difference may be attributed to the use of the minimum required shear strengths instead of the actual shear resistance of the bridges.

A comparison between Figure 5.37(a) and Figure 5.37(b) indicates that, with reduced live loads, the reliability for moment is scaled down by 20 – 79% with an average of 46% for the 14 bridges. However, the reliability index for shear is only reduced by approximately 19%. Figure 5.37(b) also indicates that the average reliability index of the 14 bridges appears above 3.5 if a live load reduction factor of 0.7 as recommended by Kwon et al. (2010) is considered for positive moment. However, cautions must be taken to implement the live load reduction factor for prestressed and solid slab bridges since their reliability indices are significantly lower than those of steel girder bridges. With reduced live loads, most of their reliability indices become

substantially lower than the target value of 3.5 when settlement effects are neglected. More importantly, with the 0.7 reduction factor, the average reliability index of the 14 bridges is lower than 3.5 for negative moment. With a live load reduction factor of 0.85, the average reliability index of the 14 bridges is slightly below 3.5 for shear.

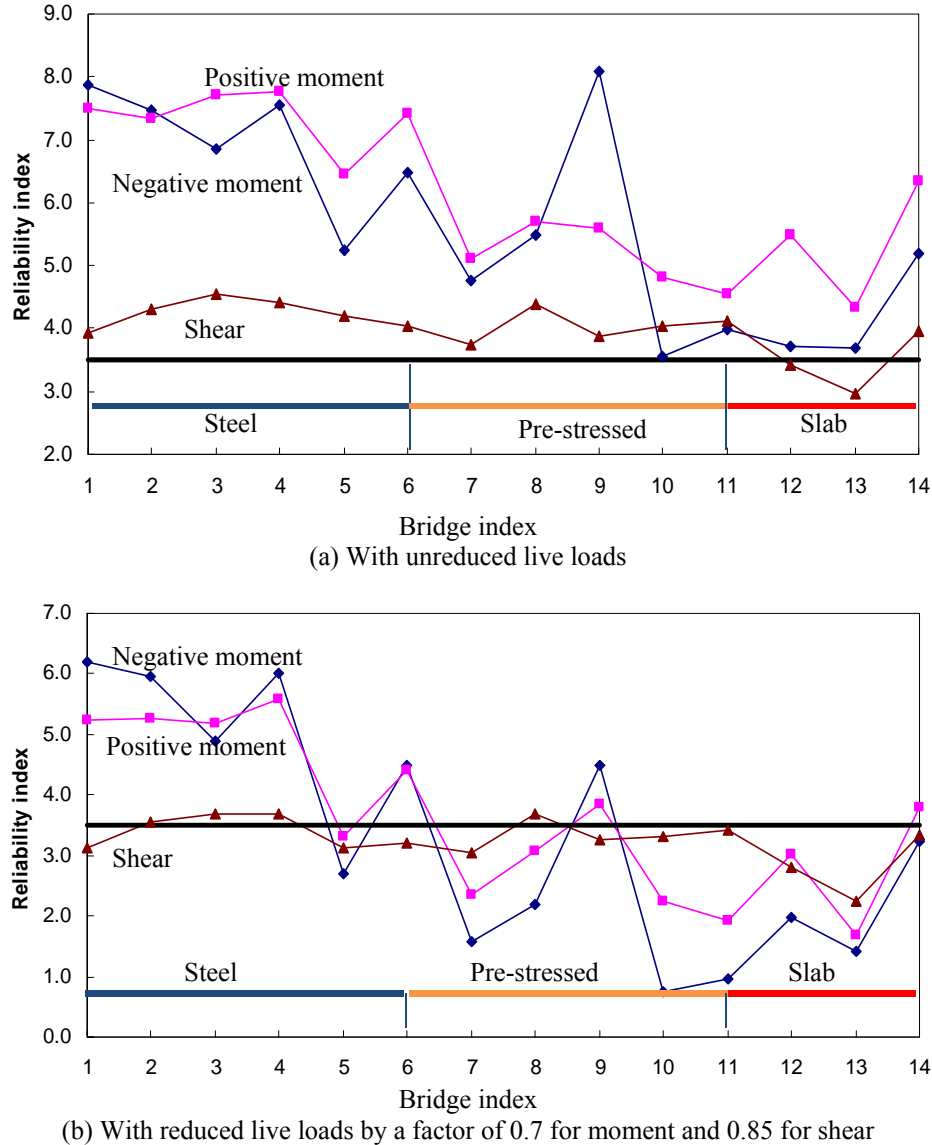


Figure 5.37 Reliability indices of 14 existing bridges without settlement effects

5.5 Uneven Settlement Effect on Diaphragm

As schematically shown in Figure 5.38, a concrete diaphragm can be treated as a continuous transverse member with infinite stiffness and short spans (girder spacing). It is expected that a concrete diaphragm is subjected to significant stress under an uneven settlement between girders when a bridge bent is tilted laterally. The steel cross diaphragm as shown in Figure 5.39 can be treated as simply-supported spans transversely. It is thus less susceptible to any uneven

settlement. In this study, only a concrete diaphragm is investigated using an intermediate bent diaphragm of Bridge A6569 as a representative example illustrated in Figure 5.40.

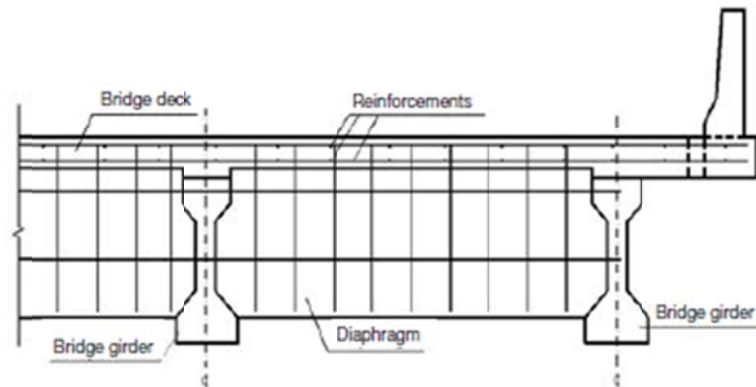


Figure 5.38 Typical concrete bent diaphragm

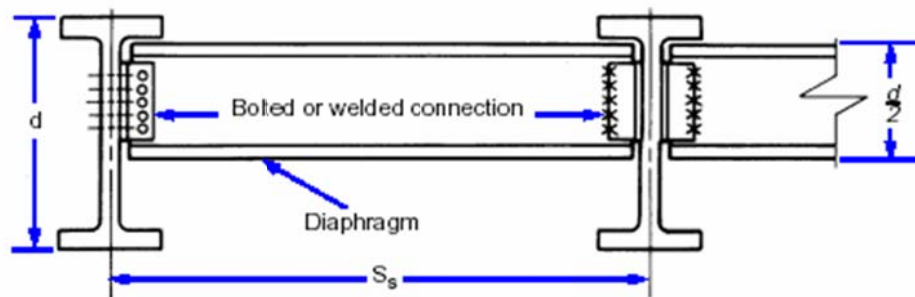


Figure 5.39 Typical steel bent diaphragm

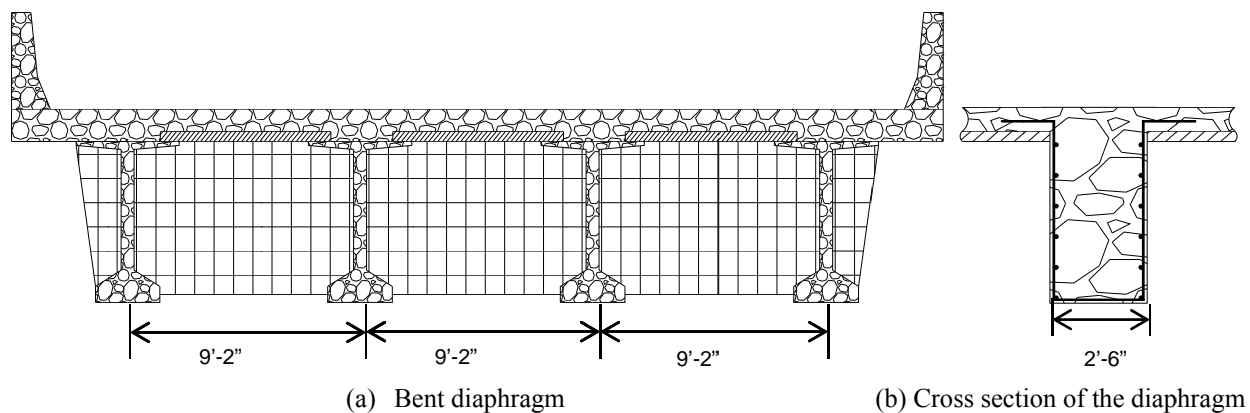


Figure 5.40 Bent diaphragm of Bridge A6569

The uneven foundation settlement of a bridge can cause a bridge bent to rotate a certain degree as schematically illustrated in Figure 5.41. This will be transferred to differential settlements in bridge girders, stressing the concrete diaphragm between the girders. The moment and shear of the diaphragm due to settlement u up to $0.004L$ (L = the distance between two adjacent columns)

were calculated using the MATLAB program developed in Section 2. The negative moment, positive moment, and shear resistance are calculated based on the diaphragm cross section in Figure 5.40(b). Together with nominal resistances, they are presented in Table 5.16.

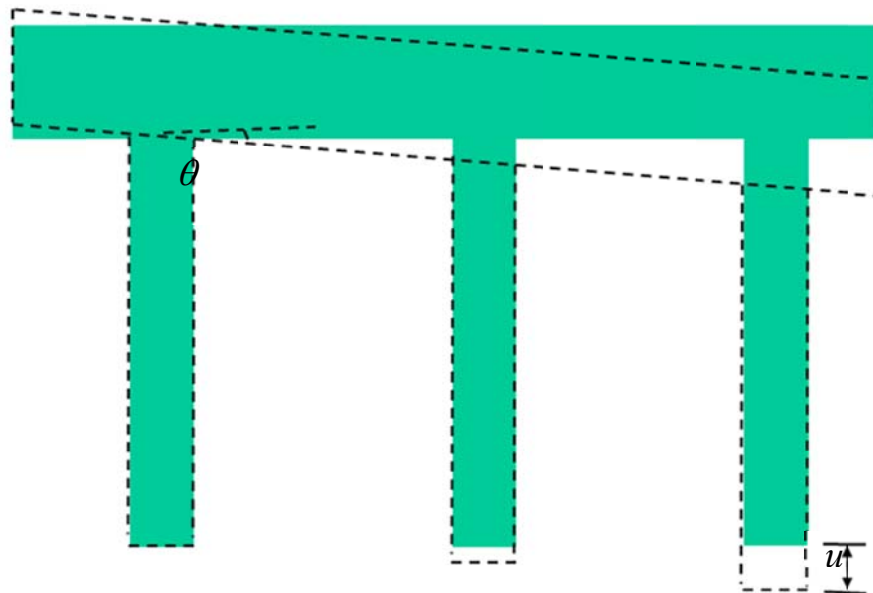


Figure 5.41 Bent rotation due to the uneven settlement of bridge foundations

Table 5.16 Nominal resistance and maximum moment and shear due to uneven settlement

Force and Moment	Nominal Resistance	Settlement (% of Column Spacing)									
		0.04	0.08	0.12	0.16	0.2	0.24	0.28	0.32	0.36	0.40
Negative moment (kip-ft)	219	64.3	128.5	192.8	257.0	321.3	385.6	449.8	514.1	578.3	642.6
Positive moment (kip-ft)	235	64.3	128.5	192.8	257.0	321.3	385.6	449.8	514.1	578.3	642.6
Shear (kip)	310	14.0	28.0	42.0	56.1	70.1	84.1	98.1	112.1	126.1	140.1

It can be observed from Table 5.16 that the continuous concrete diaphragm is very susceptible to differential settlement. The moment resulting from a small settlement (e.g. 0.16% of the column spacing or $L/625$) exceeds the nominal moment resistance, potentially damaging the concrete diaphragm. In terms of shear resistance, the concrete diaphragm can tolerate a differential settlement of over $L/250$. As an example, consider a column spacing of 12.75 ft for a three-column pier as illustrated in Figure 5.41. $L/625$ corresponds to a differential settlement of 0.245 in. This level of settlement is difficult to prevent in practice. As such, special attention must be paid to the design of concrete diaphragms when a bridge is located in an area with potential settlements.

6 CONCLUSIONS AND RECOMMENDATIONS

This study is focused on the effect of support settlement on the reliability of bridges under gravity loads. Dead and live loads were respectively modeled as random variables with a normal distribution and a Gumbel Type I distribution. Settlement was characterized by a random variable with lognormal distribution or a deterministic extreme value. The reliability indices for positive and negative moments as well as shear of 14 existing bridges and 31 new bridges were evaluated and compared. The tolerable settlements without requiring foundation mitigation as a result of settlement load effects on structural design were determined for various cases. The conclusions and recommendations from this study are presented as follows.

6.1 Conclusions

Based on the extensive simulation results for continuous bridges, the following conclusions can be drawn:

- (1) The settlement effect on the moment and shear of multi-span bridges depends upon the moment of inertia, span length, and their change among various spans. As the number of spans increases, the moment and shear of the bridges become more sensitive to support settlement. While the reliability indices for positive and negative moments increase with the increasing of span length, the reliability index can also be high for spans as short as 20 ft due to shear effect.
- (2) The maximum settlement-induced moment always occurs at supports, which coincides with the location of maximum negative moment. Depending upon the span length ratio, the settlement-induced moment can be as high as 100% of the moment due to dead and live loads alone. Therefore, the reliability index for negative moment is more sensitive to differential settlement effects than positive moment. However, their difference for both negative and positive moments appears small in general.
- (3) When settlement is defined as a random variable with a mean value and a given COV = 0.25, the average tolerable settlements (represented by the mean value) in all cases are between 50% and 100% of their corresponding values when settlement is defined as an extreme value. This is because some sample settlements in the random model exceed the extreme value.
- (4) The reliability indices for prestressed concrete-girder and slab bridges are significantly lower than those of steel-girder bridges due partially to the fact that concrete-girder and slab bridges are often stiffer and the reliability indices (3.8~4.5 for shear and 5.1~7.9 for negative moment) of the existing steel-girder bridges without settlement are significantly higher. Their corresponding tolerable settlements are much smaller, particularly for prestressed concrete-girder bridges. Since prestressed concrete-girder bridges are simply supported for dead loads and continuous for live loads, the settlement-induced negative moments at various supports have a higher percentage of their respective negative moments induced by dead plus live loads, making concrete-girder bridges particularly sensitive to support settlement.
- (5) For steel-girder bridges, the average tolerable settlements in extreme value are $L/450$ and $L/3500$ for the current MoDOT practice with unreduced live loads (Case 2) and the potential future MoDOT practice with reduced live loads (Case 6), respectively, when settlement is not considered in design. With due consideration of settlement in structural design, the tolerable settlement reaches the AASHTO recommended settlement limit of

0.004L with unreduced live loads (Case 4) but is limited by 0.0019L with reduced live loads (Case 8, shear governs).

- (6) For prestressed concrete-girder bridges, the average tolerable settlements in extreme value are $L/3500$ and virtually zero for the current MoDOT practice with unreduced live loads (Case 2) and the potential future MoDOT practice with reduced live loads (Case 6), respectively, when settlement is not considered in design. With due consideration of settlement in structural design, the tolerable settlement becomes 0.0017L under unreduced live loads (Case 4, negative moment governs) and 0.0001L under reduced live loads (Case 8, positive moment governs).
- (7) For slab bridges, the average tolerable settlements in extreme value are $L/2500$ and virtually zero for the current MoDOT practice with unreduced live loads (Case 2) and the potential future MoDOT practice with reduced live loads (Case 6), respectively, when settlement is not considered in design. With due consideration of settlement in structural design, the tolerable settlement is limited by 0.0013L with unreduced live loads (Case 4, shear governs) but virtually zero with reduced live loads (Case 8, shear governs).
- (8) When reduced live loads are used, the average tolerable settlements are substantially smaller than those when no reduction in live loads is considered. With reduced live loads, the reliability for moment is significantly scaled down while that for shear is slightly reduced when settlement is negligible.
- (9) When the length ratio among any two adjacent spans is less than 0.75, the reliability index of a multi-span bridge drops significantly at small settlements.

6.2 Recommendations

The extreme values of settlement depend on the confidence in the estimation of associated parameters and the roadway class. The extreme settlement used in this report is defined as a factored settlement that corresponds to a probability of being exceeded based on the target probabilities established by MoDOT for various roadway classes and bridge capital investments (MoDOT, 2010a; 2010b; 2010c; Abu El-Ela et al., 2011; Song et al., 2011; Vu and Loehr, 2011).

Based on extensive simulations on the reliability of existing and new bridges under gravity loads (with no live load reduction), the settlement effect in bridge design for Strength I Limit State requirements can be addressed with one of the following two methods:

- (1) Extreme settlement is considered in structural design and no special requirement is needed for foundation design unless the settlement exceeds the AASHTO recommended limit of $L/250$. For consistency, L represents the minimum span length of a multi-span bridge.
- (2) Extreme settlement is not considered in structural design as in the current MoDOT practice but ensured below what structures can tolerate in terms of reliability index. The tolerable settlement is $L/450$ for steel-girder bridges, $L/2500$ for slab bridges, and $L/3500$ for prestressed concrete-girder bridges.

Both methods represent minimum efforts in structural design as far as settlement load effects are concerned. They can be implemented in design according to the flow chart in Figure 6.1. The first method is a direct approach to deal with bridge settlement and has potential to reduce the overall cost of a new bridge. Although it may lead to larger superstructure and substructure members with additional calculations on settlement load effects, the increase in associated

material and labor costs expects to be trivial unless otherwise demonstrated for very short spans, based on the numerical analyses in this study. For new bridges, there is virtually no additional construction cost except in highly congested areas where clearance is critical.

The second method provides an indirect approach to deal with support settlement and may require larger and longer foundations with piles or drilled shafts to limit settlement to the level that can be tolerated by the superstructure and substructure of a bridge designed without due consideration of settlement. Other than additional material and labor costs, excavation costs associated with the oversized foundations, particularly when drilling into rock for pile/shaft sockets is otherwise not required, could be significant. As a result, although with less effort in the design of the superstructure and substructure, the second method may increase the overall cost of a bridge system.

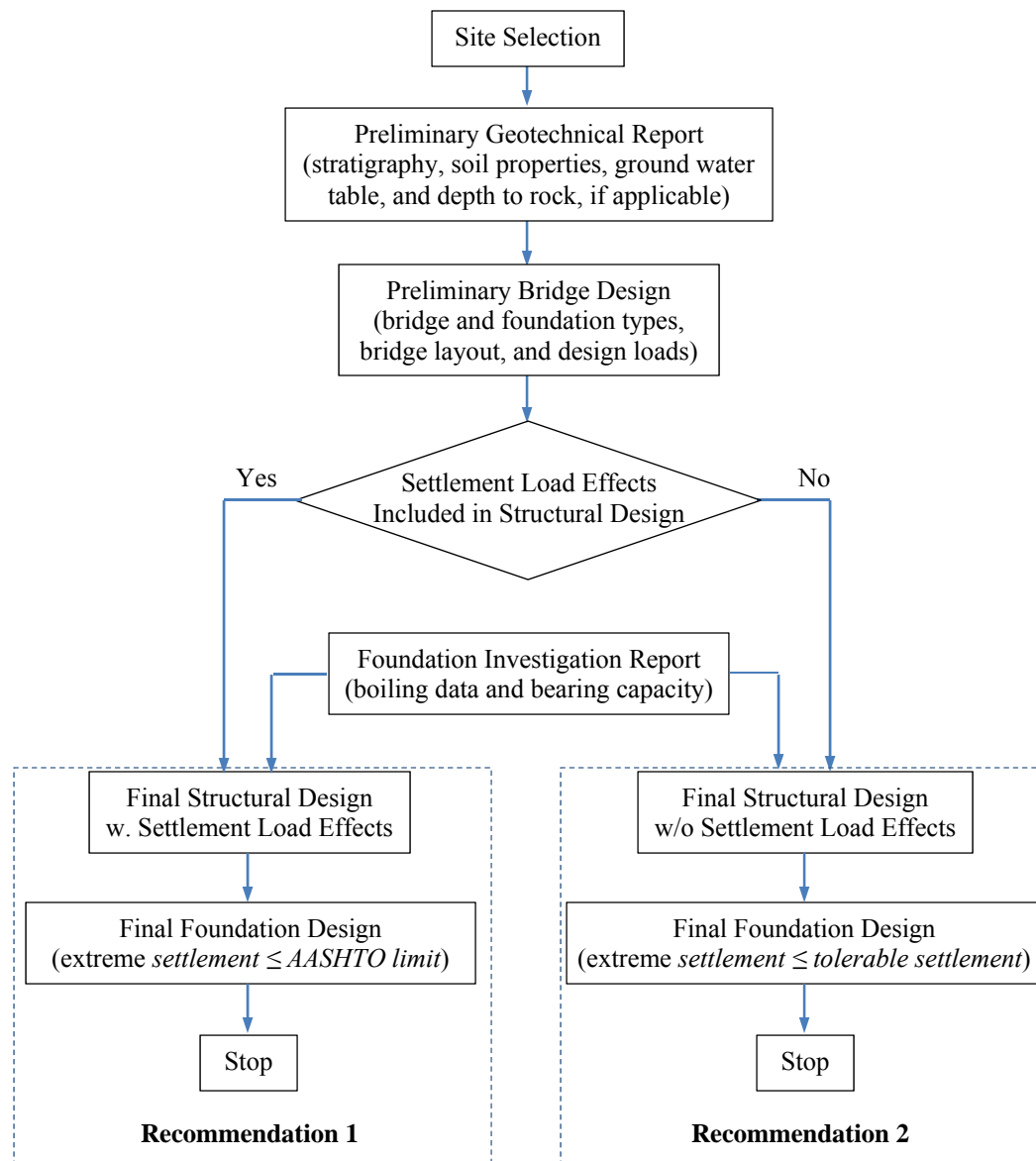


Figure 6.42 Design flow chart with two recommendations

REFERENCES

- [1]. AASHTO (2007), LRFD bridge design specifications, 4th Edition, Washington, DC.
- [2]. AASHTO (1996), Standard specifications for highway bridge design, 16th Edition, Washington, DC.
- [3]. Abramowitz, M. (1952), Remarks on a multivariate transformation, *Ann. of Mathematical Statistics*, Vol. 23, pp. 470-472.
- [4]. Abu El-Ela, A.A., J.J. Bowders, and L.E. Loehr (2011), Calibration of LRFD resistance factors for design of spread footings in hard and soft rock, MoDOT Final Report OR11-xxx, Missouri Department of Transportation, Jefferson City, MO, xxpp.
- [5]. Allen, T.M., A.S. Nowak, and R.J. Bathurst (2005), Calibration to determine load and resistance factors for geotechnical and structural design, Transportation Research Board, Washington, DC.
- [6]. Ang, A.H.S., and W.H. Tang (1975), Probability concepts in engineering planning and design, Volume I – Basic Principles, John Wiley & Sons, Inc., New York.
- [7]. Ang, A.H.S., and W.H. Tang (1984), Probability concepts in engineering planning and design, Volume II– Decision, Risk and Reliability, John Wiley & Sons, Inc., New York.
- [8]. Barker, R.M., J.M. Duncan, K.B. Rojiani, P.S.K. Ooi, C.K. Tan, and S.G. Kim (1991), Manuals for the design of bridge foundations, NCHRP Report 343, Transportation Research Board, National Research Council, Washington DC.
- [9]. Choi, S.K., R.V. Grandhi, and R.A. Canfield (2006), Reliability-based structural design, Springer-Verlag, London.
- [10]. Der Kiureghian, A. (2005), First- and second-order reliability method, Engineering Design Reliability Handbook, CRC, Boca Raton, FL.
- [11]. DiMillio, A.F., and K.E. Robinson (1982), Performance of highway bridge abutments supported by spread footing on compacted fill, FHWA/RD-81/184, (NTIS PB83-201822). (FHWA Staff Study).
- [12]. Gumbel, E.J. (1958), Statistics of extremes, Columbia University Press.
- [13]. Hearn, G., and K. Nordheim (1998), Differential settlements and inelastic response in steel bridge beams, Transportation Research Board, Vol. 1633, No. 09, pp. 68-73.
- [14]. Hwang, E.S., and A.S. Nowak (1991), Simulation of dynamic load for bridges, Journal of Structural Engineering, ASCE, Vol.117, No.5, pp.1413-1434.
- [15]. Kwon, O.S., S. Orton, H. Salim, E. Kim, and T. Hazlett (2010), Calibration of the live load factor in LRFD design guidelines, MoDOT Final Report OR11-003, Missouri Department of Transportation, Jefferson City, MO, 106pp.
- [16]. MoDOT (2010a), Guidelines for Design of Driven Piles (draft), EPG 751.36, Missouri Department of Transportation, Jefferson City, MO.
- [17]. MoDOT (2010b), Guidelines for Design of Drilled Shafts (draft), EPG 751.37, Missouri Department of Transportation, Jefferson City, MO.
- [18]. MoDOT (2010c), Guidelines for Design of Shallow Foundations (draft), EPG 751.38, Missouri Department of Transportation, Jefferson City, MO.
- [19]. Moulton, L.K., H.V.S. GangaRao, and G.T. Halverson (1985), Tolerable movement criteria for highway bridges, FHWA/RD-85/107, Federal Highway Administration, U.S. Department of Transportation, Washington, DC.
- [20]. Moulton, L.K. (1986), Tolerable movement criteria for highway bridges, FHWA-86/228, Federal Highway Administration, U.S. Department of Transportation, Washington, DC.

- [21]. Nour, A., A. Slimani, and N. Laouami (2002), Foundation settlement statistics via finite element analysis, *Computers and Geotechnics*, Vol. 29, No. 8, pp. 641-672.
- [22]. Nowak, A.S. (1999), NCHRP Report 368: Calibration of LRFD Bridge design code, Transportation Research Board, National Research Council, Washington, DC.
- [23]. Nowak, A.S., A.S. Yamani, and S.W. Tabsh (1994), Probabilistic models for resistance of concrete bridge girders, *ACI Structural Journal*, Vol. 91, No. 3, pp.269-276.
- [24]. Song, C., J.J. Bowders, A.A. Abu El-Ela, and J.E. Loehr (2011), Calibration of LRFD resistance factors for design of spread footings and embankments in cohesive soils at serviceability limit states, MoDOT Final Report OR11-xxx, Missouri Department of Transportation, Jefferson City, MO, xxxpp.
- [25]. Vu, T.T., and J.E. Loehr (2011), Calibration of LRFD resistance factors for design of drilled shafts at serviceability limit states, MoDOT Final Report OR11-xxx, Missouri Department of Transportation, Jefferson City, MO, xxxpp.

APPENDIX A: SUPPORT MOMENTS DUE TO UNIT SETTLEMENTS AT VARIOUS SUPPORTS

Table A.1 Support moments due to unit settlements for 2-span continuous bridges

Bridge No.	Bridge Description	Support Locations of Unit Settlement	Moment (kip-ft)		
			1	2	3
A3101	120+120ft continuous steel girder bridge	1	0.0	-164.3	0.0
		2	0.0	328.5	0.0
		3	0.0	-164.3	0.0
		1 and 3	0.0	-328.5	0.0
A6754	142+110ft continuous steel girder bridge	1	0.0	-181.4	0.0
		2	0.0	415.6	0.0
		3	0.0	-234.2	0.0
		1 and 3	0.0	-415.6	0.0
A4840	128+141ft continuous steel girder bridge	1	0.0	-159.7	0.0
		2	0.0	315.9	0.0
		3	0.0	-156.3	0.0
		1 and 3	0.0	-315.9	0.0
A7300	64.75+64.75 ft continuous steel girder bridge	1	0.0	-127.6	0.0
		2	0.0	255.2	0.0
		3	0.0	-127.6	0.0
		1 and 3	0.0	-255.2	0.0

Table A.2 Support moments due to unit settlements for 3-span continuous bridges

Bridge No.	Bridge Description	Support Locations of Unit Settlement	Moment (kip-ft)			
			1	2	3	4
A3386	75+97+75 ft continuous steel girder bridge	1	0.0	-477.8	137.1	0.0
		2	0.0	953.2	-608.5	0.0
		3	0.0	-612.4	944.0	0.0
		4	0.0	137.1	-472.6	0.0
		1 and 3	0.0	-1090.2	1081.1	0.0
		2 and 4	0.0	1090.2	-1081.1	0.0
A4058	37+65+42 ft continuous pre-stressed girder bridge	1	0.0	-585.7	177.9	0.0
		2	0.0	1020.4	-597.0	0.0
		3	0.0	-591.4	910.9	0.0
		4	0.0	156.7	-491.9	0.0
		1 and 3	0.0	-1177.1	1088.8	0.0
		2 and 4	0.0	1177.1	-1088.8	0.0
A4256	19.5+26+23.5 ft continuous steel girder bridge	1	0.0	-440.2	115.6	0.0
		2	0.0	857.0	-505.7	0.0
		3	0.0	-512.7	725.9	0.0
		4	0.0	95.9	-335.7	0.0
		1 and 3	0.0	-952.9	841.5	0.0
		2 and 4	0.0	952.9	-841.5	0.0
A4999	58+119+54 ft continuous steel	1	0.0	-393.8	144.3	0.0
		2	0.0	656.1	-410.9	0.0

	girder bridge	3	0.0	-417.3	699.0	0.0
		4	0.0	155.0	-432.4	0.0
		1 and 3	0.0	-811.1	843.3	0.0
		2 and 4	0.0	811.1	-843.3	0.0
A5161	38+65+40 ft continuous pre-stressed girder bridge	1	0.0	-696.9	215.7	0.0
		2	0.0	1230.4	-741.4	0.0
		3	0.0	-738.4	1175.1	0.0
		4	0.0	204.9	-649.4	0.0
		1 and 3	0.0	-1435.3	1390.8	0.0
		2 and 4	0.0	1435.3	-1390.8	0.0
A6569	65+100+74ft continuous pre-stressed girder bridge	1	0.0	-716.3	205.8	0.0
		2	0.0	1315.6	-781.1	0.0
		3	0.0	-780.1	1171.9	0.0
		4	0.0	180.8	-596.6	0.0
		1 and 3	0.0	-1496.4	1377.7	0.0
		2 and 4	0.0	1496.4	-1377.7	0.0
A3562	34+46+34 ft continuous slab bridge	1	0.0	-1012.8	291.2	0.0
		2	0.0	1976.7	-1255.0	0.0
		3	0.0	-1255.0	1976.7	0.0
		4	0.0	291.2	-1012.8	0.0
		1 and 3	0.0	-2267.9	2267.9	0.0
		2 and 4	0.0	2267.9	-2267.9	0.0
A6450	18+23+18 ft continuous slab bridge	1	0.0	-520.4	146.0	0.0
		2	0.0	1041.8	-667.4	0.0
		3	0.0	-667.4	1041.8	0.0
		4	0.0	146.0	-520.4	0.0
		1 and 3	0.0	-1187.8	1187.8	0.0
		2 and 4	0.0	1187.8	-1187.8	0.0

Table A.3 Support moments due to unit settlements for 4- and 5-span continuous bridges

Bridge No.	Bridge Description	Support Locations of Unit Settlement	Moment (kip-ft)					
			1	2	3	4	5	6
A3973	59+59+43+43 ft continuous pre-stressed girder bridge	1	0.0	-265.0	80.9	-20.2	0.0	
		2	0.0	611.0	-485.5	121.4	0.0	
		3	0.0	-484.7	959.7	-700.8	0.0	
		4	0.0	166.5	-666.1	1088.2	0.0	
		5	0.0	-27.8	111.0	-488.6	0.0	
		1, 3, and 5	0.0	-777.5	1151.6	-1209.6	0.0	
		2 and 4	0.0	777.5	-1151.6	1209.6	0.0	
A4582	38+38+65+38 ft continuous pre-stressed girder bridge	1	0.0	-622.0	127.4	-40.2	0.0	
		2	0.0	1371.4	-764.5	241.2	0.0	
		3	0.0	-847.4	1029.1	-579.3	0.0	
		4	0.0	138.2	-552.8	864.4	0.0	
		5	0.0	-40.2	160.8	-486.2	0.0	
		1, 3, and 5	0.0	-1509.6	1317.3	-1105.6	0.0	
		2 and 4	0.0	1509.6	-1317.3	1105.6	0.0	

A7086	120+125+125+1 20 ft continuous pre-stressed girder bridge	1	0.0	-184.3	49.2	-12.6	0.0	
		2	0.0	408.4	-281.6	71.8	0.0	
		3	0.0	-283.4	464.8	-283.4	0.0	
		4	0.0	71.8	-281.6	408.4	0.0	
		5	0.0	-12.6	49.2	-184.3	0.0	
		1, 3, and 5	0.0	-480.3	563.2	-480.3	0.0	
		2 and 4	0.0	480.3	-563.2	480.3	0.0	
A3390	48+60+48+55 ft continuous slab bridge	1	0.0	-424.5	124.4	-29.0	0.0	
		2	0.0	863.7	-582.0	135.6	0.0	
		3	0.0	-592.5	1009.7	-644.2	0.0	
		4	0.0	178.6	-643.1	915.7	0.0	
		5	0.0	-25.3	91.0	-378.1	0.0	
		1, 3, and 5	0.0	-1042.3	1225.2	-1051.3	0.0	
		2 and 4	0.0	1042.3	-1225.2	1051.3	0.0	
A4528	48+48+65+48+4 8 ft continuous slab bridge	1	0.0	-564.2	131.3	-39.9	10.0	0.0
		2	0.0	1259.7	-787.8	239.3	-59.8	0.0
		3	0.0	-821.9	1162.2	-705.1	176.3	0.0
		4	0.0	176.3	-705.1	1162.2	-821.9	0.0
		5	0.0	-59.8	239.3	-787.8	1259.7	0.0
		6	0.0	10.0	-39.9	131.3	-564.2	0.0
		1, 3, and 5	0.0	-1446.0	1532.8	-1532.8	1446.0	0.0
		2, 4, and 6	0.0	1446.0	-1532.8	1532.8	-1446.0	0.0

APPENDIX B: SHEAR IN SPAN DUE TO UNIT SETTLEMENTS AT VARIOUS SUPPORTS

Table B.1 Shear in spans due to unit settlements for 2-span continuous bridges

Bridge No.	Bridge Description	Support Locations of Unit Settlement	Shear (kips)		
			1	2	3
A3101	120+120ft continuous steel girder bridge	1	1.4	-1.4	-1.4
		2	-2.7	2.7	2.7
		3	1.4	-1.4	-1.4
		1 and 3	2.7	-2.7	-2.7
A6754	142+110ft continuous steel girder bridge	1	1.3	-1.6	-1.6
		2	-2.9	3.8	3.8
		3	1.6	-2.1	-2.1
		1 and 3	2.9	-3.8	-3.8
A4840	128+141ft continuous steel girder bridge	1	1.2	-1.1	-1.1
		2	-2.3	2.2	2.2
		3	1.1	-1.1	-1.1
		1 and 3	2.3	-2.2	-2.2
A7300	64.75+64.75 ft continuous steel girder bridge	1	2.0	-2.0	-2.0
		2	-3.9	3.9	3.9
		3	2.0	-2.0	-2.0
		1 and 3	3.9	-3.9	-3.9

Table B.2 Shear in spans due to unit settlements for 3-span continuous bridges

Bridge No.	Bridge Description	Support Locations of Unit Settlement	Shear (kips)			
			1	2	3	4
A3386	75+97+75 ft continuous steel girder bridge	1	6.4	-6.3	1.8	1.8
		2	-12.7	16.1	-8.1	-8.1
		3	8.2	-16.0	12.6	12.6
		4	-1.8	6.3	-6.3	-6.3
		1 and 3	14.5	-22.4	14.4	14.4
		2 and 4	-14.5	22.4	-14.4	-14.4
A4058	37+65+42 ft continuous pre-stressed girder bridge	1	15.8	-11.7	4.2	4.2
		2	-27.6	24.9	-14.2	-14.2
		3	16.0	-23.1	21.7	21.7
		4	-4.2	10.0	-11.7	-11.7
		1 and 3	31.8	-34.9	25.9	25.9
		2 and 4	-31.8	34.9	-25.9	-25.9
A4256	19.5+26+23.5 ft continuous steel girder bridge	1	22.6	-21.4	4.9	4.9
		2	-43.9	52.4	-21.5	-21.5
		3	26.3	-47.6	30.9	30.9
		4	-4.9	16.6	-14.3	-14.3
		1 and 3	48.9	-69.0	35.8	35.8
		2 and 4	-48.9	69.0	-35.8	-35.8
A4999	58+119+54 ft continuous steel girder	1	6.8	-4.5	2.7	2.7
		2	-11.3	9.0	-7.6	-7.6
		3	7.2	-9.4	12.9	12.9

	bridge	4	-2.7	4.9	-8.0	-8.0
		1 and 3	14.0	-13.9	15.6	15.6
		2 and 4	-14.0	13.9	-15.6	-15.6
A5161	38+65+40 ft continuous pre-stressed girder bridge	1	18.3	-14.0	5.4	5.4
		2	-32.4	30.3	-18.5	-18.5
		3	19.4	-29.4	29.4	29.4
		4	-5.4	13.1	-16.2	-16.2
		1 and 3	37.8	-43.5	34.8	34.8
		2 and 4	-37.8	43.5	-34.8	-34.8
A6569	65+100+74ft continuous pre-stressed girder bridge	1	11.0	-9.2	2.8	2.8
		2	-20.2	21.0	-10.6	-10.6
		3	12.0	-19.5	15.8	15.8
		4	-2.8	7.8	-8.1	-8.1
		1 and 3	23.0	-28.7	18.6	18.6
		2 and 4	-23.0	28.7	-18.6	-18.6
A3562	34+46+34 ft continuous slab bridge	1	29.8	-28.3	8.6	8.6
		2	-58.1	70.3	-36.9	-36.9
		3	36.9	-70.3	58.1	58.1
		4	-8.6	28.3	-29.8	-29.8
		1 and 3	66.7	-98.6	66.7	66.7
		2 and 4	-66.7	98.6	-66.7	-66.7
A6450	18+23+18 ft continuous slab bridge	1	28.9	-29.0	8.1	8.1
		2	-57.9	74.3	-37.1	-37.1
		3	37.1	-74.3	57.9	57.9
		4	-8.1	29.0	-28.9	-28.9
		1 and 3	66.0	-103.3	66.0	66.0
		2 and 4	-66.0	103.3	-66.0	-66.0

Table B.3 Shear in spans due to unit settlements for 4- and 5-span continuous bridges

Bridge No.	Bridge Description	Support Locations of Unit Settlement	Shear (kips)					
			1	2	3	4	5	6
A3973	59+59+43+43 ft continuous pre-stressed girder bridge	1	4.5	-5.9	2.4	-0.5	-0.5	
		2	-10.4	18.6	-14.1	2.8	2.8	
		3	8.2	-24.5	38.6	-16.3	-16.3	
		4	-2.8	14.1	-40.8	25.3	25.3	
		5	0.5	-2.4	13.9	-11.4	-11.4	
		1 ,3, and 5	13.2	-32.7	54.9	-28.1	-28.1	
		2 and 4	-13.2	32.7	-54.9	28.1	28.1	
A4582	38+38+65+38 ft continuous pre-stressed girder bridge	1	16.4	-19.7	2.6	-1.1	-1.1	
		2	-36.1	56.2	-15.5	6.3	6.3	
		3	22.3	-49.4	24.7	-15.2	-15.2	
		4	-3.6	18.2	-21.8	22.7	22.7	
		5	1.1	-5.3	10.0	-12.8	-12.8	
		1 ,3, and 5	39.7	-74.4	37.3	-29.1	-29.1	
		2 and 4	-39.7	74.4	-37.3	29.1	29.1	
A7086	120+125+125+120 ft continuous pre-	1	1.5	-1.9	0.5	-0.1	-0.1	
		2	-3.4	5.5	-2.8	0.6	0.6	

	stressed girder bridge	3	2.4	-6.0	6.0	-2.4	-2.4	
		4	-0.6	2.8	-5.5	3.4	3.4	
		5	0.1	-0.5	1.9	-1.5	-1.5	
		1,3, and 5	4.0	-8.3	8.3	-4.0	-4.0	
		2 and 4	-4.0	8.3	-8.3	4.0	4.0	
A3390	48+60+48+55 ft continuous slab bridge	1	8.8	-9.1	3.2	-0.5	-0.5	
		2	-18.0	24.1	-15.0	2.5	2.5	
		3	12.3	-26.7	34.5	-11.7	-11.7	
		4	-3.7	13.7	-32.5	16.6	16.6	
		5	0.5	-1.9	9.8	-6.9	-6.9	
		1,3, and 5	21.7	-37.8	47.4	-19.1	-19.1	
		2 and 4	-21.7	37.8	-47.4	19.1	19.1	
A4528	48+48+65+48+48 ft continuous slab bridge	1	11.8	-14.5	2.6	-1.0	0.2	0.2
		2	-26.2	42.7	-15.8	6.2	-1.2	-1.2
		3	17.1	-41.3	28.7	-18.4	3.7	3.7
		4	-3.7	18.4	-28.7	41.3	-17.1	-17.1
		5	1.2	-6.2	15.8	-42.7	26.2	26.2
		6	-0.2	1.0	-2.6	14.5	-11.8	-11.8
		1, 3, and 5	30.1	-62.1	47.2	-62.1	30.1	30.1
		2, 4, and 6	-30.1	62.1	-47.2	62.1	-30.1	-30.1

APPENDIX C: SUPPORT REACTIONS DUE TO UNIT SETTLEMENTS AT VARIOUS SUPPORTS

Table C.1 Support reactions due to unit settlements for 2-span continuous bridges

Bridge No.	Bridge Description	Support Locations of Unit Settlement	Reaction (kips)		
			1	2	3
A3101	120+120ft continuous steel girder bridge	1	-1.4	2.7	-1.4
		2	2.7	-5.5	2.7
		3	-1.4	2.7	-1.4
		1 and 3	-2.7	5.5	-2.7
A6754	142+110ft continuous steel girder bridge	1	-1.3	2.9	-1.6
		2	2.9	-6.7	3.8
		3	-1.6	3.8	-2.1
		1 and 3	-2.9	6.7	-3.8
A4840	128+141ft continuous steel girder bridge	1	-1.2	2.3	-1.1
		2	2.3	-4.5	2.2
		3	-1.1	2.2	-1.1
		1 and 3	-2.3	4.5	-2.2
A7300	64.75+64.75 ft continuous steel girder bridge	1	-2.0	3.9	-2.0
		2	3.9	-7.9	3.9
		3	-2.0	3.9	-2.0
		1 and 3	-3.9	7.9	-3.9

Table C.2 Support reactions due to unit settlements for 3-span continuous bridges

Bridge No.	Bridge Description	Support Locations of Unit Settlement	Reaction (kips)			
			1	2	3	4
A3386	75+97+75 ft continuous steel girder bridge	1	-6.4	12.7	-8.2	1.8
		2	12.7	-28.8	24.2	-8.1
		3	-8.2	24.2	-28.6	12.6
		4	1.8	-8.1	12.6	-6.3
		1 and 3	-14.5	36.9	-36.8	14.4
		2 and 4	14.5	-36.9	36.8	-14.4
A4058	37+65+42 ft continuous pre-stressed girder bridge	1	-15.8	27.6	-16.0	4.2
		2	27.6	-52.5	39.1	-14.2
		3	-16.0	39.1	-44.8	21.7
		4	4.2	-14.2	21.7	-11.7
		1 and 3	-31.8	66.7	-60.8	25.9
		2 and 4	31.8	-66.7	60.8	-25.9
A4256	19.5+26+23.5 ft continuous steel girder bridge	1	-22.6	43.9	-26.3	4.9
		2	43.9	-96.4	73.9	-21.5
		3	-26.3	73.9	-78.5	30.9
		4	4.9	-21.5	30.9	-14.3
		1 and 3	-48.9	117.9	-104.8	35.8
		2 and 4	48.9	-117.9	104.8	-35.8
A4999	58+119+54 ft continuous steel girder bridge	1	-6.8	11.3	-7.2	2.7
		2	11.3	-20.3	16.6	-7.6
		3	-7.2	16.6	-22.3	12.9

		4	2.7	-7.6	12.9	-8.0
		1 and 3	-14.0	27.9	-29.5	15.6
		2 and 4	14.0	-27.9	29.5	-15.6
A5161	38+65+40 ft continuous pre- stressed girder bridge	1	-18.3	32.4	-19.4	5.4
		2	32.4	-62.7	48.9	-18.5
		3	-19.4	48.9	-58.8	29.4
		4	5.4	-18.5	29.4	-16.2
		1 and 3	-37.8	81.2	-78.2	34.8
		2 and 4	37.8	-81.2	78.2	-34.8
A6569	65+100+74ft continuous pre- stressed girder bridge	1	-11.0	20.2	-12.0	2.8
		2	20.2	-41.2	31.5	-10.6
		3	-12.0	31.5	-35.4	15.8
		4	2.8	-10.6	15.8	-8.1
		1 and 3	-23.0	51.8	-47.4	18.6
		2 and 4	23.0	-51.8	47.4	-18.6
A3562	34+46+34 ft continuous slab bridge	1	-29.8	58.1	-36.9	8.6
		2	58.1	-128.4	107.2	-36.9
		3	-36.9	107.2	-128.4	58.1
		4	8.6	-36.9	58.1	-29.8
		1 and 3	-66.7	165.3	-165.3	66.7
		2 and 4	66.7	-165.3	165.3	-66.7
A6450	18+23+18 ft continuous slab bridge	1	-28.9	57.9	-37.1	8.1
		2	57.9	-132.2	111.4	-37.1
		3	-37.1	111.4	-132.2	57.9
		4	8.1	-37.1	57.9	-28.9
		1 and 3	-66.0	169.3	-169.3	66.0
		2 and 4	66.0	-169.3	169.3	-66.0

Table C.3 Support reactions due to unit settlements for 4- and 5-span continuous bridges

Bridge No.	Bridge Description	Support Locations of Unit Settlement	Reaction (kips)					
			1	2	3	4	5	6
A3973	59+59+43+43 ft continuous pre- stressed girder bridge	1	-4.5	10.4	-8.2	2.8	-0.5	
		2	10.4	-28.9	32.7	-16.9	2.8	
		3	-8.2	32.7	-63.1	54.9	-16.3	
		4	2.8	-16.9	54.9	-66.1	25.3	
		5	-0.5	2.8	-16.3	25.3	-11.4	
		1, 3, and 5	-13.2	45.9	-87.6	83.0	-28.1	
		2 and 4	13.2	-45.9	87.6	-83.0	28.1	
A4582	38+38+65+38 ft continuous pre-stressed girder bridge	1	-16.4	36.1	-22.3	3.6	-1.1	
		2	36.1	-92.3	71.7	-21.8	6.3	
		3	-22.3	71.7	-74.1	40.0	-15.2	
		4	3.6	-21.8	40.0	-44.6	22.7	
		5	-1.1	6.3	-15.2	22.7	-12.8	
		1, 3, and 5	-39.7	114.1	-111.7	66.4	-29.1	
		2 and 4	39.7	-114.1	111.7	-66.4	29.1	
A7086	120+125+125+	1	-1.5	3.4	-2.4	0.6	-0.1	

	120 ft continuous pre- stressed girder bridge	2	3.4	-8.9	8.3	-3.4	0.6	
		3	-2.4	8.3	-12.0	8.3	-2.4	
		4	0.6	-3.4	8.3	-8.9	3.4	
		5	-0.1	0.6	-2.4	3.4	-1.5	
		1, 3, and 5	-4.0	12.4	-16.7	12.4	-4.0	
		2 and 4	4.0	-12.4	16.7	-12.4	4.0	
A3390	48+60+48+55 ft continuous slab bridge	1	-8.8	18.0	-12.3	3.7	-0.5	
		2	18.0	-42.1	39.0	-17.4	2.5	
		3	-12.3	39.0	-61.2	46.2	-11.7	
		4	3.7	-17.4	46.2	-49.1	16.6	
		5	-0.5	2.5	-11.7	16.6	-6.9	
		1, 3, and 5	-21.7	59.5	-85.2	66.5	-19.1	
		2 and 4	21.7	-59.5	85.2	-66.5	19.1	
A4528	48+48+65+48+ 48 ft continuous slab bridge	1	-11.8	26.2	-17.1	3.7	-1.2	0.2
		2	26.2	-68.9	58.5	-22.0	7.5	-1.2
		3	-17.1	58.5	-70.1	47.1	-22.0	3.7
		4	3.7	-22.0	47.1	-70.1	58.5	-17.1
		5	-1.2	7.5	-22.0	58.5	-68.9	26.2
		6	0.2	-1.2	3.7	-17.1	26.2	-11.8
		1, 3, and 5	-30.1	92.2	-109.2	109.2	-92.2	30.1
		2, 4, and 6	30.1	-92.2	109.2	-109.2	92.2	-30.1

APPENDIX D: BRIDGE ANALYSIS REPORT FROM ANSYS SOFTWARE

Three existing bridges with curved steel girders were analyzed with the ANSYS probabilistic design system. Bridge A3848 is a 3-span (68'+70'+68'), continuous steel plate girder structure with a curve radius of 250 ft. Bridge A6723 is a 3-span (90'+200'+90'), continuous steel plate curved girder structure. Bridge A6477 is a 3-span (110'+190'+110'), continuous steel plate curved girder structure. This section only reports the analysis results of the bridges under a random settlement at the second support. The random settlement is assumed to have a lognormal distribution with a mean value of 1 in. and a standard deviation of 25%.

The statistics of random output parameters are computed using the ANSYS software and illustrated with histogram plots, cumulative distribution curves, and/or history plots. The influence of random input variables on individual output parameters (known as the "sensitivity") are illustrated as bar and pie charts. All units in Section D are in lbs for force and ft for length.

D.1 Deterministic Finite Element Model

ANSYS runs multiple times to account for various sample sets during a probabilistic analysis. The finite element models of the three bridges are shown in Figure D.1. The details of the finite element models and material properties are given in Table D.1 and Table D.2, respectively.

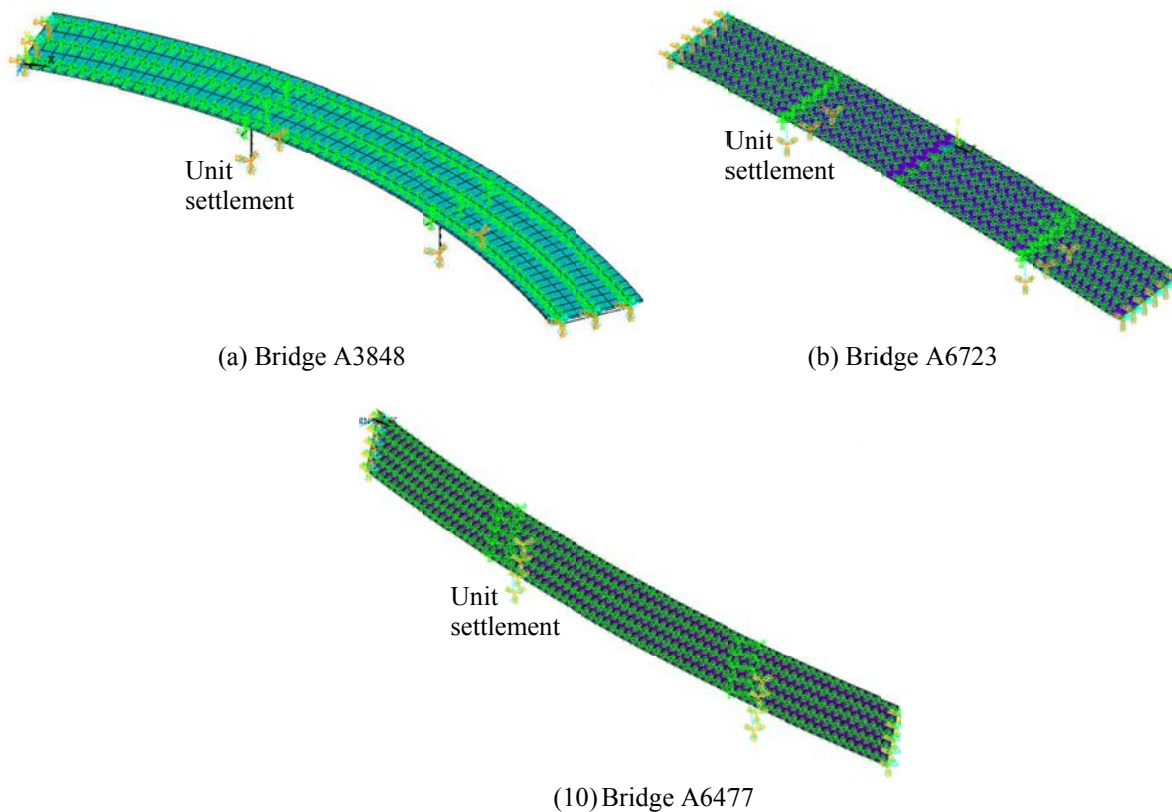


Figure D.1 Finite element model of each bridge

Table D.1 Details of the finite element model

Bridge No.	No. of BEAM4 Elements	No. of SHELL63 Elements	No. of Nodes
A3848	435	360	823
A6723	868	672	1467
A6477	933	740	1625

Table D.2 Material properties

Material	Modulus of Elasticity (lb/ft ²)	Density (lb/ft ³)	Poisson's Ratio
Steel	4,176,000,000	490	0.30
Concrete	518,400,000	150	0.17

D.2 Probabilistic Model

The settlement at support 2 was considered as a random input variable for each of the bridge models. A list of random input variables, their distribution, and statistical parameters are provided in Table D.3. The probability density functions and cumulative distribution functions are shown in Figure D.2. Note that the remaining tables and figures in Section D are presented in the format from the ANSYS software for easy references to the original computation if needed.

Table D.3 Random input variable specifications

No.	Name	Type	Par1 (mean)	Par2 (STD)
1	A	LOG1	0.0833	0.0208

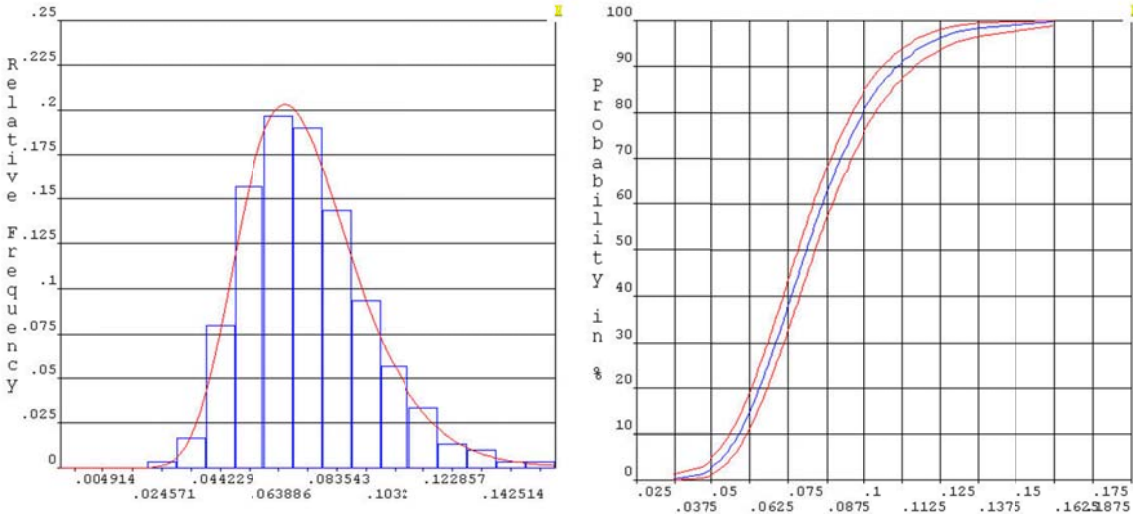


Figure D.2 Probability density function and probability distribution function of input random variable A defined in Table D.3

D.3 Probabilistic Analysis Results

The following selected results are reported:

- (1) Statistics of probabilistic results
- (2) Sample history plots
- (3) Histogram plots
- (4) Probability distribution function or cumulative distribution function plots

The distributions of output parameters are shown in Table D.4 and Figures D.3 - D.6. Sample histories of output parameters are shown in Figures D.7 - D.10. Probability distribution functions of output parameters are shown in Figures D.11 - D.14. The correlation between the random input settlement and the output moment are shown in Figures D.15 and D.16.

Table D.4 Statistics of the random output parameters
(a) Bridge A3848

Name	Mean	Standard Deviation	Skewness	Kurtosis	Minimum	Maximum
MMAXI	4.4643E+04	1.1137E+04	0.6978	0.7611	1.7457E+04	8.6772E+04
MMINI	-3.0574E+04	7628.	-0.6978	0.7611	-5.9426E+04	-1.1955E+04
SMAXI	-1816.	453.1	-0.6978	0.7611	-3530.	-710.3
SMINI	-857.7	214.0	-0.6978	0.7611	-1667.	-335.4

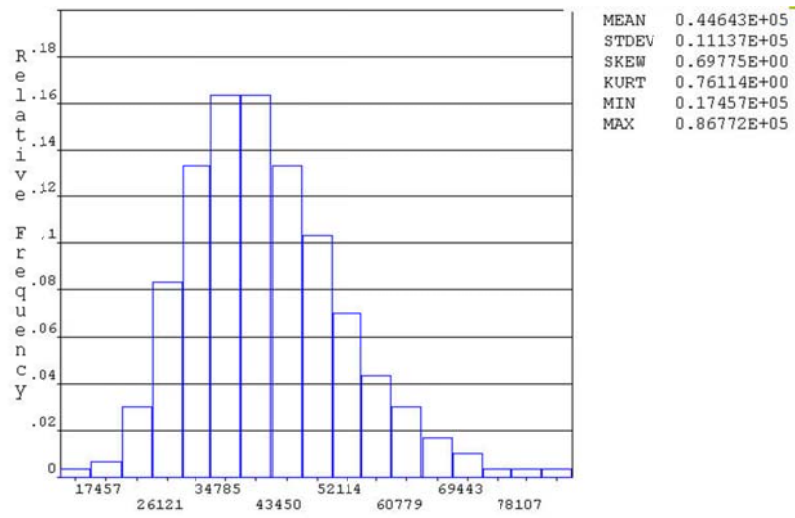
(b) Bridge A6723

Name	Mean	Standard Deviation	Skewness	Kurtosis	Minimum	Maximum
MMAXI	6800.	1711.	0.8457	1.556	3316.	1.5060E+04
MMINI	-4935.	1242.	-0.8457	1.556	-1.0930E+04	-2407.
SMAXI	-1197.	301.1	-0.8457	1.556	-2650.	-583.5
SMINI	-291.0	73.22	-0.8457	1.556	-644.4	-141.9

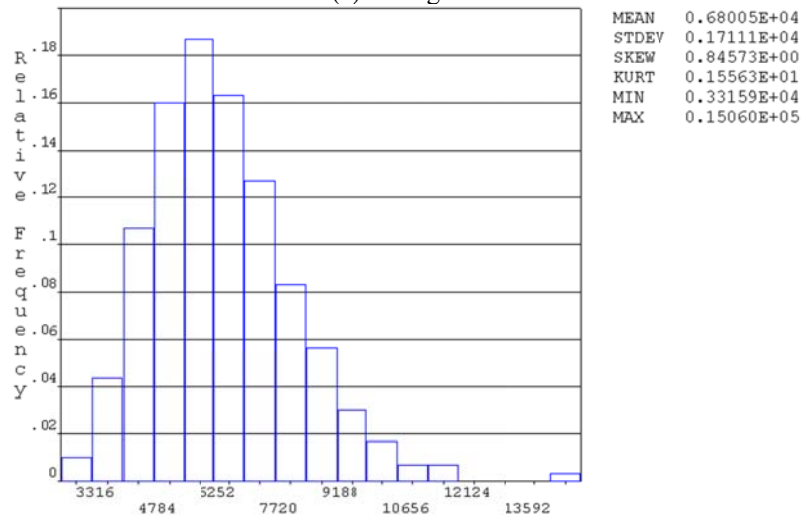
(c) Bridge A6477

Name	Mean	Standard Deviation	Skewness	Kurtosis	Minimum	Maximum
MMAXI	4.1610E+04	1.0393E+04	0.7679	1.036	2.0674E+04	8.7073E+04
MMINI	-1.6581E+04	4141.	-0.7679	1.036	-3.4696E+04	-8238.
SMAXI	1.2942E+04	3233.	0.7679	1.036	6430.	2.7081E+04
SMINI	-323.8	80.88	-0.7679	1.036	-677.6	-160.9

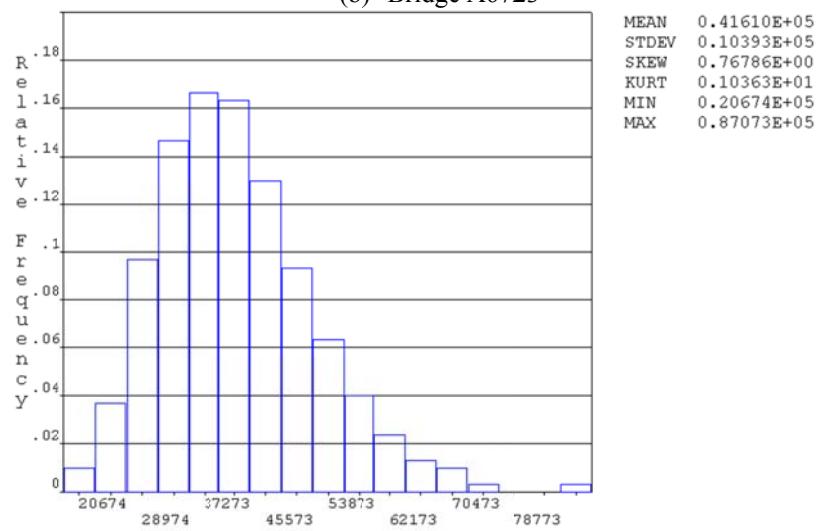
Note: MMAXI: Maximum Positive Moment; MMIMI: Maximum Negative Moment;
SMAXI: Maximum Absolute Shear Force; SMINI: Minimum Absolute Shear Force



(a) Bridge A3848

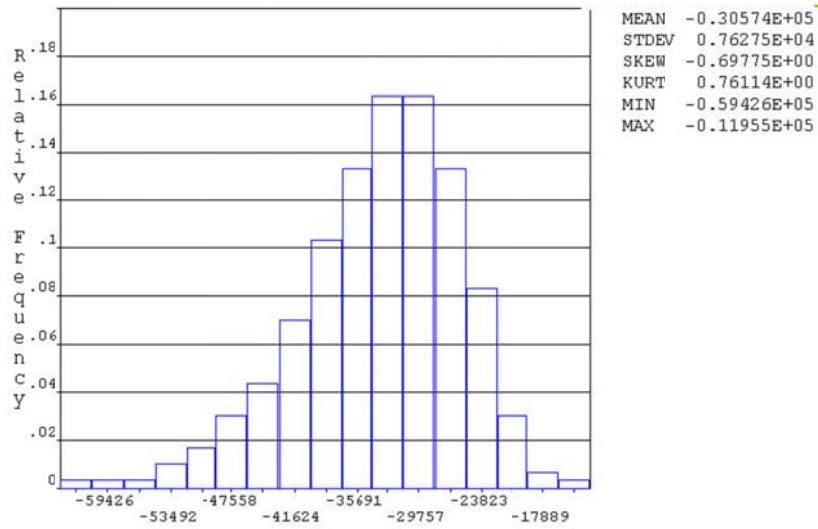


(b) Bridge A6723

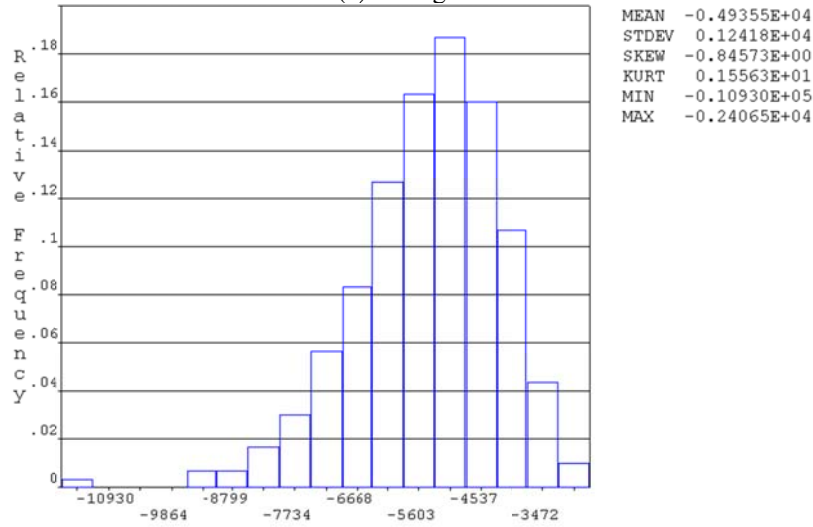


(c) Bridge A6477

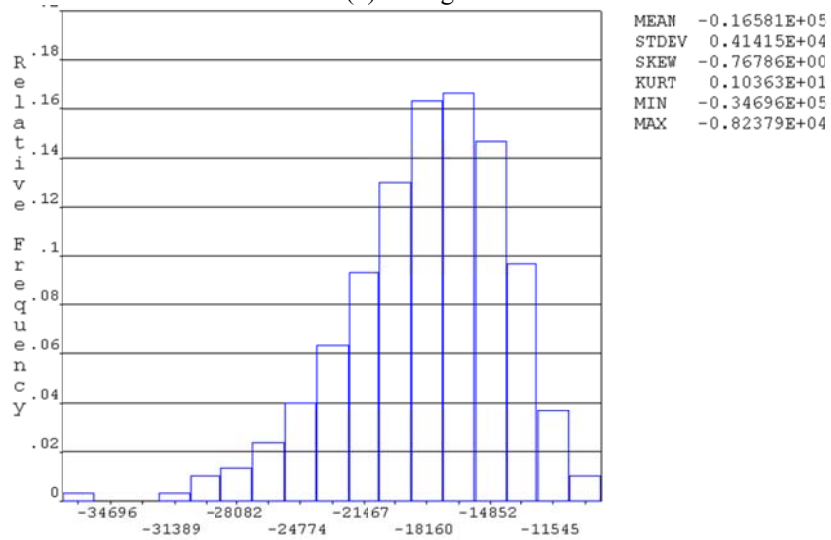
Figure D.3 Histograms of maximum moment



(a) Bridge A3848

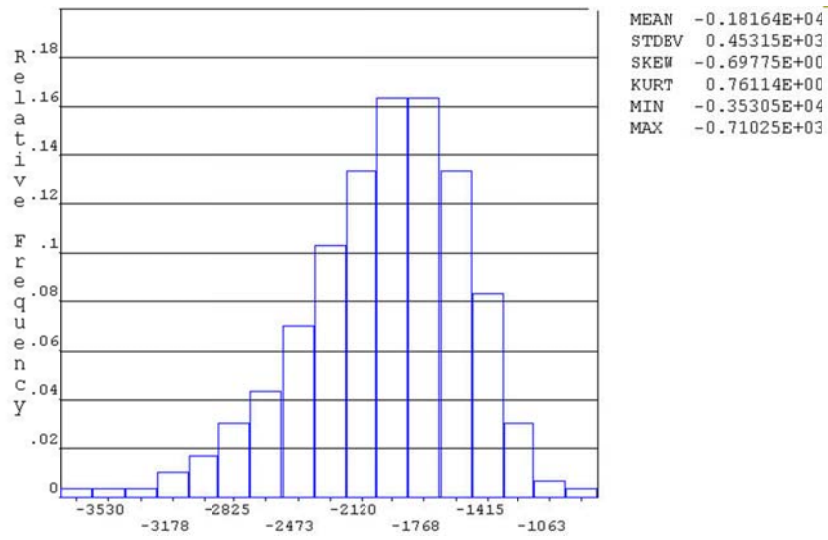


(b) Bridge A6723

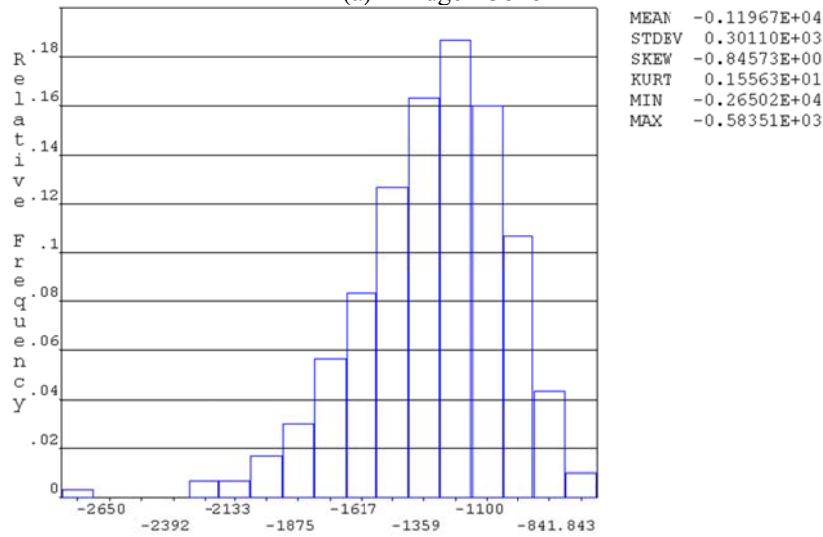


(c) Bridge A6477

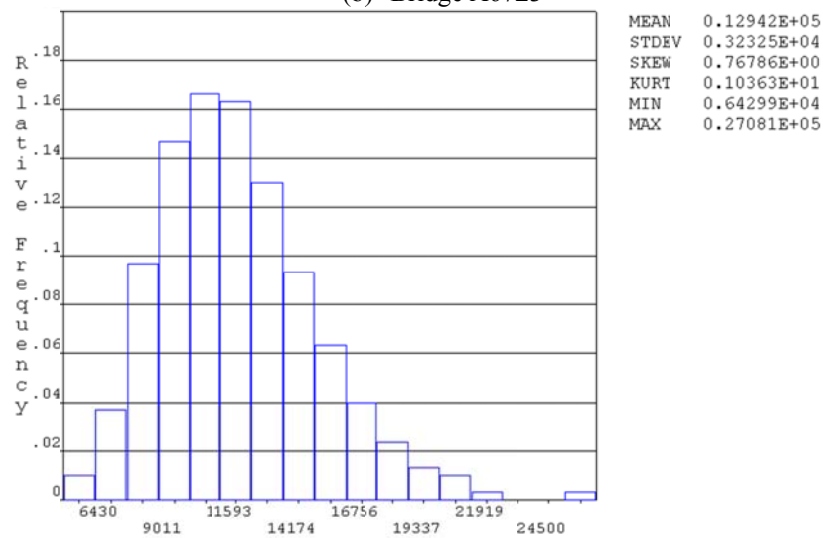
Figure D.4 Histograms of minimum moment



(a) Bridge A3848

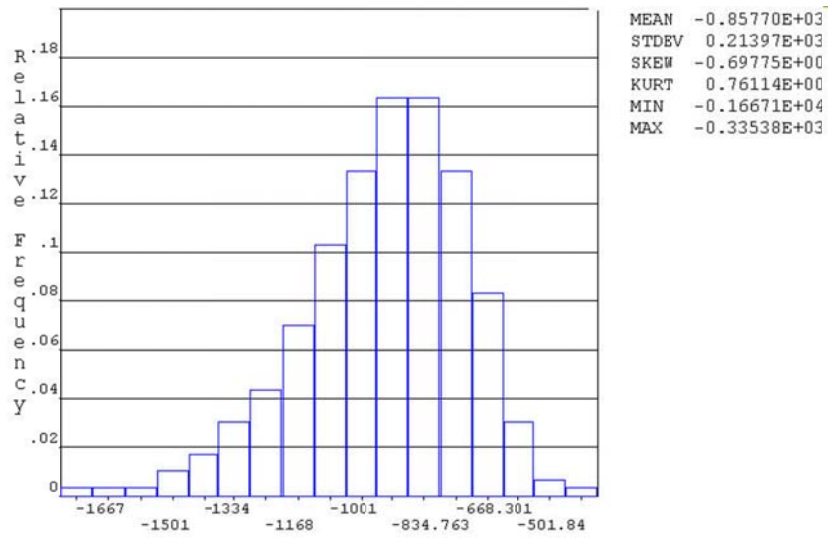


(b) Bridge A6723

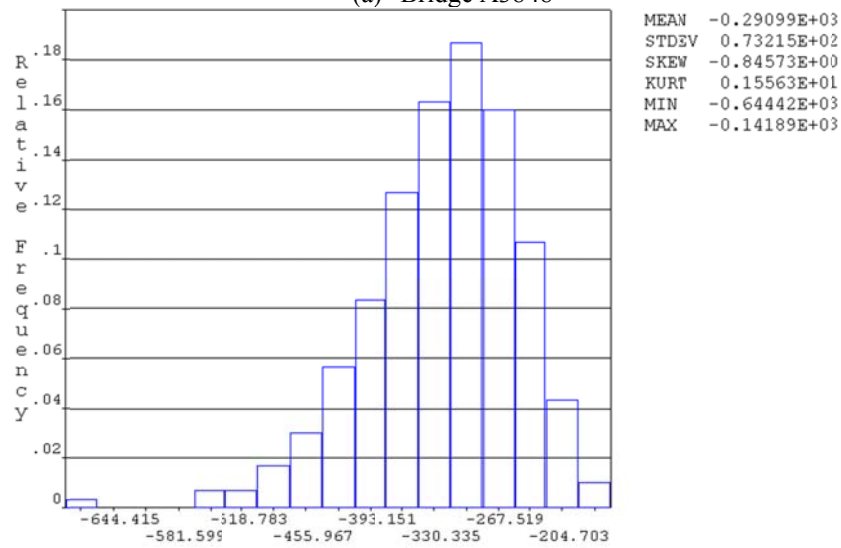


(c) Bridge A6477

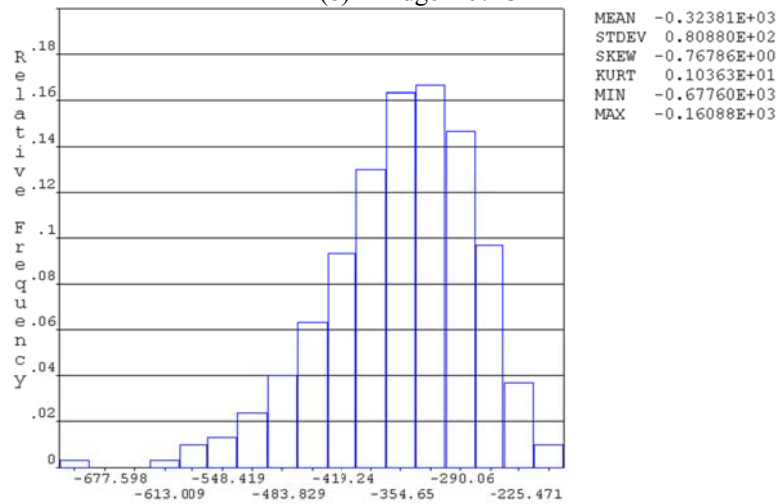
Figure D.5 Histograms of maximum absolute shear force



(a) Bridge A3848

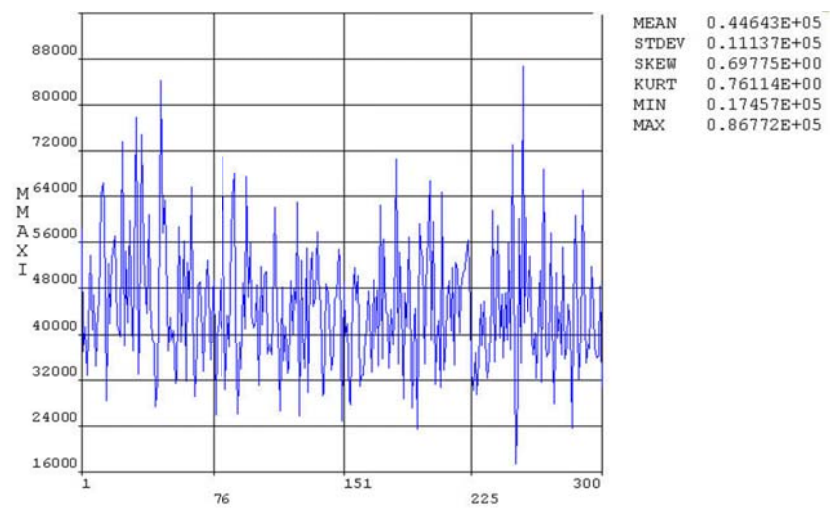


(b) Bridge A6723

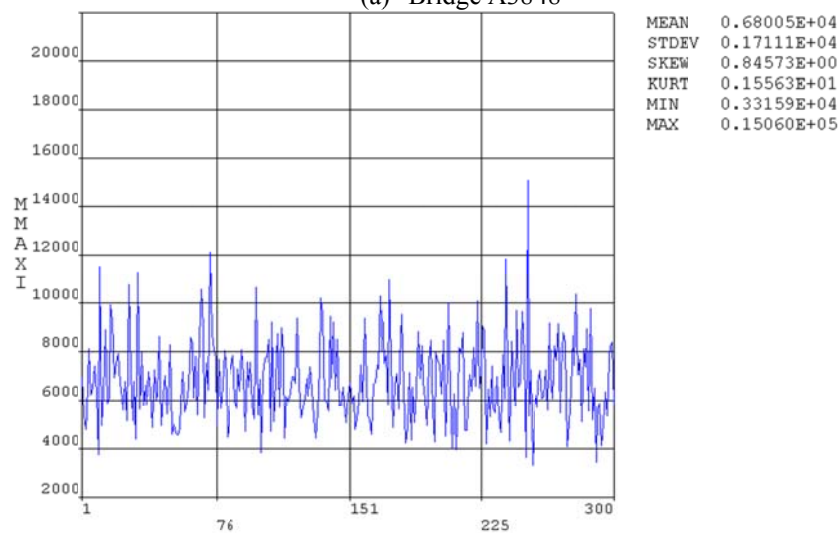


(c) Bridge A6477

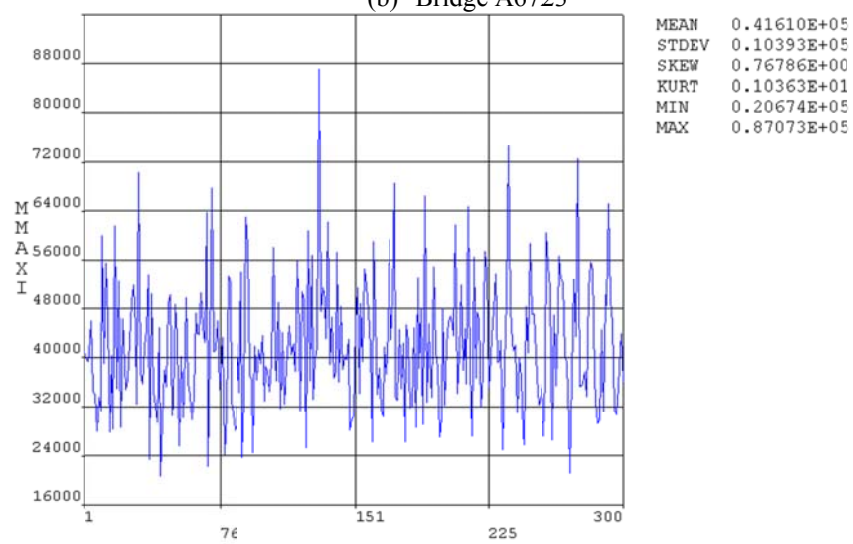
Figure D.6 Histograms of minimum absolute shear force



(a) Bridge A3848

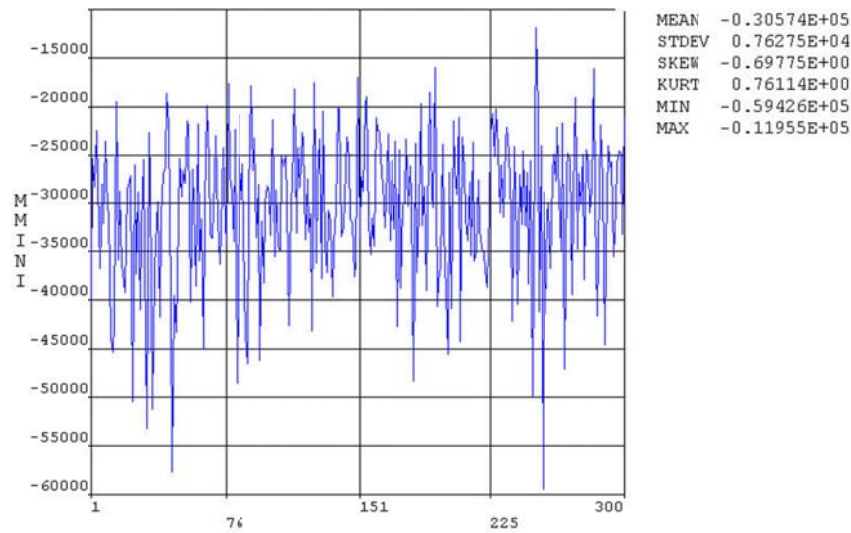


(b) Bridge A6723

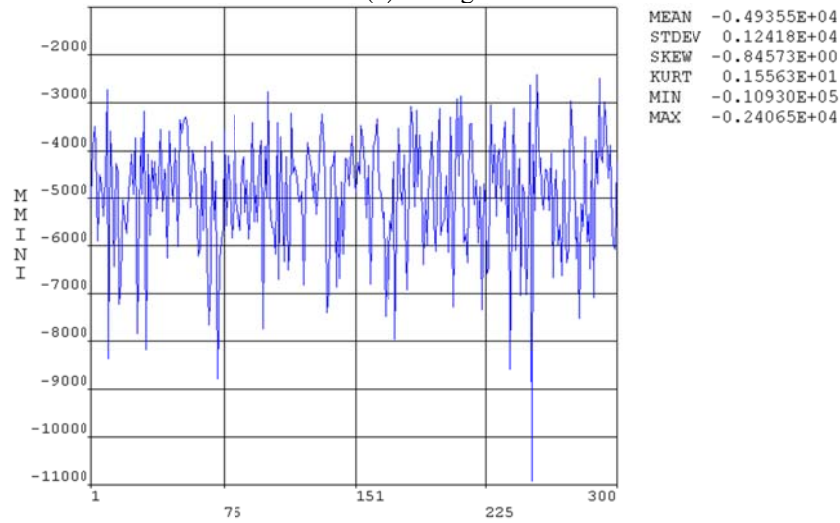


(c) Bridge A6477

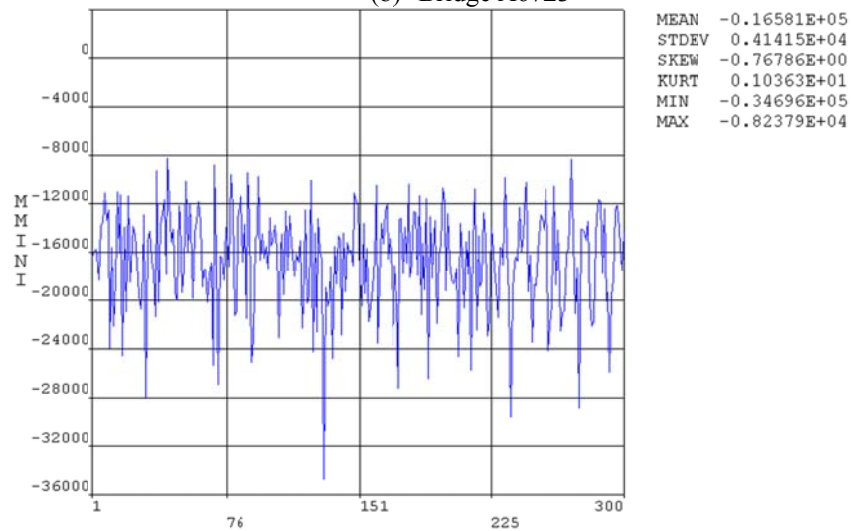
Figure D.7 Sample histories of maximum moment



(a) Bridge A3848

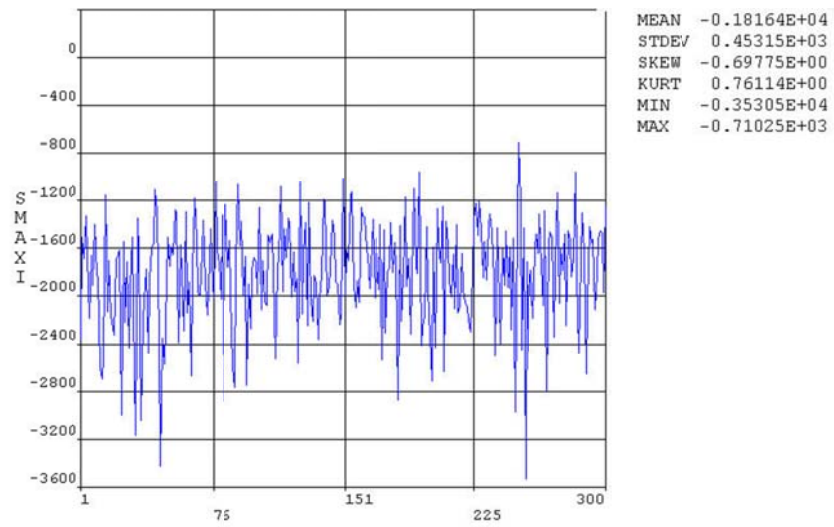


(b) Bridge A6723

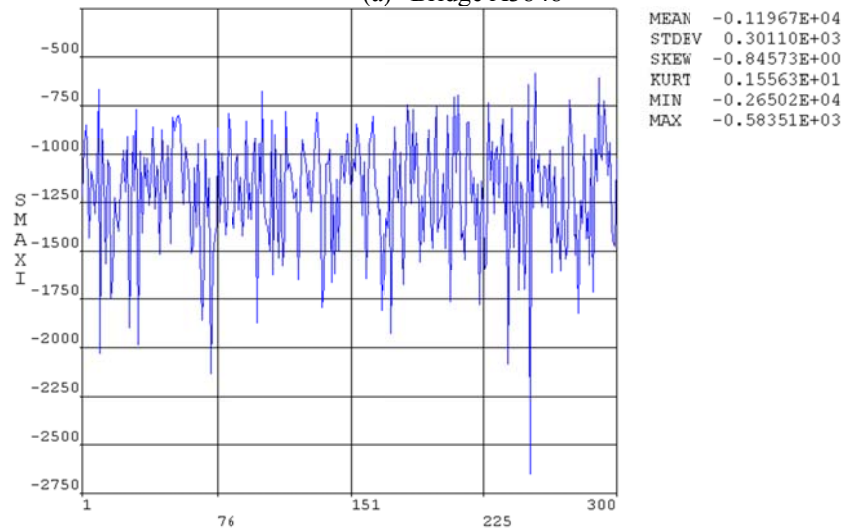


(c) Bridge A6477

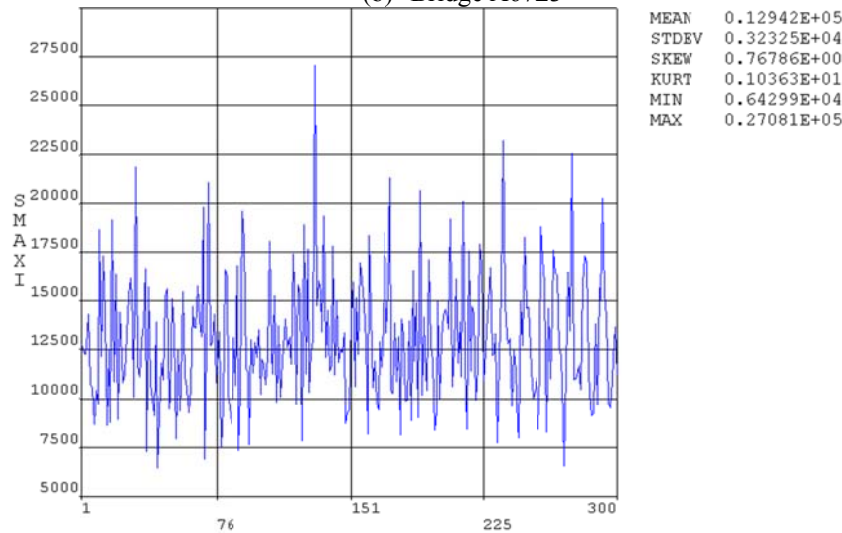
Figure D.8 Sample histories of minimum moment



(a) Bridge A3848

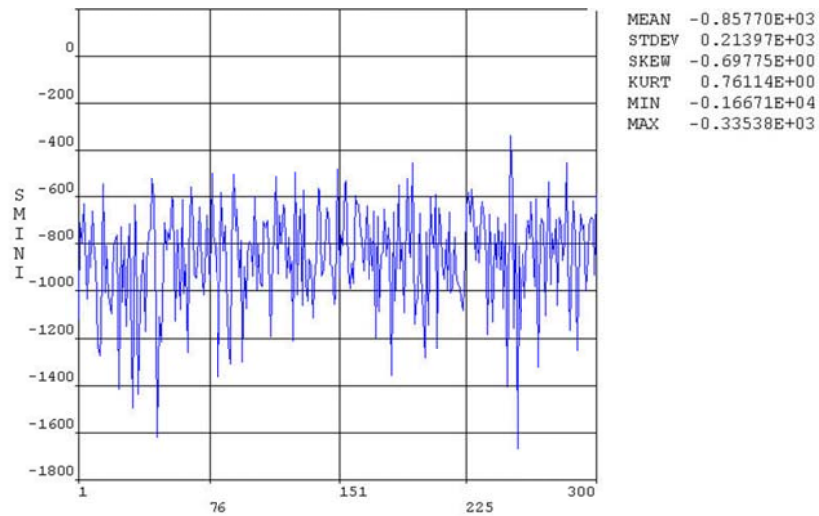


(b) Bridge A6723

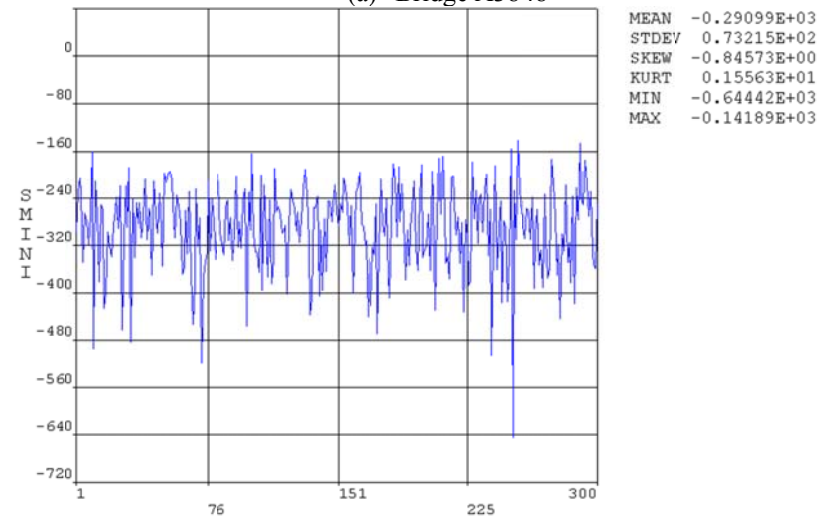


(c) Bridge A6477

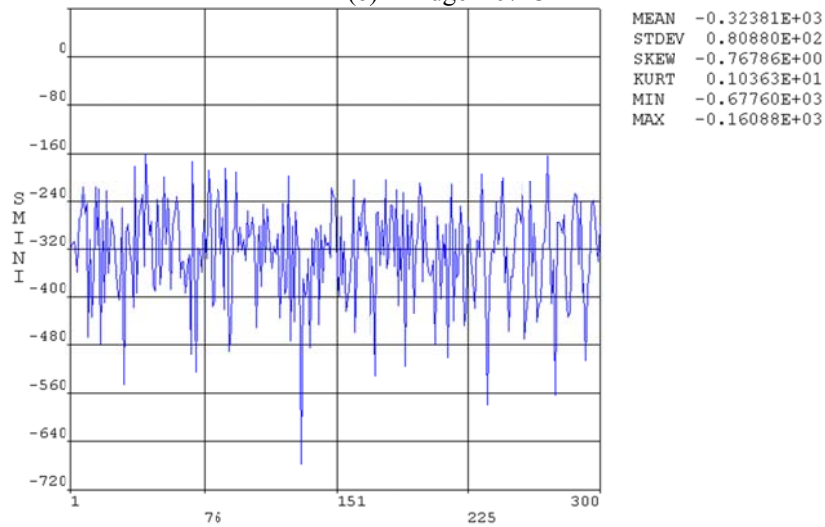
Figure D.9 Sample histories of maximum shear force



(a) Bridge A3848

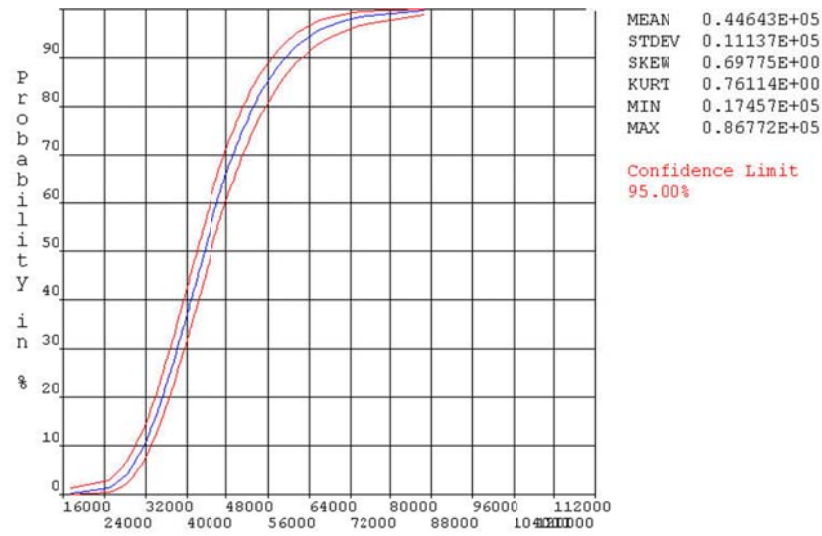


(b) Bridge A6723

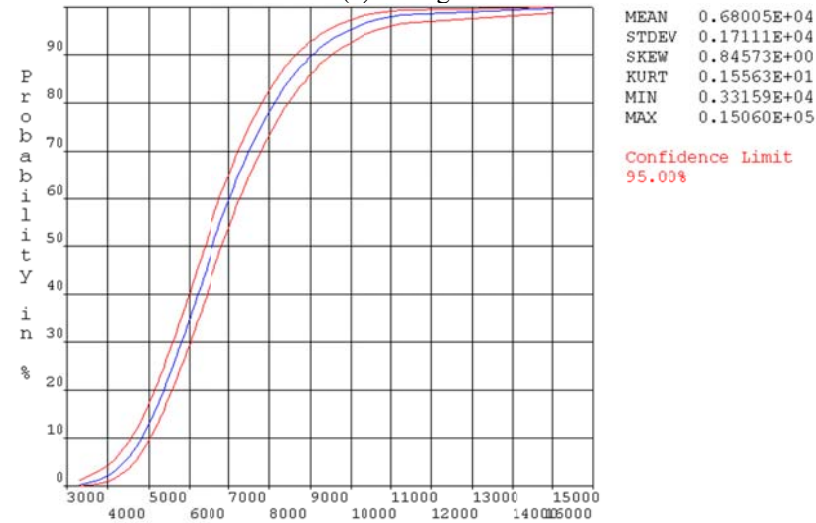


(c) Bridge A6477

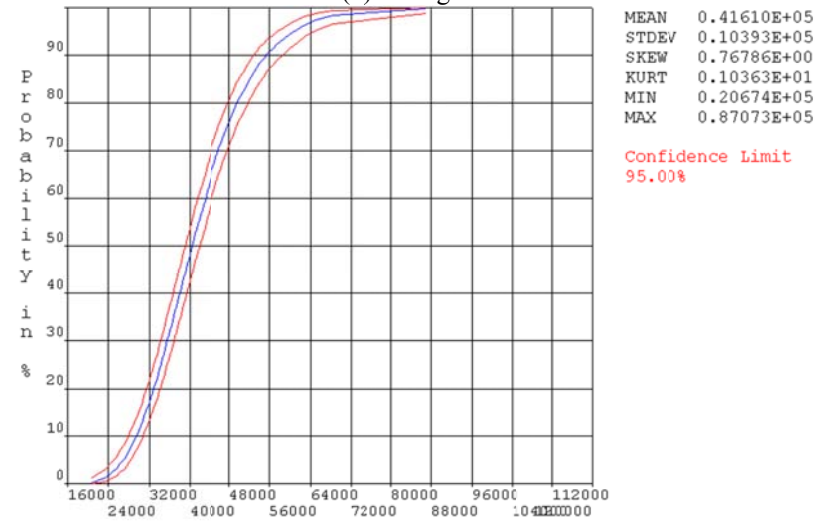
Figure D.10 Sample histories of minimum shear force



(a) Bridge A3848

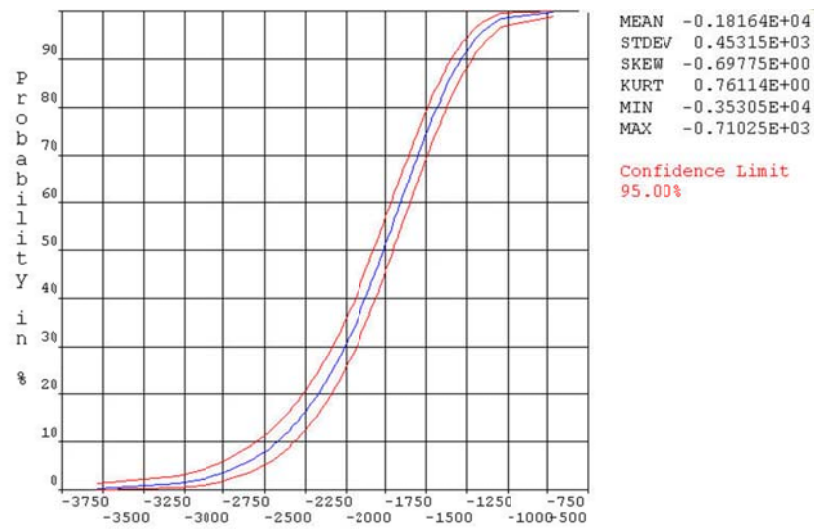


(b) Bridge A6723

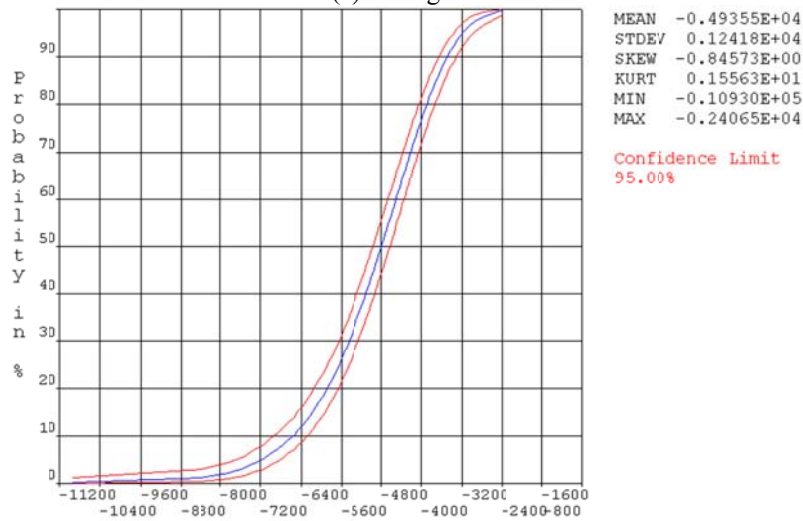


(c) Bridge A6477

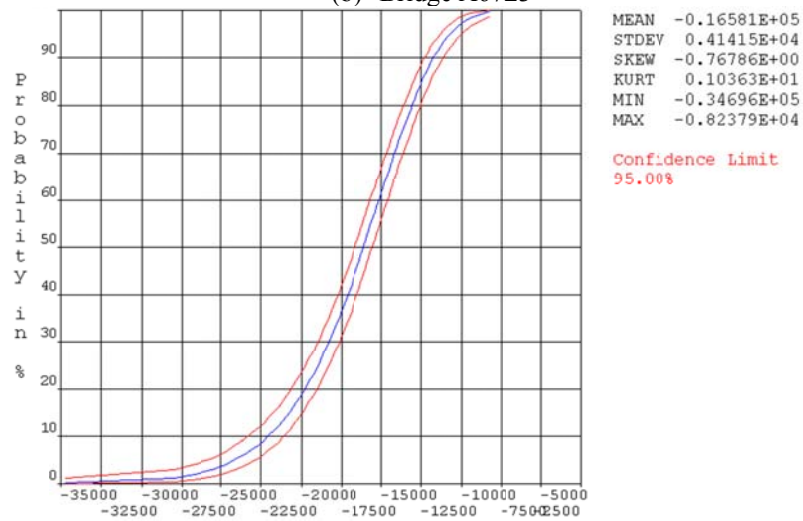
Figure D.11 Probability distribution functions of maximum moment



(a) Bridge A3848

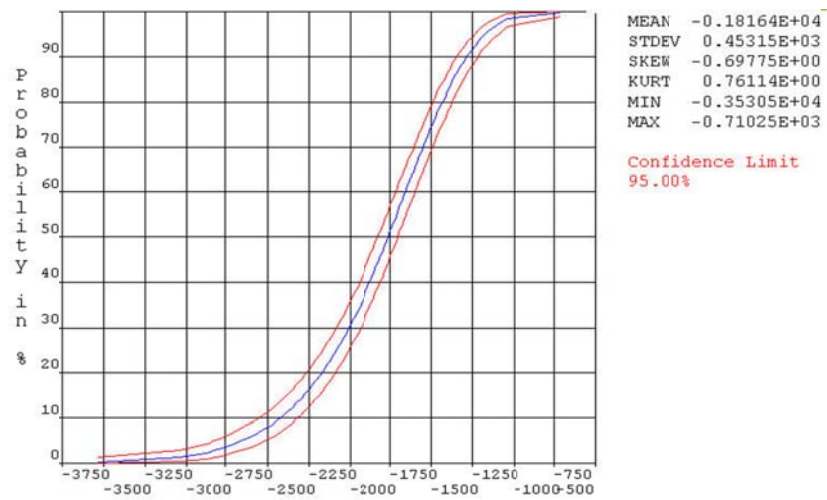


(b) Bridge A6723

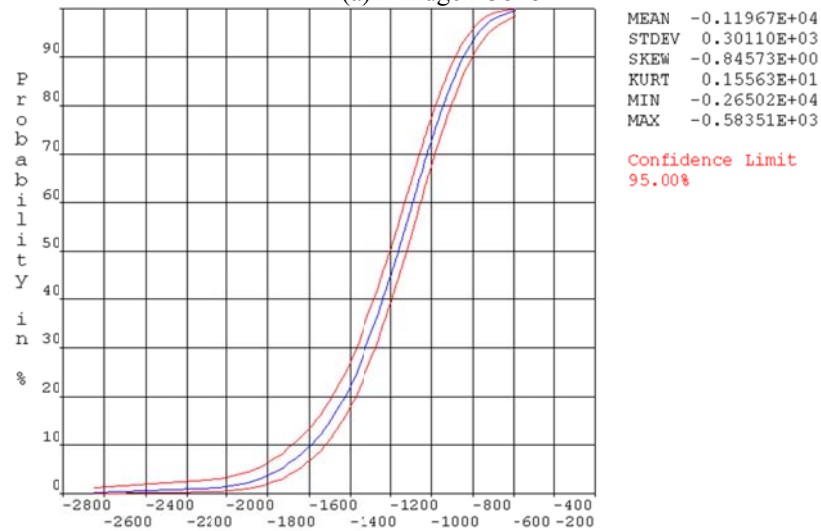


(c) Bridge A6477

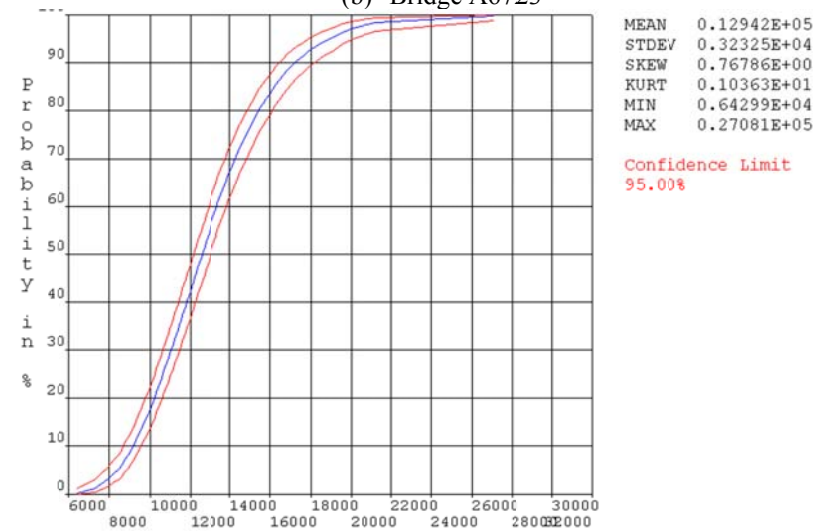
Figure D.12 Probability distribution function of minimum moment



(a) Bridge A3848

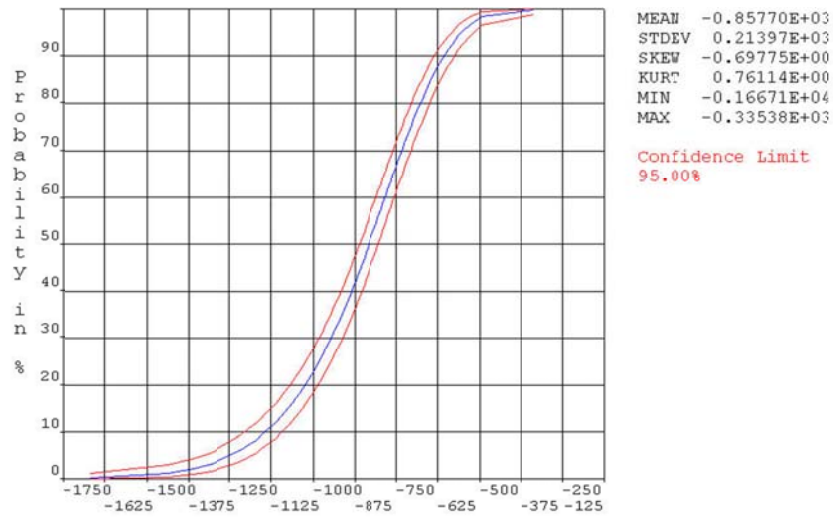


(b) Bridge A6723

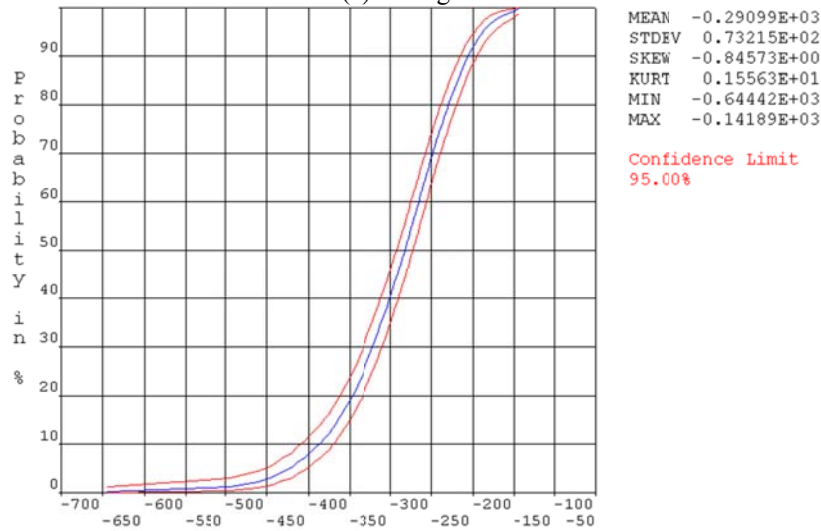


(c) Bridge A6477

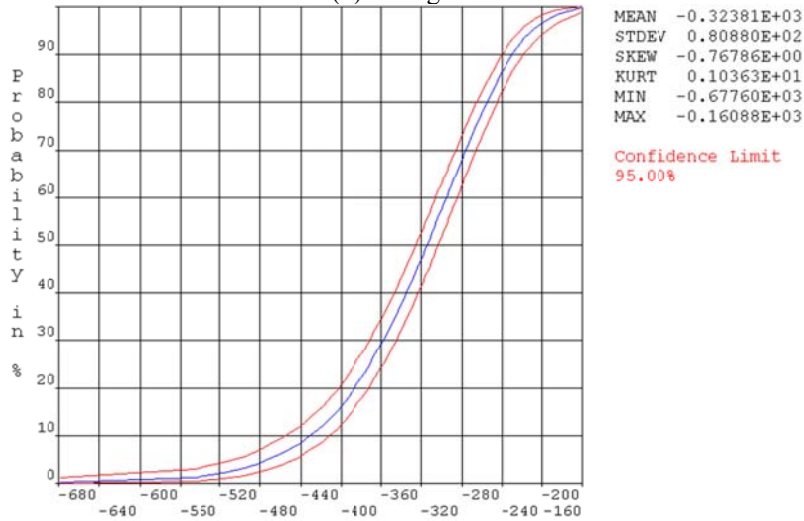
Figure D.13 Probability distribution function of maximum shear force



(a) Bridge A3848

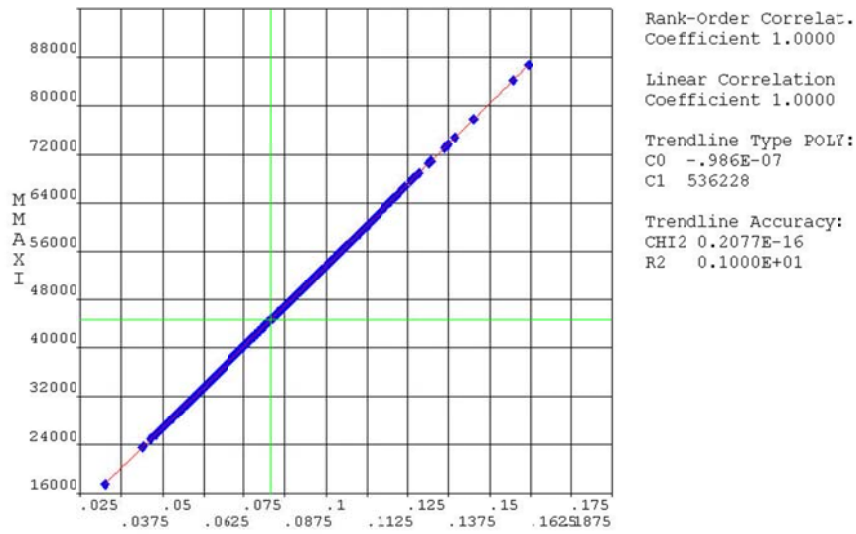


(b) Bridge A6723

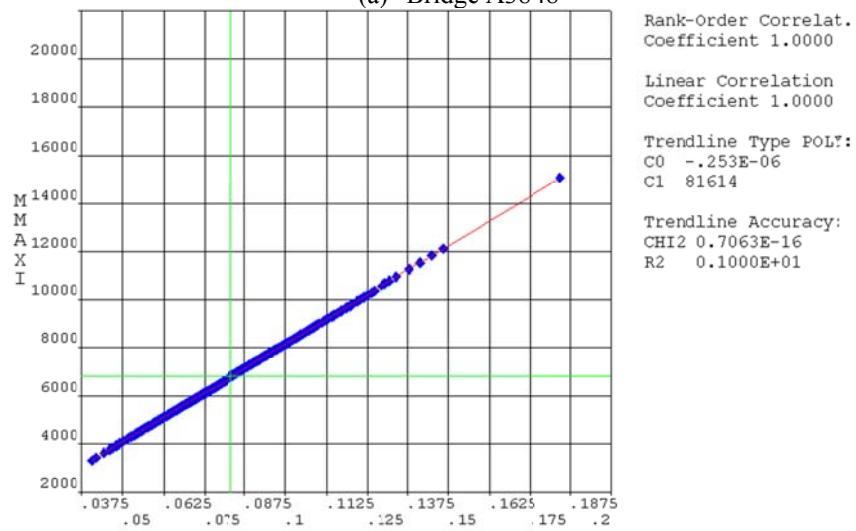


(c) Bridge A6477

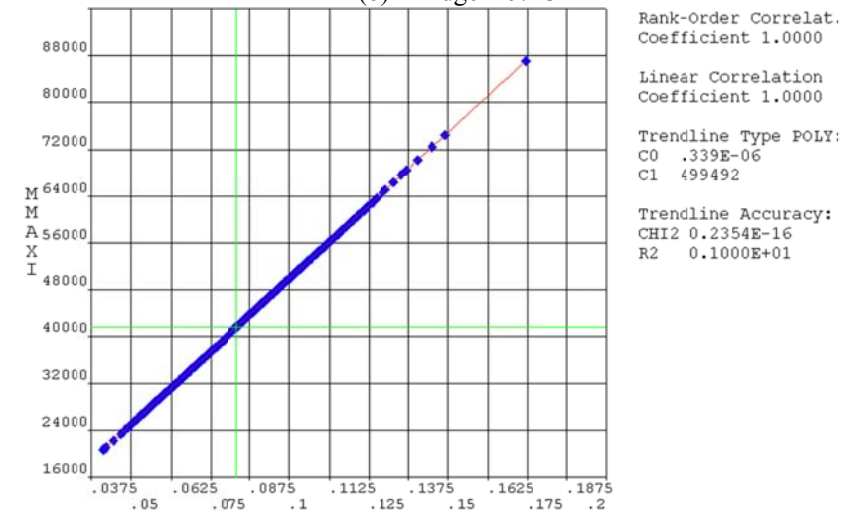
Figure D.14 Probability distribution function of minimum shear force



(a) Bridge A3848

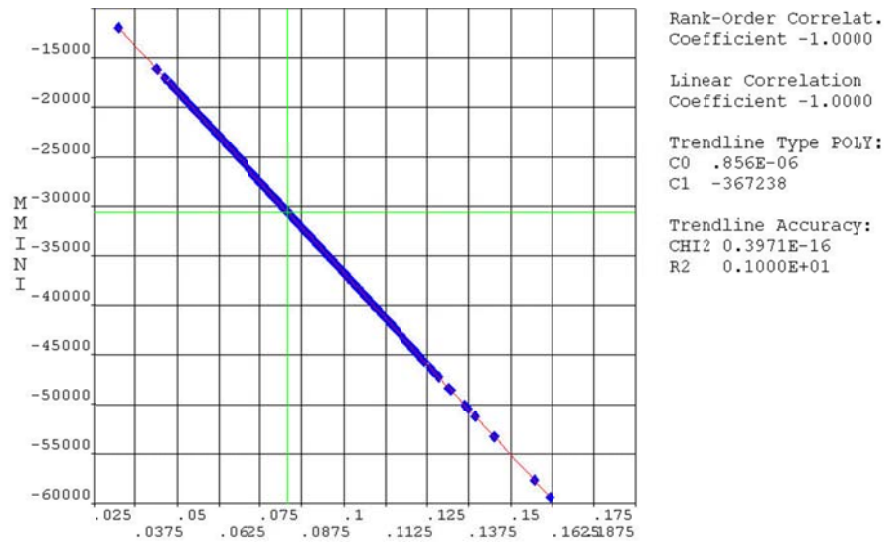


(b) Bridge A6723

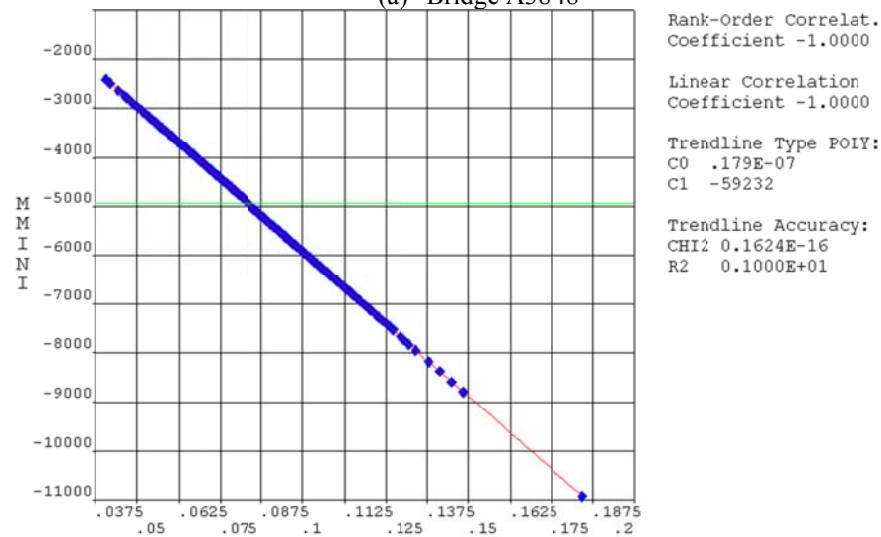


(c) Bridge A6477

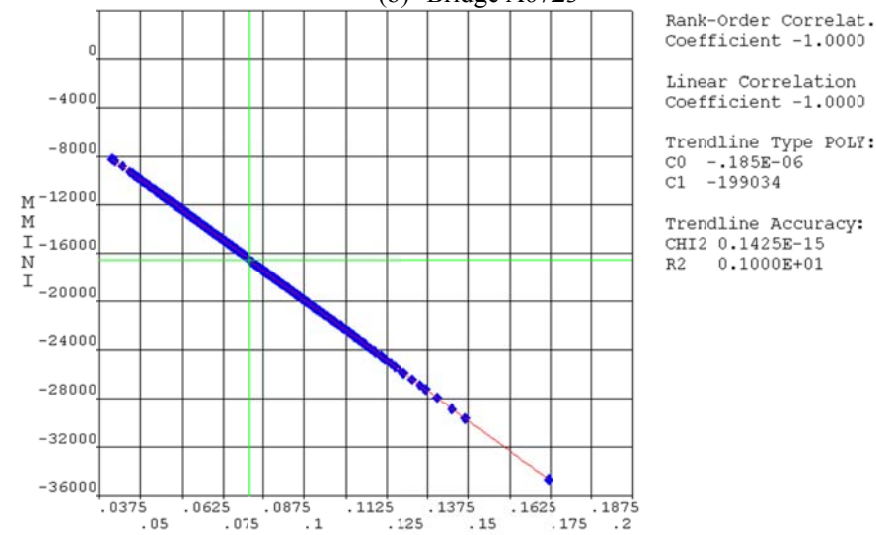
Figure D.15 Settlement versus maximum moment



(a) Bridge A3848



(b) Bridge A6723



(c) Bridge A6477

Figure D.16 Settlement versus minimum moment

**APPENDIX E: FORCES AND MOMENTS OF 31 NEW BRIDGES DUE TO A UNIT
SETTLEMENT AT SUPPORT 1**

Table E.1 Moments at various supports

Bridge No.	Moment (kip-ft)				
	Support 1	Support 2	Support 3	Support 4	Support 5
1	0.0	-344.7	0.0		
2	0.0	-341.8	0.0		
3	0.0	-349.6	0.0		
4	0.0	-325.6	0.0		
5	0.0	-340.9	0.0		
6	0.0	-354.1	0.0		
7	0.0	-356.9	0.0		
8	0.0	-368.7	0.0		
9	0.0	-375.9	0.0		
10	0.0	-381.9	0.0		
11	0.0	-388.7	0.0		
12	0.0	-458.4	458.4	0.0	
13	0.0	-432.1	432.1	0.0	
14	0.0	-454.6	454.6	0.0	
15	0.0	-400.3	400.3	0.0	
16	0.0	-527.3	527.3	0.0	
17	0.0	-553.4	553.4	0.0	
18	0.0	-483.7	483.7	0.0	
19	0.0	-501.1	501.1	0.0	
20	0.0	-512.4	512.4	0.0	
21	0.0	-522.2	522.2	0.0	
22	0.0	-533.0	533.0	0.0	
23	0.0	-489.3	587.2	-489.3	0.0
24	0.0	-447.8	537.4	-447.8	0.0
25	0.0	-449.3	539.2	-449.3	0.0
26	0.0	-530.7	636.9	-530.7	0.0
27	0.0	-556.1	667.4	-556.1	0.0
28	0.0	-588.4	706.0	-588.4	0.0
29	0.0	-512.3	614.8	-512.3	0.0
30	0.0	-529.0	634.8	-529.0	0.0
31	0.0	-544.5	653.4	-544.5	0.0

Table E.2 Shear forces at various supports

Bridge No.	Shear Force (kip)			
	Span 1	Span 2	Span 3	Span 4
1	17.2	-17.2		
2	11.4	-11.4		
3	8.7	-8.7		
4	6.5	-6.5		
5	5.7	-5.7		
6	5.1	-5.1		
7	4.5	-4.5		
8	4.1	-4.1		
9	3.8	-3.8		
10	3.5	-3.5		
11	3.2	-3.2		
12	22.9	-45.8	22.9	
13	14.4	-28.8	14.4	
14	11.4	-22.7	11.4	
15	8.0	-16.0	8.0	
16	8.8	-17.6	8.8	
17	7.9	-15.8	7.9	
18	6.0	-12.1	6.0	
19	5.6	-11.1	5.6	
20	5.1	-10.2	5.1	
21	4.7	-9.5	4.7	
22	4.4	-8.9	4.4	
23	24.5	-53.8	53.8	-24.5
24	14.9	-32.8	32.8	-14.9
25	11.2	-24.7	24.7	-11.2
26	10.6	-23.4	23.4	-10.6
27	9.3	-20.4	20.4	-9.3
28	8.4	-18.5	18.5	-8.4
29	6.4	-14.1	14.1	-6.4
30	5.9	-12.9	12.9	-5.9
31	5.4	-12.0	12.0	-5.4

Table E.3 Reactions at various supports

Bridge No.	Reaction (kip)				
	Support 1	Support 2	Support 3	Support 4	Support 5
1	-17.2	34.5	-17.2		
2	-11.4	22.8	-11.4		
3	-8.7	17.5	-8.7		
4	-6.5	13.0	-6.5		
5	-5.7	11.4	-5.7		
6	-5.1	10.1	-5.1		
7	-4.5	8.9	-4.5		
8	-4.1	8.2	-4.1		
9	-3.8	7.5	-3.8		
10	-3.5	6.9	-3.5		
11	-3.2	6.5	-3.2		
12	-22.9	68.8	-68.8	22.9	
13	-14.4	43.2	-43.2	14.4	
14	-11.4	34.1	-34.1	11.4	
15	-8.0	24.0	-24.0	8.0	
16	-8.8	26.4	-26.4	8.8	
17	-7.9	23.7	-23.7	7.9	
18	-6.0	18.1	-18.1	6.0	
19	-5.6	16.7	-16.7	5.6	
20	-5.1	15.4	-15.4	5.1	
21	-4.7	14.2	-14.2	4.7	
22	-4.4	13.3	-13.3	4.4	
23	-24.5	78.3	-107.7	78.3	-24.5
24	-14.9	47.8	-65.7	47.8	-14.9
25	-11.2	35.9	-49.4	35.9	-11.2
26	-10.6	34.0	-46.7	34.0	-10.6
27	-9.3	29.7	-40.8	29.7	-9.3
28	-8.4	26.9	-37.0	26.9	-8.4
29	-6.4	20.5	-28.2	20.5	-6.4
30	-5.9	18.8	-25.9	18.8	-5.9
31	-5.4	17.4	-24.0	17.4	-5.4

APPENDIX F: FORCES AND MOMENTS OF 31 NEW BRIDGES DUE TO DEAD AND LIVE LOADS

Table F.1 Maximum negative moments due to dead load excluding wearing surface

Bridge No.	Negative Moment (kip-ft)				
	Support 1	Support 2	Support 3	Support 4	Support 5
1	0.0	47.3	0.0		
2	0.0	109.5	0.0		
3	0.0	198.5	0.0		
4	0.0	316.9	0.0		
5	0.0	464.7	0.0		
6	0.0	644.0	0.0		
7	0.0	888.9	0.0		
8	0.0	1146.1	0.0		
9	0.0	1438.6	0.0		
10	0.0	1769.9	0.0		
11	0.0	2144.9	0.0		
12	0.0	37.8	37.8	0.0	
13	0.0	87.2	87.2	0.0	
14	0.0	158.0	158.0	0.0	
15	0.0	251.2	251.2	0.0	
16	0.0	380.5	380.5	0.0	
17	0.0	529.0	529.0	0.0	
18	0.0	713.2	713.2	0.0	
19	0.0	920.3	920.3	0.0	
20	0.0	1156.0	1156.0	0.0	
21	0.0	1423.3	1423.3	0.0	
22	0.0	1725.9	1725.9	0.0	
23	0.0	40.5	40.5	40.5	0.0
24	0.0	93.0	93.0	93.0	0.0
25	0.0	168.2	168.2	168.2	0.0
26	0.0	276.7	276.7	276.7	0.0
27	0.0	406.8	406.8	406.8	0.0
28	0.0	566.1	566.1	566.1	0.0
29	0.0	762.5	762.5	762.5	0.0
30	0.0	983.1	983.1	983.1	0.0
31	0.0	1236.4	1236.4	1236.4	0.0

Table F.2 Maximum positive moments due to dead load excluding wearing surface

Bridge No.	Positive Moment (kip-ft)			
	Span 1	Span 2	Span 3	Span 4
1	27.0	27.0		
2	61.8	61.8		
3	111.6	111.6		
4	178.4	178.4		
5	261.7	261.7		
6	362.7	362.7		
7	500.5	500.5		
8	645.2	645.2		
9	809.6	809.6		
10	995.8	995.8		
11	1206.5	1206.5		
12	30.7	9.9	30.7	
13	70.3	21.8	70.3	
14	126.9	40.0	126.9	
15	201.4	62.8	201.4	
16	304.9	95.7	304.9	
17	423.7	132.2	423.7	
18	571.1	178.9	571.1	
19	736.8	230.1	736.8	
20	925.3	289.6	925.3	
21	1139.2	355.8	1139.2	
22	1381.3	432.1	1381.3	
23	29.6	14.0	14.0	29.6
24	67.5	32.0	32.0	67.5
25	121.6	57.4	57.4	121.6
26	199.7	94.1	94.1	199.7
27	293.4	138.5	138.5	293.4
28	408.1	192.5	192.5	408.1
29	549.5	258.8	258.8	549.5
30	708.4	334.1	334.1	708.4
31	890.8	420.0	420.0	890.8

Table F.3 Maximum shear forces due to dead load excluding wearing surface

Bridge No.	Shear Force (kip)			
	Span 1	Span 2	Span 3	Span 4
1	11.0	11.0		
2	17.3	17.3		
3	23.9	23.9		
4	30.7	30.7		
5	37.7	37.7		
6	45.0	45.0		
7	54.5	54.5		
8	62.6	62.6		
9	70.8	70.8		
10	79.3	79.3		
11	88.2	88.2		
12	10.5	8.6	10.5	
13	16.5	13.6	16.5	
14	22.8	18.8	22.8	
15	29.2	24.2	29.2	
16	37.0	30.7	37.0	
17	44.3	36.7	44.3	
18	52.4	43.5	52.4	
19	60.2	50.0	60.2	
20	68.2	56.7	68.2	
21	76.5	63.5	76.5	
22	85.1	70.7	85.1	
23	10.6	9.3	9.3	10.6
24	16.7	14.6	14.6	16.7
25	22.9	20.1	20.1	22.9
26	30.4	26.7	26.7	30.4
27	37.4	32.9	32.9	37.4
28	44.8	39.4	39.4	44.8
29	52.9	46.6	46.6	52.9
30	60.8	53.5	53.5	60.8
31	68.9	60.7	60.7	68.9

Table F.4 Maximum negative moments due to weight of wearing surface

Bridge No.	Negative Moment (kip-ft)				
	Support 1	Support 2	Support 3	Support 4	Support 5
1	0.0	11.9	0.0		
2	0.0	26.9	0.0		
3	0.0	47.9	0.0		
4	0.0	74.9	0.0		
5	0.0	107.9	0.0		
6	0.0	146.9	0.0		
7	0.0	191.9	0.0		
8	0.0	242.9	0.0		
9	0.0	299.9	0.0		
10	0.0	362.9	0.0		
11	0.0	431.9	0.0		
12	0.0	9.5	9.5	0.0	
13	0.0	21.5	21.5	0.0	
14	0.0	38.3	38.3	0.0	
15	0.0	59.9	59.9	0.0	
16	0.0	86.3	86.3	0.0	
17	0.0	117.5	117.5	0.0	
18	0.0	153.5	153.5	0.0	
19	0.0	194.3	194.3	0.0	
20	0.0	239.9	239.9	0.0	
21	0.0	290.3	290.3	0.0	
22	0.0	345.5	345.5	0.0	
23	0.0	10.2	10.2	10.2	0.0
24	0.0	23.0	23.0	23.0	0.0
25	0.0	41.0	41.0	41.0	0.0
26	0.0	64.2	64.2	64.2	0.0
27	0.0	92.5	92.5	92.5	0.0
28	0.0	125.9	125.9	125.9	0.0
29	0.0	164.5	164.5	164.5	0.0
30	0.0	208.2	208.2	208.2	0.0
31	0.0	257.0	257.0	257.0	0.0

Table F.5 Maximum positive moments due to weight of wearing surface

Bridge No.	Positive Moment (kip-ft)			
	Span 1	Span 2	Span 3	Span 4
1	6.8	6.8		
2	15.2	15.2		
3	26.9	26.9		
4	42.2	42.2		
5	60.8	60.8		
6	82.7	82.7		
7	108.0	108.0		
8	136.7	136.7		
9	168.8	168.8		
10	204.2	204.2		
11	242.9	242.9		
12	7.7	2.5	7.7	
13	17.3	5.4	17.3	
14	30.8	9.7	30.8	
15	48.0	15.0	48.0	
16	69.2	21.7	69.2	
17	94.1	29.4	94.1	
18	122.9	38.5	122.9	
19	155.6	48.6	155.6	
20	192.0	60.1	192.0	
21	232.4	72.6	232.4	
22	276.5	86.5	276.5	
23	7.4	3.5	3.5	7.4
24	16.7	7.9	7.9	16.7
25	29.7	14.0	14.0	29.7
26	46.3	21.8	21.8	46.3
27	66.7	31.5	31.5	66.7
28	90.8	42.8	42.8	90.8
29	118.5	55.8	55.8	118.5
30	150.0	70.7	70.7	150.0
31	185.2	87.3	87.3	185.2

Table F.6 Maximum shear forces due to weight of wearing surface

Bridge No.	Shear Force (kip)			
	Span 1	Span 2	Span 3	Span 4
1	2.8	2.8		
2	4.3	4.3		
3	5.8	5.8		
4	7.3	7.3		
5	8.8	8.8		
6	10.3	10.3		
7	11.8	11.8		
8	13.3	13.3		
9	14.8	14.8		
10	16.3	16.3		
11	17.8	17.8		
12	2.6	2.2	2.6	
13	4.1	3.4	4.1	
14	5.5	4.6	5.5	
15	7.0	5.8	7.0	
16	8.4	7.0	8.4	
17	9.8	8.2	9.8	
18	11.3	9.4	11.3	
19	12.7	10.6	12.7	
20	14.2	11.8	14.2	
21	15.6	13.0	15.6	
22	17.0	14.2	17.0	
23	2.7	2.3	2.3	2.7
24	4.1	3.6	3.6	4.1
25	5.6	4.9	4.9	5.6
26	7.0	6.2	6.2	7.0
27	8.5	7.5	7.5	8.5
28	10.0	8.8	8.8	10.0
29	11.4	10.0	10.0	11.4
30	12.9	11.3	11.3	12.9
31	14.3	12.6	12.6	14.3

Table F.7 Maximum negative moments due to 75-year live load including dynamic effect

Bridge No.	Negative Moment (kip-ft)				
	Support 1	Support 2	Support 3	Support 4	Support 5
1	0.0	373.9	0.0		
2	0.0	480.1	0.0		
3	0.0	617.7	0.0		
4	0.0	767.3	0.0		
5	0.0	1112.2	0.0		
6	0.0	1423.3	0.0		
7	0.0	2174.3	0.0		
8	0.0	2461.3	0.0		
9	0.0	2711.1	0.0		
10	0.0	2941.2	0.0		
11	0.0	3161.2	0.0		
12	0.0	354.1	354.1	0.0	
13	0.0	425.3	425.3	0.0	
14	0.0	561.4	561.4	0.0	
15	0.0	660.6	660.6	0.0	
16	0.0	1226.7	1226.7	0.0	
17	0.0	1601.4	1602.8	0.0	
18	0.0	2034.0	2034.0	0.0	
19	0.0	2315.7	2319.7	0.0	
20	0.0	2569.8	2570.2	0.0	
21	0.0	2797.4	2797.4	0.0	
22	0.0	3006.4	3006.8	0.0	
23	0.0	354.7	354.7	355.1	0.0
24	0.0	410.8	410.8	410.8	0.0
25	0.0	518.9	518.9	519.3	0.0
26	0.0	888.6	888.6	886.4	0.0
27	0.0	1230.9	1230.9	1229.6	0.0
28	0.0	1606.4	1606.4	1606.1	0.0
29	0.0	2042.5	2042.5	2042.9	0.0
30	0.0	2330.8	2330.8	2331.8	0.0
31	0.0	2587.0	2587.0	2587.1	0.0

Table F.8 Maximum positive moments due to 75-year live load including dynamic effect

Bridge No.	Positive Moment (kip-ft)			
	Span 1	Span 2	Span 3	Span 4
1	463.9	463.9		
2	591.2	597.3		
3	756.2	756.2		
4	979.0	986.7		
5	1186.3	1199.3		
6	1418.2	1418.2		
7	2075.8	2075.8		
8	2370.4	2358.4		
9	2628.7	2635.9		
10	2894.1	2897.2		
11	3174.3	3170.5		
12	460.0	370.9	460.0	
13	549.6	451.7	555.0	
14	720.7	589.3	720.7	
15	867.1	695.4	873.9	
16	1423.6	1147.2	1437.6	
17	1723.0	1378.5	1723.0	
18	2080.1	1670.2	2080.1	
19	2379.4	1911.7	2369.2	
20	2645.5	2132.3	2650.3	
21	2916.3	2345.9	2918.1	
22	3201.7	2574.2	3199.5	
23	458.7	369.6	369.6	458.7
24	532.2	433.7	433.7	532.2
25	654.4	541.0	540.7	659.8
26	1160.8	928.2	929.5	1145.2
27	1415.0	1135.7	1135.7	1415.0
28	1714.5	1384.4	1384.4	1714.5
29	2059.9	1673.3	1671.0	2068.5
30	2346.3	1900.7	1903.7	2338.0
31	2639.1	2142.9	2147.4	2625.4

Table F.9 Maximum shear forces due to 75-year live load including dynamic effect

Bridge No.	Shear (kip)			
	Span 1	Span 2	Span 3	Span 4
1	59.0	59.0		
2	70.5	70.2		
3	78.4	78.4		
4	85.8	86.5		
5	91.8	92.8		
6	96.9	97.5		
7	101.6	102.1		
8	106.0	107.1		
9	110.2	111.8		
10	114.2	115.2		
11	118.1	119.9		
12	59.1	56.8	59.1	
13	70.4	66.6	70.3	
14	78.5	73.3	78.5	
15	85.9	81.7	86.5	
16	91.8	88.3	92.8	
17	96.9	93.1	97.5	
18	101.5	97.7	102.0	
19	105.9	102.8	106.9	
20	110.0	107.7	111.6	
21	114.0	110.8	114.9	
22	117.8	115.6	119.6	
23	61.0	56.1	59.4	61.0
24	67.6	63.1	63.1	67.6
25	81.9	74.8	75.0	79.7
26	85.0	84.7	81.7	87.4
27	90.9	87.0	86.6	91.6
28	96.1	96.6	96.6	97.2
29	104.5	98.4	98.1	102.7
30	105.1	104.2	103.1	107.6
31	109.3	108.6	106.0	110.8

Table F.10 Maximum negative moments due to HL-93 load including dynamic effect

Bridge No.	Negative Moment (kip-ft)				
	Support 1	Support 2	Support 3	Support 4	Support 5
1	0.0	562.3	0.0		
2	0.0	721.9	0.0		
3	0.0	928.9	0.0		
4	0.0	1153.9	0.0		
5	0.0	1672.5	0.0		
6	0.0	2140.2	0.0		
7	0.0	3269.7	0.0		
8	0.0	3701.3	0.0		
9	0.0	4076.9	0.0		
10	0.0	4422.9	0.0		
11	0.0	4753.7	0.0		
12	0.0	532.4	532.4	0.0	
13	0.0	639.6	639.6	0.0	
14	0.0	844.2	844.2	0.0	
15	0.0	993.4	993.4	0.0	
16	0.0	1844.7	1844.6	0.0	
17	0.0	2408.1	2410.2	0.0	
18	0.0	3058.6	3058.6	0.0	
19	0.0	3482.3	3488.2	0.0	
20	0.0	3864.3	3865.0	0.0	
21	0.0	4206.6	4206.5	0.0	
22	0.0	4520.9	4521.6	0.0	
23	0.0	533.3	533.3	534.0	0.0
24	0.0	617.8	617.8	617.8	0.0
25	0.0	780.4	780.4	780.9	0.0
26	0.0	1336.3	1336.3	1332.9	0.0
27	0.0	1851.0	1851.0	1849.0	0.0
28	0.0	2415.7	2415.7	2415.1	0.0
29	0.0	3071.4	3071.4	3072.1	0.0
30	0.0	3505.0	3505.0	3506.4	0.0
31	0.0	3890.3	3890.3	3890.4	0.0

Table F.11 Maximum positive moments due to HL-93 load including dynamic effect

Bridge No.	Positive Moment (kip-ft)			
	Span 1	Span 2	Span 3	Span 4
1	697.5	697.5		
2	889.1	898.1		
3	1137.2	1137.2		
4	1472.1	1483.8		
5	1783.9	1803.5		
6	2132.6	2132.6		
7	3121.4	3121.4		
8	3564.6	3546.5		
9	3953.0	3963.8		
10	4352.0	4356.6		
11	4773.4	4767.7		
12	691.8	557.7	691.8	
13	826.5	679.3	834.6	
14	1083.8	886.2	1083.8	
15	1304.0	1045.7	1314.2	
16	2140.7	1725.0	2161.8	
17	2591.0	2073.0	2591.0	
18	3128.0	2511.6	3128.0	
19	3578.0	2874.7	3562.7	
20	3978.2	3206.5	3985.4	
21	4385.5	3527.6	4388.1	
22	4814.5	3871.0	4811.2	
23	689.7	555.9	555.9	689.7
24	800.2	652.2	652.2	800.2
25	984.1	813.5	813.1	992.2
26	1745.5	1395.8	1397.8	1722.1
27	2127.8	1707.7	1707.7	2127.8
28	2578.2	2081.8	2081.8	2578.2
29	3097.7	2516.2	2512.8	3110.6
30	3528.3	2858.2	2862.7	3515.7
31	3968.6	3222.4	3229.1	3948.0

Table F.12 Maximum shear forces due to HL-93 load including dynamic effect

Bridge No.	Shear (kip)			
	Span 1	Span 2	Span 3	Span 4
1	80.0	80.0		
2	95.5	95.1		
3	106.2	106.2		
4	116.3	117.1		
5	124.3	125.7		
6	131.3	132.1		
7	137.7	138.4		
8	143.6	145.1		
9	149.3	151.5		
10	154.7	156.1		
11	160.1	162.5		
12	80.1	77.0	80.1	
13	95.4	90.2	95.3	
14	106.4	99.4	106.4	
15	116.4	110.7	117.3	
16	124.4	119.7	125.8	
17	131.3	126.1	132.1	
18	137.6	132.4	138.2	
19	143.4	139.3	144.9	
20	149.0	145.9	151.2	
21	154.4	150.1	155.7	
22	159.7	156.7	162.0	
23	82.7	76.0	80.4	82.7
24	91.6	85.5	85.5	91.6
25	110.9	101.4	101.6	108.0
26	115.1	114.8	110.8	118.4
27	123.2	117.9	117.4	124.1
28	130.2	130.9	130.9	131.7
29	141.6	133.3	132.9	139.1
30	142.4	141.2	139.7	145.8
31	148.1	147.2	143.6	150.1